NUCLEAR REACTOR MULTI-PHYSICS SIMULATIONS WITH COUPLED MCNP5 AND STAR-CCM+

BY

JEFFREY NEIL CARDONI

THESIS

Submitted in partial fulfillment of the requirements
for the degree of Master of Science in Nuclear, Plasma, and Radiological Engineering
in the Graduate College of the
University of Illinois at Urbana-Champaign, 2011

Urbana, Illinois

Master's Committee:

Professor Rizwan-uddin, Chair
Associate Professor Magdi Ragheb

Abstract

NUCLEAR REACTOR MULTI-PHYSICS SIMULATIONS
WITH COUPLED MCNP5 AND STAR-CCM+

Jeffrey N. Cardoni
Department of Nuclear, Plasma, and Radiological Engineering
University of Illinois at Urbana-Champaign, 2011
Dr. Rizwan-uddin, Advisor

The MCNP5 Monte Carlo particle transport code has been coupled to the computational fluid dynamics code, STAR-CCM+, to provide a high fidelity multi-physics simulation tool for analyzing the steady state properties of a PWR core. The codes are executed separately and coupled externally through a Perl script. The Perl script automates the exchange of temperature, density, and volumetric heating information between the codes using ASCII text data files. Fortran90 and Java utility programs the assist job automation with data post-processing and file management. The MCNP5 utility code, MAKXSF, pre-generates temperature dependent cross section libraries for the thermal feedback calculations.

The MCNP5–STAR-CCM+ coupled simulation tool, dubbed MULTINUKE, is applied to two steady state, PWR models to demonstrate its usage and capabilities. The first demonstration model, a single fuel element surrounded by water, consists of 9,984 CFD cells and 7,489 neutronic cells. The second model is a 3 x 3 PWR lattice model, consisting of 89,856 CFD cells and 67,401 neutronic cells. Fission energy deposition (fission and prompt gamma heating) is tallied over all UO_2 cells in the models using the F7:N tally in MCNP5. The demonstration calculations show reasonable results that agree with PWR values typically reported in literature. Temperature and fission reaction rate distributions are realistic and intuitive. Reactivity coefficients are also deemed reasonable in comparison to historically reported data. Mesh count is held to a minimum in both models to expedite computation time on a 2.8 GHz quad core machine with 1 GB RAM. The simulations on a quad core machine indicate that a massively parallelized implementation of MULTINUKE could be used to assess larger multi-million cell models with more complicated, time-dependent neutronic and thermal-hydraulic feedback effects.

To my love, Denise

Acknowledgments

Many thanks are due to the Department of Nuclear, Plasma, and Radiological Engineering at the University of Illinois. The unlimited patience and guidance of Idell Dollison, Gail Krueger, Becky Meline, Dr. Stubbins, and my adviser, Dr. Uddin, greatly facilitated my graduate studies at the University. I would also like to thank Dr. Ragheb for acting as the second reader for this thesis.

I would also like to acknowledge the financial support from the National Academy of Nuclear Training and the Institute of Nuclear Power Operations. Moreover, the boundless support, financial and otherwise, from family and friends was particularly conducive for my graduate studies.

Jeff Cardoni

TABLE OF CONTENTS

LIST OF FIGURES

LIST OF TABLES

ACRONYMS AND SYMBOLS

ANSI	American National Standards Institute
BWR	Boiling Water Reactor
CFD	Computational Fluid Dynamics
DES	Detached-Eddy Simulation
DNS	Direct Numerical Simulation of the Navier-Stokes Equations
US DOE	Department of Energy
ENDF	Evaluated Nuclear Data File
LES	Large-Eddy Simulation
MCNP5	Monte Carlo N-Particle Version 5, A Monte Carlo Particle Transport Code
PCT	Peak Cladding Temperature
PWR	Pressurized Water Reactor
RANS	Reynolds-Averaged Navier-Stokes Equations
RSICC	Radiation Safety Information Computational Center
RST	Reynolds Stress Transport Model
STAR-CCM+	A Computational Fluid Dynamics Code developed by CD-adapco

$S(\alpha,\beta)$	Thermal Scattering Function, Tabular Thermal Data Scattering Treatment
F_i	Reaction Rate
$\sum_\mathrm{i}$	Macroscopic Cross section (i = f = fission, i = s = scattering, i = t = total)
ϕ	Scalar Neutron Flux
ψ	Angular Neutron Flux
$\boldsymbol{r}$	Position Vector
E	Neutron Energy
$\boldsymbol{\Omega}$	Unit Vector of Neutron Direction
$d\boldsymbol{\Omega}$	Solid Angle of Neutron Direction
t	Time
n	Angular Neutron Density
N	Scalar Neutron Density
$\sum_\mathrm{s}(\boldsymbol{r},E'\rightarrow E,\boldsymbol{\Omega}'\rightarrow\boldsymbol{\Omega})$	Double Differential Macroscopic Scattering Cross section
H_f	Deposited Fission Energy
Q	Energy Released per Fission
$\boldsymbol{u}$	Velocity Field of Fluid
ρ	Fluid Density
$\mathbf{F}$	Volume Body Force per Unit Mass of Fluid
p	Static Gauge Pressure
μ	Dynamic Viscosity
$\boldsymbol{\sigma}$	Stress Tensor. $\boldsymbol{\sigma} = -\mathrm{p}\mathbf{I} + \mathbf{T}$, where $\mathbf{I}$ is the identity tensor and $\mathbf{T}$ is the deviatoric stress tensor.
c_p	Specific Heat Capacity at Constant Pressure
T	Fluid Temperature
$\overline{\phi}$	Dissipation Function in Energy Conservation Equation

Chapter 1. Introduction

This thesis is aimed at developing tools for coupled multi-physics analysis of nuclear reactors. The primary goal of the research was to incorporate state of the art, science-based neutronic and thermal-hydraulic simulators into an integrated tool for coupled and automated reactor core neutronics and thermal-hydraulics calculations. For this purpose, the Monte Carlo neutron transport code, MCNP5, was coupled to the computational fluid dynamics code, STAR-CCM+, to simulate self-consistent thermal-hydraulic and neutronic conditions in pressurized light-water reactors. The coupled solver, called MULTINUKE, is used to calculate the converged steady state neutronic and thermal-hydraulic properties of a single PWR cell model and a 3 x 3 PWR lattice model. Essential mechanisms of thermal reactivity feedback in PWRs and a brief overview of the remainder of the thesis are given in Chapter 1.

1.1. Background

Consistent gains in microprocessor speed and memory size have made highly accurate and computationally expensive computer codes more practical in simulating complex systems behavior. In the past, computation time limited high fidelity techniques to simplified models, and limited their use as audit tools for less accurate methods. With speed and memory size increasing approximately by a factor of two every eighteen months [1], modern nuclear reactor simulation practices have shifted to full three-dimensional models described by increasingly realistic physics codes. This includes the coupling of several different physics solvers into an integrated multi-physics analysis tool. The use of state of the art physics codes, combined into a coupled physics solver, represents the cutting edge of engineering and scientific simulations. The US Department of Energy's Innovation Hub, Nuclear Energy Modeling and Simulation, specifically calls for the development of first-principles based multi-physics simulations for nuclear reactors [2, 3]. High accuracy simulations, based on first-principles physics, can reduce design costs and uncertainty, thereby enhancing the economic feasibility and safety of nuclear energy.

Several physical processes are involved in modeling a large and complex system like a nuclear reactor. Codes simulating the neutronic, thermal-hydraulic, chemical, and mechanical aspects of the reactor can separately model these processes in the reactor. However, there exist feedback effects amongst the nuclear, fluid, thermal, chemical, and structural behavior of a nuclear reactor. The interplay between the neutronic and thermal-hydraulic properties of a nuclear reactor core, called thermal or reactivity feedback, is a fundamental aspect of nuclear core performance. The negative temperature reactivity coefficient – the negative reactivity feedback from an increase in temperature – contributes to a nuclear reactor's inherent operational stability and safety. In pressurized water reactors, thermal feedback and temperature coefficients are primarily from microscopic cross section's temperature dependence and from the change in moderator density with temperature. Water coolant in a PWR also acts as the neutron moderator. Other thermal feedback effects include coolant voiding (mostly important in BWRs), and the thermal expansion of fuel and core structural materials. Feedback from the neutronics to the thermal-hydraulics in the reactor is through the much more obvious heat generation rate, which is proportional to the fission reaction rate.

Microscopic cross section's temperature dependence is a result of the Doppler effect. The Doppler effect is a change in cross section due to temperature changes altering the thermal motion of nuclei [4]. In general, an increase in temperature lowers and widens resonance peaks to preserve the total area under the resonance. This usually leads to an increase in resonance absorption, because the heights of many significant cross section resonances in reactor materials are saturated – that is, due to self-shielding, the drop in resonance height does not lead to a proportional drop in resonance absorption (since Doppler broadening corresponds to a decrease in self-shielding) [5, 6]. As neutrons scatter to lower energy levels through collisions with the moderator, the broadened resonance will outweigh the effect of the slightly lowered resonance peak, increasing the probability of resonance absorption [6]. Although numerically smaller than the reactivity coefficient due to moderator temperature change, the reactivity feedback from the Doppler effect is almost instantaneous, making it a vital characteristic in nuclear reactor performance. In a low enriched PWR, the Doppler effect decreases reactivity due to parasitic absorption in epithermal U-238 resonances. However, reactors with different fuel materials and neutron spectra could have positive Doppler reactivity coefficients [7].

The delayed reactivity effect from the moderator temperature variation is the dominant link between the neutronic and thermal-hydraulic behavior in a pressurized water reactor. There exists a time delay between changes in fission heating in the fuel and the temperature response in the coolant; heat transport from the fuel, across the fuel-clad gap, through the cladding, and into the coolant takes a measurable amount of time. Assuming a near constant pressure, as in the case of a steady state PWR, coolant temperature determines the density of the moderator (water) through thermal expansion. Even with the density held constant, increased moderator temperature lowers reactivity by hardening the neutron spectrum and increasing resonance absorption; but it is the effect of temperature on moderator density that influences reactivity the most [6]. An increase in moderator temperature lowers the moderator density, altering the neutron transport and energy spectrum characteristics of the core. Decreased moderator density reduces the number of moderator atoms in a given region of the core, which in turn reduces scattering and macroscopic absorption cross sections. This results in an increased neutron mean free path, increased leakage from the core, and decreased neutron thermalization. Therefore, in a PWR, the increased coolant/moderator temperature decreases reactivity, creating a negative reactivity coefficient of greater magnitude than that of the Doppler effect [7]. Lower moderator density also reduces parasitic absorption of thermal neutrons (light water has a significant absorption cross section), which tends to increase reactivity. However, in a typical PWR lattice, this positive reactivity contribution is small compared to the negative reactivity effect associated with a loss of neutron thermalization [8].

It is important to stress the significance of moderator temperature and neutron thermalization. Accurate modeling of neutron scattering requires consideration of the thermal motion of other nearby atoms and molecules. In the free gas thermal treatment (neutron energy above 4 eV), the temperature of the moderator influences the velocity of the target atom in (neutron) elastic scattering events [4]. Although relevant for scattering events at higher neutron energies with heavy materials, nuclear inelastic scattering is not a concern for low energy neutrons in light moderating media [6]. References to inelastic scattering in the following discussion refer to thermal neutron scattering events where entire molecules or crystal lattices are left in an excited state after the collision. For neutron energies below approximately 4 eV, thermal neutron cross sections are complicated functions of moderator temperature [4, 6]. Thermal cross sections are in the form of tabular thermal scattering data, commonly referred to as the *S(α,β)* scattering treatment, where *S(α,β)* is the scattering function. In some literature, *S(α,β)* may be specifically referring to incoherent inelastic scattering [9, 7]. When neutron energy is comparable to the thermal energy of target molecules and crystals, colliding neutrons tend to interact with the entire molecule or crystal lattice. The use of thermal cross section tables is essential in simulating neutron thermalization in nuclear reactors. There are three thermal scattering types [10]:

- Coherent elastic: important in crystalline materials such as graphite, beryllium, and beryllium oxide. Interference from scattering planes creates jagged cross section profiles called Bragg edges.
- Incoherent elastic: related to reactors with solid hydrogen moderators.
- Incoherent inelastic: related to bound scattering problems, such as hydrogen in liquid water. For PWR simulations, incoherent inelastic scattering is a crucial aspect of neutron thermalization.

1.2. Methods

Two fundamental quantities describing PWR core behavior are nuclear reaction rates and the thermo-physical behavior of the water coolant and moderator. In a fission reactor, the neutron population drives the most important nuclear reaction rates – including fission heating in the fuel, and neutron heating in structures and water coolant. [Photon particle transport is important for determining gamma heating, but will not be considered here. However, estimating gamma heating in the fuel from prompt fission gamma rays does not require explicit photon particle transport.]

Calculating reaction rates is vital in coupling neutronic and thermal-hydraulic physics. A nuclear reaction rate F_i for reaction type i is given by

$$F_i = \int d\boldsymbol{r} \int dE \sum_i(\boldsymbol{r}, E)\, \phi(\boldsymbol{r}, E). \tag{1.1}$$

Here, $\sum_i$ is the macroscopic cross section of the desired reaction type, and ϕ is the scalar neutron flux. The macroscopic cross section can be determined from energy dependent microscopic cross section libraries and the atom density in the target material. The macroscopic cross section is defined as the product of atom density and microscopic cross section, which is written as

$$\sum_i \equiv N\sigma_i. \tag{1.2}$$

Computing nuclear reaction rates requires the determination of the neutron flux distribution. Neutron transport methods provide one of the most accurate means for simulating the transport of neutrons in a nuclear reactor core. Neutron transport codes actually solve for the angular flux, ψ, which is related to the scalar flux simply by

$$\phi \equiv \int_0^{4\pi} \psi \, d\boldsymbol{\Omega}\,. \tag{1.3}$$

Here, ψ is the angular flux of neutrons traveling in solid angle $d\boldsymbol{\Omega}$ about direction $\boldsymbol{\Omega}$.

Using the Monte Carlo method, stochastic neutron transport solvers often employ general three-dimensional regions and surfaces, and use highly accurate continuous energy cross section libraries. With proper modeling techniques, Monte Carlo transport codes allow for nearly “exact” modeling of neutron transport problems by permitting users to avoid approximating reactor geometries and materials with approximate meshes and smeared material properties. With a continuous energy cross section database, Monte Carlo transport codes also avoid the tedious process of generated multi-energy group cross section libraries. From these perspectives, Monte Carlo neutron transport is a conceptually easier, “brute force” method for solving reactor physics problems. The problem can be modeled nearly exactly and solved stochastically by simulating individual neutron histories. The ease in modeling comes at a cost of computation speed: sufficient (many) particle transport histories must be run to reduce stochastic uncertainty to acceptable levels. Consistent developments in computer speed, computational science, and parallel computing have made simulating nuclear reactors with Monte Carlo methods a reality. For this thesis, the well-established code from Los Alamos National Laboratory, MCNP5 (Monte Carlo N-Particle Version 5), is used without any variance reduction techniques to determine the nuclear physics aspects of a PWR reactor core.

The other part of a coupled nuclear and thermal-hydraulic solver involves the calculation of the temperature distribution in fuel elements and core structures, and the density distribution of the coolant. Therefore, simulating the thermal-hydraulic behavior of a PWR requires the solution of the heat conduction equation in the fuel rod, and the solution to the mass, momentum, and energy transport equations for the fluid. Computational fluid dynamics (CFD) provides a state of the art method for simulating the turbulent fluid flow and heat transfer in a nuclear reactor. For this thesis, the CFD code STAR-CCM+ (from the company CD-adapco) shall be used to calculate temperature and density distributions in a PWR. STAR-CCM+ is capable of solving the Navier-Stokes equations in complex 3D geometries. STAR-CCM+ is distributed with a model-building program, STAR-DESIGN, to streamline the process of creating 3D geometries. STAR-CCM+ has the ability to generate automated CFD meshes. It also features several turbulence models, and allows volumetric heat sources to be read from external data files and automatically assigned to the appropriate CFD cells, a feature that will be used to couple it with the neutronics code.

1.3. Thesis Overview

For this thesis, MCNP5 and STAR-CCM+ are coupled into an integrated neutronic and thermal-hydraulic PWR simulation tool, called MULTINUKE. This high fidelity multi-physics solver calculates and automatically exchanges:

1. Fission heating rate in the fuel region, including prompt gamma heating in the fuel, (calculated by MCNP5) for use as a volumetric (W/m^3) heat source in STAR-CCM+.
2. Temperature distributions in the fuel, cladding, and coolant regions (calculated by STAR-CCM+) for use in determining MCNP5 cross section libraries.

3. The density distribution in the coolant/moderator, calculated by STAR-CCM+, for use in MCNP5 input files.

The kinetic energy of the fission fragments and local prompt gamma heating deposit over 80% of the energy from nuclear fission in the fuel, and ~97% of all recoverable fission energy is eventually deposited in the fuel [5, 6]. Therefore, neutron and gamma heating in the clad and coolant regions are neglected. Along with the mesh data of the MCNP5 and STAR-CCM+ models, the variables listed above are the only information automatically exchanged between the two codes by the MULTINUKE Perl script. However, any data normally available in MCNP5 or STAR-CCM+ can be used in post-processing the coupled solution. There are no modifications made to the source codes of MCNP5 and STAR-CCM+; the codes are executed separately and coupled through the Perl script. Therefore, the coupling scheme is explicit, i.e. several systems of equations are solved in an iterative fashion until the solution *appears* converged. Data exchange is through ASCII data files, and automated by the MULTINUKE Perl script. The term MULTINUKE refers to the solver processes involving MCNP5 and STAR-CCM+, and the automation programs linking the two codes.

The MCNP5 utility code, MAKXSF, is used to pre-generate temperature dependent cross section libraries for use by MULTINUKE. The creation of the cross section libraries is not an automated process in MULTINUKE; rather, it is performed before the iterations between MCNP5 and STAR-CCM+ for the sake of computational speed (saving hours of computation time for typical PWR materials and temperatures). It would be more accurate, and much slower, to run MAKXSF in-between the STAR-CCM+ and MCNP5 calculations, adjusting cross sections to the actual temperatures in each cell. Fortunately, work performed by Seker et al. at Purdue University and Argonne National Laboratory demonstrated sufficient accuracy using pre-generated cross section libraries binned by discrete temperature increments [11]. Chapter 2 presents details about this work, and other previous work related to coupled Monte Carlo and CFD simulations of nuclear reactors.

Chapters 3 and 4 discuss the theory of neutron transport and computational fluid dynamics, and how these tools are specifically used in this thesis. Brief descriptions of the governing neutronic and thermal-hydraulic equations are given in order to point out the computational challenges of using high-fidelity methods for reactor simulations. The details of the MULTINUKE processes, including any necessary manual preparations, are discussed in Chapter 5. Results for two PWR models (a single fuel cell and a 3 x 3 lattice of fuel cells), analyzed using MULTINUKE, are presented in Chapter 6. Potential further research and the thesis summary are discussed in Chapter 7. Appendices A, B, and C contain sample input files, the coding of MULTINUKE coupling programs, and data file formats. Finally, Appendix D provides a quick summary of how to prepare a directory to contain all of the files necessary for execution of MULTINUKE.

Chapter 2. Literature Review of Coupled Neutronics and Thermal-Hydraulics

A traditional multi-physics analysis of a nuclear reactor involved scientists and engineers performing calculations in their respective disciplines (nuclear, thermal-hydraulic…), and manually exchanging relevant data to couple the physical behavior of the nuclear reactor [6]. To simulate thermal feedback, these simulations generally approximated the neutronics with diffusion theory, and approximated the thermal-hydraulics with 1D methods based on empirical correlations [12]. Automated and coupled deterministic neutronic–thermal-hydraulic codes now exist with varying degrees of accuracy in the context of using first-principles physics. With modern computational capabilities, this includes the coupling of deterministic neutron transport and computational fluid dynamics for practical nuclear reactor problems. In 2004, D.P. Weber et al. of Argonne National Laboratory reported successfully linking the CFD code, STAR-CD, to the 3D deterministic neutron transport code, DeCART, in their work on the Numerical Nuclear Reactor (NNR) [13, 23].

2.1. McSTAR: MCNP5 and STAR-CD

Expanding upon the deterministic work of D.P. Weber et al., V. Seker and colleagues coupled stochastic neutron physics with computational fluid dynamics. The work of Seker et al. involved the automated linking of MCNP5 and STAR-CD for single pin and small PWR assembly applications [11]. This coupled code system, called McSTAR, coupled MCNP5 to STAR-CD by a Fortran90 program, two Perl scripts, and modified STAR-CD user subroutines to assist in data exchange. Similar to MULTINUKE, the principal quantities exchanged between the two codes are fission heating rates calculated using MCNP5, and temperatures and densities calculated using STAR-CD. Temperature dependent cross section libraries were pre-generated using NJOY [10]. Of particular interest are the various methods used to update the cross sections between the STAR-CD and MCNP5 calculations.

The McSTAR work of Seker et al. examined three approaches to generate temperature dependent cross section libraries. The first method modified the cross sections of each nuclide during the execution of McSTAR, in each region, to the exact new temperatures determined by STAR-CD. This approach was deemed too computationally expensive, even though it yields the most exact temperature dependent cross sections. The second and third methods were similar in that cross section libraries were generated before running MCNP5 and STAR-CD, and binned into discrete temperature intervals over a temperature range typical of PWR problems. The second method used fine 2 K to 5 K temperature bins, which caused memory problems in the MCNP5 calculation. The third method used coarser 25 K to 50 K temperature bins, and linearly interpolated the cross sections. Although the least accurate of the three approaches, pre-generated coarse 25 K to 50 K binned cross section libraries still yielded high accuracy solutions in comparison to the other methods. A calculation of the effective multiplication factor, k_{eff}, for a single PWR pin problem at 325 K showed very low error in using coarsely binned, pre-generated cross sections. The use of coarse pre-generated cross section libraries produced an error of only 30 pcm in k_{eff} compared to the k_{eff} value obtained using cross sections at exactly 325 K [11]. The demonstrated accuracy of the pre-generated cross sections justifies a similar approach for pre-generating cross sections for MULTINUKE, which is described in detail in Chapter 3 and Chapter 5.

2.2. MCNP5 and FLUENT

At the University of Illinois at Urbana-Champaign, Jianwei Hu also successfully demonstrated the coupling of Monte Carlo transport with computational fluid dynamics [14]. The general solution methodology was similar to McSTAR: a coupling program links the two codes externally, where temperature, density, and nuclear heating data were transferred via text data files. In this work, the FLUENT code was used for the CFD component instead of STAR-CD. Furthermore, the scope of the demonstration model was reduced to a very simple 64 cell cube, half of which was UO_2 fuel and the other half was water. Because of the simplicity of the model, neutron and gamma heating were calculated for the entire model, along with the fission heating in the fuel, by running coupled neutron-photon MCNP5 calculations. The MCNP5 mesh and the FLUENT mesh for the 64 cell model were exactly alike, allowing a Perl script to automatically locate the appropriate donor-receiver cell pairs for data transfer between the meshes. For each cell in the donor mesh, the Perl script calculated the distance to each cell in the receiver mesh.

The minimum distance between donor and receiver cells determined the data exchange between the two meshes [14]. Although convenient and accurate for identical or nearly identical meshes, this simple method will not work with two meshes of sufficiently different size and type. Cross sections were updated using NJOY by discrete temperature increments after each FLUENT calculation.

2.3. Coupled Monte Carlo and CFD Developments in MULTINUKE

The general methodology of MULTINUKE, described in detail in Chapter 5, is comparable to Seker's McSTAR [11] and Hu's MCNP5-FLUENT work [14]. The major differences are the use of the STAR-CCM+ as the CFD solver, and the use of MAKXSF to generate temperature dependent cross section libraries. McSTAR's STAR-CD code is similar to STAR-CCM+ and developed by the same company (CD-adapco), but STAR-CCM+ is touted as an integrated engineering tool with an intuitive graphical user interface with automated meshing capabilities [15]. For example, MULTINUKE does not require modified user subroutines to input a heat source from MCNP5 and create thermal-hydraulic output data files. Instead, MULTINUKE uses the external table and Java macro features in STAR-CCM+ to read in the heat generation rate, run the CFD calculation, and write temperature and density data files. The CFD mesh in MULTINUKE is created using STAR-CCM+ without the use of additional meshing programs. The test problems solved using MULTINUKE are less complicated than the problem solved earlier using McSTAR [11], but more complicated than the 64 cell cube problem solved using the MCNP5-FLUENT coupled code. However, compared to McSTAR's test problems, the MCNP5 models investigated by MULTINUKE are more detailed, since the neutronic mesh is not reduced compared to the CFD mesh. (In the test problem for McSTAR, the MCNP5 mesh was simplified compared to the STAR-CD mesh [11].) Finally, MULTINUKE does not rely on an external cross section code like NJOY. MAKXSF can perform most of the functions of NJOY for reactor applications, and is included in MCNP5 distributions that follow the MCNP5-1.50 release [16].

Chapter 3. Overview of Neutron Transport Theory

Neutron transport governs fundamental aspects of nuclear reactor performance. Neutron interactions cause heating, nuclear fission, and induce radioactivity in reactor materials. These interactions determine numerous essential core properties including reactor safety, reactivity control, reactor kinetics, xenon stability, fuel depletion, and isotope production. Neutron interactions play a central role in creating the power distributions that drive the heat transfer process. There are strong feedback effects between nuclear physics and the other physical processes in the reactor, particularly thermal-hydraulics.

Chapter 3 gives an overview of neutron transport theory, *in the context of its role in calculating power distributions for coupling with steady state CFD*. The neutron transport equation is presented to highlight the computational challenges of high-fidelity reactor physics, particularly the fact that discretizing the seven variables of the equation over the spatial and energy domain of a PWR creates an enormous computational burden. The neutron diffusion equation is also presented in order to describe how its simplifications that have allowed its past coupling with thermal-hydraulics in traditional reactor analysis methods. The deterministic transport method is then compared to the Monte Carlo method, which is the neutron transport method used in the MULTINUKE code. Although MULTINUKE currently only analyzes steady state models, the time dependence in the neutronic equations is retained to illustrate the full complexity of neutron transport theory. (Further work with MULTINUKE will expand its applicability to time-dependent simulations.) Finally, the basic features of the MCNP5 Monte Carlo transport code and the nuclear data code, MAKXSF, are introduced.

3.1. Theory

3.1.1. Deterministic Transport

The fundamental technique to simulate the nuclear properties of a PWR involves solving the neutron transport equation to obtain nuclear reaction distributions in the core. The solution to the neutron transport equation yields the neutron flux as a function of position, energy, neutron direction, and time. This entails seven independent variables: three in space, one in energy, two for angular direction, and one in time. The neutron transport equation, which is a linearized form of the Boltzmann transport equation, is given by [6]:

$$\frac{1}{\mathrm{v}(E)}\frac{\partial\psi}{\partial t} + \boldsymbol{\Omega}\cdot\boldsymbol{\nabla}\psi(\boldsymbol{r},E,\boldsymbol{\Omega},t) + \textstyle\sum_t(\boldsymbol{r},E)\,\psi(\boldsymbol{r},E,\boldsymbol{\Omega},t) = S(\boldsymbol{r},E,\boldsymbol{\Omega},t). \qquad (3.1)$$

For steady state problems, the time derivative of the angular flux in equation (3.1) is zero, and the time dependence in the angular flux ψ and the neutron source S can be removed. The angular flux is defined as

$$\psi(\boldsymbol{r},E,\boldsymbol{\Omega},\boldsymbol{t}) \;\equiv\; \mathrm{v}(E)n(\boldsymbol{r},E,\boldsymbol{\Omega},t). \qquad (3.2)$$

In equation (3.2), $\mathrm{v}(E)$ is the neutron speed, and $n(\boldsymbol{r},E,\boldsymbol{\Omega},t)$ is the angular neutron density. In words, $n(\boldsymbol{r},E,\boldsymbol{\Omega},t)\,d^3rdEd\boldsymbol{\Omega}$ is the average number of neutrons in volume element d^3r about position $\boldsymbol{r}$, with energy in dE about E, moving in the solid angle $d\boldsymbol{\Omega}$ about unit vector $\boldsymbol{\Omega}$, at time t [6]. For criticality problems, the neutron source is from fission, elastic scattering, and inelastic scattering. Therefore, the total neutron source is

$$S(\boldsymbol{r},E,\boldsymbol{\Omega},t) = S_{scatter}(\boldsymbol{r},E,\boldsymbol{\Omega},t) + \; S_{fission}(\boldsymbol{r},E,\boldsymbol{\Omega},t). \qquad (3.3)$$

The neutron source from elastic and inelastic scattering is written as

$$S_{scatter}(\boldsymbol{r},E,\boldsymbol{\Omega},t) = \;\int_0^{4\pi} d\boldsymbol{\Omega}'\int_0^{\infty} dE'\,\textstyle\sum_s(\boldsymbol{r},E'\rightarrow E,\boldsymbol{\Omega}'\rightarrow\boldsymbol{\Omega})\,\psi(\boldsymbol{r},E',\boldsymbol{\Omega}',t). \qquad (3.4)$$

The double differential macroscopic cross section in equation (3.4), $\sum_s(\boldsymbol{r},E'\rightarrow E,\boldsymbol{\Omega}'\rightarrow\boldsymbol{\Omega})$, is the scattering cross section that characterizes the probability per path length that neutrons at $\boldsymbol{r}$ scatter from energy interval about E' into dE about E, and from incident direction $\boldsymbol{\Omega}'$ to a final direction in $d\boldsymbol{\Omega}$ about $\boldsymbol{\Omega}$ [6]. The fission source, considering only prompt fission neutrons, is given by

$$S_{fission}(\boldsymbol{r},E,\boldsymbol{\Omega},t) = \frac{\chi(E)}{4\pi}\int_0^{4\pi} d\boldsymbol{\Omega}'\int_0^{\infty} dE'\,\nu(E')\textstyle\sum_f(\boldsymbol{r},E')\,\psi(\boldsymbol{r},E',\boldsymbol{\Omega}',t). \qquad (3.5)$$

Equation (3.5) assumes ν neutrons, on average, are released isotropically from fission with an energy distribution given by the fission spectrum $\chi(E)$. Once again, E' is the incident neutron energy and $\boldsymbol{\Omega}'$ is the incident neutron direction.

For reactor applications, a high accuracy discrete-ordinates solution to the time independent neutron transport equation requires solving some 10^{15} simultaneous equations [2]. The discrete-ordinates method discretizes the neutron transport equation in each variable. A first-principles approach to the discrete-ordinates method for neutron transport, as in the case of Argonne National Laboratory's Ultimate Neutronic Investigation Code (UNIC), discretizes the reactor model into millions to billions of spatial grid points, thousands of energy groups, and hundreds of angles [17]. This enormous computational effort may not be practical even on petascale supercomputers, owing to the inherent parallel algorithm difficulties in handling neutron transport source iteration [2]. Furthermore, the memory requirements of direct neutron transport solutions may challenge the memory capabilities of current and next generation supercomputers [17].

However challenging direct solutions to the neutron transport equation may be, it allows for an approximate reactor model with discretized physics to be solved through the neutron transport equation. In contrast, Monte Carlo transport methods are generally considered to model a reactor's geometry exactly, and solve the problem approximately by simulating many neutron histories. The DOE Innovation Hub, Nuclear Energy Modeling and Simulation, considered Monte Carlo transport to be the longer-term goal over deterministic methods for reactor analysis, due to Monte Carlo's ability to model space, energy, and neutron angle in a continuous and more accurate manner [3]. Therefore, this thesis investigated the usage of coupling Monte Carlo transport with thermal-hydraulics as a science-based multi-physics tool for nuclear reactor analysis.

3.1.2. Neutron Diffusion Approximation

Another deterministic method for reactor physics is the neutron diffusion approximation to neutron transport. The principal difference from neutron transport is that neutron diffusion does not take into account the angular dependence of the neutron flux. The neutron diffusion equation can be derived from a simple neutron balance or directly from the neutron transport equation. Similar to thermal conduction and gaseous diffusion, it assumes that neutrons diffuse from regions of high neutron population to low neutron population. The neutron diffusion approximation uses three main assumptions in its formulation [7]:

1. Scalar neutron flux is sufficiently slowly varying in space to be approximated by a Taylor series expansion where only the first two terms are retained.

2. Neutron absorption is small relative to scattering. Thus, absorption is much less likely than scattering and $\sum_{\text{total}} \approx \sum_{\text{scatter}}$.
3. Neutron scattering is linearly anisotropic.

These assumptions allow the neutron continuity equation, which has the two unknowns of scalar flux $\phi(\boldsymbol{r}, E, t)$ and scalar neutron current $\mathbf{J}(\boldsymbol{r}, E, t)$, to be reduced to an equation with only one unknown. Specifically, the three diffusion approximations relate scalar flux to scalar current by Fick's Law [7]:

$$\mathbf{J}(\boldsymbol{r}, E, t) = -D(\boldsymbol{r}, E)\boldsymbol{\nabla}\phi(\boldsymbol{r}, E, t). \tag{3.6}$$

Here, $D(\boldsymbol{r}, E)$ is the diffusion coefficient. Transport theory can be used to show that $D(\boldsymbol{r}, E)$ is a function of the macroscopic cross sections; thus the diffusion coefficient also has spatial and energy dependence. The neutron diffusion equation for prompt neutrons is then given by

$$\frac{1}{\mathrm{v}(E)}\frac{\partial\phi}{\partial t} - \boldsymbol{\nabla}\cdot D(\boldsymbol{r}, E)\boldsymbol{\nabla}\phi(\boldsymbol{r}, E, t) + \textstyle\sum_t(\boldsymbol{r}, E)\,\phi(\boldsymbol{r}, E, t) = S(\boldsymbol{r}, E, t). \tag{3.7}$$

The source on the right side of equation (3.7) is again the sum of the in-scattering source and fission source, which are respectively written as

$$S_{scatter}(\boldsymbol{r}, E, t) = \int_0^\infty dE' \textstyle\sum_s(\boldsymbol{r}, E' \to E)\,\phi(\boldsymbol{r}, E', t). \tag{3.8}$$

$$S_{fission}(\boldsymbol{r}, E, t) = \frac{\chi(E)}{4\pi}\int_0^\infty dE'\,\nu(E')\textstyle\sum_f(\boldsymbol{r}, E')\,\phi(\boldsymbol{r}, E', t). \tag{3.9}$$

Once again, the time derivative of flux in equation (3.7) for steady state problems is zero, and the time dependence in equations (3.6) through (3.9) can be removed. Though similar in appearance to the neutron transport equation, the diffusion equation does not directly address angular dependence of neutron flux or scattering, and it is a second order equation [7].

Diffusion theory is applicable under certain conditions for reactor analysis. The first diffusion theory assumption results in diffusion being valid in large homogeneous media. The second approximation makes diffusion theory acceptable away from highly absorbing materials (fuel and poison). The third assumption only works for neutron scattering events with heavy nuclei. Thus, it is clear that neutron diffusion theory cannot be *directly* applied to a pressurized water reactor where: neutron mean free path is comparable to the lattice spacing of very heterogeneous reactor materials, highly absorbing fuel and neutron poison materials are prevalent, and neutron thermalization is accomplished by scattering with light nuclei. Transport theory corrections, such as linear extrapolations for neutron flux to better model neutron leakage, extend the applicability of diffusion theory. Properly spatially homogenized multigroup cross sections allow diffusion theory based reaction rates to capture averaged reaction rates that match neutron transport solutions. However, even with these laborious efforts, fine-resolution neutron diffusion results may still need modification through empirical methods in order to match experimental or transport theory results [6, 7].

Despite its shortcomings, neutron diffusion theory has been the historical workhorse for reactor analysis. Its various approximations and lack of angular dependence in the diffusion equations allow 3D neutron diffusion codes to be very fast compared to 3D neutron transport codes. Like deterministic neutron transport codes, a discretized mesh that approximates the model geometry is created using finite difference, finite element, finite volume, or nodal discretization. Unlike deterministic transport, however, a coarser mesh is usually employed, typically ranging from hundreds of nodes (nodal diffusion) to several million grid points [7]. Diffusion methods use approximately 2-20 energy groups for light water reactors. The computational speeds of neutron diffusion codes have facilitated their coupling to other physics modules over the years, particularly in thermal-hydraulic feedback codes. With modern computing, many such multi-physics codes are also fully time-dependent, such as Idaho National Laboratory's RELAP5-3D [18].

3.1.3. Monte Carlo Neutron Transport

Monte Carlo neutron transport methods do not solve the linearized Boltzmann equation directly in the sense that deterministic methods do; average particle behavior in Monte Carlo codes is not resolved from a direct solution of the transport equation. Instead, Monte Carlo transport simulates neutron transport with *computational particles*, essentially solving the neutron transport equation stochastically. With a sufficiently large sample of particle histories, the central limit theorem can infer the average physical characteristics of particles in a nuclear reactor within a confidence interval, including the neutron flux distribution [4]. This numerical experiment is inherently realistic, especially when individual nuclear reactions are based on first-principles physics, since particle transport is an intrinsically stochastic phenomenon [7]. In contrast to deterministic transport, Monte Carlo methods generally allow for exact geometry modeling and continuous treatments of neutron energy and direction. Monte Carlo codes also have an advantage in the ease of developing massively parallel algorithms [17].

Monte Carlo geometry modeling can be considered nearly exact because the stochastic transport of particles does not require an approximate mesh of the geometry. In deterministic transport solvers, the discrete ordinate method transfers particles between discretized elements of space, energy, and angle. Monte Carlo transport, where energy and angle are treated as continuous independent variables, transfers particles between events separated in space [4]. For example, in calculating the criticality of a simple Godiva sphere, a Monte Carlo model consists of only one geometric region – just a simple sphere. On the other hand, a deterministic transport code needs to subdivide the sphere into several grids/cells/nodes to create an approximate spatial mesh of the sphere.

Although Monte Carlo codes can model particle transport without discretized physics, unless specific steps are taken they only yield gross information for the problem. This includes data such as total reaction rates in entire geometric regions, effective multiplication factors, and reactivity coefficients. Even when every fuel pin is modeled in an entire PWR core, Monte Carlo codes can calculate integral data for the core relatively efficiently. Nonetheless, to obtain the fine-level detail for 3D reaction rate distributions required for thermal-hydraulic coupling, Monte Carlo codes generally tally data using one of three methods:

1. Subdividing Monte Carlo geometry cells into several smaller cells.
2. Implementing tally surfaces, unused by the actual problem geometry, to obtain data distributions.
3. Superimposing a separate tally mesh over the actual reactor geometry.

Therefore, in order to tally highly detailed reaction rate distributions, a mesh of sorts must still be created. Many particle histories must be run to reduce stochastic uncertainty to acceptable levels in all of the numerous small regions of the tally mesh. It is for this reason that practical use of the Monte Carlo method for reactor analysis is extremely computationally expensive. For instance, the relative error in each tally region is proportional to $\sigma/\sqrt{N}$, where σ is the variance and N is the number of histories used in the calculation of the tally in the particular region. In order to decrease the relative error in each region by one-half, the number of histories in each region would have to increase by at least a factor of four, assuming no method of variance reduction is used. In contrast to direct Monte Carlo simulation, variance reduction techniques can be used to decrease the variance (σ). It becomes clear that a high-resolution reaction rate distribution, which requires a fine tally mesh in a large PWR, needs an enormous amount of particle histories in order to adequately sample each region so that relative error is reduced to acceptable levels. Generally, the precision of a Monte Carlo calculation is acceptable for relative errors less than 0.10 [4].

Nuclear events for a particle in Monte Carlo codes are simulated sequentially by using pseudo-random number generators to sample probability distributions describing the physical events. For reactor applications, a typical neutron history can begin as a source neutron with isotropic direction and an energy distribution given by the fission spectrum. The source distribution can be spatially uniform, or it can be the exact spatial fission source distribution, since Monte Carlo codes can store the location of fission sites for use as source locations for subsequent neutron histories. Monte Carlo codes typically run neutron histories in discrete batches or cycles. Thus for criticality problems, fission neutrons in one neutron batch are terminated for use as source neutrons for the next batch. After an adequate number of cycles, a uniform or approximate spatial source distribution converges to the true fission source distribution [4].

Random numbers are generated to sample the source distributions. When a neutron undergoes an event or collision, additional random numbers are used to sample nuclear reaction probability distributions. The determination of whether a reaction occurs, and the type of reaction to take place, is found by considering physical rules and probabilistic transport data for the reaction and material involved [4].

To determine the heating reaction rates required for multi-physics coupling to thermal-hydraulics, Monte Carlo codes can use the *track length estimator*. The length of a neutron track in a cell allows Monte Carlo solvers to tally neutron flux and fission heating [4]. Neutrons stream in straight lines through materials between collisions. For a region of constant composition, the track length (l_i) of a neutron is

$$l_i = -\frac{1}{\Sigma_t} ln\, \lambda_i. \tag{3.10}$$

In equation (3.10), $\sum_t$ is the total macroscopic cross section of the material in the region, and λ is a random number between 0 and 1 [7]. The average scalar flux in a particular mesh cell is then the sum of the path lengths traversing through the volume (per unit volume per unit time):

$$\phi = \frac{1}{V} \int dE \int d^3r \int ds\, N(\boldsymbol{r}, E, t) = \frac{1}{V} \sum_i l_i. \tag{3.11}$$

The term $dsN(\boldsymbol{r}, E, t)$ in equation (3.11) is the track length density and V is the volume of the region. The flux distribution can then be obtained by assembling the calculated fluxes in each mesh cell [4].

3.2. MCNP5

Continuously developed by Los Alamos National Laboratory since the 1940s and with roots in the Manhattan Project for World War II, MCNP is considered the "gold standard" in Monte Carlo transport codes [17]. MCNP5 is capable of modeling the transport of neutrons, photons, and electrons for a variety of applications. For this thesis, a Linux MPI executable is compiled using the ANSI-Standard Fortran90 source code obtained from RSICC (Radiation Safety Information Computational Center at Oak Ridge National Laboratory). This release included the MAKXSF utility program for modifying the cross section libraries.

MCNP5 features general 3D geometry modeling and the best available, continuous nuclear data and physics. Reactor physics and data are discretized where appropriate, such as with the S(α,β) thermal scattering treatment, where the angular probability distribution has discrete angles for Bragg scattering [4]. MCNP5 uses the free-gas thermal treatment to account for the thermal motion of target atoms during low-energy neutron collisions. For very low energy neutron thermalization, MCNP5 can use the *S(α,β)* thermal scattering treatment to account for molecular binding and crystalline effects that influence neutron scattering. MCNP5 has access to nuclear and atomic data for: continuous-energy neutron, discrete-reaction neutron, continuous-energy photoatomic interaction, continuous-energy electron interaction, continuous-energy photonuclear interaction, neutron dosimetry, *S(α,β)* thermal, neutron multigroup, and photoatomic multigroup. Neutronic data used in this thesis is from the ENDF/B-VII.0, nuclear data cross sections evaluated in 2006. MCNP5 neutron cross section data is separated into different datasets by element, isotope, temperature, and the source of the data. Unique datasets are identified by *ZAID*s, where *Z* is the atomic number, *A* is the mass number, and *ID* is the library specifier. For a given isotope and evaluation source (such as ENDF/B-VII.0), the *ID* number changes for different temperatures. There are special ZAIDs for *S(α,β)* thermal scattering data [4].

A collection of dataset *ZAID*s constitutes a cross section library. Cross section libraries are organized for MCNP5 by the XSDIR directory file. When utilizing a variety of temperature dependent cross section libraries (created by MAKXSF), as in the case of coupled MCNP5 and STARCCM+ calculations, MCNP5 allows for a modified XSDIR file to be specified during code execution. The temperature dependent *ZAID* identifiers are listed in the MCNP5 input file for the appropriate materials.

The MCNP5 input file is an ASCII text file arranged in the following order [4]:

- MCNP5 geometry cell cards: closed volumes comprised of logical combinations of surfaces. It is in this section of the input file that temperature and density distributions from STAR-CCM+ calculations can be input into MCNP5. Each cell is given a material that determines the cross sections to be used for that cell (and thus the cross section's temperature dependence), a density value, and a temperature. The cell temperature is specified in the TMP free-gas thermal temperature card. Cell temperature is needed to properly sample the velocity of target nuclei that is important for many physics effects, and to modify elastic scattering cross sections. Track length tallies, such as fission heating, can be defined for cells to obtain 3D reaction rate distributions.
- Surface cards: general three-dimensional surfaces used to define MCNP5 cells. Surface cards can also be ignored by the actual problem's geometry cells and used solely for creating tally surfaces to obtain flux distributions.
- Data cards: contains material information such as isotopic compositions and cross section libraries, the type of particles to be transported, and whether the problem is a source or criticality problem. This section contains user specified source information, tally specifications, the total number of neutron batches, and the number of neutrons per batch. Options to include special physics and a variety of other data can also be in this section. There is a special mesh tally data card for obtaining spatial tally distributions.

MCNP5's mesh tally capability provides another option for calculating reaction rate distributions, besides tallying by cells or surfaces. Mesh tallies superimpose a mesh over the problem that need not correspond to the actual problem geometry in order to calculate spatially distributed data.

Blank lines serve as delimiters between these three main sections, and each line record is limited to 80 characters. Chapter 5, Chapter 6, and Appendix A contain examples of MCNP5 input files.

To calculate fission heating in the fuel, MCNP5 has a fission energy deposition tally labeled the F7:N tally. It computes cell fission heating in units of MeV/g. The F7:N tally includes local photon heating in the fuel, because energy from prompt fission photons are deposited locally [4]. The F7:N tally is equivalent to a F4:N track length flux estimator tally multiplied by an energy multiplier on the FM card. The F7:N tally is a track length tally that calculates the quantity

$$H_{\mathrm{f}} = \frac{\rho_{\mathrm{a}}}{m}\, Q \int dE \int dt \int d^3r \int d\boldsymbol{\Omega}\, \sigma_{\mathrm{f}}(E)\psi(\boldsymbol{r}, E, \boldsymbol{\Omega}, t). \tag{3.12}$$

In this expression, H_{f} is the cell's deposited fission energy (MeV/g), ρ_{a} is the atom density (atoms/barn-cm), m is the mass of the cell (g), Q is the fission heating Q-value (MeV), and $\sigma_{\mathrm{f}}(E)$ is the microscopic fission cross section (barns). MCNP5 tallies for criticality problems are normalized to "per fission neutron created" [4].

3.3. MAKXSF

The integrated MULTINUKE solver developed in this thesis makes use of temperature dependent cross section libraries pre-generated by MAKXSF and stored into discrete temperature bins. The temperature for each fuel and moderator cell in the MCNP5 input file is calculated by STAR-CCM+, and is listed on each cell data card by the TMP entry. MCNP5 uses temperatures in the TMP entry for each cell to modify elastic scattering cross sections. However, temperatures listed on the TMP entries have no effect on absorption cross sections or thermal scattering data. For more accurate temperature dependent data, an external cross section code such as NJOY [10] or MAKXSF was necessary. Hence, the MULTINUKE Perl script is written to take cell temperatures from STAR-CCM+ and modify the cells in the MCNP5 input file to use the material numbers with the appropriate data libraries. The MCNP5 input file contains a number of material numbers for each material (fuel, clad, water) with references to cross section data ZAIDs at different temperature bins [19].

MAKXSF is capable of altering data file formats, copying and moving data libraries, and creating nuclide datasets at new temperatures. MAKXSF generates temperature dependent libraries by using Doppler-broadened resolved resonance data, interpolating unresolved resonance probability tables, and interpolating *S(α,β)* thermal scattering kernel data. In order to modify cross section data to a new temperature, MAKXSF requires two existing cross section datasets (such as those available in the ENDF/B-VII.0 cross section library). One cross section dataset must be at a temperature *less* than desired new temperature, and the second dataset must be at a temperature *greater* than the new temperature. MAKXSF has an input file called *specs*. The commands to modify cross section datasets to new temperatures are listed in the *specs* input file. The command to modify an existing cross section dataset to a new temperature is given by:

$$ZAID_{new} \quad T_{new} \quad ZAID_{low} \quad ZAID_{high}.$$

Here, $ZAID_{new}$ is the *ZAID* identifier for the new cross section dataset and T_{new} is the new temperature. $ZAID_{low}$ is the existing cross section dataset at a temperature less than T_{new}, and $ZAID_{high}$ is the existing cross section dataset at a temperature greater than T_{new}. Every *ZAID* in the command must be for the same isotope; thus, the atomic number *Z* and the mass number *A* are the same [19]. For example, the command to generate a new U-235 dataset (*Z* = 92, *A* = 235) at a temperature of 625 K is given by:

```
92235.01c  625.00   92235.71c   92235.73c
```

In this command, `92235.01c` is the new U-235 *ZAID* at the new temperature of 625 K. The *ZAID* given by `92235.71c` designates the cross section dataset for U-235 at 600 K (less than 625 K) from the ENDF/B-VII.0 library. The *ZAID* given by `92235.73c` is the U-235 dataset at 1200 K (greater than 625) from ENDF/B-VII.0. The complete *specs* input file used in this thesis is given in Appendix A.3.

When MAKXSF is executed, it creates and stores the new cross section datasets into a new cross section library. In the process, MAKXSF creates a new XSDIR directory file, which MCNP5 uses to locate the newly created cross section data [19].

Chapter 4. Overview of Computational Fluid Dynamics

Energy is extracted from a reactor by transferring the heat generated by nuclear reactions to a working fluid. Modeling the coolant behavior in a PWR requires the solution to mass, momentum, and energy transport equations. In fact, nuclear reactor power output is usually determined by thermal limitations of reactor materials and coolant. This chapter gives an overview on the theory of computational fluid dynamics and its use for calculating the thermal-hydraulic conditions in a PWR. Computational fluid dynamics is a state of the art method for solving the Navier-Stokes equations in complicated 3D geometries. Prior to CFD, simple thermal-hydraulic simulations for reactors were generally one-dimensional and used empirical correlations.

The state of the art code, STAR-CCM+, is used in this thesis for the CFD component of MULTINUKE. A description of the capabilities and features of the STAR-CCM+ CFD code follows the discussion of the theoretical basis of CFD codes. Compared to the options for modeling neutron transport, there are many approaches to representing fluid flow and heat transfer, and there are many commercially available CFD codes. Therefore, the discussion in this chapter will be limited to information relevant to STAR-CCM+ and its coupling to MCNP5 for applications involving steady state, turbulent, incompressible flow typical of PWRs. The governing equations for PWR thermal-hydraulics are presented in their most basic form in order to illustrate the computational challenge of using high-fidelity methods, such as CFD, for the analysis of PWR thermal-hydraulics. Although MULTINUKE currently only analyzes steady state models, the time dependence in the governing equations is retained to fully demonstrate the complexity of the theory behind PWR thermal-hydraulics.

4.1. Theory

Heat transfer and fluid flow in a nuclear reactor core are difficult to simulate due to the nature of fluid dynamics phenomena and the geometries involved. The Reynolds number of turbulent flow in a typical coolant channel ranges from 10,000 to 100,000 [17]. Traditional thermal-hydraulic methods, especially with neutronic coupling, usually are based on simplified one-dimensional treatments that rely heavily on empirical correlations. Simple thermal-hydraulic methods use one-dimensional coolant channels divided into relatively large nodes or control volumes. Mass, momentum, and energy are conserved over each of these large size cells. To model an entire PWR core, such simple thermal-hydraulic methods are applied to a number of representative coolant channels, all with unique axial power distributions determined using a neutronic code. The resulting temperature and density profiles are then input back into the neutronics solver, with updated cross sections, and the process is repeated iteratively until a converged solution is obtained [5, 6, 7]. These simple thermal-hydraulic methods only yield information averaged over the cross section of the fuel assembly.

Computational fluid dynamics is a state of the art method for thermal-hydraulics analysis. For reactor analysis, it entails discretizing and solving the Navier-Stokes equations over the domain of the reactor. The geometric domain is discretized into a mesh, and the conservation equations are solved using finite difference, finite element, or finite volume discretization methods. In a direct numerical solution (DNS), the Navier-Stokes equations are solved without the use of any turbulence modeling assumptions; hence, the spatial scale of the computational mesh must be fine enough to capture the scales of turbulence effects. A direct numerical solution for reactor applications is a daunting task, even with modern petascale computing. It involves solving for ~10^{16} unknowns in the governing equations for a time-independent solution, a more formidable task than deterministic neutronics (10^{15} unknowns) [2]. Fluid flow in nuclear reactors is highly turbulent. Turbulence modeling and the nonlinear nature of the momentum transport equation make the modeling of reactor thermal-hydraulics a challenge. In BWRs, science-based descriptions of critical heat flux and two-phase flow are difficult, and empirical correlations have traditionally been used to model such processes [17].

The governing mass and momentum equations for single-phase flow are given respectively by

$$\frac{1}{\rho}\frac{D\rho}{Dt} + \boldsymbol{\nabla}\cdot\boldsymbol{u} = 0, \tag{4.1}$$

$$\rho\frac{D\boldsymbol{u}}{Dt} = \rho\mathbf{F} + \boldsymbol{\nabla}\cdot\boldsymbol{\sigma}. \tag{4.2}$$

In the momentum equation (4.2), the term $\frac{D\boldsymbol{u}}{Dt} = \frac{\partial \boldsymbol{u}}{\partial t} + \boldsymbol{u} \cdot \boldsymbol{\nabla u}$ gives rise to the nonlinear nature of the Navier-Stokes equations, and is a source of some of the computational challenge of PWR thermal-hydraulics [20]. In these equations, $\boldsymbol{u}$ is velocity, ρ is density, $\mathbf{F}$ is the body force per unit of fluid mass, and $\boldsymbol{\sigma}$ is the stress tensor. For an incompressible Newtonian fluid, the Navier-Stokes equations are [21]:

$$\boldsymbol{\nabla} \cdot \boldsymbol{u} = 0 \tag{4.3}$$

$$\rho \left(\frac{\partial \boldsymbol{u}}{\partial t} + \boldsymbol{u} \cdot \boldsymbol{\nabla u} \right) = \rho \mathbf{F} - \boldsymbol{\nabla} \mathrm{p} + \mu \boldsymbol{\nabla}^2 \boldsymbol{u} \tag{4.4}$$

$$\rho c_{\mathrm{p}} \left(\frac{\partial T}{\partial t} + \boldsymbol{u} \cdot \boldsymbol{\nabla} T \right) = \boldsymbol{\nabla} \cdot (k \boldsymbol{\nabla} T) + q''' + \overline{\phi}. \tag{4.5}$$

The time derivatives vanish for the steady state applications studied in this thesis. In these equations, T is temperature, p is pressure, c_{p} is the specific heat capacity at constant pressure, k is thermal conductivity, q''' is a volumetric heat source in the fluid (such as gamma or neutron heating), and $\overline{\phi}$ is the dissipation function. The energy equation above neglects any radiation heat fluxes. For general three-dimensional flows where the governing equations are coupled, an equation of state in the form $\rho = \rho(\mathrm{p}, T)$ must be specified for the fluid. The equation for heat conduction in the solid fuel and clad regions can be deduced from equation (4.5) and is given by

$$\rho c_{\mathrm{p}} \frac{\partial T}{\partial t} = \boldsymbol{\nabla} \cdot (k \boldsymbol{\nabla} T) + q'''. \tag{4.6}$$

In equation (4.6), q''' is a volumetric heat source such as fission heating in the fuel or neutron/gamma heating in the clad. In this thesis, q''' in the fuel region is one of the primary means of coupling STAR-CCM+ to MCNP5, because MCNP5 generates the volumetric fission heat source for STAR-CCM+. Neutron and gamma heating are neglected in the cladding, thus $q''' = 0$ for the clad region in this thesis.

As mentioned before, the discretization of the governing equations (4.3 - 4.6) over the domain of a PWR core results in ~10^{16} unknowns for a time-independent DNS. Therefore, turbulence models are necessary to reduce the computational burden of CFD for PWR applications, especially when CFD is coupled to Monte Carlo neutronics.

Turbulence modeling is a major challenge, including for PWR thermal-hydraulics. A variety of turbulence models have been developed for modern CFD methods. Higher fidelity turbulence models are generally more computationally expensive, since they must use smaller scales to capture the fine scale effects of turbulence. Usually requiring lower computational expense, the Reynolds-averaged Navier-Stokes (RANS) equations can describe the average effects of turbulence for complex geometries, where closure is given by models such as k-ε or k-ω models. A superior method to RANS is the large-eddy simulation (LES) method, where only large-scale turbulence is solved for explicitly, while the effect of small-scale eddies is modeled. However, the higher computational costs of large-eddy simulations can limit their application to simple geometries. Hybrid methods (combining features of RANS and LES), such as the detached-eddy simulation (DES) model, provide more accurate results than RANS methods while being computationally quicker than LES methods. LES and DES models require the use of a computational grid of sufficient resolution, and their higher accuracy solutions should justify their slower computation times. The second-order closure model, the Reynolds Stress Transport model (RST or RSM), is a RANS method that directly computes Reynolds stresses instead of the eddy viscosity approach. RST models are quite accurate but computationally slow [22].

4.2. STAR-DESIGN

STAR-DESIGN is a utility program included with STAR-CCM+ to facilitate CFD geometry creation, meshing, and solution. It is intended to assist new users in getting started with using STAR-CCM+. For this thesis, STAR-DESIGN was primarily used for its CAD abilities. Different regions of a geometric model, such as fuel, clad, and coolant are created separately in STAR-DESIGN. STAR-CCM+ imports the STAR-DESIGN geometries, and generates the computational grid (a STAR-CCM+ volumetric mesh). The STAR-DESIGN GUI is capable of meshing and executing the STAR-CCM+ solver, but with less functionality than the main STAR-CCM+ GUI. Since STAR-DESIGN is primarily a CAD code intended to assist a new user in learning STAR-CCM+, the user has less control over mesh options and physics modeling [22].

4.3. STAR-CCM+

STAR-CCM+ is the thermal-hydraulic component of the MULTINUKE integrated solver. STAR-CCM+ is a commercially available computational fluid dynamics code developed by CD-adapco. It features an elaborate graphical user interface to facilitate model creation, meshing, solver execution, and post-processing of data. STAR-CCM+ has a macro feature that records user GUI actions and automatically creates a Java-based file to reproduce the steps. This feature is used to run STAR-CCM+ without the GUI (in batch mode), and to assist with data input/output for repeated runs. For coupled physics with MCNP5, the *external-data-table* feature is used to input the volumetric fission heating rate into STAR-CCM+ (in W/m^3). This heat source, called an energy source in STAR-CCM+, is a text data file that lists fission heat generation rate at each MCNP5 cell centroid. With support from Java macros, STAR-CCM+ automatically reads in each centroid coordinate (x, y, z) and the volumetric heat source (calculated using MCNP5), and applies the data to the nearest STAR-CCM+ fuel cell. The energy source from MCNP5 could also have been linked to STAR-CCM+ by user code, available in C and FORTRAN languages [22].

STAR-CCM+ models fluid flow and heat transfer, as well as heat transfer in solids, in complex three-dimensional geometries. It solves the Navier-Stokes equations discretized using the finite-volume approach for steady state and time-dependent problems. STAR-CCM+ can represent solid, liquid, gaseous, and porous media. Porous media models are especially useful for representing spacers and flow mixers in nuclear fuel assemblies when full geometric models of such structures are not required. Heat may be transferred via conduction, radiation, and convection. STAR-CCM+ models both single and multi-phase flow, with the ability to model boiling and cavitation phase changes. The code can solve the governing equations simultaneously (coupled), or in a segregated fashion more appropriate for simpler incompressible and isothermal flows. The coupled flow solver is more rigorous and accurate, and it can employ either implicit integration or explicit integration using a Runge-Kutta multi-stage scheme [22].

Surface and volume meshes can be created using STAR-CCM+, or imported from other software in a variety of formats. Meshing in STAR-CCM+ is highly automated, but allows substantial user control if desired. The overall resolution of a finite-volume mesh is user controlled. Mesh cells can be manipulated by scaling, translating, rotating, splitting, combining, or deleting. The *surface remesher* and *surface wrapper* can improve a surface mesh for a better finite-volume grid. STAR-CCM+ can generate tetrahedral, polyhedral, and trimmed (hexahedral) meshes. Prism layers of mesh cells can be included for modeling heat transfer and turbulence at important surfaces. STAR-CCM+ also features automatic tools for checking the quality and validity of a volume mesh [22].

STAR-CCM+ features a host of turbulence models – the most complex and slow being the Reynolds stress transport model [22]. Some of the available turbulence models include:

- Models that provide closure to the Reynolds-averaged Navier-Stokes (RANS) equations
    - k-epsilon (k-ε)
    - k-omega (k-ω)
    - Reynolds stress transport model (RST/RSM)
- Large-eddy simulation (LES)
- Detached-eddy simulation (DES)
- Wall treatments

Chapter 5. MULTINUKE Solver

MULTINUKE is an integrated set of computer codes. Developed as part of this thesis, it automates the coupling of neutronic and thermal-hydraulic solutions for steady state PWR simulations. It is comprised of MCNP5, STAR-CCM+, a master Perl script, and Fortan90 and Java data management programs. MULTINUKE needs cross section data pre-generated using NJOY or MAKXSF in order to include fully temperature dependent neutronics. The code runs serially or in parallel mode, since both MCNP5 and STAR-CCM+ have built-in parallel capabilities. The techniques and procedures implemented in MULTINUKE for PWR thermal feedback calculations are described in Section 5.1. Next, the manual preparations required to use MULTINUKE are described in Section 5.2. This includes MCNP5 and STAR-CCM+ model creation, mesh interpolation, and input file formats.

5.1. MULTINUKE Automated Solver

5.1.1. MULTINUKE Perl Script Processes

MULTINUKE automatically executes MCNP5 and STAR-CCM+ in a cyclical fashion, exchanging data through ASCII data files. Figure 1 illustrates the order of the primary MULTINUKE procedures. To begin the process, MULTINUKE reads the *multiSpecs_base.txt* input file and the mesh correlation files (these files are described in Section 5.2.3 and Section 5.2.4). It then creates an isothermal MCNP5 input file, with initial cell temperatures at a user specified value, and runs an isothermal MCNP5 calculation that tallies an initial fission energy distribution. After each neutronic calculation, MULTINUKE calls the Fortran90 post-processor, GETHEAT, to extract and normalize tally data from the MCNP5 output file. GETHEAT creates the data file *Heat_n.xy* (*n* is the MULTINUKE iteration number) that contains centroid and heat source information for each cell. MULTINUKE also extracts the eigenvalue from the MCNP5 output file for monitoring convergence of the coupled solution. GETHEAT is described in detail in Section 5.1.2.

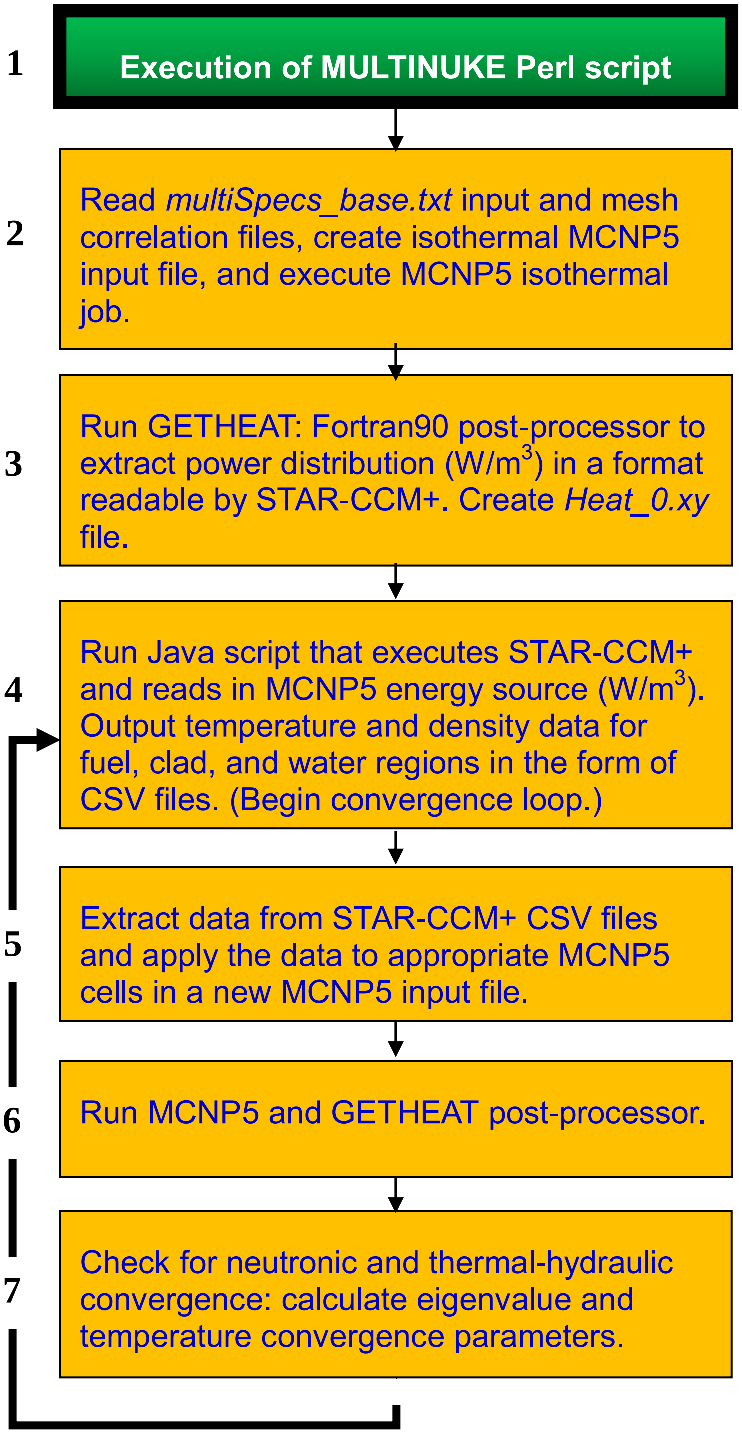
1
Execution of MULTINUKE Perl script
2
Read *multiSpecs_base.txt* input and mesh correlation files, create isothermal MCNP5 input file, and execute MCNP5 isothermal job.
3
Run GETHEAT: Fortran90 post-processor to extract power distribution (W/m^3) in a format readable by STAR-CCM+. Create *Heat_0.xy* file.
4
Run Java script that executes STAR-CCM+ and reads in MCNP5 energy source (W/m^3). Output temperature and density data for fuel, clad, and water regions in the form of CSV files. (Begin convergence loop.)
5
Extract data from STAR-CCM+ CSV files and apply the data to appropriate MCNP5 cells in a new MCNP5 input file.
6
Run MCNP5 and GETHEAT post-processor.
7
Check for neutronic and thermal-hydraulic convergence: calculate eigenvalue and temperature convergence parameters.

Files Created at Each Step
MCNP5 isothermal input file MCNP5 isothermal output file
Heat_0.xy
STARCCMfuel_out_n.csv STARCCMwater_out_n.csv STARCCMclad_out_n.csv
MCNP5 input file for iteration *n*
MCNP5 output file for iteration n Heat_n.xy
convergenceSummary.txt

Loop until convergence criteria are satisfied, or until maximum iteration count is reached.

Figure 1. MULTINUKE Solver Processes.

After the isothermal neutronic calculation, the solver enters a loop that terminates once the solution converges. The loop begins with MULTINUKE executing the STAR-CCM+ Java script. The Java script initiates the STAR-CCM+ simulation file by reading in the data from *Heat_n.xy* and applying the fission energy source to the fuel region of the model. STAR-CCM+ automatically allocates heat generation rate data from each MCNP5 cell to the appropriate STAR-CCM+ cell. This is accomplished by calculating the minimum distances between the MCNP5 centroids in the *Heat_n.xy* file and the centroids in the CFD simulation file. Finally, the Java script runs the CFD solver in STAR-CCM+ and generates output files in CSV format. These CSV files contain cell index, temperature, density, and centroid data for all cells in the STAR-CCM+ model. These CSV (output) files are named *STARCCMfuel_out_n.csv*, *STARCCMwater_out_n.csv*, and *STARCCMclad_out_n.csv* (*n* is the iteration number). After each STAR-CCM+ run, the Perl script in MULTINUKE calculates the average percent difference in cell temperatures between subsequent iterations. A description of the processes performed by the STAR-CCM+ Java script is given in Section 5.1.3, and development of the Java script is described in Section 5.1.2.

The MULTINUKE Perl script extracts the cell indices, temperature, density, and centroid information from STAR-CCM+ output files. With the cell indices related by the mesh correlation files, MULTINUKE creates a new MCNP5 input file. Each MCNP5 cell's material (and associated temperature dependent cross section libraries), temperature, and density (if moderator) are updated by the Perl script during the creation of each new MCNP5 input file. Once again, MULTINUKE executes MCNP5 and then the GETHEAT post-processor. The process of alternating between CFD and neutronic solutions is repeated until the eigenvalue and temperature distributions converge. Figure 2 provides a simple illustration that summarizes MULTINUKE's data exchange process and the various programs involved. The Perl source code can be found in Appendix B.1.

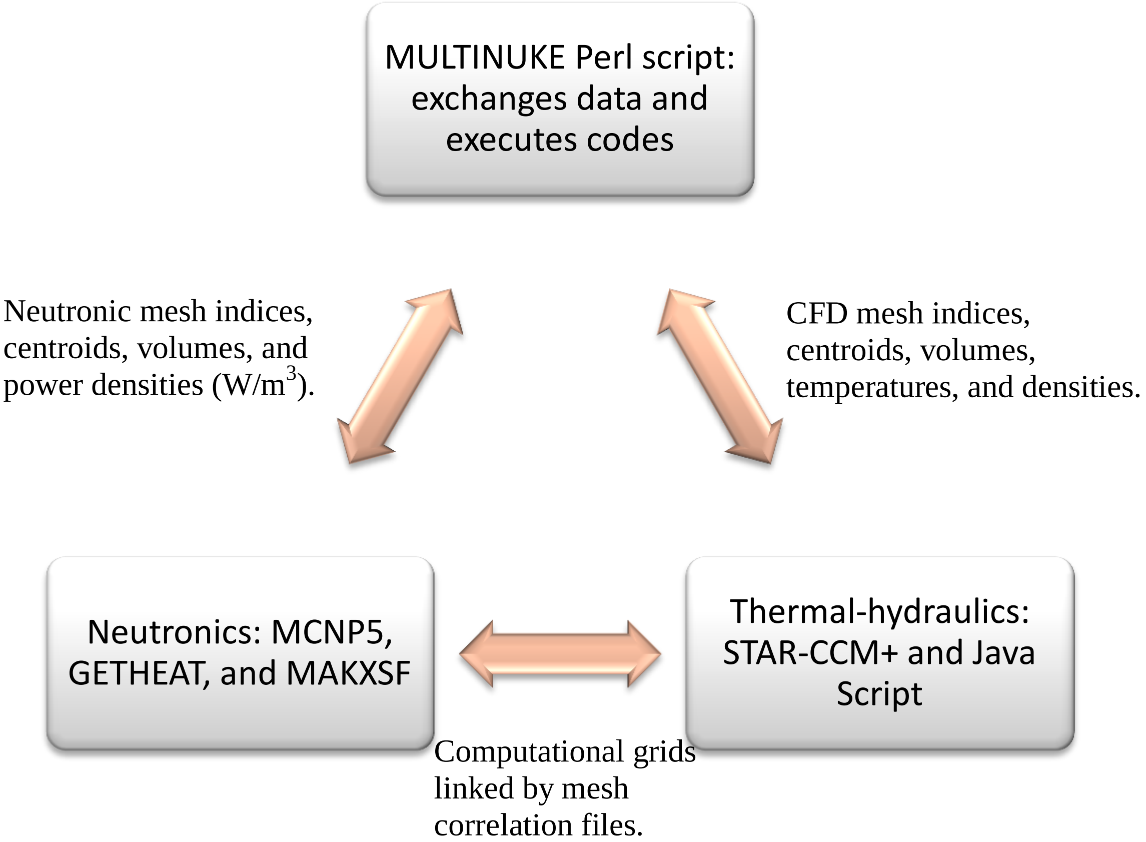
MULTINUKE Perl script: exchanges data and executes codes
Neutronic mesh indices, centroids, volumes, and power densities (W/m3).
CFD mesh indices, centroids, volumes, temperatures, and densities.
Neutronics: MCNP5, GETHEAT, and MAKXSF
Thermal-hydraulics: STAR-CCM+ and Java Script
Computational grids linked by mesh correlation files.

Figure 2. MULTINUKE Programs and Data Exchange.

5.1.2. GETHEAT – MCNP5 Post Processor Calculations

After each neutronic calculation, MULTINUKE runs the MCNP5 post-processing code GETHEAT. This Fortran90 program reads *multiSpecs_base.txt* to get the name of the MCNP5 input file, and to obtain information necessary for converting MCNP5 tally data into a STAR-CCM+ heat source (in W/m^3). MCNP5 normalizes tallies in criticality mode by the fission neutrons generated, and the F7:N heat deposition tally is in unit of MeV/g. Therefore, GETHEAT calculates a constant multiplier that is applied to F7:N tally data to obtain the heat generation rate in units of W/m^3. The multiplier depends on the number of neutrons released per fission, power level, and k_{eff}. The number of neutrons released per fission (ν) and k_{eff} vary with each MCNP5 iteration in a single MULTINUKE run, thus the tally multiplier is updated after each MCNP5 execution. GETHEAT extracts k_{eff}, ν, and tally data from the MCNP5 output file. The equation for calculating fission energy in correct STAR-CCM+ units is given by [4, 24, 25]:

$$H_{\mathrm{f}}\left[\frac{W}{m^3}\right] = \frac{P\,\nu}{\left(1.602x10^{-13}\frac{J}{MeV}\right) Q\, k_{eff}}\; H_{\mathrm{f}}[MCNP5]\, \rho_f \left(10^6\, \frac{cm^3}{m^3}\right)\left(1.602x10^{-13}\, \frac{J}{MeV}\right). \quad (5.1)$$

In equation (5.1), $H_{\mathrm{f}}\left[\frac{W}{m^3}\right]$ is the real fission power density deposited in each fuel cell, and $H_{\mathrm{f}}[MCNP5]$ is the normalized tally data directly from the MCNP5 output file. P is the system's power level in Watts, ν is the average number of neutrons released per fission, Q is the energy released per fission (MeV), and ρ_f is the fuel density (g/cm^3). This equation accounts for MCNP5 tally normalization and converts the resulting MeV/g data into W/m^3 data. $H_{\mathrm{f}}\left[\frac{W}{m^3}\right]$ is the quantity printed out for each cell in the *Heat_n.xy* data file. Appendix B.2 contains the source code of GETHEAT.

5.1.3. STAR-CCM+ Java Script

The STAR-CCM+ Java script, *loadHeat_runStarJob_base.java*, is edited by the MULTINUKE Perl script before each thermal-hydraulic calculation. With the working directory and current iteration number obtained from the MULTINUKE Perl script, the Java script loads the *Heat_n.xy* file and applies the fission power density to the fuel region in the CFD model, executes the STAR-CCM+ solver, and writes thermal-hydraulic results in files in CSV format for the subsequent neutronic calculation. The Java script also allows STAR-CCM+ to be run without using the graphical user interface (batch mode). MULTINUKE and the Java script do not modify the STAR-CCM+ base simulation file. Each CFD run uses the same base simulation file and saves the results in a new file indexed by the iteration number. Manual preparation of the Java script is described in Section 5.2.2. Appendix B.3 contains the source code of the STAR-CCM+ Java script.

5.2. Solver Preparation

Although MULTINUKE automatically exchanges heat generation rate, temperature, and density data, the code requires some manual preparation. Before the MULTINUKE is executed, MAKXSF pre-generates tables of temperature dependent neutron transport data, including thermal *S(α,β)* tables, over a temperature range appropriate for PWR temperatures. Likewise, STAR-CCM+ and MCNP5 models prepared for MULTINUKE contain specific facets for neutronic–thermal-hydraulic coupling. Finally, input files used by MULTINUKE are to be prepared to simulate the desired PWR model.

5.2.1. MCNP5 Input File Preparations

In order for MULTINUKE to couple MCNP5 to STAR-CCM+, the fuel and moderator regions described in the MCNP5 input file need to be divided into small cells that correspond to the CFD mesh. Additionally, each cell card in the input file needs to be specifically formatted so that MULTINUKE can modify the neutronic model with updated thermal-hydraulic data. The MULTINUKE Perl script requires that the MCNP5 input file contain unique "dummy" character string designators in cell data cards (where there would normally be real data), so that it may locate and edit the material, temperature, and density (if H_2O) of each cell. This necessitates the creation of an MCNP5 "base" input file, which is an actual MCNP5 input file with cell data replaced with character strings. When the MULTINUKE Perl script is executed, it locates and replaces the character strings in the base input file with appropriate data, and creates a *real* MCNP5 input file for the next neutronic iteration. Specifically, MULTINUKE looks for "f_####" for fuel material numbers, "ft####" for fuel temperatures, "w_####" for moderator material numbers, "wden_####" for moderator densities, "wt####" for moderator temperatures, "mclad" for clad material number, and "cladt" for cladding temperature (#### is a 4 digit cell index). Below, Figure 3 shows examples of base input data for fuel, water, and clad cells. Note that solid material densities (fuel and clad) are assumed to be constant. The cell data in the base input file must fit within the 80-column MCNP5 limit.

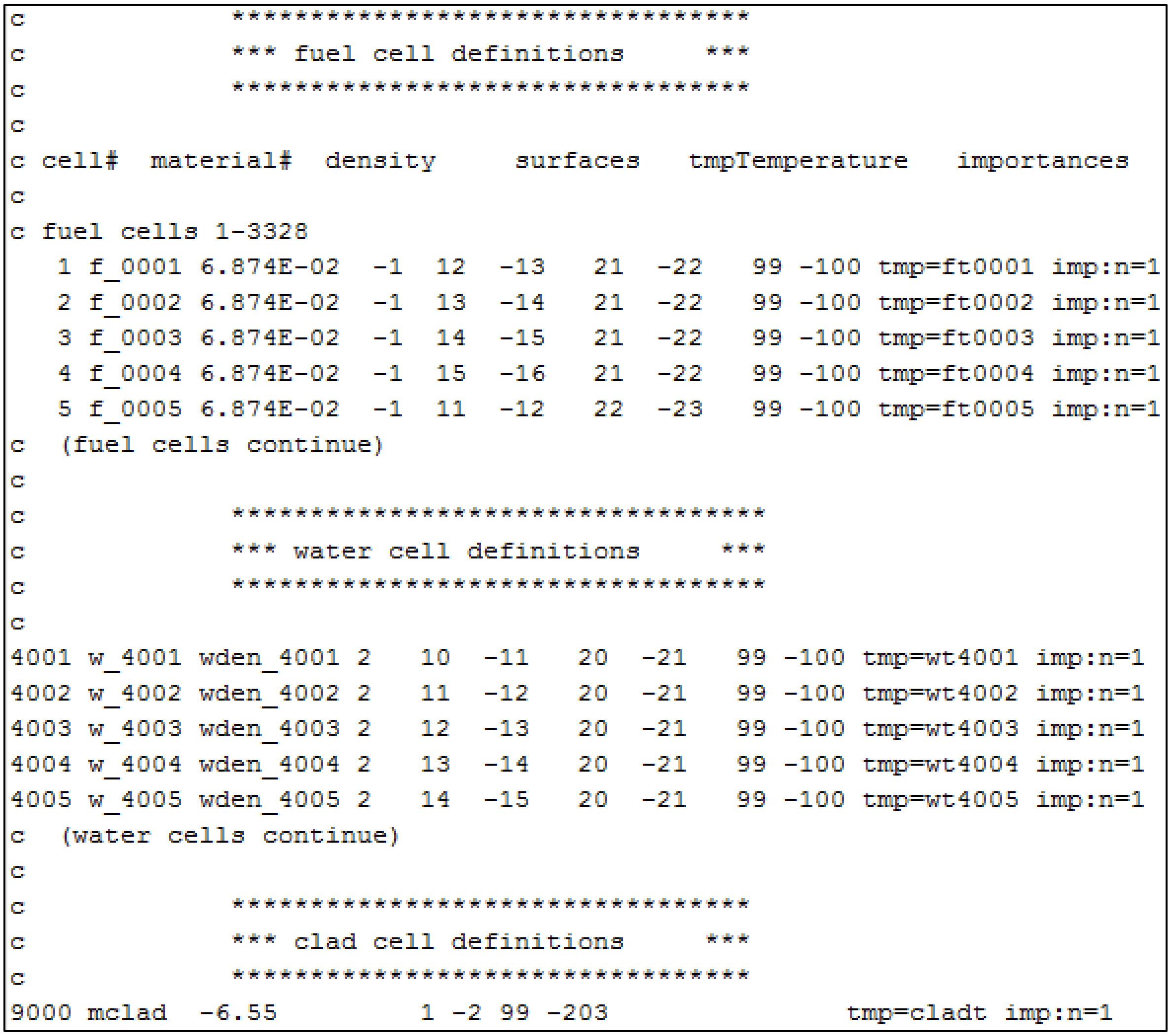

```
c             *********************************
c             *** fuel cell definitions     ***
c             *********************************
c
c cell#  material#  density     surfaces   tmpTemperature   importances
c
c fuel cells 1-3328
   1 f_0001 6.874E-02  -1  12  -13   21  -22   99 -100 tmp=ft0001 imp:n=1
   2 f_0002 6.874E-02  -1  13  -14   21  -22   99 -100 tmp=ft0002 imp:n=1
   3 f_0003 6.874E-02  -1  14  -15   21  -22   99 -100 tmp=ft0003 imp:n=1
   4 f_0004 6.874E-02  -1  15  -16   21  -22   99 -100 tmp=ft0004 imp:n=1
   5 f_0005 6.874E-02  -1  11  -12   22  -23   99 -100 tmp=ft0005 imp:n=1
c  (fuel cells continue)
c
c             **********************************
c             *** water cell definitions     ***
c             **********************************
c
4001 w_4001 wden_4001 2   10  -11   20  -21   99 -100 tmp=wt4001 imp:n=1
4002 w_4002 wden_4002 2   11  -12   20  -21   99 -100 tmp=wt4002 imp:n=1
4003 w_4003 wden_4003 2   12  -13   20  -21   99 -100 tmp=wt4003 imp:n=1
4004 w_4004 wden_4004 2   13  -14   20  -21   99 -100 tmp=wt4004 imp:n=1
4005 w_4005 wden_4005 2   14  -15   20  -21   99 -100 tmp=wt4005 imp:n=1
c  (water cells continue)
c
c             *********************************
c             *** clad cell definitions     ***
c             *********************************
9000 mclad  -6.55         1 -2 99 -203               tmp=cladt imp:n=1
```

Figure 3. Sample MCNP5 Base Input File Excerpt.

MCNP5 input files are developed to represent an accurate model of a PWR core at steady state conditions. Currently, MULTINUKE is intended to only analyze steady state PWR problems. [However, MULTINUKE can be used to analyze any nuclear reactor with a single-phase coolant, such as liquid metal cooled reactors with fast neutron spectra. Only the cross section database would require significant alteration.] In order to tally reaction distributions and exchange data with STAR-CCM+, the fuel and moderator regions of the model are divided into several smaller cells, corresponding to mesh cells in the CFD grid. The cladding regions of the model may also be built of many small cells, but the cladding temperature distribution is not as significant as fuel and moderator temperatures for thermal feedback. There is essentially no limit to the size of the model – it could range from a single pin to an entire core. Computer limitations determine the maximum size of the MCNP5 model.

Fission heat generation rate, or flux modified to calculate fission heating, is tallied over MCNP5 cells. By tallying over several cells, MULTINUKE calculates reaction rate distributions from MCNP5 output files. Tallying by cells allows MCNP5 to store heat generation rate, temperature, and density (if a moderator cell) data for each cell that corresponds to its equivalent cell in the CFD mesh, thereby facilitating code coupling. In MCNP5, heat generation rate is most easily calculated using the F7:N fission energy deposition tally. The F7:N tally may require the cell masses to be listed on tally data cards (SD cards) in the MCNP5 input file, because MCNP5 does not automatically calculate masses for asymmetric cells. The F7:N tally computes fission heating in units of MeV/g. Hence, the tallied heating value must be converted to STAR-CCM+ energy source units (W/m^3). The details have already been described in Section 5.1.2.

There should be a list of reactor material numbers in the data card section of the MCNP5 input file containing references to the pre-generated data libraries. Each material number corresponds to a particular reactor material at a certain temperature. Therefore, each reactor material (UO_2, Zirc, and H_2O) will have several material numbers referencing cross section library ZAIDs generated at different temperatures.

5.2.2. STAR-CCM+ Model Preparations

MULTINUKE requires an appropriate CFD model of the core (or part of the core) of a pressurized water reactor. The CFD mesh needs to be sufficiently fine for accurate fluid flow and heat transfer simulation, while being simple enough to "link" with MCNP5 geometry cells. This means that complex, unstructured polyhedral meshes are not appropriate for use with MULTINUKE without additional processing of mesh data. Complex CFD meshes that lack axial symmetry (with cells at various orientations) are very difficult to model in MCNP5. Therefore, the STAR-CCM+ model should use a relatively simple mesh – most importantly one that is axially uniform (meaning each axial segment has the same radial mesh structure). When there is a pattern to the mesh structure, simple scripts or programs can create MCNP5 cell input, even when there are several thousand cells. The two meshes should have cells with very similar volumes and centroids to allow for accurate data exchange. Without simple meshes and the automated creation of MCNP5 input files, the grid used for MCNP5 tallies would need to be axially simplified, as was done in the work of Seker et al. with McSTAR [11].

Mesh compatibility and transfer of data from one code to another are long recognized to be some of the most challenging steps in externally linked multi-physics problems. Current work linking MCNP5 and STARCCM+ is based on the premise that the meshes are simple and compatible. An additional layer of code between MCNP5 and STARCCM+ that interpolates and averages data from the mesh in one code, to be suitably used by a very different mesh in the other code, will allow significantly different meshes to be used by the two codes. However, this is expected to add a significant computational cost.

Once a simple mesh is in place for a PWR core model, the macro feature in the STAR-CCM+ GUI can be used to record a Java macro that performs the following actions:

1. Read in the MCNP5 heating data in the form of an external data table, and apply it to the fuel region as an energy source term. STAR-CCM+ software can automatically assign each MCNP5 cell's heating value to the appropriate CFD mesh cell, since the heating data file (*Heat_n.xy*) contains the centroid coordinates of each MCNP5 cell. (This data exchange should be accurate if the MCNP5 and STAR-CCM+ meshes are identical, or very similar.)
2. Execute the STAR-CCM+ solver for a sufficient number of CFD iterations (typically 3000-4000 for small PWR problems presented in this thesis).
3. Output the temperature and density of each cell, along with CFD mesh cell index and centroid coordinates.

After STAR-CCM+ creates the file for the Java macro, the absolute directories in the Java code are replaced with the character string "_WORKDIR_". This allows the Perl script to identify the location for the directory names and update the working directory name each time MULTINUKE is executed. As described in Section 5.1.1, the Perl script executes the Java macro in the convergence loop for each MULTINUKE iteration (see step 4 in Figure 1). The Perl script looks for the file called *loadHeat_runStarJob_base.java*; it updates the Java code in this file with the current working directory and iteration number for file management purposes.

Then, the Perl script creates a new Java macro file that is actually executed, labeled *loadHeat_runStarJob.java* (that has current directory and iteration number). Execution of the Java macro controls the data input, solver execution, and data output for STAR-CCM+.

5.2.3. Relating the MCNP5 and STAR-CCM+ Meshes

The creation of similar MCNP5 and STAR-CCM+ meshes is straightforward, given a simple enough grid structure. However, STAR-CCM+ does not index the mesh cells conveniently for automated MCNP5 input file creation. Thus, the neutronic and CFD meshes will typically be indexed differently. Relating the indices of the MCNP5 mesh to indices of the STAR-CCM+ mesh is a manual preparatory task of upmost importance.

A simple pattern for numbering the cells in the MCNP5 input file is therefore used to write scripts to produce large blocks of MCNP5 input deck, such as with Fortran "DO" loops. For the PWR cell models discussed in Chapter 6, the cell data in the MCNP5 input file is created using two "DO" loops in a very simple Fortran90 code. The MCNP5 cells are numbered (starting from cell number 1) left-to-right in the *x*-direction and bottom-to-top in the *y*-direction. After the cell input for an entire axial level is written, this cell-numbering scheme continues in the same fashion for the next axial node. The *x*, *y*, and *z* surfaces that bound the MCNP5 cells are also numbered in an appropriate (sequential) manner for writing large blocks of MCNP5 input using Fortran90 code. The cell-numbering scheme for the MCNP5 input file is apparent in Appendix A.1, which provides excerpts of the MCNP5 input file used for the single PWR cell simulation described in Chapter 6. The MCNP5 input file for the 3 x 3 PWR cell model is very similar, but substantially longer.

When the MULTINUKE Perl script is executed, it looks for the files *fuel_STARcell_equals_MCNPcell.txt* and *water_STARcell_equals_MCNPcell.txt*. These files are required for data coupling in MULTINUKE. The mesh correlation files are formatted as "STARcell# = MCNPcell#," as shown below in Figure 4. To find the relationship between the mesh indices, one can manually examine both mesh data and match each appropriate cell. Since this can be excessively time consuming for large meshes, a simple script or program can find the minimum distances between each cell in the two meshes. If the meshes are nearly identical, zero distance (or nearly zero) should separate the correct cell pairs between the meshes. The program can then generate the mesh correlation files with cells paired by minimum distance. In this thesis, the CFD and neutronic meshes for the PWR simulations (in Chapter 6) are correlated by a simple Fortran90 code that associates mesh cells by minimum distance.

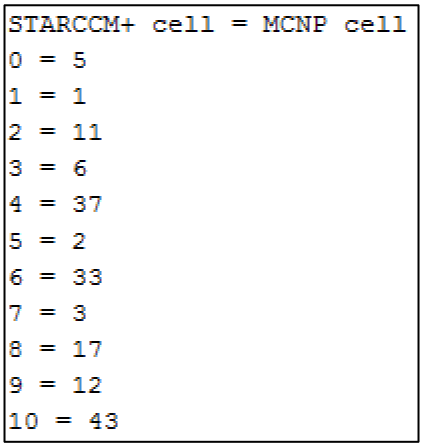

```
STARCCM+ cell = MCNP cell
0 = 5
1 = 1
2 = 11
3 = 6
4 = 37
5 = 2
6 = 33
7 = 3
8 = 17
9 = 12
10 = 43
```

Figure 4. Mesh Correlation File Format Excerpt.

5.2.4. MULTINUKE Input File

The primary MULTINUKE input file, called *multiSpecs_base.txt*, is edited prior to executing the coupled codes. The input file *multiSpecs_base.txt* contains the job name of the problem (the file name of the MCNP5 and STAR-CCM+ simulation files). It also specifies the nuclear fuel density (g/cm^3), power rating (Watts), energy released per fission event (MeV/fission), iteration convergence parameters, initial neutronic isothermal temperature (K), and the starting cell index of the moderator in the MCNP5 input file. MULTINUKE solutions are considered converged when MCNP5 k_{eff} values and STAR-CCM+ cell temperatures change less than a user-specified tolerance between two consecutive iterations. The *multiSpecs_base.txt* file contains data input for the eigenvalue tolerance, and another tolerance level for average percent difference for cell temperatures. The MULTINUKE code terminates when both convergence criteria are satisfied in two successive MCNP5–STAR-CCM+ iterations. Some editing of the MULTINUKE Perl script and data processing programs may be needed when simulating reactors that diverge significantly from the PWR models simulated in this thesis. Figure 5 shows sample input data in *multiSpecs_base.txt*. MULTINUKE extracts parameters for the model by searching for the keywords, which can be in any order, to the left of the equal sign. The program terminates if a keyword is missing or if the input file is incorrectly formatted. Table 1 describes the required input data in the *multiSpecs_base.txt* file.

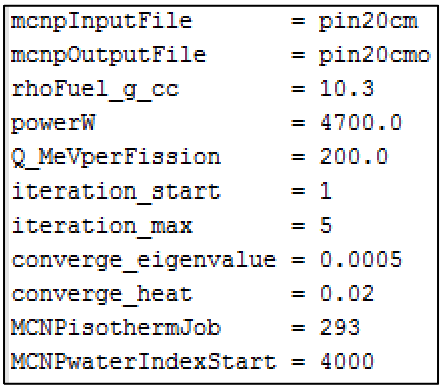

```
mcnpInputFile        = pin20cm
mcnpOutputFile       = pin20cmo
rhoFuel_g_cc         = 10.3
powerW               = 4700.0
Q_MeVperFission      = 200.0
iteration_start      = 1
iteration_max        = 5
converge_eigenvalue  = 0.0005
converge_heat        = 0.02
MCNPisothermJob      = 293
MCNPwaterIndexStart  = 4000
```

Figure 5. Sample *multiSpecs_base.txt* Input Data for MULTINUKE.

Table 1. Required MULTINUKE Inputs and Formats in *multiSpecs_base.txt*.

Keyword	**Type**	**Description**
mcnpInputFile	String	Files names of MCNP5 and STAR-CCM+ input files
mcnpOutputFile	String	MCNP5 output file name
rhoFuel_g_cc	Real	Nuclear fuel density (g/cm^3)
powerW	Real	Total thermal power produced in nuclear fuel
Q_MeVperFission	Real	Energy released per fission event (MeV)
iteration_start	Integer	Starting MULTINUKE iteration number – can be greater than 1 for restarts
iteration_max	Integer	Maximum permitted MULTINUKE iterations
converge_eigenvalue	Real	Eigenvalue convergence criterion (Δk)
converge_heat	Real	Temperature convergence criterion (% fraction)
MCNPisothermJob	Real	Temperature of isothermal MCNP5 calculation (K)
MCNPwaterIndexStart	Integer	Starting MCNP5 cell number for moderator cells (i.e. where fuel cells end and water cells begin)

Chapter 6. PWR Test Calculations

The MULTINUKE solver is applied to a single cell model and a 3 x 3 lattice model to investigate the steady state, coupled neutronics and thermal-hydraulics of a PWR representative cell. The PWR models are run on a 64 bit, quad core, Intel 2.8 GHz microprocessor with 1 GB RAM. The MCNP5 source code is compiled and a Linux MPI executable is generated for parallel neutronics. STAR-CCM+ is released fully capable of parallel processing, and is executed in parallel mode on the machine's four cores. The PWR models and the coupled nuclear and thermal-hydraulic results calculated using MULTINUKE are described below.

6.1. PWR Cell Model Description

The PWR cell model consists of a cylindrical fuel rod (fuel, cladding) surrounded by the coolant contained within boundaries in the *x* and *y* directions. With symmetric boundary conditions imposed in the *x* and *y* directions, the PWR cell model simulates a PWR core as an infinite array of identical fuel cells. However, the model is finite in the axial direction, allowing axial neutron leakage and coolant to flow in and out of the model. Figure 6 illustrates the single pin model. The purpose of the simple PWR cell model is twofold: to debug various functionalities of MULTINUKE using a problem that runs fast, and to calculate pseudo-realistic PWR conditions using coupled neutronics/thermal-hydraulic simulations. Although coupled, multi-physics reactor simulations are intended to analyze large complex models on massively parallel computing platforms, and MULTINUKE is envisioned for this purpose, the single cell model is meant to demonstrate the usage of MULTINUKE on a quad core machine. Therefore, the number of mesh cells in the model is held to a minimum by reducing the height of the model to 20 cm. This allows STAR-CCM+ to generate a simple prismatic hexahedral CFD mesh with only 9,984 computational cells, which consequently facilitates the creation of an equivalent neutronic mesh in MCNP5 (excluding the clad region that is lumped into one MCNP5 cell). All axial nodes have the same radial mesh structure.

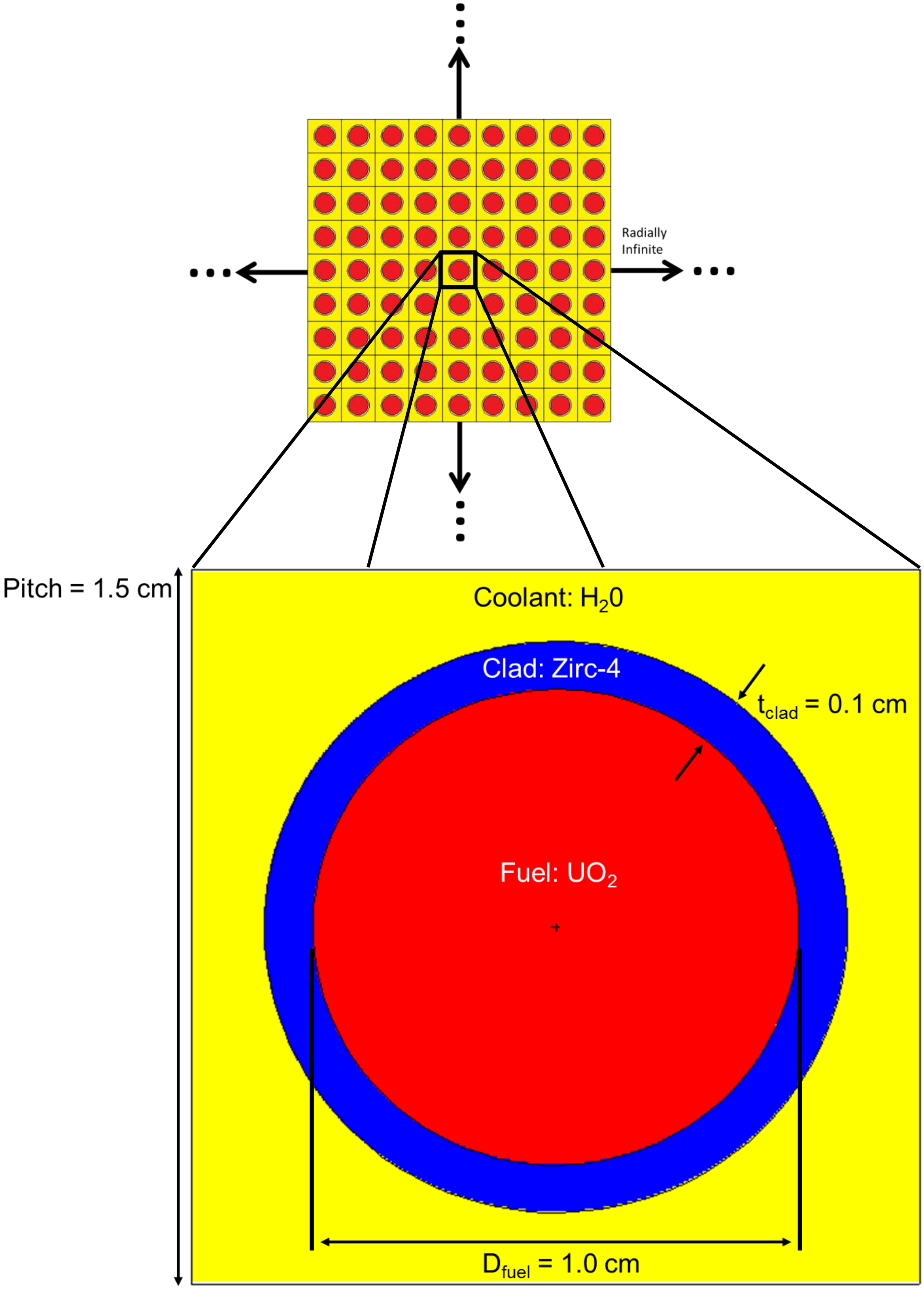

Figure 6. PWR Cell Model.

Table 2 contains important data for the PWR cell model, and subsequent mesh and simulation. The fuel diameter is 1.0 cm, and the outer clad diameter is 1.2 cm, resulting in a 0.1 cm cladding thickness with no fuel-clad gap modeled. The lattice has a pitch of 1.5 cm and an axial height of 20.0 cm. The nuclear fuel material is UO_2 with 5 w/o U-235 enrichment. Cladding is made of Zircaloy-4 and liquid water is the coolant and neutron moderator.

Table 2. PWR Cell Model Data.

Lattice Data	Value
Fuel Outer Diameter (cm)	1.0
Fuel Cladding Outer Diameter (cm)	1.2
Fuel Cladding Thickness (cm)	0.1
Fuel Rod Pitch (cm)	1.5
Axial Height (cm)	20.0
Fuel Material	UO_2
Fissile Material Enrichment	5 w/o U-235
Cladding Material	Zircaloy-4
Coolant/Moderator Material	Liquid H_2O
Mesh Data	**Value**
Mesh Type	Prismatic Hexahedral
Total STAR-CCM+ Cells	9,984
Number of Radial STAR-CCM+ Cells per Axial Node	96
Number of STAR-CCM+ Axial Nodes	104
Total MCNP5 Cells	7488 + 1 Clad Cell
Number of Radial MCNP5 Cells per Axial Node	72
Number of MCNP5 Axial Nodes	104
Number of MCNP5 Tally Regions (UO_2 Cells)	3328

6.1.1. Computational Grid

STAR-DESIGN is used to create CAD geometries of the fuel, clad, and coolant regions of the PWR cell model. These are then imported into STAR-CCM+, which is used to generate the volumetric computational mesh. The resolution of the mesh automatically generated by STAR-CCM+ is determined by the surface mesh and the size of the model. For a long and slender CFD geometry, such as a lattice cell, the axial length determines the mesh size since it is the longest dimension of the model. To generate the surface mesh, the surface mesh size is specified to be 1% of the axial length. With the surface mesh generated, STAR-CCM+ automatically creates the volumetric mesh where base computational cell size is specified to be 1% of the length of the model. A 3D view of the surface mesh used to create the volume mesh is shown in Figure 7.

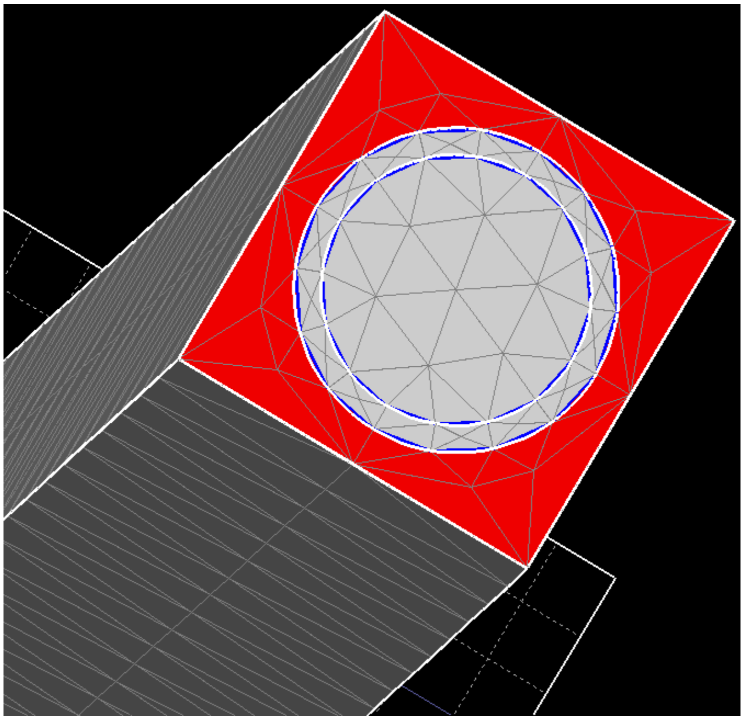

Figure 7. CFD Surface Mesh for Single PWR Cell.

An axially uniform mesh is desired to facilitate coupling with the neutronics mesh; thus, a prismatic hexahedral CFD mesh is generated using the “trimmer” mesh model option in STAR-CCM+. The trimmer option can generate better quality meshes than the STAR-CCM+ tetrahedral mesher, needing five to eight times less number of cells for the same accuracy [22]. Trimmed meshes also lead to better quality volumetric meshes than the polyhedral mesh model when the surface mesh is low quality. A summary of mesh data for the PWR cell model is given in Table 2. The model has 96 radial CFD cells per axial node, with 104 axial nodes, resulting in 9,984 CFD computational cells. An equivalent neutronic grid is created in MCNP5 with help from a simple Fortran90 program. The MCNP5 computational cells have almost identical centroids and volumes compared to the STAR-CCM+ cells, except for the clad region that is reduced to one cell in the MCNP5 input file. The cladding temperature for MCNP5 is calculated as the volume weighted average of the STAR-CCM+ clad cells’ temperatures. The MCNP5 model has 7,489 computational cells, including 3,328 tallied fuel cells. Figure 8 and Figure 9 depict the STAR-CCM+ mesh and MCNP5 mesh, respectively. The upper-right quadrant of the coolant mesh is numbered for the results presented in Section 6.2.8 (see Figure 28).

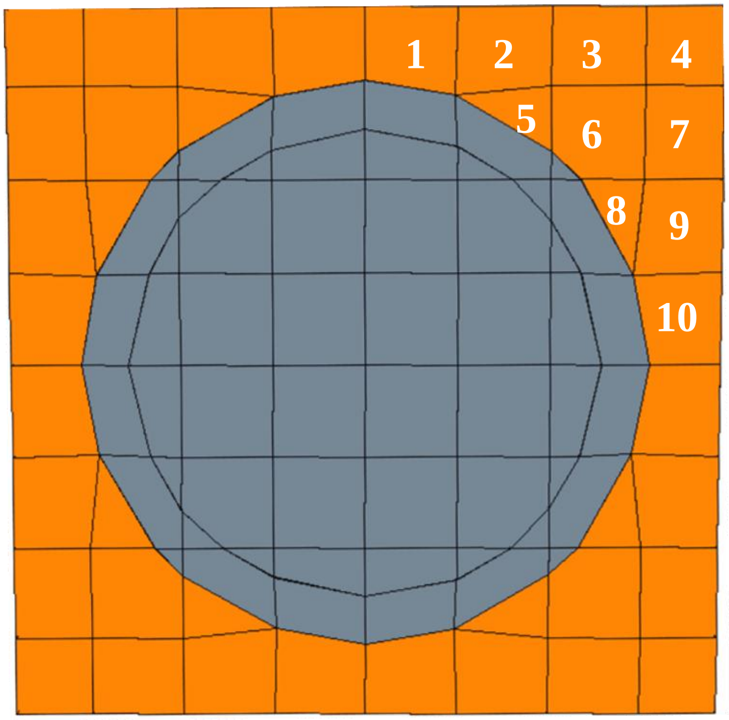

Figure 8. STAR-CCM+ Mesh for PWR Cell Model.

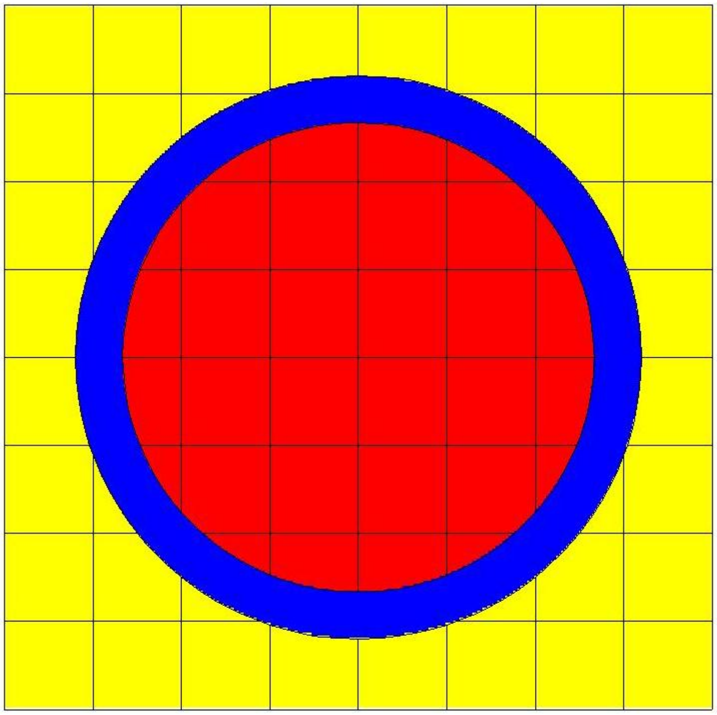

Figure 9. MCNP5 Geometry Cells for PWR Cell Model.

6.1.2. MAKXSF Pre-generated Cross Section Data

Prior to execution of MULTINUKE, MAKXSF is run to pre-generate cross section data over a temperature range appropriate for a typical PWR. MAKXSF copies cross section data from ENDF/B-VII.0 for the initial isothermal MCNP5 calculation. The MAKXSF input file used to create the cross section data for the PWR cell model is given in Appendix A.3. In order for MCNP5 to locate the required data, the code is executed for each MULTINUKE iteration using the command:

```
mpirun -n 4 mcnp5.mpi n=$JOB_NAME xsdir=xsdir_broad1 .
```

This command executes the Linux MPI MCNP5 executable over all of the cores of the machine’s processor. The code also locates the temperature dependent cross section data using the information in the command line. For the PWR cell model, a temperature dependent library designated “broad1” is specified for MCNP5 by the XSDIR file called “xsdir_broad1.”

After each STAR-CCM+ calculation, MULTINUKE assigns material numbers to all cells in MCNP5 by comparing each cell’s calculated temperature to the nearest pre-generated temperature bin for that particular material. Hence, cells at very different temperatures for the same material are assigned different material numbers. Tables 3, 4, and 5 list the temperature bins used by MAKXSF to pre-generate cross section data, along with the associated material numbers and ZAIDs that are in the PWR cell model’s base MCNP5 input file. (ZAIDs are explained in Sec. 3.2.) The ID extension refers to the suffix on the ZAID numbers in the MCNP5 input file. For example, for a UO_2 fuel cell that has temperature close to 925 K, MULTINUKE assigns the material number 7 (with ID suffix “.07c”) to that cell. Material 7 appears in data card section of the MCNP5 input file, as shown in Figure 10.

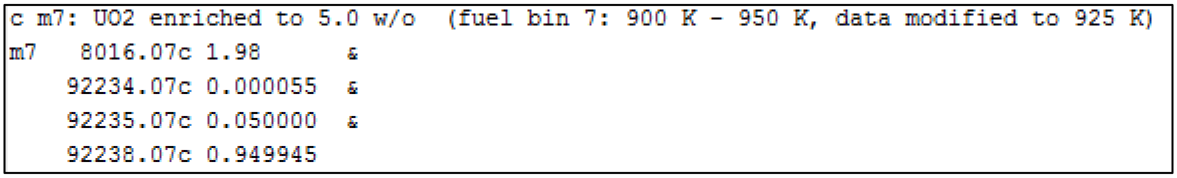

```
c m7: UO2 enriched to 5.0 w/o  (fuel bin 7: 900 K - 950 K, data modified to 925 K)
m7   8016.07c 1.98      &
    92234.07c 0.000055  &
    92235.07c 0.050000  &
    92238.07c 0.949945
```

Figure 10. Example MCNP5 Material Data Card for PWR Cell Model.

Table 3. MAKXSF Temperature-Binned Fuel Cross Sections.

Fuel Material Number	MCNP5 ZAID ID Extension	Bin T_{min} (K)	Bin T_{max} (K)	Temperature at which Data is Evaluated (K)
1	.01c	600	650	625
2	.02c	650	700	675
3	.03c	700	750	725
4	.04c	750	800	775
5	.05c	800	850	825
6	.06c	850	900	875
7	.07c	900	950	925
8	.08c	950	1000	975
9	.09c	1000	1050	1025
10	.10c	1050	1100	1075
11	.11c	1100	1150	1125
12	.12c	1150	1200	1175
13	.13c	1200	1250	1225
14	.14c	1250	1300	1275
15	.15c	1300	1350	1325

Table 4. MAKXSF Temperature-Binned Cladding Cross Sections.

Clad Material Number	MCNP5 ZAID ID Extension	Bin T_{min} (K)	Bin T_{max} (K)	Temperature at which Data is Evaluated (K)
21	.21c	500	600	550
22	.22c	600	700	650
23	.23c	700	800	750

Table 5. MAKXSF Temperature-Binned Moderator Cross Sections.

Coolant Material Number	MCNP5 ZAID ID Extension	Bin T_{min} (K)	Bin T_{max} (K)	Temperature at which Data is Evaluated (K)
31	.31c (.31t for $S(\alpha,\beta)$)	550	560	555
32	.32c (.32t for $S(\alpha,\beta)$)	560	570	570
33	.33c (.33t for $S(\alpha,\beta)$)	570	575	572.5
34	.34c (.34t for $S(\alpha,\beta)$)	575	580	577.5
35	.35c (.35t for $S(\alpha,\beta)$)	580	585	582.5
36	.36c (.36t for $S(\alpha,\beta)$)	585	590	587.5
37	.37c (.37t for $S(\alpha,\beta)$)	590	595	592.5
38	.38c (.38t for $S(\alpha,\beta)$)	595	600	597.5
39	.39c (.39t for $S(\alpha,\beta)$)	600	610	605

6.1.3. Neutronics Modeling

The nuclear physics of the PWR cell model are treated using steady state, three-dimensional, Monte Carlo neutron transport. Gamma and neutron heating in the clad and moderator are neglected; only fission heating and local prompt gamma heating in the fuel are tallied by MCNP5 in order to create a heat generation rate for STAR-CCM+.

The MCNP5 model has 3328 fuel cells and 4160 moderator/coolant cells, matching the CFD mesh for the fuel and water regions. The CFD mesh of the clad region is collapsed to a single MCNP5 cell. The MCNP5 geometry has dimensions identical to the STAR-CCM+ geometry. After each CFD run, MULTINUKE assigns the appropriate temperature, material number, and density (if a moderator cell) to the corresponding MCNP5 cells by modifying the MCNP5 base input deck (the "base" input file for MCNP5 is discussed Sec. 5.2.1).

Reflective boundary conditions are specified on the surfaces in the x and y directions in the MCNP5 model. Neutron leakage is permitted from the top and bottom axial surfaces. The simple 20 cm cell model is not representative of any realistic nuclear reactor design. High axial leakage leads to low k_{eff} values of about 0.6 to 0.8. Since the PWR cell model does not have any axial reflector regions, no reflector power peaking at the top and bottom of the model will be shown for the results in Section 6.2. The PWR cell model is not a criticality search problem – but a steady state thermal feedback simulation for a hypothetical PWR.

As discussed in Section 5.1.2, the tallies for heat generation rate are dependent on the eigenvalue and average neutrons released per fission (ν) (see equation (5.1)). Because ν remains relatively constant compared to the reactivity feedback, the overall power level will fluctuate as k_{eff} changes during the iterations. Therefore, the (fission) heat generation rate data transferred to STAR-CCM+ is scaled by a constant (which is updated after each MCNP5 calculation) to keep the overall power level equal to the value specified in the MULTINUKE input file, *multiSpecs_base.txt*.

For the PWR cell simulation, MCNP5 is executed in neutron transport mode (*mode n*) with no explicit photon particle transport. Delayed neutrons are accounted for by using the *TOTNU* data card in the MCNP5 input file. Each MULTINUKE neutronic calculation ran 160 batches of neutrons with 15,000 neutron histories in each batch, while discarding the first 10 batches for proper eigenvalue and fission source convergence. Source neutrons are uniformly distributed over a cylindrical region that encompasses all fissionable material in the model. There were no warnings from MCNP5 of unsampled cells containing fissionable material. Figure 11 shows the MCNP5 physics data card used for the PWR cell model, also showing that default MCNP5 neutron physics are used since special physics options are not specified.

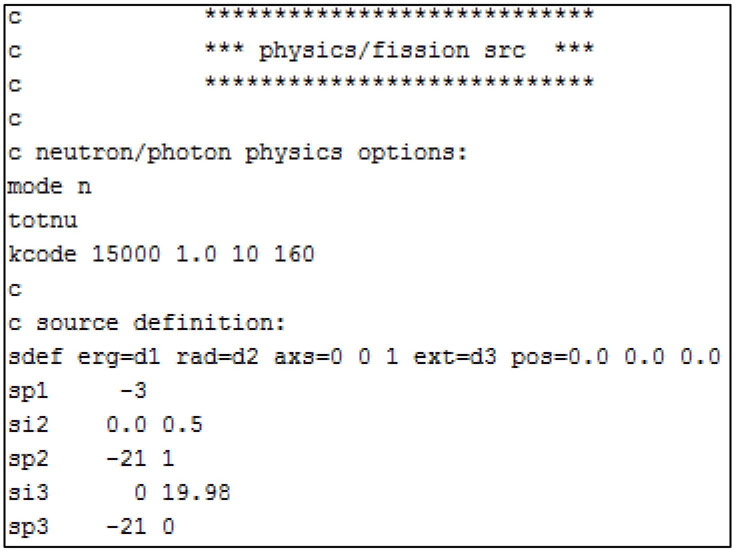

```
c             ****************************
c             *** physics/fission src  ***
c             ****************************
c
c neutron/photon physics options:
mode n
totnu
kcode 15000 1.0 10 160
c
c source definition:
sdef erg=d1 rad=d2 axs=0 0 1 ext=d3 pos=0.0 0.0 0.0
sp1     -3
si2    0.0 0.5
sp2    -21 1
si3      0 19.98
sp3    -21 0
```

Figure 11. MCNP5 Physics Data Cards for PWR Cell Model.

6.1.4. Thermal-Hydraulics Modeling: CFD Solver

The thermal-hydraulics of the PWR cell model are simulated using single-phase, three-dimensional, steady state, computational fluid dynamics in conjunction with 3D heat conduction in solids. The coupled flow solver in STAR-CCM+ (for conjugate heat transfer) is used so that the governing equations can be solved simultaneously, since it intrinsically provides more robust solutions. It is advised in the STAR-CCM+ manual to use the coupled flow solver for problems with large energy sources and if the computational burden is not too high [22]. (The segregated flow and energy solvers could have been used because the flow is essentially incompressible;

however, the presence of the large fission energy source in the fuel region (~10^8 W/m^3) necessitates the use of the coupled flow solver.) The PWR model simulates heat conduction in the solid fuel and clad regions using the coupled solid energy solver in STAR-CCM+. For the steady state PWR cell model, the coupled flow solver incorporates a pseudo-time marching approach to solve the governing equations simultaneously. The coupled flow solver uses implicit-steady integration to solve the discretized equations, providing relatively faster convergence rates than explicit-steady integration with a multi-stage Runge-Kutta scheme [22].

Table 6 summarizes the parameters used in simulating the PWR cell model using STAR-CCM+. For the steady coupled solver, the Courant number specifies the maximum size of the local pseudo-time steps used by the solver when integrating the governing equations. When faced with convergence difficulties during initial iterations, it may be necessary to decrease the Courant number. The governing equations are discretized using a second-order discretization scheme. For the PWR model, a Gauss-Seidel relaxation scheme with a convergence tolerance of 0.01 is used.

Table 6. CFD Solver Options in STAR-CCM+ for PWR Cell Model.

STAR-CCM+ Solver Parameter	Value
Solver Type	Coupled Implicit
Equation Discretization Method	2nd Order Upwind
Courant Number	5.0
Relaxation Scheme	Gauss-Seidel
Solver Convergence Tolerance	0.01

6.1.5. Modeling Turbulence in the PWR Cell Simulation

The coolant in the PWR cell model is treated as a viscous and turbulent liquid. Turbulence modeling is accomplished using the realizable two-layer k-ε model that provides closure to the Reynolds-averaged Navier-Stokes (RANS) equations. The k-ε turbulence method is a two-equation eddy viscosity model that solves the transport equation for turbulent kinetic energy (k) and dissipation rate (ε). It usually gives reasonable results for simple models that have a relatively coarse mesh [22]. There are more accurate turbulence models in STAR-CCM+ available for future work with MULTINUKE. In STAR-CCM+, the realizable two-layer *k-ε* turbulence model is a combination of the realizable *k-ε* model and the two-layer turbulence model.

The realizable two-layer *k-ε* turbulence model for the PWR model uses the default turbulence options in STAR-CCM+, some of which are listed in Table 7. The turbulence model uses a shear driven (Wolfstein) two-layer formulation with an all-*y*+ wall treatment. The Boussinesq approximation is used for a linear constitutive relation, which is recommended for all *k-ε* models in the STAR-CCM+ manual. The PWR cell model has a second-order convection scheme, which is superior to first-order convection schemes [22]. The under-relaxation factor of the turbulence solver is set to 0.8, the default for *k-ε* turbulence in STAR-CCM+. The turbulence solver under-relaxation factor affects solution convergence – lowering it may help convergence but also slows down the solver. The algebraic multigrid (AMG) linear solver values in Table 7 set the parameters for STAR-CCM+ to solve the discretized linear systems of equations in an iterative fashion. The details on these parameters can be found in the STAR-CCM+ user guide [22]. With the *k-ε* viscosity under-relaxation factor set to 1.0 (as shown in Table 7), the entire turbulent viscosity is updated after each CFD iteration computes a new turbulent viscosity field.

Table 7. CFD Turbulence Options in STAR-CCM+ for PWR Cell Model.

Parameter	Value
Turbulence Model	Realizable Two-Layer *k-ε*
Two-Layer Type Formulation	Shear Driven (Wolfstein)
Wall Treatment	All-*y*+
Constitutive Relation	Linear
Convection Scheme	2nd Order
k-ε Under-Relaxation Factor	0.8
Algebraic Multigrid Linear Solver Convergence Tolerance	0.1
Algebraic Multigrid Linear Solver Maximum Cycles	30
Algebraic Multigrid Linear Solver Group Size	2
k-ε Turbulence Viscosity Under-Relaxation Factor	1.0

6.1.6. Thermo-Physical Material Properties

The thermo-physical properties of the solid UO_2 and Zircaloy-4 regions are assumed to be constant. Still, an effort is made to input solid material data at temperatures appropriate for the PWR cell model. Table 8 and Table 9 designate the constant material properties for the fuel and clad regions of the PWR model, and the source from which the data was obtained.

Table 8. UO_2 Thermo-Physical Properties for PWR Cell Model.

Thermal Property	Value	Source of Data and Reference #
ρ, Density (g/cm^3)	10.3	Duderstadt, 1976 [6]
k, Thermal Conductivity (W/m-K)	3.0	Argonne National Laboratory [26]
c_p, Specific Heat Capacity (J/kg-K)	310	Todreas, 1993 [21]

Table 9. Zircaloy-4 Thermo-Physical Properties for PWR Cell Model.

Thermal Property	Value	Source of Data and Reference #
ρ, Density (g/cm^3)	6.50	Duderstadt, 1976 [6]
k, Thermal Conductivity (W/m-K)	11.0	Argonne National Laboratory [27]
c_p, Specific Heat Capacity (J/kg-K)	330	Argonne National Laboratory [28]

The coolant is assumed to have constant thermal conductivity, as well as constant dynamic viscosity and turbulent Prandtl number. Table 10 gives the water properties chosen from the stated source at the approximate coolant temperatures of the PWR model. The density and specific heat capacity of the coolant in STAR-CCM+ are however not constant, but rather polynomial functions of the cell temperature. The thermal expansion of the coolant is discussed in the next section.

Table 10. H_2O Thermo-Physical Properties for PWR Cell Model.

Thermal Property	Value	Source of Data and Reference #
μ, Dynamic Viscosity (Pa-s)	$9.177\text{x}10^{-5}$	El-Wakil, 1993 [5]
k, Thermal Conductivity (W/m-K)	0.53	El-Wakil, 1993 [5]
Pr, Turbulent Prandtl Number	0.90	STAR-CCM+ Manual, 2007 [22]

The specific heat capacity for H_2O is modeled by the following temperature dependent equation in STAR-CCM+:

$$c_p(T) = \begin{cases} 4570, \ if\ T < 500 \\ 5.0\text{x}10^{-5}\, T^4 - 0.11\, T^3 + 85.2\, T^2 - 3.0\text{x}10^4\, T + 4.03\text{x}10^6, \ if\ 500 \le T \le 600 \\ 6778, \ if\ T > 600. \end{cases} \qquad (6.1)$$

In equation (6.1), temperature (*T*) has units of Kelvin, and the specific heat capacity (c_p) has units of J/kg-K. The polynomial is a fourth-order fit of specific heat data in *Nuclear Heat Transport* by M. M. El-Wakil [5]. Figure 12 depicts the H_2O heat capacity for the PWR cell model, where the red curve denotes the heat capacity equation (6.1) and the blue dots are data from El-Wakil [5]. (The H_2O heat capacity is assumed to be constant outside the coolant temperature range of interest.)

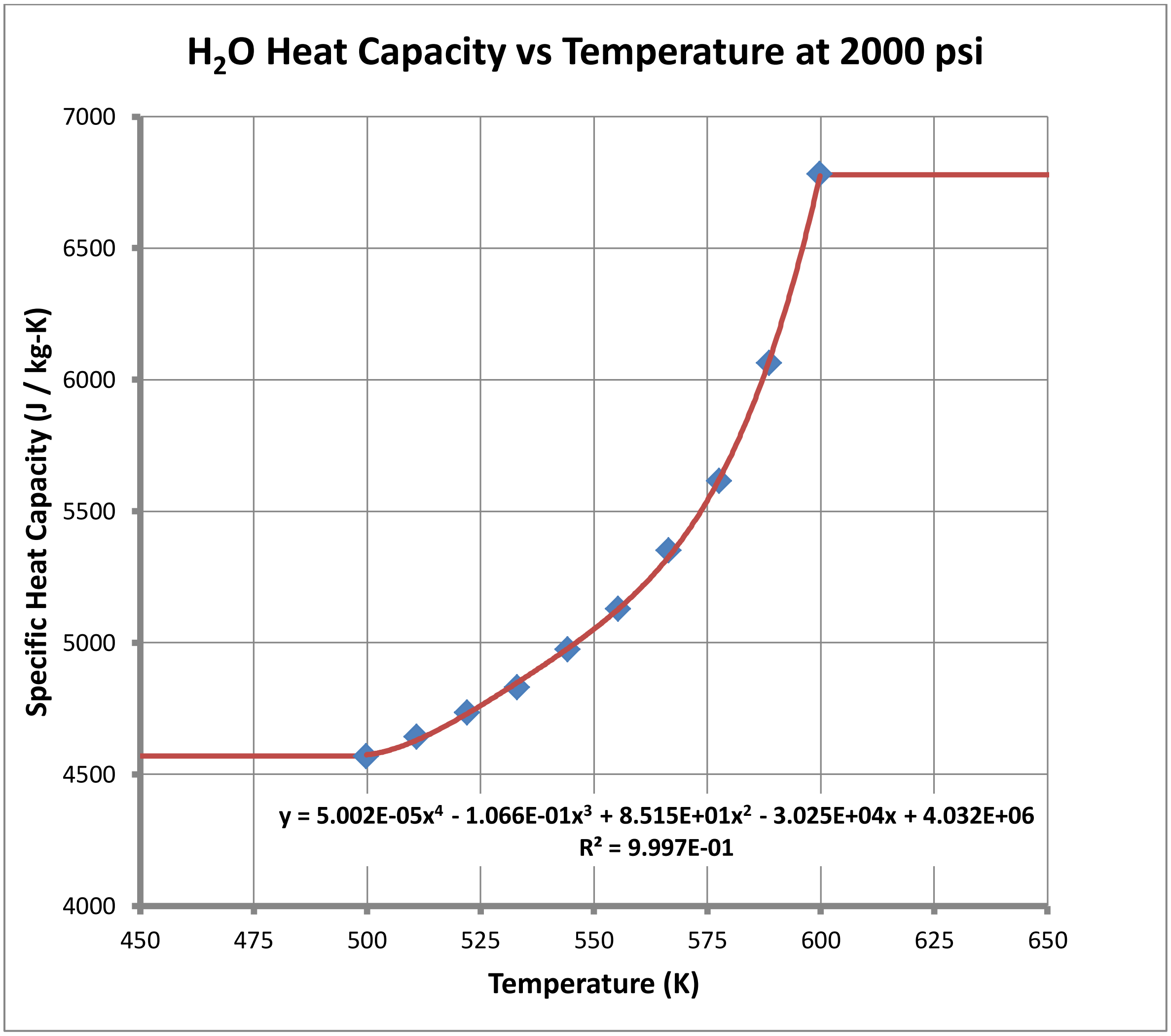

Figure 12. Specific Heat Capacity for Coolant in PWR Cell Model.

6.1.7. Equation of State and Moderator Density

When simulating a single-phase fluid with the steady state, coupled flow solver, STAR-CCM+ allows for constant density, density varying as a polynomial, and ideal gas treatment for the equation of state. To model the equation of state, STAR-CCM+ simulates the thermal expansion of coolant in the PWR cell model using a user-specified polynomial fluid density. A user-specified equation of state is specified making use of the water density data from El-Wakil. The equation for coolant density as a function of temperature at 2000 psi pressure in the PWR cell mode is [5]:

$$\rho(T) = \begin{cases} 1006, \; if \; T < 277.6 \\ -4.12\text{x}10^{-8}\, T^4 + 6.74\text{x}10^{-5}\, T^3 - 4.31\text{x}10^{-2}\, T^2 + 11.8\, T - 154, \; if \; 277.6 \leq T \leq 600 \\ 657.4, \; if \; T > 600. \end{cases} \quad (6.2)$$

In equation (6.2), ρ is the H_2O density in kg/m^3, temperature (T) is in Kelvin and coolant density is assumed to be constant outside the temperature range of interest for the PWR model. Figure 13 shows the variation of coolant density with temperature. The red curve represents equation (6.2) and the blue dots are the data points for water density from El-Wakil [5].

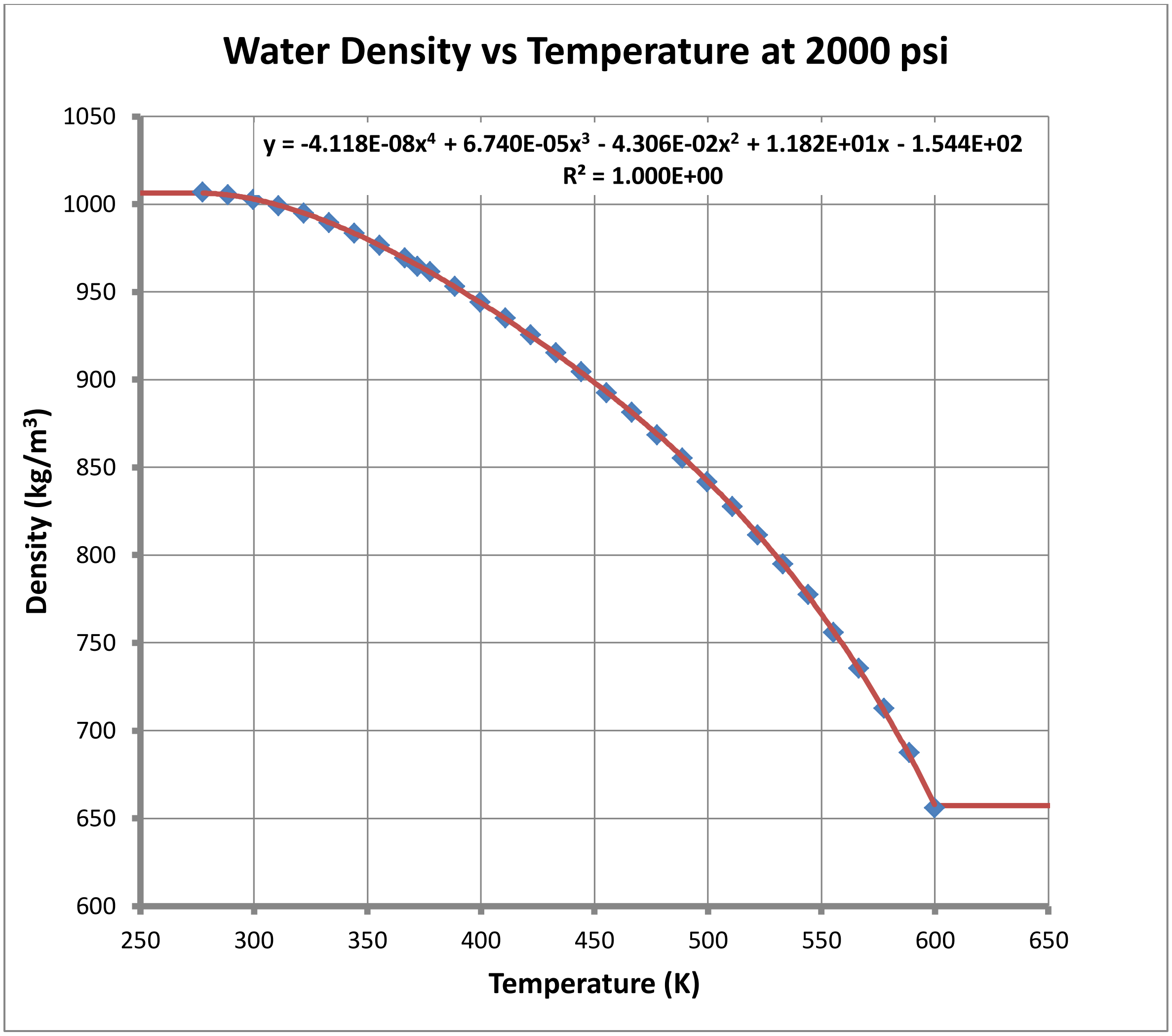

Figure 13. Water Density Temperature Dependence in PWR Cell Simulation.

6.1.8. STAR-CCM+ Initial Conditions and Boundary Conditions

The STAR-CCM+ simulation file for the PWR model contains three mesh continua and three physics continua, corresponding to the three geometry regions in the model ("continua" is a STAR-CCM+ term referring to data input sections in the GUI where mesh data and physical quantities are specified by the user). The trimmer mesh generator can only generate a hexahedral mesh for one region at a time; therefore, three mesh continua are necessary for the model. There exist two interfaces: one between the fuel and clad regions, and one between the clad and coolant regions. The physics continua specify the material properties of the regions and the initial conditions for the CFD solver. Table 11 shows the initial thermal-hydraulic conditions for the PWR model. These initial conditions only serve as the “initial guess” for the steady state problem.

Table 11. Initial Thermal-Hydraulic Conditions for PWR Cell Model.

Initial Parameter	Value
UO_2 Fuel Continua Temperature (K)	1000.0
Fuel-Clad Interface Temperature (K)	900.0
Zircaloy-4 Clad Continua Temperature (K)	800.0
Clad-Coolant Interface Temperature (K)	800.0
H_2O Coolant Continua Temperature (K)	580.0
H_2O Coolant Inlet Temperature (K)	570.0
H_2O Coolant Inlet Speed (m/s)	1.0
H_2O Coolant Initial Pressure (Pa)	$1.55x10^7$
H_2O Coolant Exit Pressure (Pa)	$1.50x10^7$
Initial Turbulence Specification	Intensity + Viscosity Ratio
Turbulence Intensity	0.01
Turbulent Viscosity Ratio	10.0

Symmetry boundary conditions are imposed on the surfaces in the *x* and *y* directions in the STAR-CCM+ simulation file. Inlet velocity is specified at the (bottom) inlet, and a pressure boundary condition is specified at the top surface. The fuel-clad and clad-coolant interfaces have continuous boundary conditions. No-slip boundary conditions are specified for the coolant on the cladding surface.

6.1.9. MULTINUKE Input Data

Assuming the PWR model represents an average fuel pin in a PWR with a power density of $3.00x10^8$ W/m^3, a power rating of 4700.0 Watts is designated in the *muliSpecs_base.txt* input file. The UO_2 fuel density is selected to be 10.3 g/cm^3, and it is assumed that each fission releases 200 MeV of energy. Rather relaxed MULTINUKE convergence criteria are selected in order to expedite development and debugging of the coupled code system. Once two successive iterations yield a difference of less than 0.0005 eigenvalue (Δk) and less than 2% average change in cell temperatures, the solution is considered to be converged. Simulations can be easily run with more strict convergence criteria. Table 12 contains some important input data for MULTINUKE to analyze the PWR cell model.

Table 12. PWR Cell Input Data for MULTINUKE.

Input Data	Value
Job Name	pin20cm
Fuel Density (g/cm^3)	10.3
Power Output (W)	4700.0
Q – Energy Released per Fission (MeV/fission)	200.0
Eigenvalue Convergence (Δk)	0.0005
Temperature Convergence (fraction % difference)	0.02
MCNP5 Initial Isothermal Temperature (K)	293

6.2. PWR Cell Model Results

This section discusses the results of neutronic and thermal-hydraulic calculations for the PWR cell model. MCNP5 and STAR-CCM+ results to validate the neutronic and thermal-hydraulic models separately are discussed in the first four subsections (6.2.1, 6.2.2, 6.2.3, and 6.2.4). Results obtained for the coupled MCNP5 and STAR-CCM+ simulations carried out using by MULTINUKE for the PWR cell model are discussed in the remaining subsections (6.2.5, 6.2.6, 6.2.7, 6.2.8, and 6.2.9).

6.2.1. MCNP5 Eigenvalue and Fission Source Convergence

Sufficient neutron history cycles must be discarded in order for the eigenvalue and fission source calculated by MCNP5 to properly converge. Figure 14 and Figure 15 respectively depict convergence of eigenvalue and fission source entropy for a typical MCNP5 simulation of the PWR model. MCNP5 is run with 15,000 neutron histories per cycle for 160 total cycles, while discarding the first 10 batches, for every MCNP5 calculation in MULTINUKE. The cycle discard number is shown at the tenth cycle in Figures 14 and 15 by the red vertical line. MCNP5 automatically calculates the Shannon entropy of the fission source and suggests the number of cycles that should be discarded. In the PWR cell model case, it recommended discarding 2-9 cycles for proper fission source convergence. Discarding the first 10 cycles of each MCNP5 calculation proved effective in allowing sufficient convergence of the eigenvalue and source distribution.

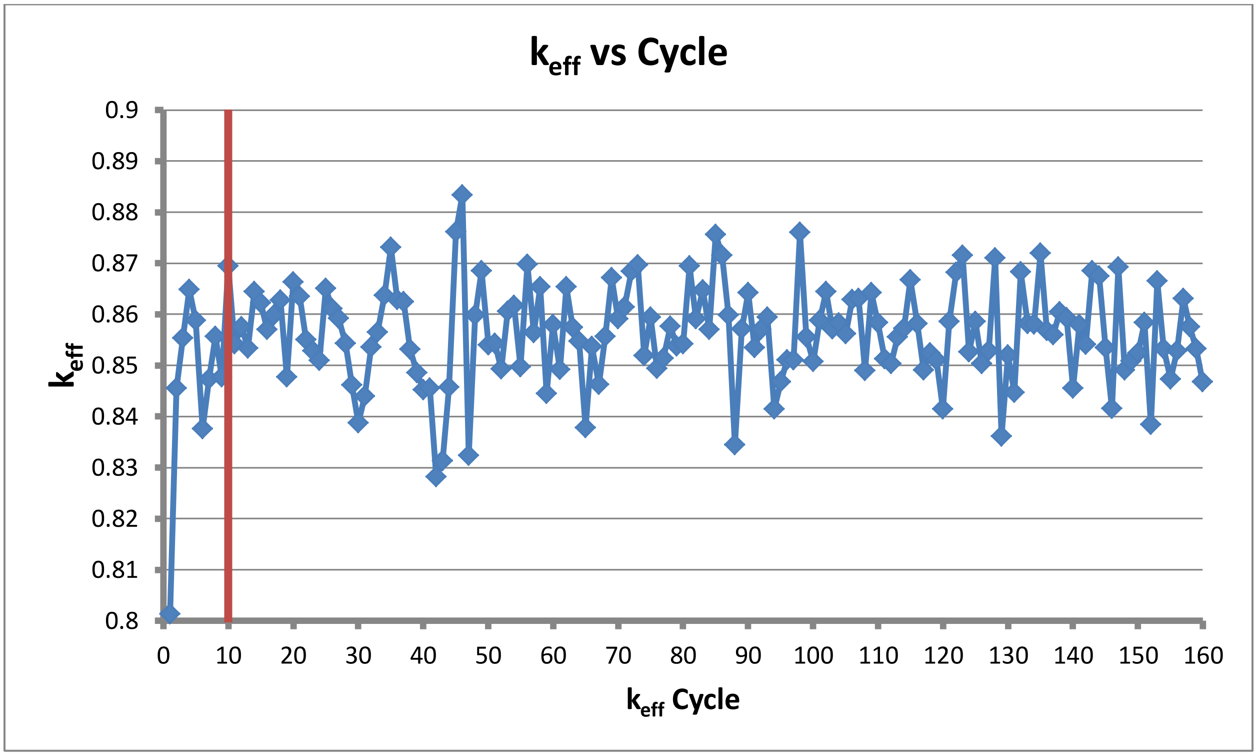

**Figure 14.	MCNP5 Eigenvalue Convergence.**

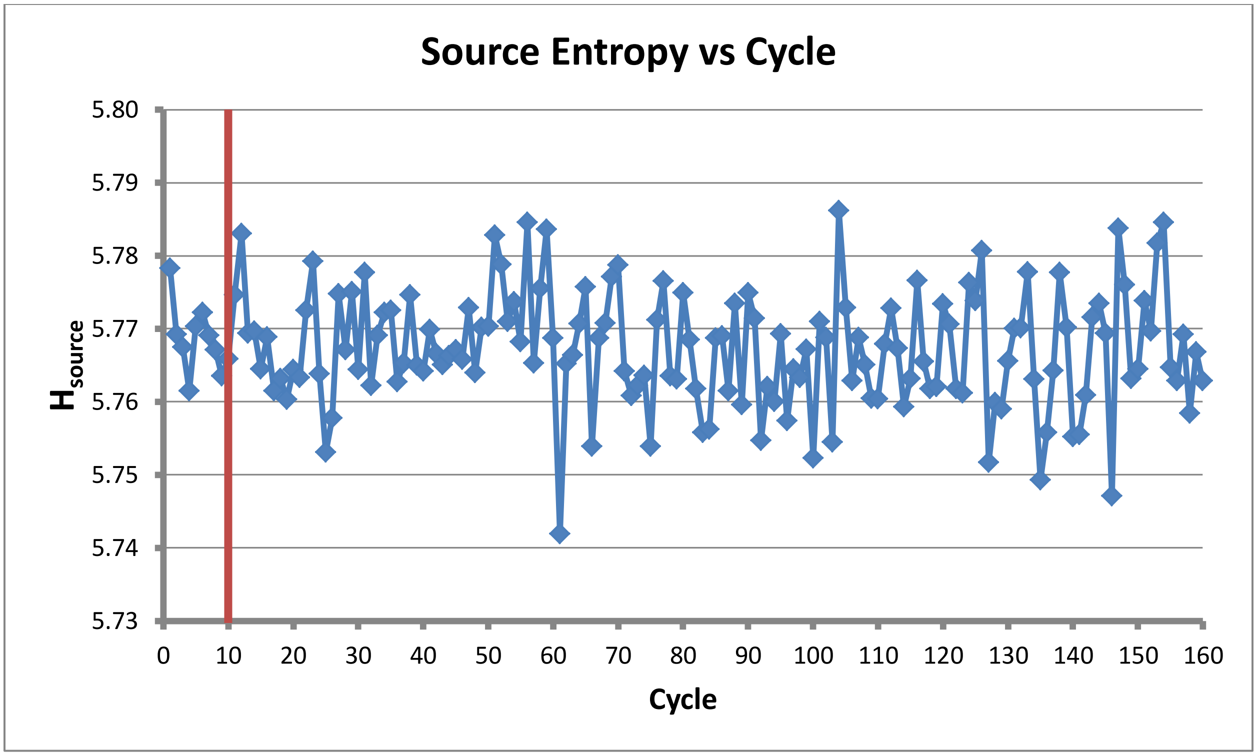

Figure 15. MCNP5 Fission Source Convergence.

6.2.2. MCNP5 Tally Statistics

According to the MCNP5 manual, tally results are usually accurate with relative errors less than 0.10. Furthermore, MCNP5 automatically performs ten standard statistical checks on all tallies listed in the input file, with details given in the MCNP5 manual [4]. For every MCNP5 calculation in the MULTINUKE assessment of the PWR model, the fission energy deposition tally passed all ten statistical checks and all of its cell tally bins had relative errors less than 0.10. Figure 16 is a scatter plot of relative error versus relative fission reaction rate, normalized to the average fission reaction rate, for a typical MCNP5 calculation of the PWR cell model. The red horizontal line represents the maximum desired relative error. All of the green data points fall below the maximum desired relative error of 0.10. The relative error in Figure 16 decreases as the normalized power distribution factor increases, because cells with higher power peaking are located in regions with relatively greater neutron flux. The trend in Figure 16 supports the neutronic validation of the pin model; MCNP5 cells with higher power peaking generate more heat, and are therefore more important in CFD coupling. High power regions should have lower stochastic errors. Cells with lower relative power generate less heat and are of lesser concern for STAR-CCM+ coupling – thereby permitting higher relative error in MCNP5.

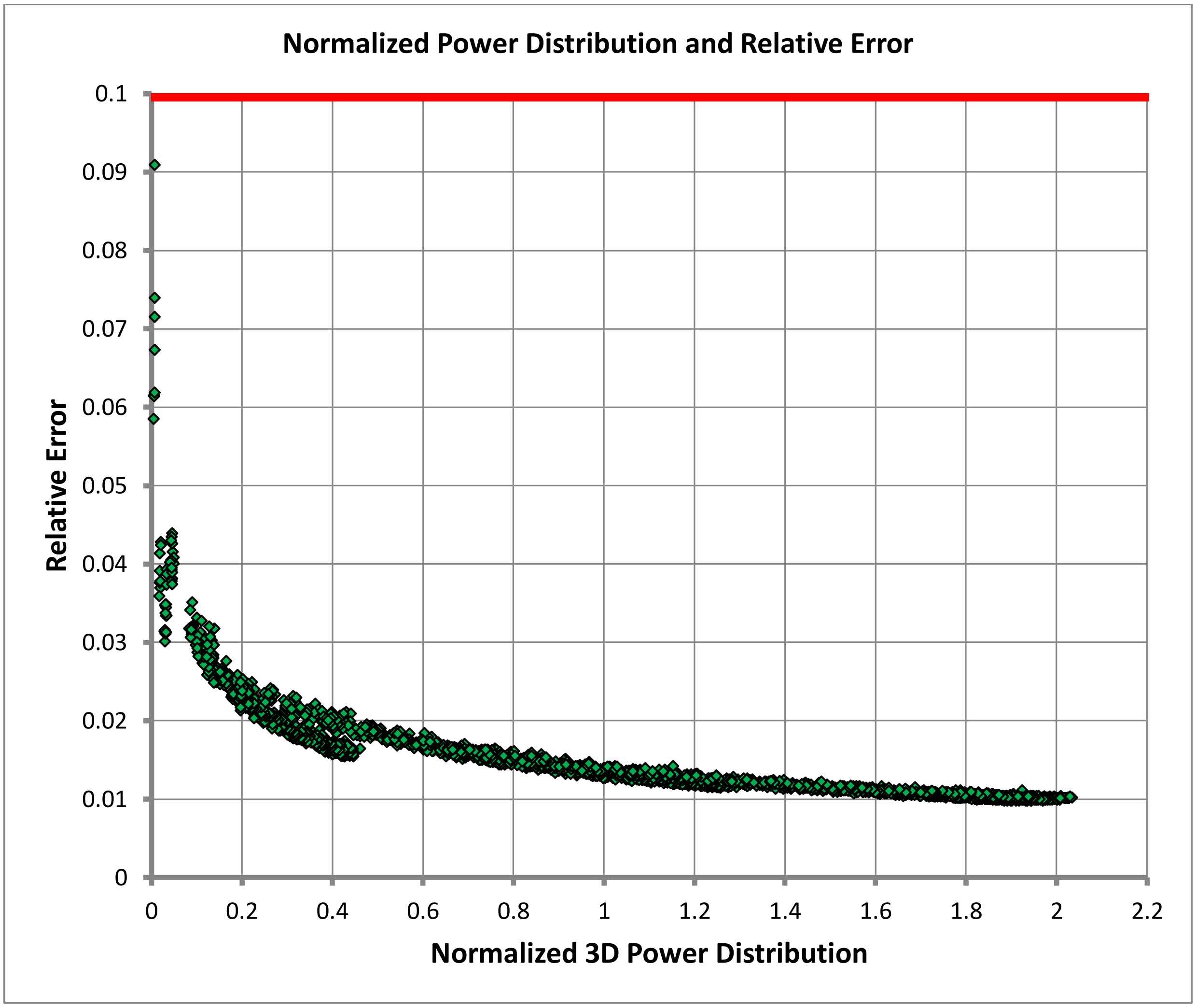

Figure 16. PWR Cell Model Tally Statistics from MCNP5.

6.2.3. MCNP5 Reactivity Coefficients

Although reactivity coefficients are temperature dependent quantities used for reactivity control of near-critical operating reactors, it is still beneficial to calculate reactivity coefficients for the PWR model as a means to validate the temperature dependent cross section libraries and the density equation for the water coolant (Section 6.1.7). Isothermal reactivity coefficients are calculated for the PWR cell model and compared to values reported in literature. For PWRs, as is well known and discussed in Chapter 1, the two primary reactivity feedback mechanisms are fuel and moderator temperature variations. The eigenvalues for the MCNP5 model are calculated for various fuel temperatures, while keeping clad and moderator temperatures constant at 293 K, allowing an estimation of the UO_2 Doppler reactivity coefficient. The eigenvalues for the MCNP5 model are also calculated at different moderator temperatures, while keeping fuel and clad temperature at a constant 293 K, in order to estimate the moderator temperature coefficient. In calculating the moderator temperature coefficient, H_2O density is modified according to the methods described in Section 6.1.7.

To assess the impact the shortened 20 cm cell height had on reactivity coefficients, the reactivity calculations are repeated with a 350 cm PWR cell with two 25 cm axial reflectors. The taller pin model is created by simply editing MCNP5 surface cards in the 20 cm pin model to stretch the axial height of the active region to 350 cm. Two 25 cm tall axial reflectors are then added to the top and bottom of the model. Table 13 gives the MCNP5 eigenvalue results for the 20 cm and 400 cm tall MCNP5 models at various isothermal temperatures, along with 95% confidence intervals. Table 14 shows the calculated fuel Doppler reactivity coefficients and moderator temperature coefficients and compared to values reported in literature.

The Doppler reactivity coefficients are in the same range as those reported in literature. The calculated moderator reactivity coefficient for the 20 cm model does not agree with values reported for PWR cores, due to excess axial leakage when the coolant density drops. However, the 400 cm model had a moderator temperature coefficient within the expected range. The results for both models are qualitatively accurate enough to justify that the MCNP5 models and pre-generated cross section database sufficiently capture the neutronics of the PWR cell model – specifically in its use for demonstrating multi-physics coupling with STAR-CCM+.

Table 13. 20 cm and 400 cm PWR Cell Model Eigenvalues at Various Temperatures.

Model	T_{fuel} (K)	$T_{coolant}$ (K)	$\rho_{coolant}$ (g/cm^3)	k_{eff} ± 95% CI
20 cm Model – Isothermal	293	293	1.0	0.85647 ± 0.0009
20 cm Model – Fuel Hot	625	293	1.0	0.84943 ± 0.0008
20 cm Model – Fuel Hot	825	293	1.0	0.84507 ± 0.0008
20 cm Model – Fuel Hot	1025	293	1.0	0.84146 ± 0.0009
20 cm Model – Fuel Hot	1325	293	1.0	0.83860 ± 0.0009
20 cm Model – Coolant Hot	293	555	0.7573	0.70149 ± 0.0008
20 cm Model – Coolant Hot	293	570	0.7278	0.67995 ± 0.0008
20 cm Model – Coolant Hot	293	582.5	0.7005	0.66100 ± 0.0009
20 cm Model – Coolant Hot	293	597.5	0.6639	0.63301 ± 0.0009
400 cm Model – Isothermal	293	293	1.0	1.46575 ± 0.0008
400 cm Model – Fuel Hot	625	293	1.0	1.45171 ± 0.0006
400 cm Model – Fuel Hot	825	293	1.0	1.44419 ± 0.0006
400 cm Model – Fuel Hot	1025	293	1.0	1.43844 ± 0.0007
400 cm Model – Fuel Hot	1325	293	1.0	1.42983 ± 0.0008
400 cm Model – Coolant Hot	293	555	0.7573	1.40974 ± 0.0007
400 cm Model – Coolant Hot	293	570	0.7278	1.40109 ± 0.0007
400 cm Model – Coolant Hot	293	582.5	0.7005	1.39271 ± 0.0007
400 cm Model – Coolant Hot	293	597.5	0.6639	1.37917 ± 0.0008

Table 14. Reactivity Coefficients for PWR Cell Models.

Parameter	20 cm Model	400 cm Model	Literature [6, 7]
Nuclear Doppler Coefficient in UO_2 (pcm/K)	-2.47	-1.66	-4 to -1
Moderator Temperature Coefficient (pcm/K)	-360 to -120	-36.0 to -12.4	-50 to -8

The reactivity coefficients in Table 14 are calculated by applying a linear regression to the data in Table 13 (slope = $\Delta\rho/\Delta T \approx$ reactivity coefficient). Figures 17-20 graphically portray the data from Table 13. These figures also show the linear regression lines and equations used for calculating the temperature reactivity coefficients in Table 14. Two linear regression lines are applied to the moderator reactivity data in an attempt to better quantify the moderator temperature coefficient for the models. For the 20 cm model, applying the linear regression to the high moderator temperature (orange trend line) results in a moderator reactivity coefficient in better agreement with reported values. Linear regressions were also fitted to the 400 cm model data in Table 13. The 400 cm model had a realistic Doppler reactivity coefficient, and a very reasonable moderator coefficient since it is a more realistic neutronic model of a PWR.

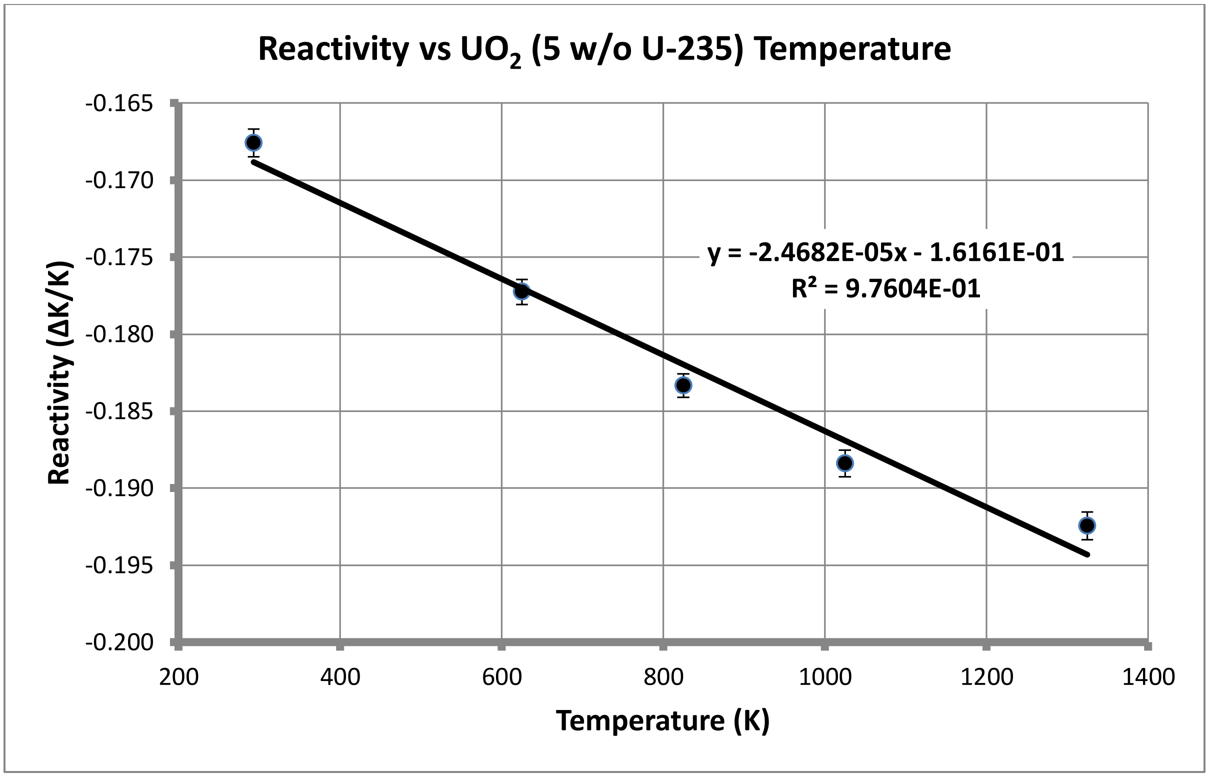

Figure 17. PWR Model (20 cm) Doppler Reactivity Coefficient.

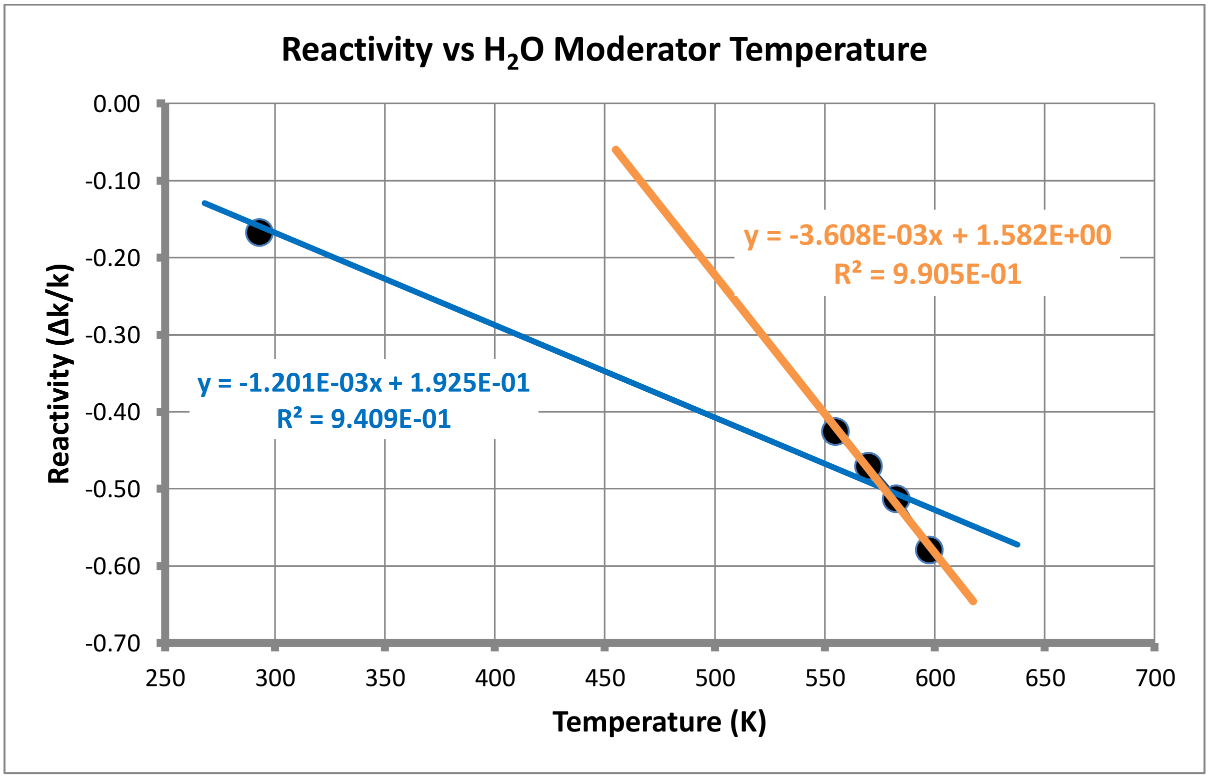

Figure 18. PWR Model (20 cm) Moderator Reactivity Coefficient.

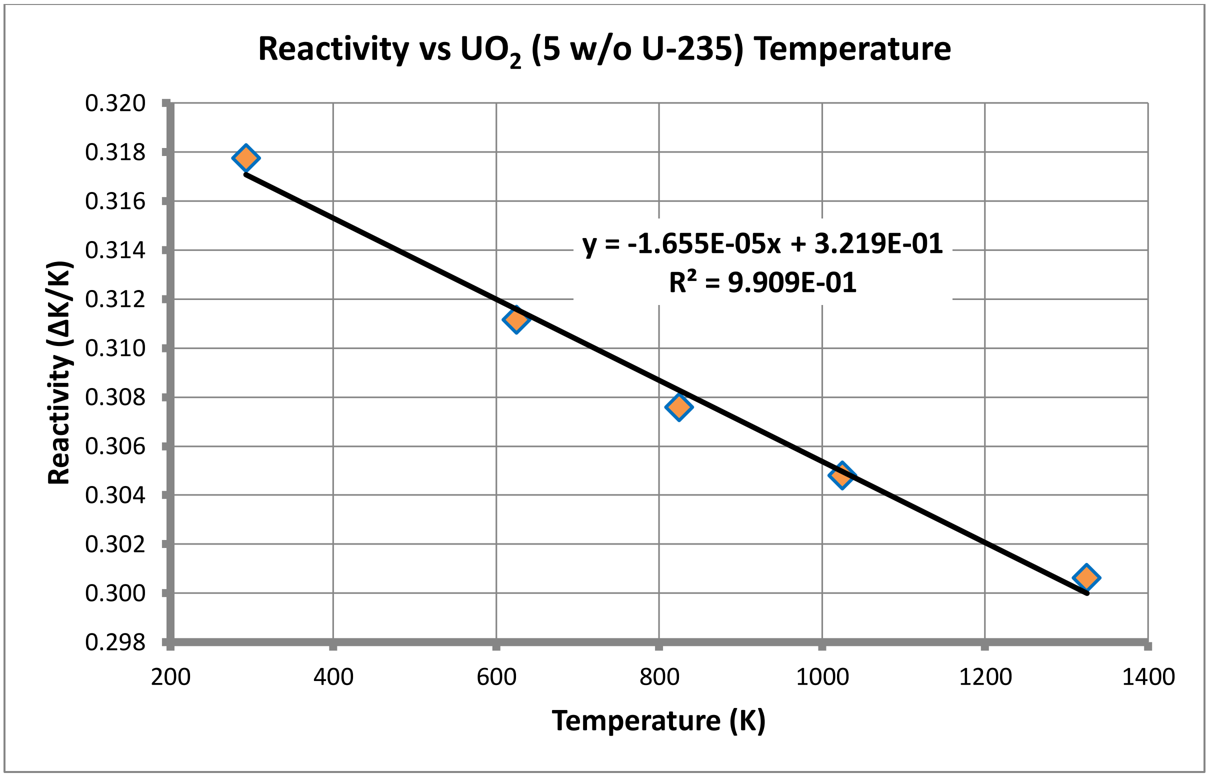

Figure 19. PWR Model (400 cm) Doppler Reactivity Coefficient.

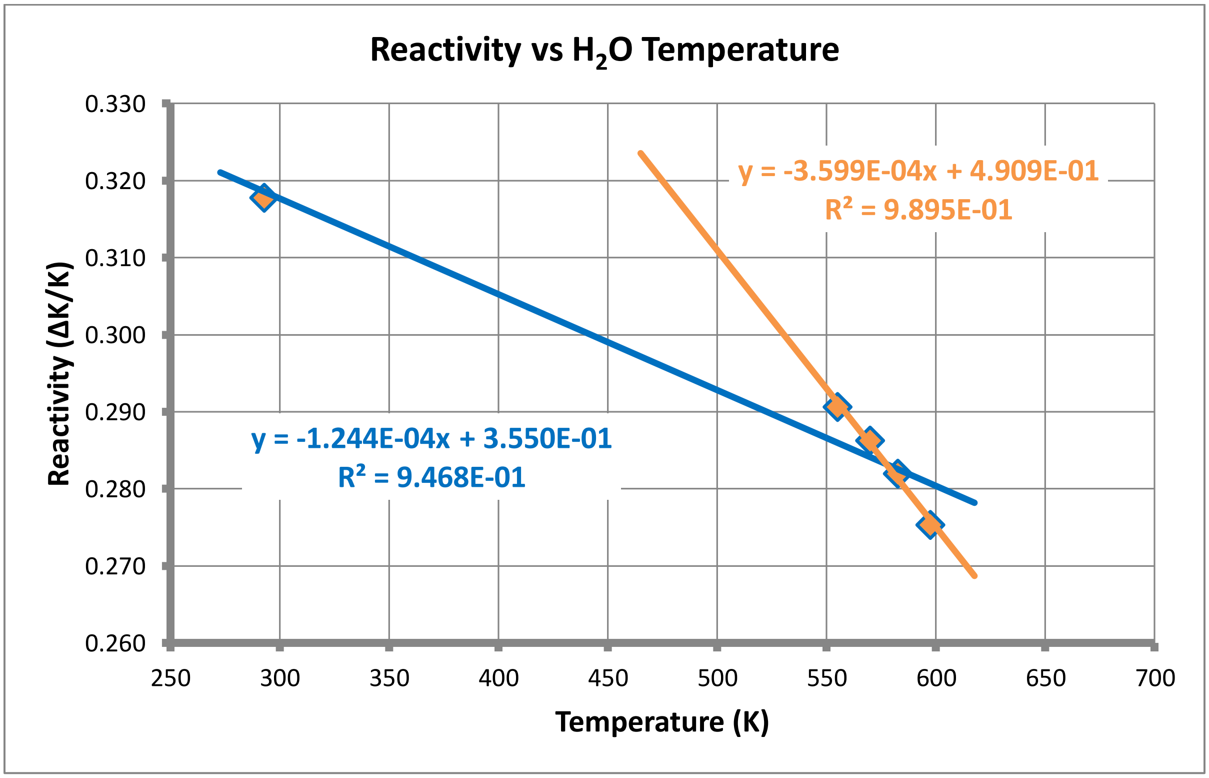

Figure 20. PWR Model (400 cm) Moderator Reactivity Coefficient.

6.2.4. STAR-CCM+ Mesh Refinement Study

In order to validate the resolution and quality of the prismatic hexahedral mesh used for the PWR cell problem, an unstructured polyhedral mesh of finer resolution is created for the PWR cell geometry as a means for comparison. Table 15 compares the meshes of the hexahedral and polyhedral models. The unstructured polyhedral mesh has 23,724 total CFD cells compared to 9,984 cells for the hexahedral mesh. The hexahedral mesh model and the polyhedral mesh model then are then used to simulate the same test case with a sinusoidal power distribution. The two thermal-hydraulic results are then compared to determine if the simpler (and faster running) hexahedral mesh provides sufficiently accurate results. Figure 21 shows a three-dimensional view of the polyhedral mesh for the PWR cell model. The polyhedral mesh also uses small prismatic cells at the fuel-clad and clad-coolant interfaces in order to better model heat transfer at these surfaces.

Table 15. Polyhedral and Hexahedral Mesh Comparison.

Parameter	Hexahedral Mesh	Polyhedral Mesh
Number of Fuel Cells	3328	6194
Number of Clad Cells	2496	6946
Number of Coolant Cells	4160	10584
Total CFD Cells	**9,984**	**23,724**

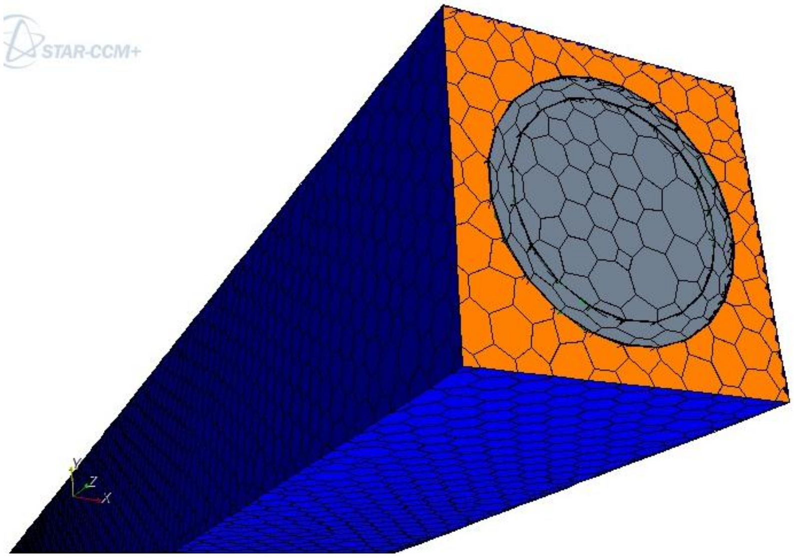

Figure 21. Unstructured Polyhedral Mesh for PWR Cell Model.

Figure 22 depicts the maximum axial temperature distribution for the fuel regions in the coarse hexahedral mesh and finer polyhedral mesh, given a sinusoidal MCNP5 power distribution at 4700 W. The red data points in Figure 22 are the maximum hexahedral mesh temperatures at each axial node. They appear to deviate less than 5% from the finer, unstructured, polyhedral mesh temperatures for most axial nodes, designated by the green data points on Figure 22. However, the polyhedral mesh does not have neatly discretized axial nodes due to its unstructured nature; thus, the maximum nodal temperatures for the polyhedral mesh appear more discontinuous when plotted against the axial dimension of the model. Furthermore, the polyhedral mesh quality at the top and bottom of the model appears to be degraded compared to the hexahedral mesh, most likely because both meshes use the same low-resolution surface mesh to generate their volumetric meshes. Compared to the polyhedral mesh generator, the STAR-CCM+ trimmer (hexahedral) mesh option can generate a higher quality mesh when surface mesh quality is low. Consequently, some of the disagreement between the axial fuel temperature distributions for the hexahedral and polyhedral mesh models could be due to differing mesh qualities at the tops and bottoms of the models.

The PWR cell models do not have axial reflectors; therefore, the temperatures near the top and bottom edges for the polyhedral model in Figure 22 are not physically realistic. The maximum fuel temperature calculated for the hexahedral mesh was 1464.9 K, which is only about 1.3% different from the polyhedral mesh result of 1445.9 K. This simple mesh refinement study was considered sufficient to validate the use of the hexahedral mesh model for demonstrating multi-physics coupling with a hexahedral MCNP5 model.

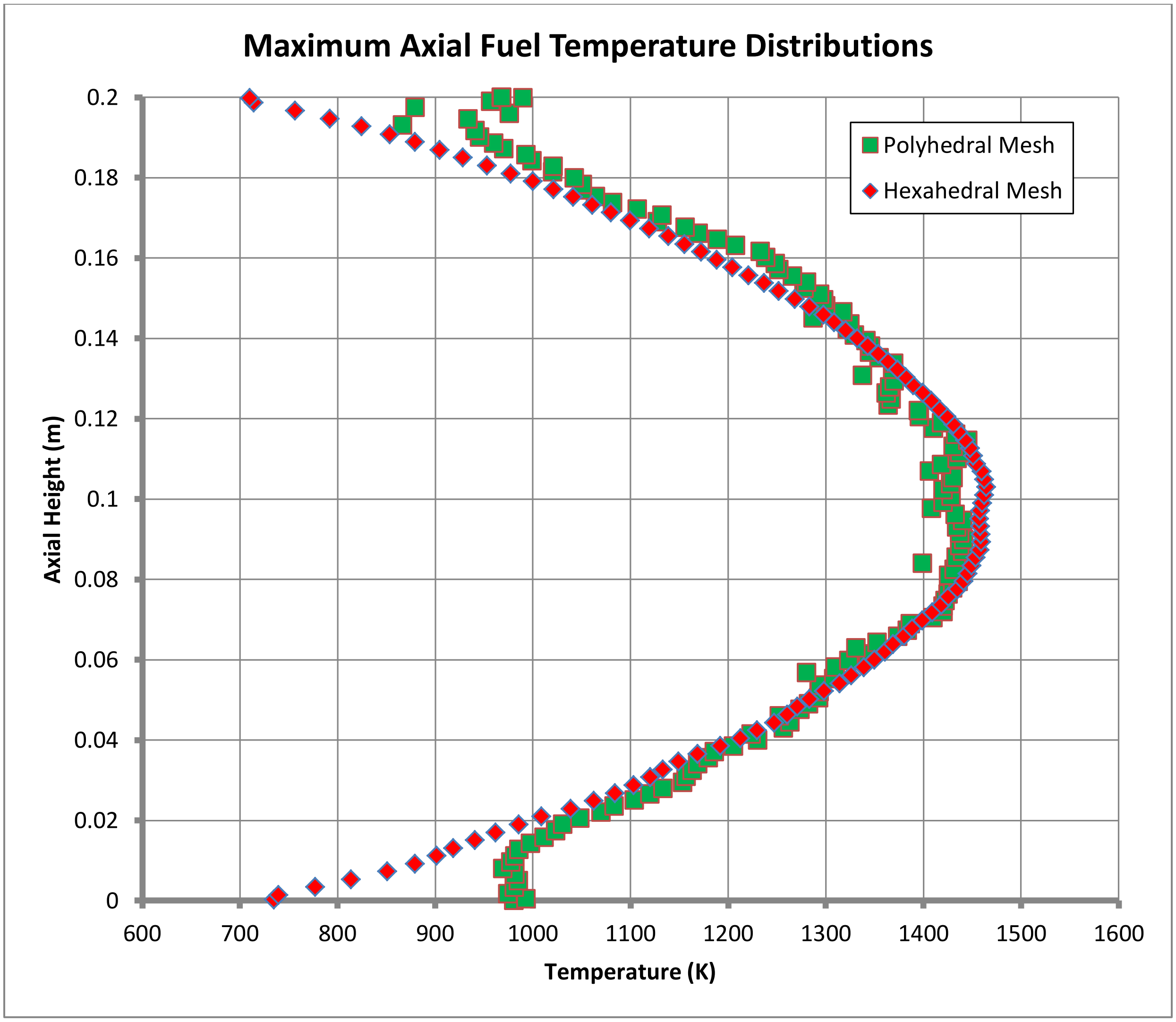

Figure 22. Maximum Axial Fuel Temperatures for Mesh Comparison.

6.2.5. STAR-CCM+ Solution Convergence

Residuals plots for a typical STAR-CCM+ run in MULTINUKE are shown in Figure 23. Between MULTINUKE iterations, the STAR-CCM+ residuals did not change noticeably, most likely because MCNP5 power profiles did not shift significantly for the PWR cell simulation. The residuals for all of the governing equations in STAR-CCM+ iterations in MULTINUKE dropped below 10^{-6} after ~3500 CFD iterations. In Figure 23, the blue “Tke” curve represents the turbulent kinetic energy residual, and the black “Tdr” curve is the turbulent dissipation rate residual.

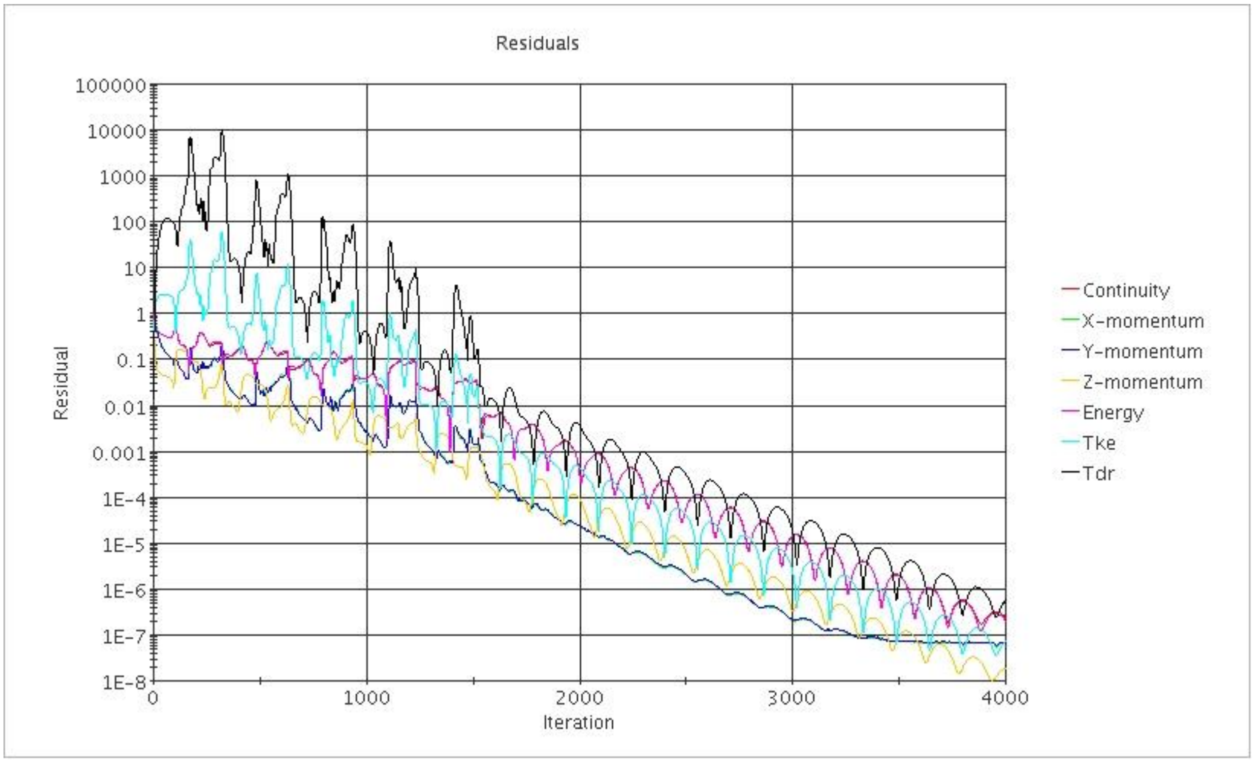

Figure 23. STAR-CCM+ Residuals for PWR Cell Model.

6.2.6. MULTINUKE Convergence and Run Time

The MULTINUKE simulation of the PWR cell model takes approximately 8 hours on a 64-bit, quad core, Intel 2.8 GHz microprocessor with 1 GB RAM. STAR-CCM+ and MCNP5 executed on all four cores of the machine's microprocessor. The coupled solution, with convergence determined by the parameters in Table 12 in Section 6.1.9, converges in only three MULTINUKE iterations due to the symmetry of the simple pin model. Table 16 summarizes the resulting convergence data for the cell model. The eigenvalue of the cell model converged within the 0.0005 Δk criteria, for a final value of 0.6601 ± 0.0009 (95% confidence interval).

Table 16. MULTINUKE Convergence Results.

Parameter	PWR Cell Model Result
Eigenvalue Change from Previous Iteration (Δk)	0.0001
Converged MCNP5 Eigenvalue	0.6601 ± 0.0009
Fractional % Change in Avg. Cell Temperature from Previous Iteration	0.0028
Total MULTINUKE Iterations to Satisfy Convergence Parameters	3

To further examine the convergence of the PWR cell model, MULTINUKE is allowed to continue the calculation for three additional iterations, for a total of six iterations. MCNP5 eigenvalues continued to hover within 0.0005 Δk of the k_{eff} from Table 16 (0.6601). The average percent change in STAR-CCM+ cell temperatures was still less than 1%, as it was in Table 16, for the three additional MULTINUKE iterations. Power distributions determined using MCNP5 and temperature distributions from STAR-CCM+ remain steady after three MULTINUKE iterations. These distributions are presented in the following sections.

6.2.7. Power Distributions

Axial power distribution data is from an F4:N (cell track length) MCNP5 tally modified to calculate the fission reaction rate in each fuel cell. In the GETHEAT post-processor, the fission reaction rates are integrated in the *x-y* directions for each axial node to determine the total fission rate for each axial node. The average fission rate for all axial nodes is also computed. The axial power peaking factor, normalized to the nodal average, is then calculated for each axial level. Figure 24 shows the converged relative axial power distribution for the PWR cell model. The relative power distribution for the pin model remains unchanged after two successive iterations.

As expected, the axial power distribution is essentially sinusoidal, owing to the fact that the model lacks axial reflectors, axial variations in fuel enrichment, or control rods. The axial power distribution in units of W/m^3 follows the profile of Figure 24. The average cell power density is calculated to be $3.855x10^8$ W/m^3, and the maximum cell power density is $9.431x10^8$ W/m^3 (taking into account axial and radial peaking). Figure 25 shows the power density in every cell in the fuel plotted against the *z*-axis for different radial locations. As expected, fuel cells near the edge of the fuel pin are exposed to greater thermal neutron flux compared to cells near the fuel center, due to self-shielding. The outer fuel cells therefore have greater fission reaction rates and higher power densities, as shown in Figure 25. When each cell's power density is multiplied by its volume and added together, the input power (4700 W) for the cell model is obtained.

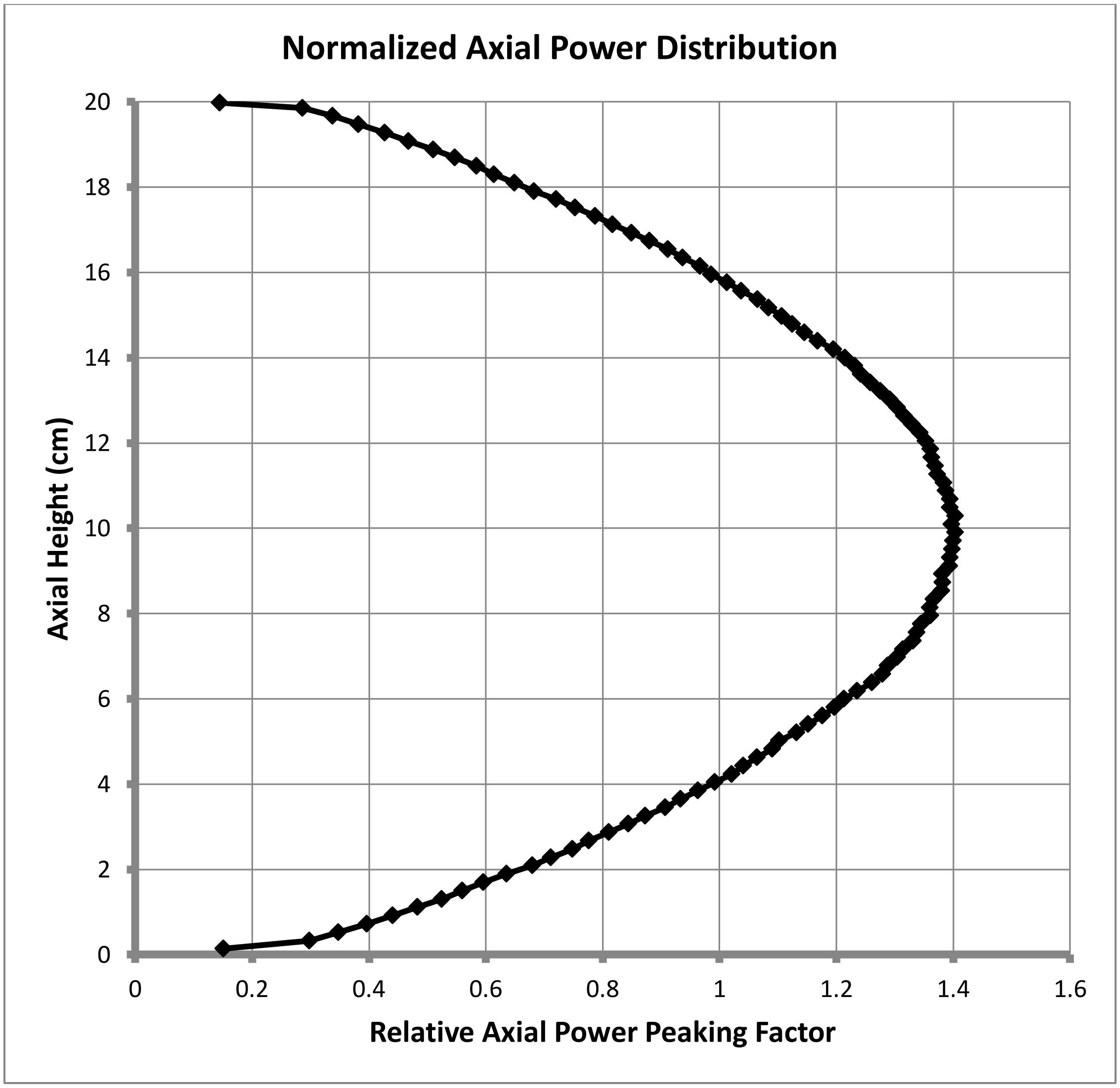

Figure 24. Axial Power Distribution for PWR Cell Model.

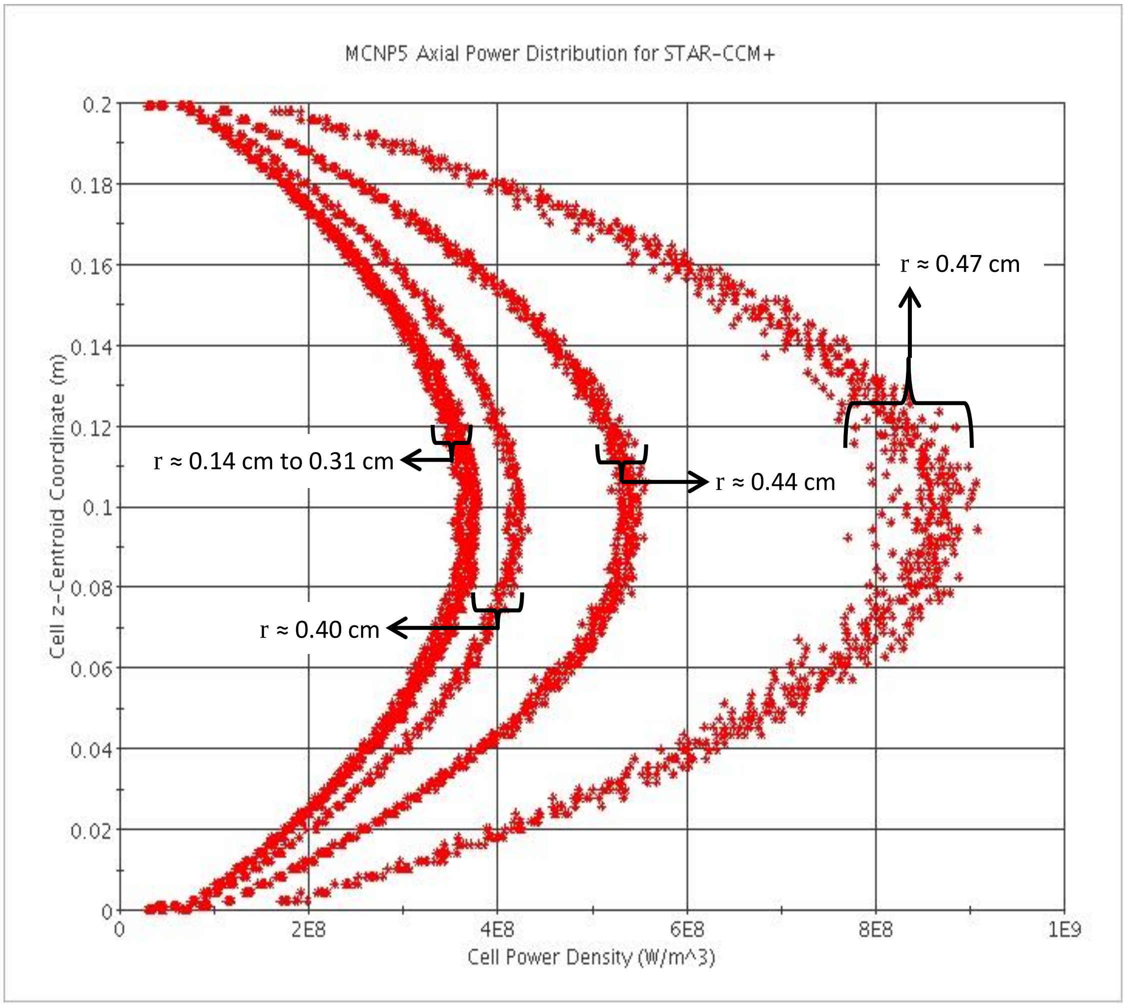

Figure 25. Axial Power Density Distributions for Different Radial Distances from Fuel Centerline.

6.2.8. Temperature Distributions

Figure 26 shows the converged temperatures for computational cells in the fuel as a function of axial location. The fuel cells closest to the center of the pin ($r \approx 0.14$ cm) have the highest temperatures. The maximum fuel temperature is 1464.9 K at $z = 10.3\ cm$ for the PWR cell model.

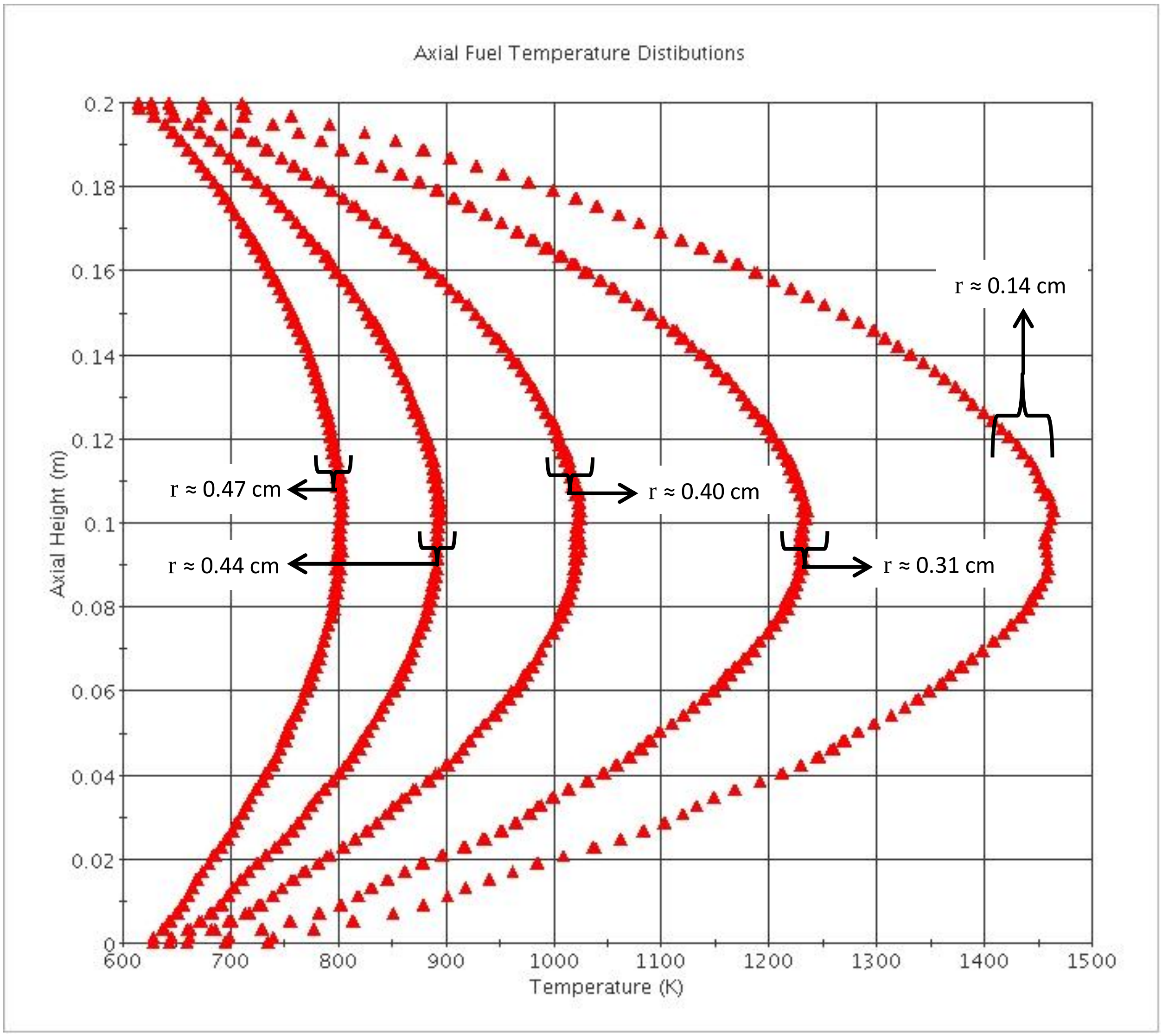

Figure 26. Axial Fuel Temperature Distributions for Different Radial Locations.

Figure 27 shows converged axial temperature distributions for the clad region. MULTINUKE calculates a peak clad temperature (PCT) of 720.1 K at z = 10.9 cm. As shown in Figure 8 in Section 6.1.1, the CFD mesh of the cladding is not radially symmetric like the fuel region, and the clad mesh has less radial cells due to its 0.01 cm thickness. Therefore, the clad cell temperatures in Figure 27 are not necessarily binned by any radial coordinate, and such markings are not included on the figure.

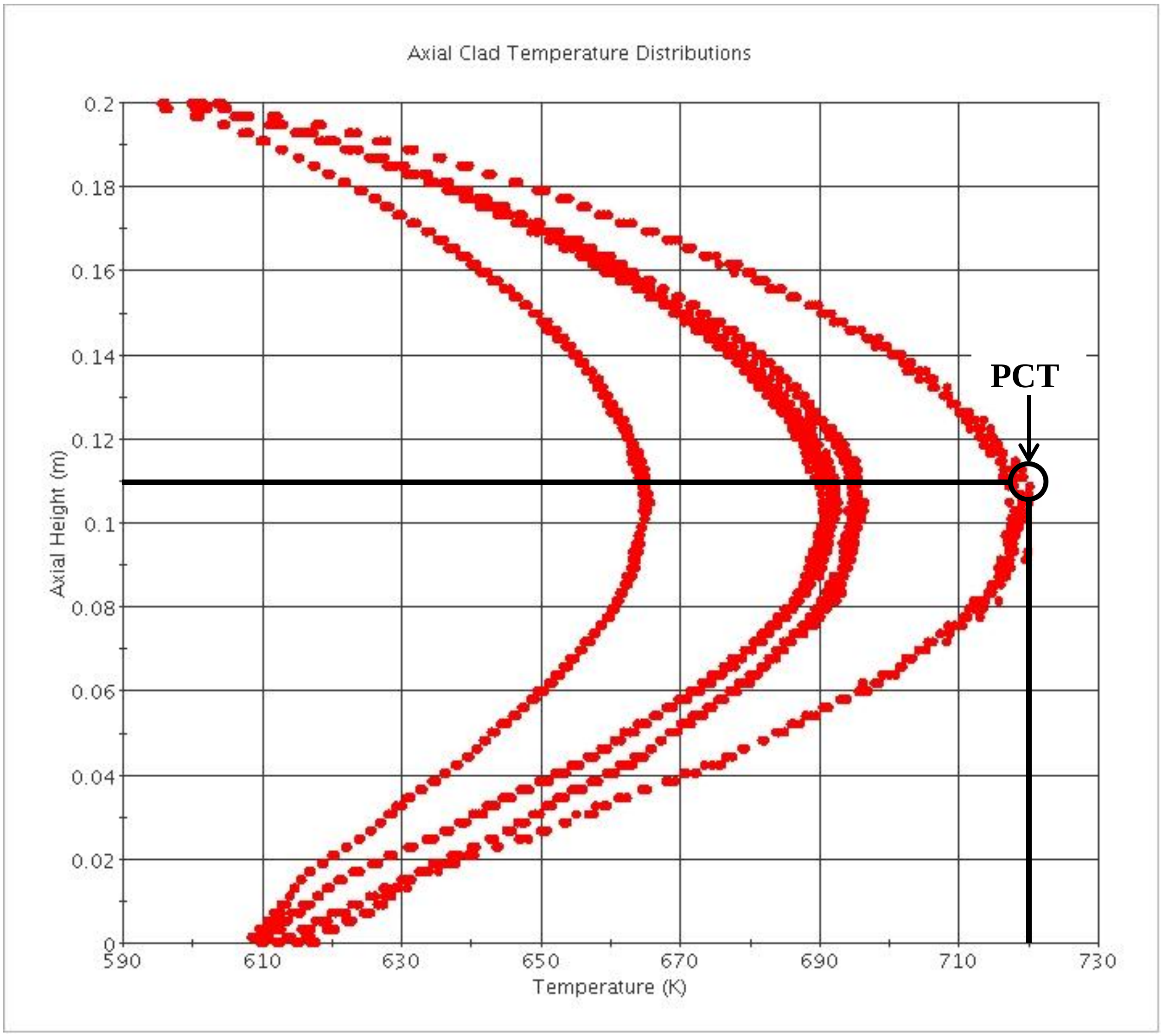

Figure 27. Axial Clad Temperature Distributions.

Figures 28 shows the axial variation of the coolant temperature. The plot contains temperature data for coolant cells in one quadrant of the model (see Figure 8). Axial temperature variation is plotted for cell numbers 1-10 identified in Figure 8. As can be seen, the temperature increases monotonically in some radial locations, while at others the coolant temperature drops near the exit. The temperature drops near the exit in the radial locations (cells 5, 8) where the temperature rise is the fastest. The slight temperature drop near the exit is a result of the shortened axial length of the model and flow mixing. The maximum coolant temperature is 587.9 K, occurring at 16.3 cm from the inlet. The average exit coolant temperature is 581 K, suggesting an average temperature rise of about 11 K for the PWR coolant ($T_{exit} – T_{inlet}$). As stated in Table 11 from Section 6.1.8, the inlet H_2O coolant temperature is set to 570 K for the simulation.

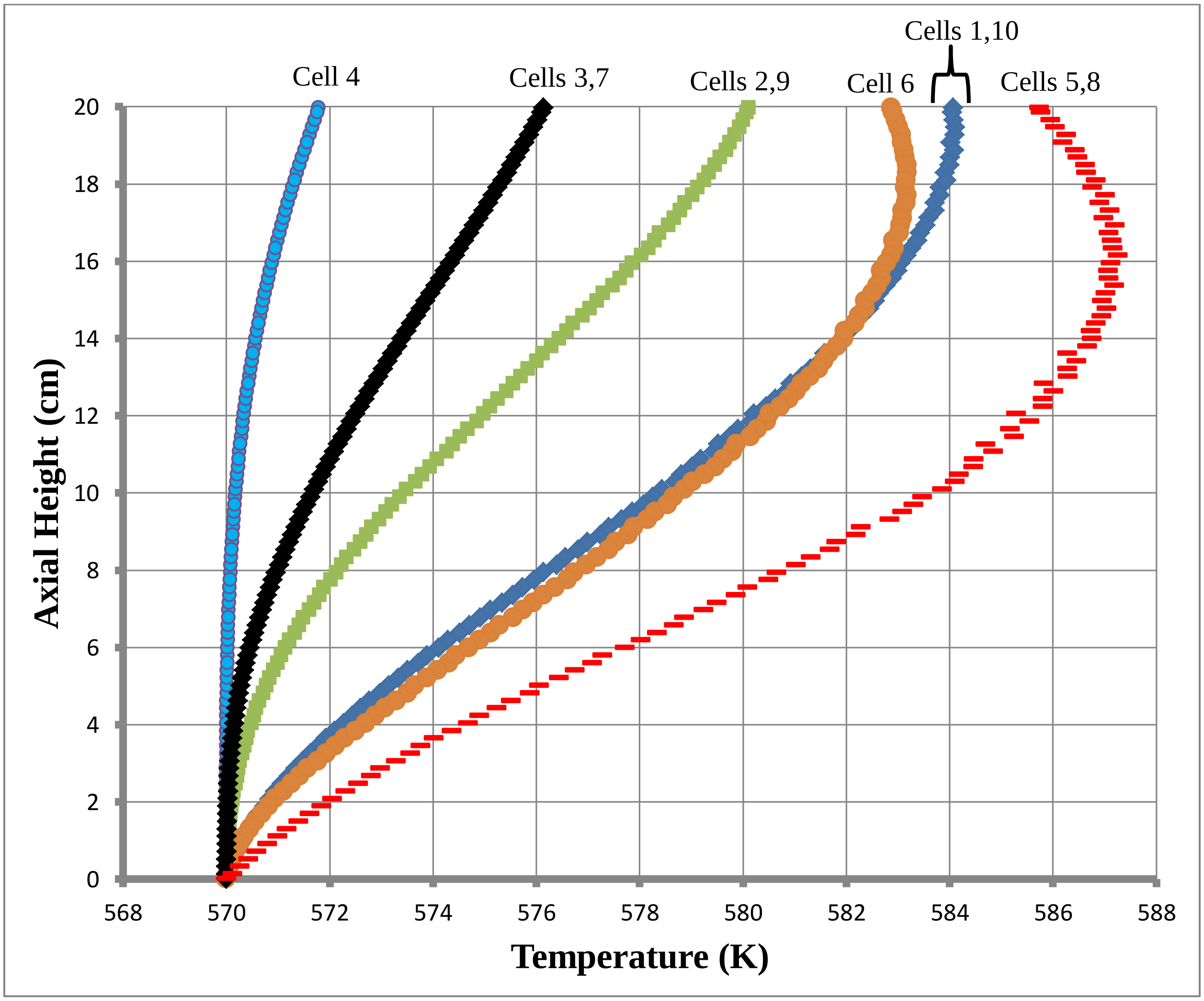

Figure 28. Axial Coolant Temperature Distributions.

Figure 29 shows the axial variation of average coolant density at each axial level. The density distribution of water is direct result of modeling the equation of state using a polynomial temperature representation of the fluid density, as discussed in Section 6.1.7. The converged MULTINUKE simulation of the PWR cell model gives a coolant density range of 687.8 kg/m^3 to 727.9 kg/m^3 (for all radial locations and axial levels). The average coolant density is 716 kg/m^3, corresponding to the average coolant temperature of 575.8 K. The coolant temperature and density variations calculated by STAR-CCM+ are the principal feedback mechanism effecting reactivity and power distributions in MCNP5.

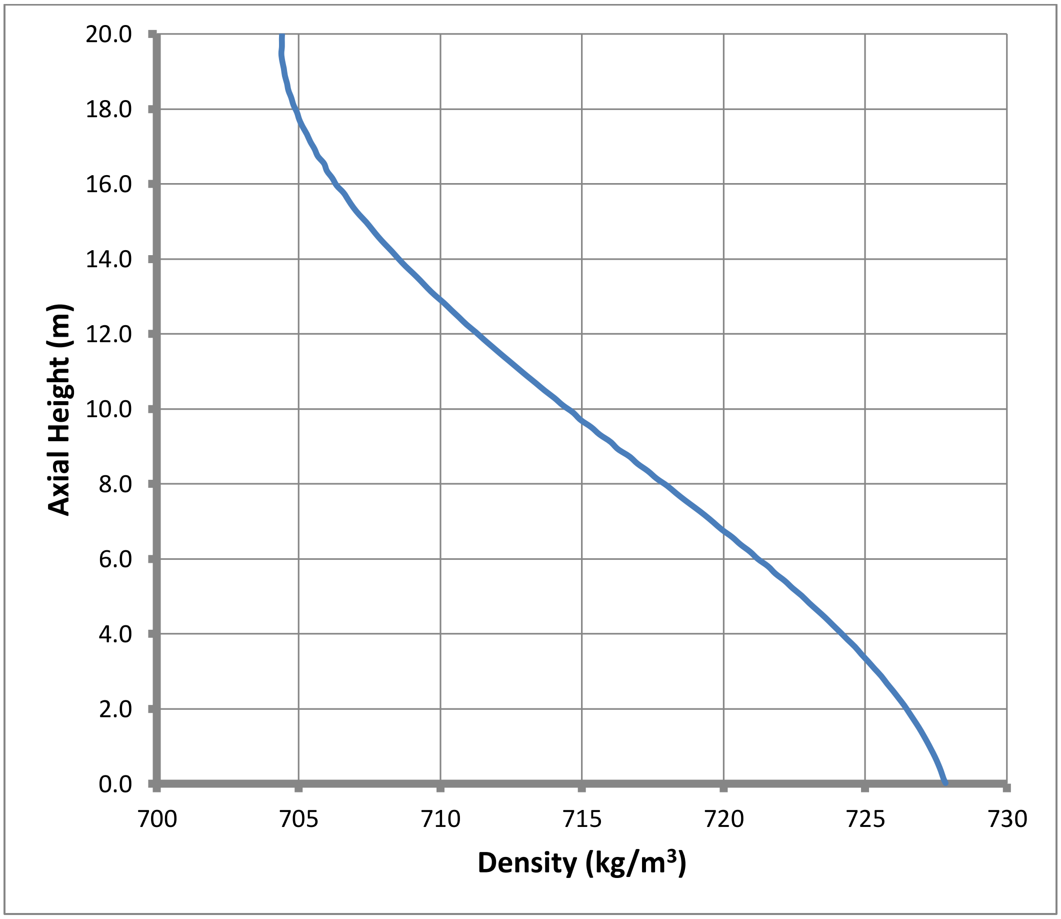

Figure 29. Axial Distribution of Average Coolant Density.

Figures 30 and 31 are three-dimensional views of the fuel and coolant regions of the PWR cell model, generated by the STAR-CCM+ GUI. Figure 30 shows the converged fuel temperature distribution overlaid on the 3D geometric model, while Figure 31 depicts the converged coolant density. The colored data bars do not reflect the entire range of data, but only the range of data on the exterior surfaces visible in the figure. These 3D representations provide further physical understanding and validation of the PWR cell model results. For instance, as shown in Figure 30, fuel temperatures are higher near the centerline and axial midplane of the fuel pin. Figure 31 shows that coolant density is smaller near the exit and clad-coolant surface, due to the fact that coolant temperature is greater in these regions.

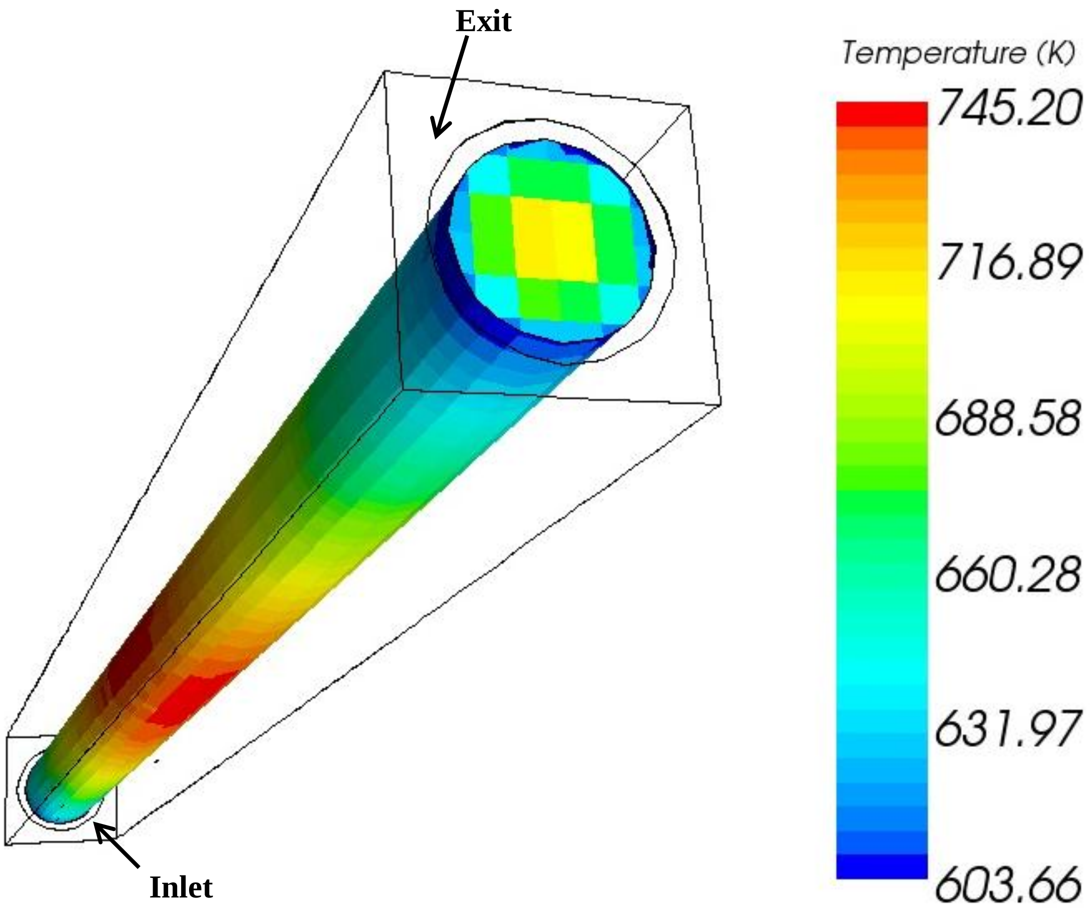

Figure 30. 3D View of Fuel Temperature for PWR Cell Model.

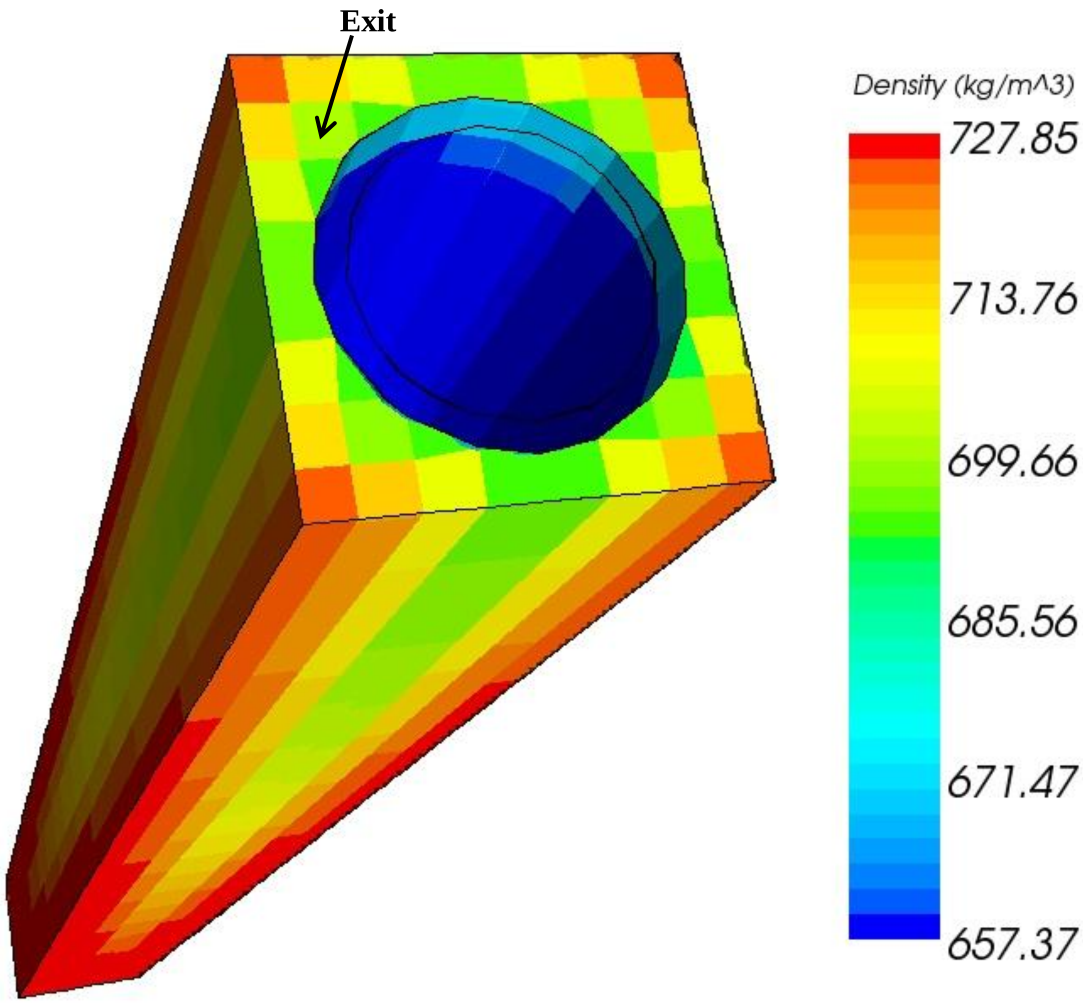

Figure 31. 3D View of Coolant Density for PWR Cell Model.

6.2.9. Reynolds Number and Flow Lines

With an average coolant density of 716 kg/m^3, velocity of 1.0 m/s, and dynamic viscosity of 9.177x10^{-5} Pa-s, the Reynolds number of the flow ($Re = \frac{\rho V D_e}{\mu}$) is approximately 20,000. Clearly, this confirms the fluid flow in the pin model is fully turbulent.

Figure 32 provides a 3D view of the coolant streamlines for the PWR model. The streamline particles are colored according to their approximate velocity magnitudes. Figure 32 illustrates that coolant cells furthest from the clad surface have the greatest velocities, while those in close proximity have lower velocity magnitudes due to no-slip conditions at solid surfaces.

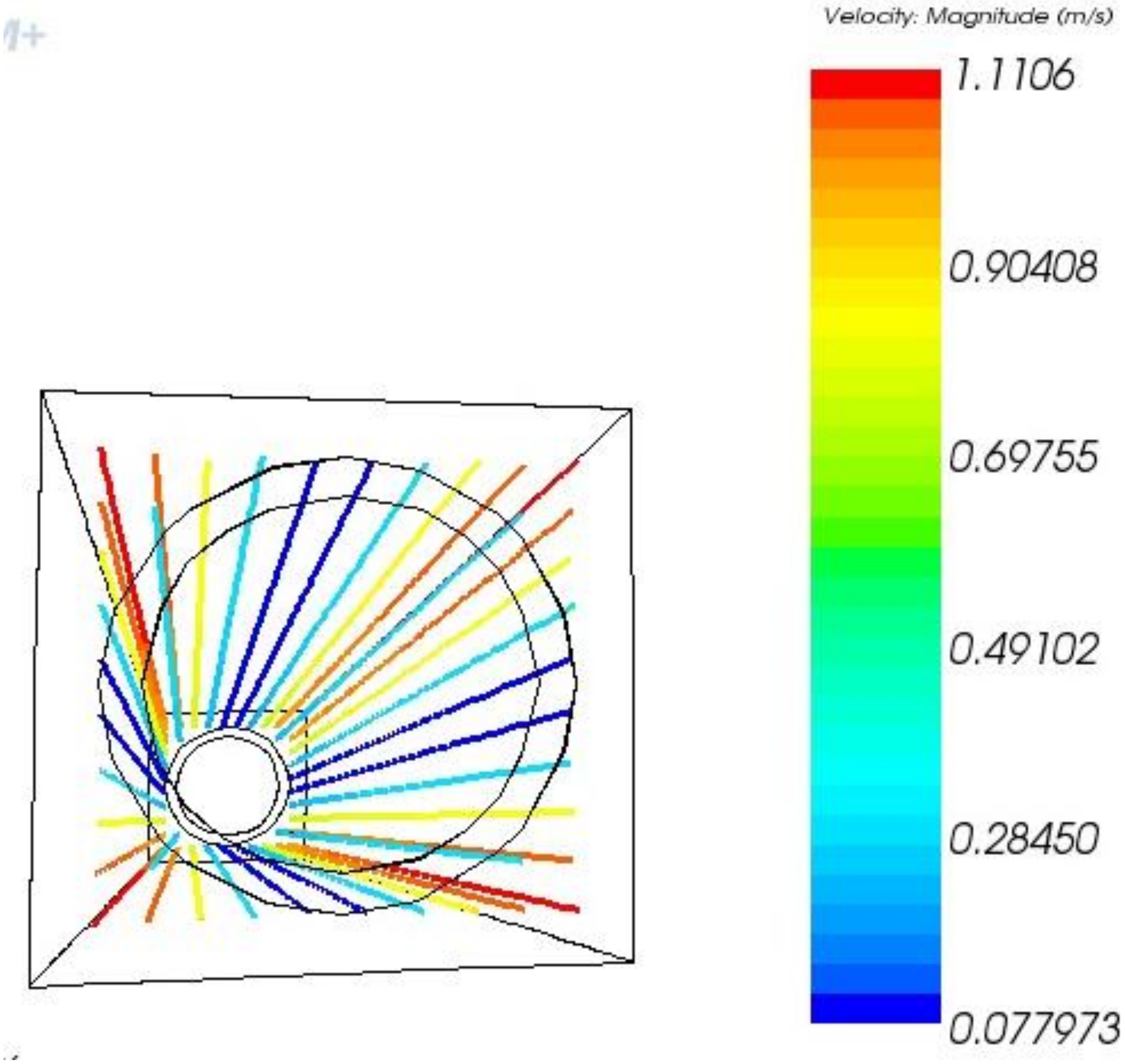

Figure 32. Streamlines for PWR Cell Model (Top-Down View).

6.3. 3 x 3 PWR Model Description

The 3 x 3 PWR model is very similar to the single PWR cell model from Sections 6.1 and 6.2. It is created by expanding the computational mesh for the single cell model in the axial and radial directions. The 3 x 3 model is a more realistic representation of a PWR – consisting of nine fuel elements arranged in a rectangular lattice, with the center fuel element replaced with a control rod guide tube, which is filled with stagnant water. The 3 x 3 model is 400 cm tall, which includes two 25 cm axial cladding and reflector regions at the top and bottom of the model. The active fuel region is 350 cm tall. The 3 x 3 PWR model uses the same cross section database and material properties that were used for the single PWR cell model. Furthermore, the same physics and solver options (including turbulence modeling) for STAR-CCM+ are used, which were described in Section 6.1.

The 3 x 3 PWR model has a computational mesh with 89,856 CFD cells distributed over 104 axial nodes (the radial grid structure is the same for each axial level). For the neutronic model, an equivalent mesh is created in MCNP5, except the clad regions are lumped into one cell for each fuel element. The mesh for the 3 x 3 model uses the mesh from the 20 cm tall PWR cell model and stretches it axially to create a model that is 400 cm tall. This 400 cm tall fuel cell is then replicated and translated in the *x* and *y* directions to create the other eight fuel cells. Figure 33 shows the CFD mesh and neutronic mesh for the 3 x 3 PWR model. Continuous boundary conditions are specified on the interfaces of the coolant regions between each fuel cell. The model is infinite in the *x* and *y* directions, with symmetry boundary conditions specified on the outer *x* and *y* surfaces. Axial neutron leakage is allowed on the top and bottom *z* surfaces. Coolant flows in through the bottom surface with a uniform speed of 1 m/s at a temperature of 550 K, and exits the top surface through a pressure outlet (the system pressure is 15.5 MPa).

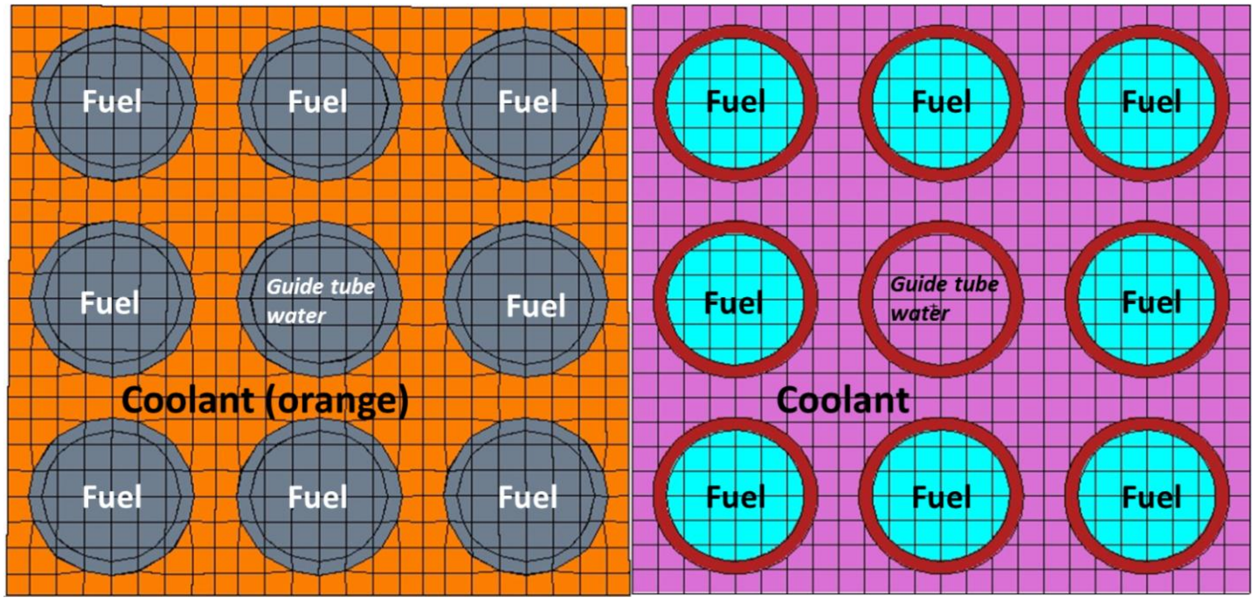

Figure 33. Computational Mesh for STAR-CCM+ (left) and MCNP5 (right) for 3 x 3 PWR Model.

The results presented in Section 6.4 are for the fuel elements with higher power output, since these fuel elements have the highest fuel, clad, and coolant temperatures. Specifically, the CFD results are for *element 2* shown below in Figure 34. The power and temperature distributions for the other fuel elements are very similar to those of *element 2*. Also depicted in Figure 34 are the relative power produced in each fuel pin normalized to the average (calculated using MCNP5). Fuel elements 2, 4, 6 and 8 produce about 22.4% more power than the other fuel elements (1.2 compared to 0.98, respectively). The relative power produced in each fuel element is constant throughout the iterative calculation process in MULTINUKE, due to the model's symmetry in the *x-y* plane.

The even-numbered fuel elements are in closer proximity to the control rod guide tube (element 5), which is filled with water. Due to the lack of a highly absorbing fuel or control material in the guide tube, the central region of the model is a source of thermal neutrons. The closer even-numbered fuel elements act as a thermal neutron shield to the other fuel elements.

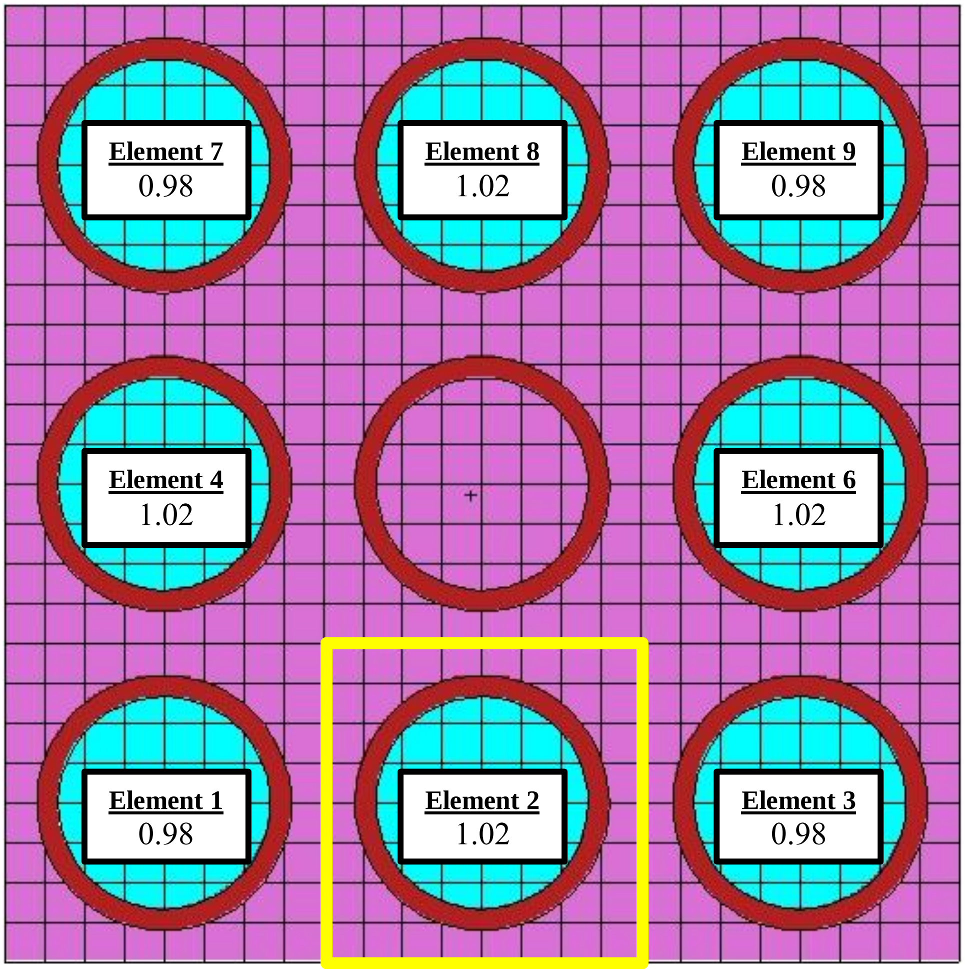

Figure 34. Fuel Element Numbering Scheme and Relative Fuel Region Powers for 3 x 3 PWR Model.

Table 17 contains parameters for the 3 x 3 PWR model, and subsequent mesh and simulation. The fuel diameter is 1.0 cm, and the outer clad diameter is 1.2 cm, resulting in a 0.1 cm cladding thickness with no fuel-clad gap modeled. The lattice has a pitch of 1.5 cm and an axial height of 400.0 cm, which includes two 25 cm axial reflector regions. The nuclear fuel material is UO_2 with 5 w/o U-235 enrichment. Cladding is made of Zircaloy-4 and liquid water is the coolant and neutron moderator.

Table 17. Model Parameters for 3 x 3 PWR Model.

Lattice Data	Value
Fuel Outer Diameter (cm)	1.0
Fuel Cladding Outer Diameter (cm)	1.2
Fuel Cladding Thickness (cm)	0.1
Fuel Rod Pitch (cm)	1.5
Active Fuel Length (cm)	350.0
Total Axial Length Including Reflector Regions (cm)	400.0
Number of Possible Fuel Pin Locations	9
Fuel Material	UO_2
Fissile Material Enrichment	5 w/o U-235
Cladding Material	Zircaloy-4
Coolant/Moderator Material	Liquid H_2O
Mesh Data	**Value**
Mesh Type	Prismatic Hexahedral
Total STAR-CCM+ Cells	89,856
Number of Radial STAR-CCM+ Cells per Axial Node	864
Number of STAR-CCM+ Axial Nodes	104
Total MCNP5 Cells	67,392 fuel/water cells + 9 clad cells
Number of Radial MCNP5 Cells per Axial Node	648 (fuel + water)
Number of MCNP5 Axial Nodes	104
Number of MCNP5 Tally Regions (UO_2 Cells)	29,952

Table 18 shows the initial thermal-hydraulic conditions for the PWR model. These initial conditions only serve as the “initial guess” for the steady state problem.

Table 18. Initial Thermal-Hydraulic Conditions for 3 x 3 PWR Model.

Initial Parameter	Value
UO_2 Fuel Continua Temperature (K)	850.0
Fuel-Clad Interface Temperature (K)	800.0
Zircaloy-4 Clad Continua Temperature (K)	650.0
Clad-Coolant Interface Temperature (K)	650.0
H_2O Coolant Continua Temperature (K)	560.0
H_2O Coolant Inlet Temperature (K)	550.0
H_2O Coolant Inlet Speed (m/s)	1.0
H_2O Coolant Initial Pressure (Pa)	$1.55x10^7$
H_2O Coolant Exit Pressure (Pa)	$1.50x10^7$
Initial Turbulence Specification	Intensity + Viscosity Ratio
Turbulence Intensity	0.01
Turbulent Viscosity Ratio	10.0

Assuming the 3 x 3 model represents an average sub-assembly of a PWR with a power density of 10^8 W/m^3, a power rating of 220 kW is designated in the *muliSpecs_base.txt* input file. The UO_2 fuel density is selected to be 10.3 g/cm^3, and it is assumed that each fission releases 200 MeV of energy. Rather relaxed MULTINUKE convergence criteria are selected in order to reduce computation time. Once two successive iterations yield a difference of less than 0.0010 eigenvalue (Δk) and less than 10% average change in cell temperatures, the solution is considered to be converged. Table 19 contains some important input data for MULTINUKE to analyze the 3 x 3 PWR model.

Table 19. 3 x 3 PWR Input Data for MULTINUKE.

Input Data	Value
Job Name	cell400cm3x3
Fuel Density (g/cm^3)	10.3
Power Output (kW)	220.0
Q – Energy Released per Fission (MeV/fission)	200.0
Eigenvalue Convergence (Δk)	0.0010
Temperature Convergence (fraction % difference)	0.10

6.4. 3 x 3 PWR Model Results

6.4.1. Neutronic Convergence of 3 x 3 PWR Model

Figure 35 and Figure 36 respectively depict convergence of eigenvalue and fission source entropy for a typical MCNP5 simulation of the 3 x 3 model. MCNP5 is run with 40,000 neutron histories per cycle for 210 total cycles, while discarding the first 60 batches, for every MCNP5 calculation in MULTINUKE. The cycle discard number is shown at the 60th cycle in Figures 35 and 36 by the red vertical line. Discarding the first 60 cycles of each MCNP5 calculation proved effective in allowing sufficient convergence of the eigenvalue and source distribution.

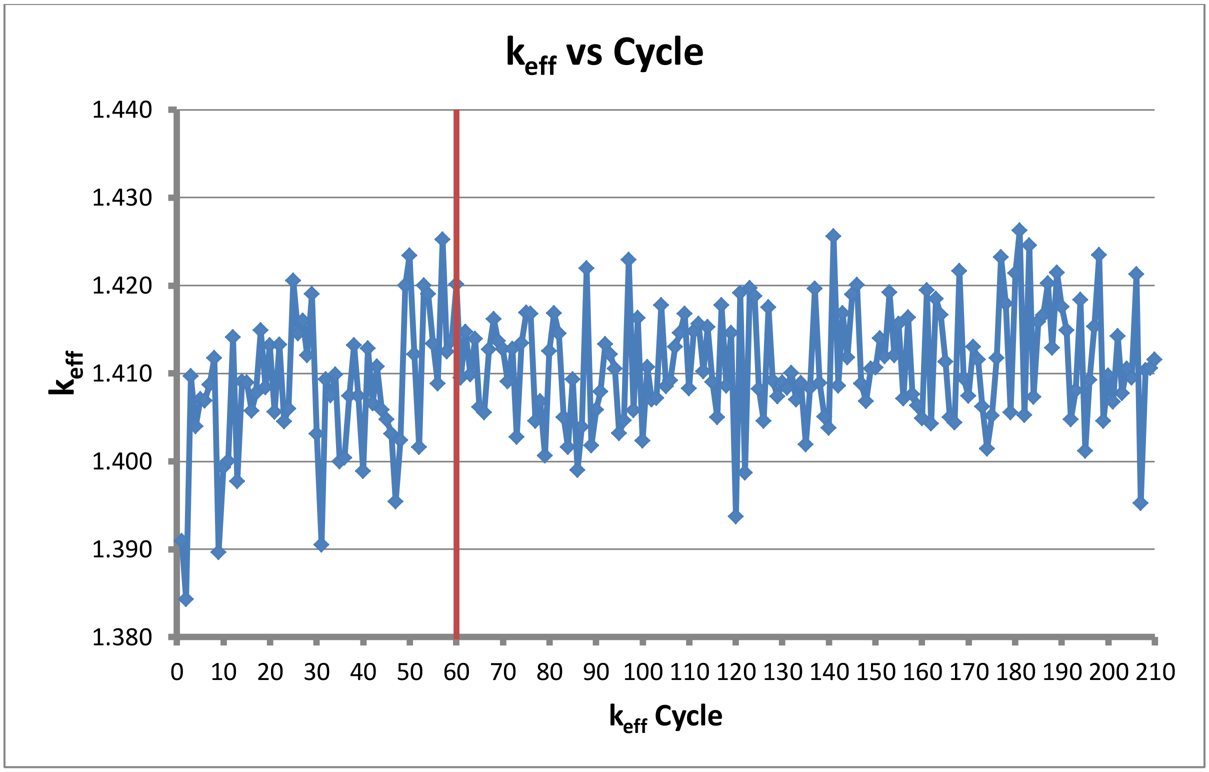

Figure 35. Eigenvalue Convergence for MCNP5 Simulation of 3 x 3 PWR Model..

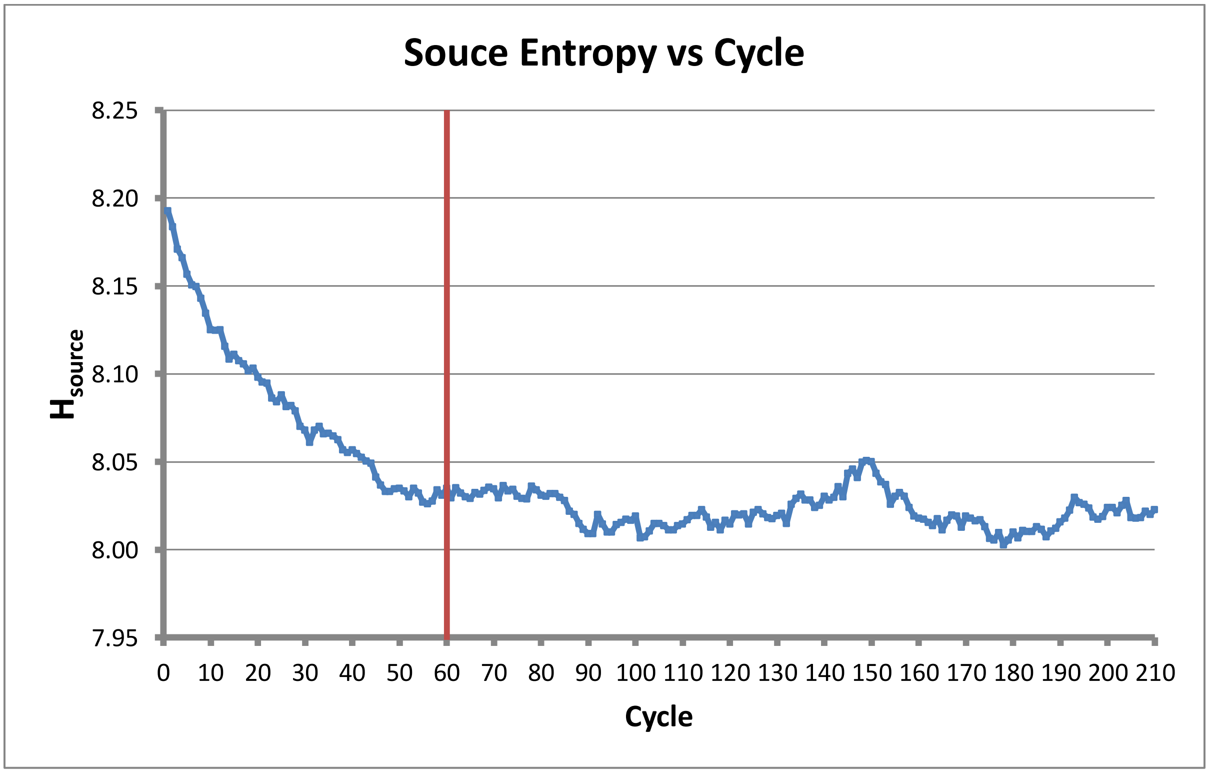

Figure 36. Fission Source Convergence for MCNP5 Simulation of 3 x 3 PWR Model..

For every MCNP5 calculation for the 3 x 3 PWR model, the fission energy deposition tally passed all ten statistical checks and nearly all of its cell tally bins had relative errors less than 0.10. Figure 37 is a scatter plot of relative error versus relative fission reaction rate, normalized to the average fission reaction rate, for a typical MCNP5 calculation of the 3 x 3 PWR model. The red horizontal line represents the maximum desired relative error. 99.98% of the green data points fall below the maximum desired relative error of 0.10.

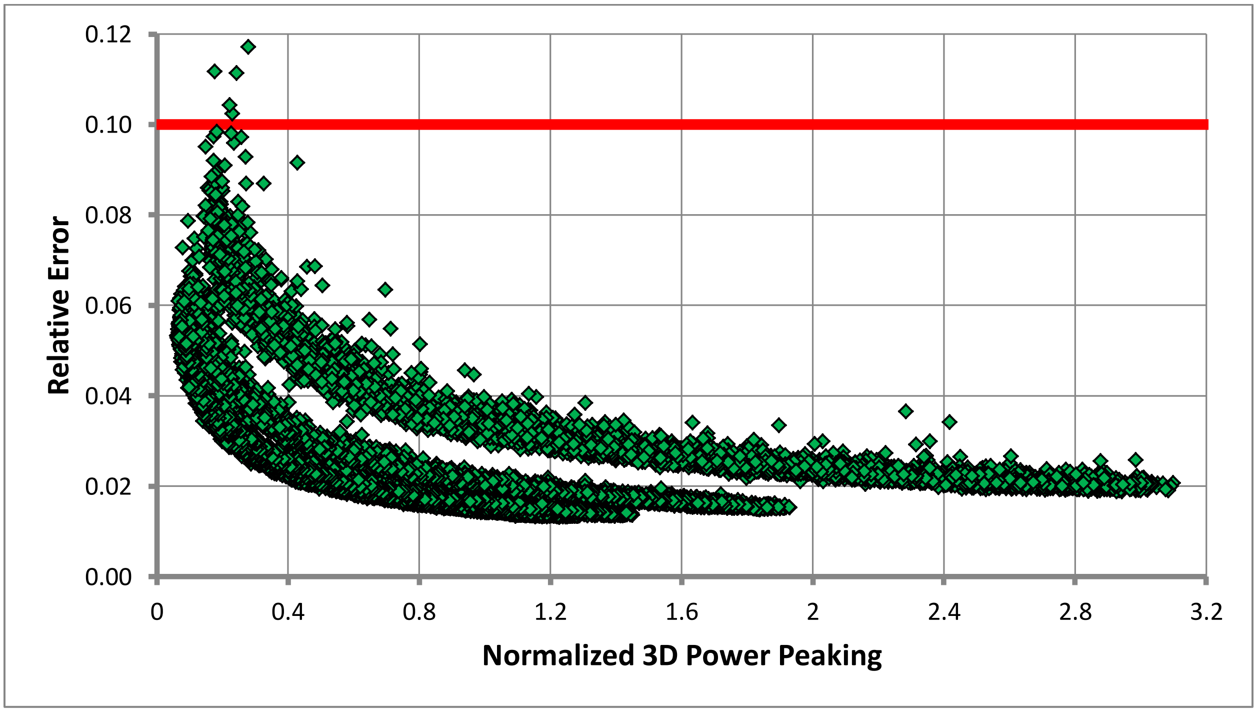

Figure 37. Relative Error vs. Relative Power for Each Fuel Cell in 3 x 3 PWR Model.

6.4.2. Coupled Neutronic and Thermal-Hydraulics Results

An eigenvalue convergence of 0.0010 Δk (see Table 19) is specified for the neutronic portion of the MULTINUKE solution. As shown in Table 20 and Figure 38, the eigenvalue calculated by MCNP5 converges to 1.41469 ± 0.0005 by the third MULTINUKE iteration, which deviates from the k_{eff} from the second iteration by only 0.00057 Δk. This variation in k_{eff} satisfies the 0.0010 Δk eigenvalue convergence criterion specified in the MULTINUKE input file, *multiSpecs_base.txt*. The MULTINUKE simulation of the 3 x 3 PWR model takes approximately 5 days and 10 hours (~7,800 minutes) to converge.

Table 20. k_{eff} Values for Each MULTINUKE Iteration.

CASE	k_{eff}	Standard Deviation	k_{eff} 95% Confidence Interval			Δk from previous iteration
iteration 0	1.41126	0.00025	1.41126	±	0.0005	----
iteration 1	1.41923	0.00023	1.41923	±	0.0005	0.00797
iteration 2	1.41412	0.00023	1.41412	±	0.0005	0.00511
iteration 3	1.41469	0.00023	1.41469	±	0.0005	0.00057

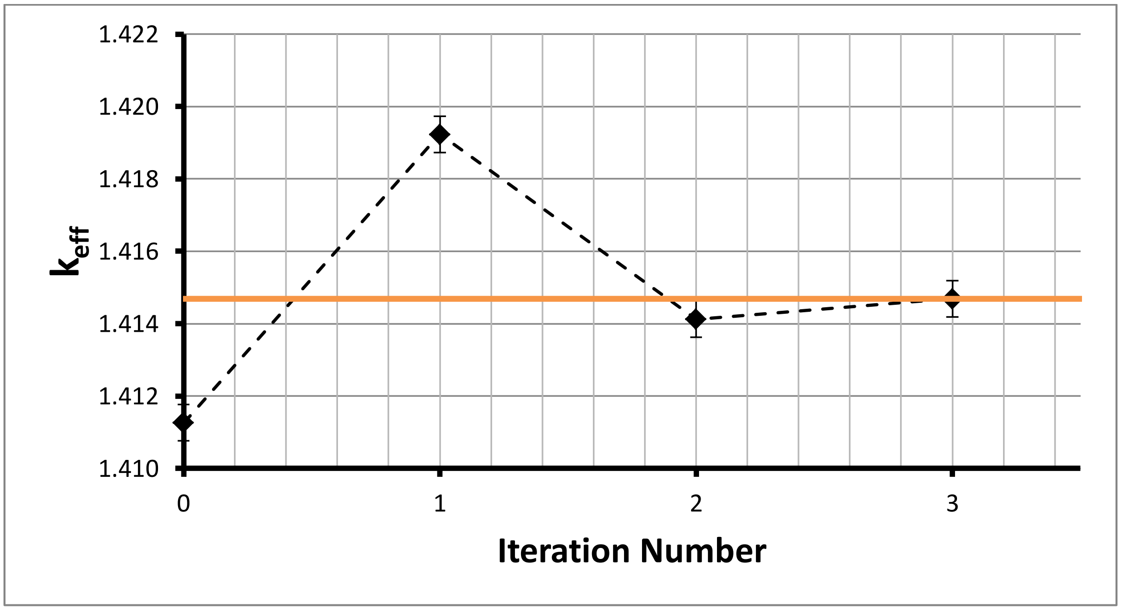

Figure 38. Eigenvalue Convergence for 3 x 3 PWR Model.

Figure 39 shows the CFD residuals for iteration 3 of the 3 x 3 PWR model. It demonstrates that STAR-CCM+ performed a sufficient number of internal CFD iterations to provide valid temperature and density distributions for the 3 x 3 PWR model. STAR-CCM+ is allowed to perform 9,000 CFD iterations before thermal-hydraulic data is extracted. As seen in Figure 39, the residuals for the governing equations are converged after about 7,000 iterations.

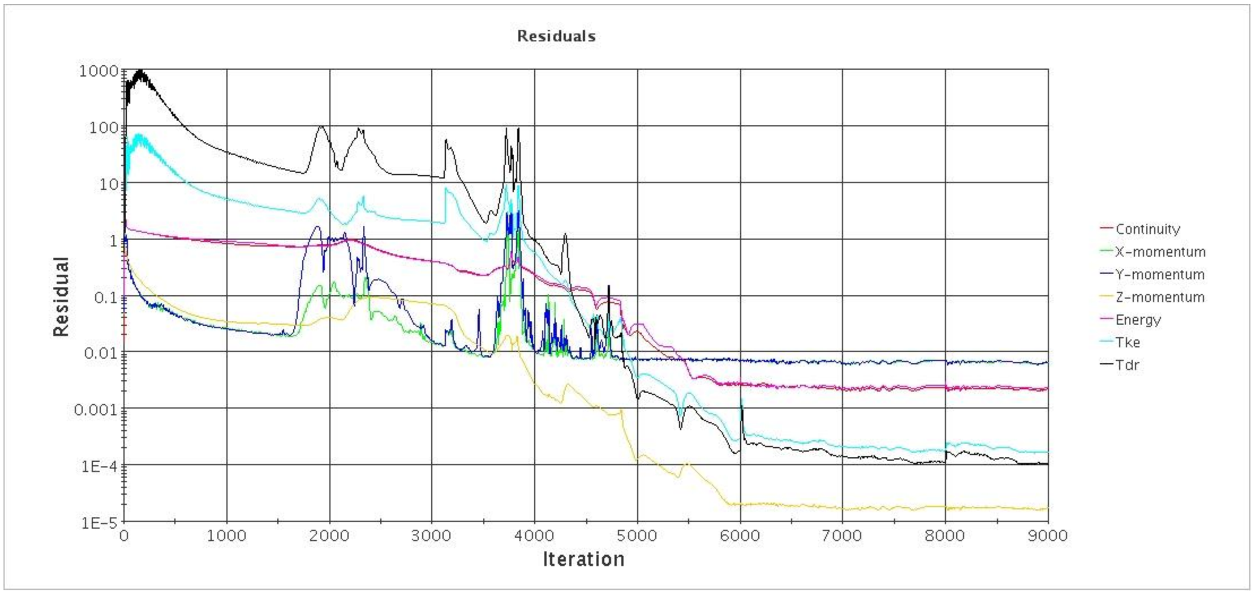

Figure 39. CFD Residuals Convergence for 3 x 3 PWR Model.

Figure 40 shows normalized axial power distributions for each MULTINUKE iteration of the PWR lattice model. Axial power peaking converges to the red curve by iteration 3. More power is generated in the lower half of the model due to significantly lower moderator temperature (and thus higher density) in this region. The coolant temperature increases by almost 50 K in the first MULTINUKE iteration, due to the model's high power level and slow coolant velocity. This causes the coolant density to be significantly less in the upper region of the model, shifting thermal neutron flux and power to the lower region.

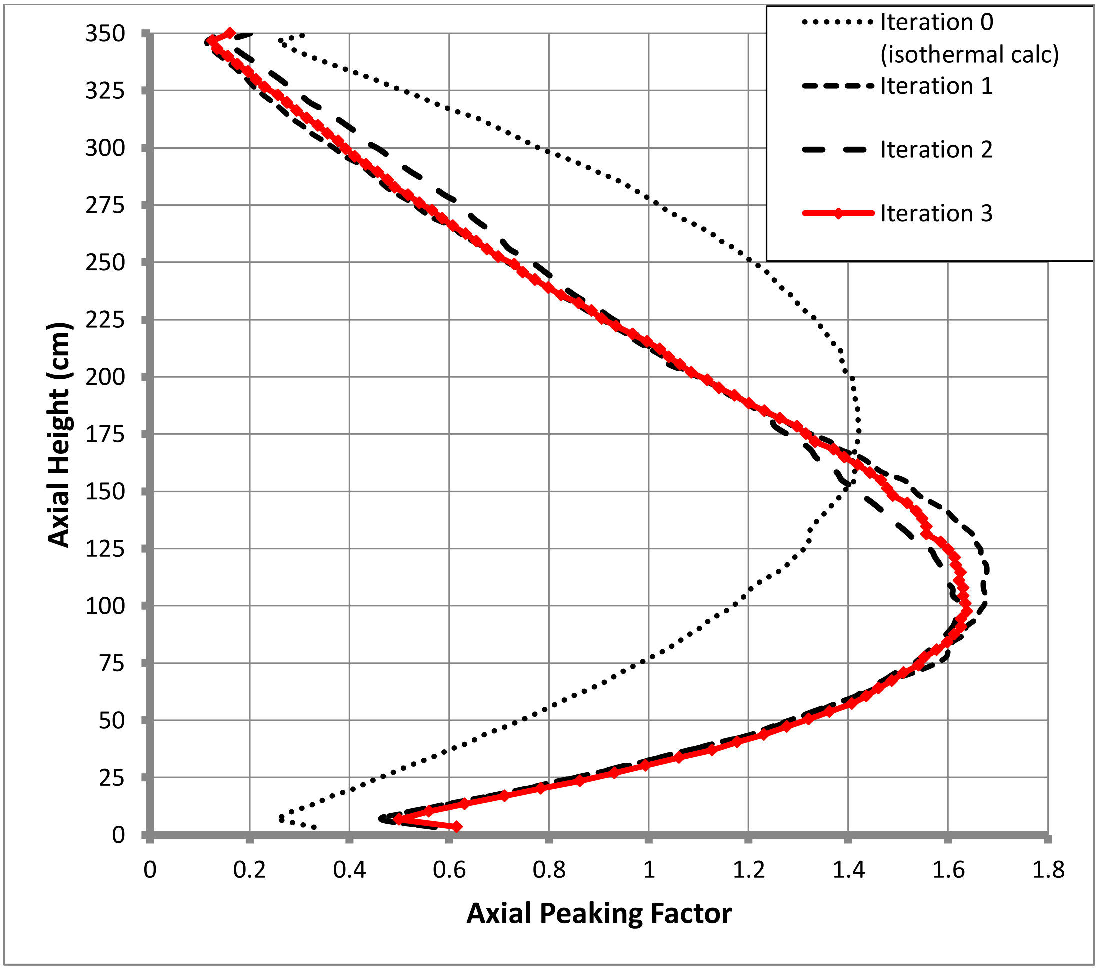

Figure 40. Converged Axial Power Peaking for 3 x 3 PWR Model.

Figure 41 shows the power density data, calculated using MCNP5, given to STAR-CCM+ for the final MULTINUKE iteration. Fuel cells near the edge of the fuel pin are exposed to greater thermal neutron flux compared to cells near the fuel center, due to self-shielding. The outer fuel cells therefore have greater fission reaction rates and higher power densities, as shown in Figure 41. However, power densities shift to the lower half of the model in iteration 3.

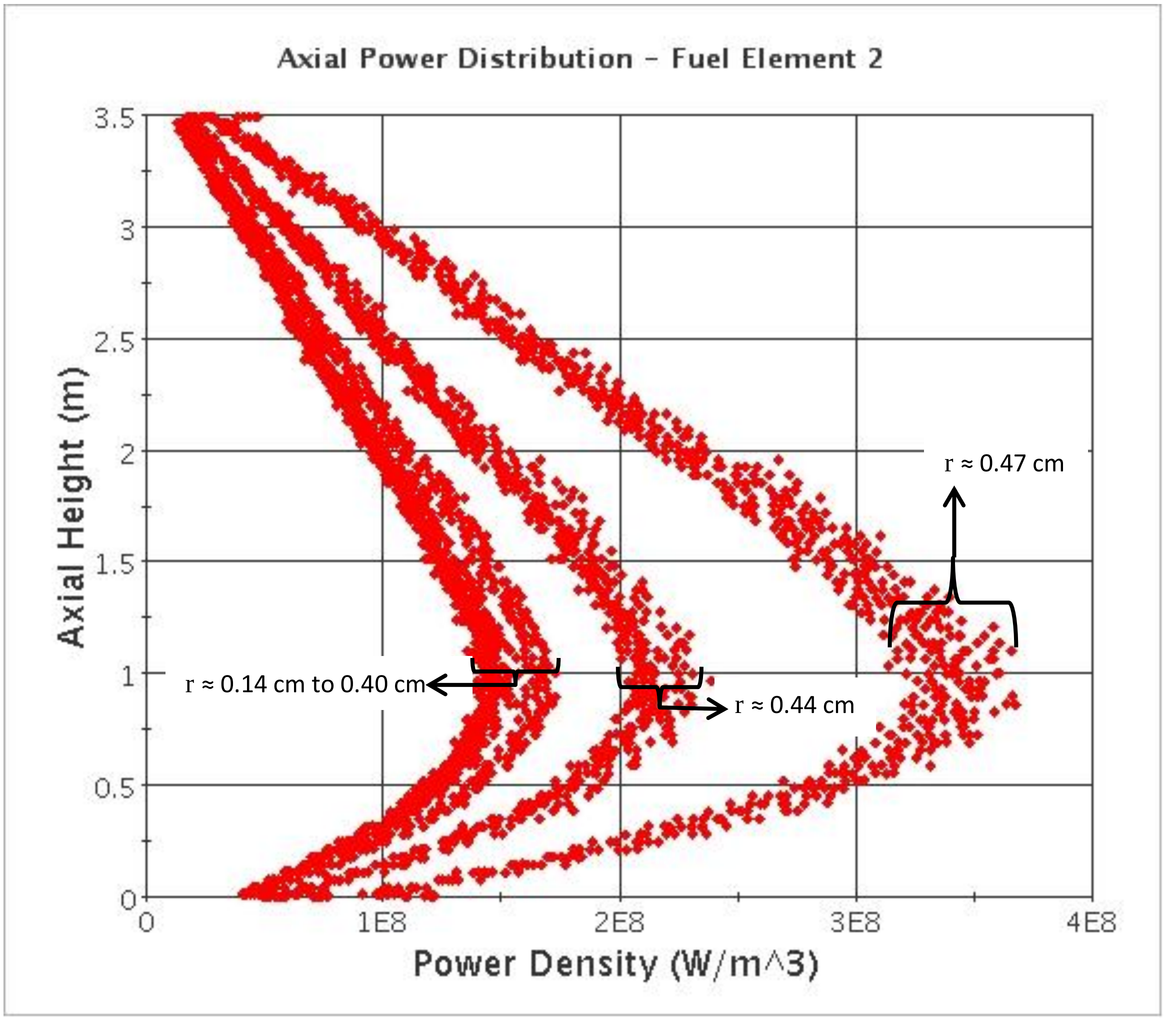

Figure 41. Axial Power Density Distributions for Different Radial Distances from Fuel Centerline in Fuel Element 2 (Iteration 3).

A contour plot of the radial power distribution at *z* = 117 cm (where power density is highest in Figure 41) is shown by Figure 42. It confirms that power density, and thus fission reaction rates, are greatest near the edge of each pin (as shown in Figure 41). The data for Figure 42 is from a MCNP5 mesh tally, where a tally grid is superimposed over the actual problem geometry. The grid used for the mesh tally in Figure 42 is of higher resolution than the computational mesh used for the coupled MULTINUKE simulation, which is shown by the black lines. Hence, the mesh tally contains more detailed radial power information than the MULTINUKE mesh in Figure 41. The contour data is normalized tally data obtained directly from MCNP5.

In Figure 42, the maximum power density is approximately 0.0087 MeV/g/s (per starting neutron). This is equivalent to 3.80x10^8 W/m^3, which is only about 2 % greater than the maximum power density calculated by MCNP5 with the coarser MULTINUKE mesh (3.73 x10^8 W/m^3 from Figure 41). Power density is greatest at the edges of the fuel regions closest to the control rod guide tube, which is filled with water and thus creates a region of high thermal neutron flux in the center of the model.

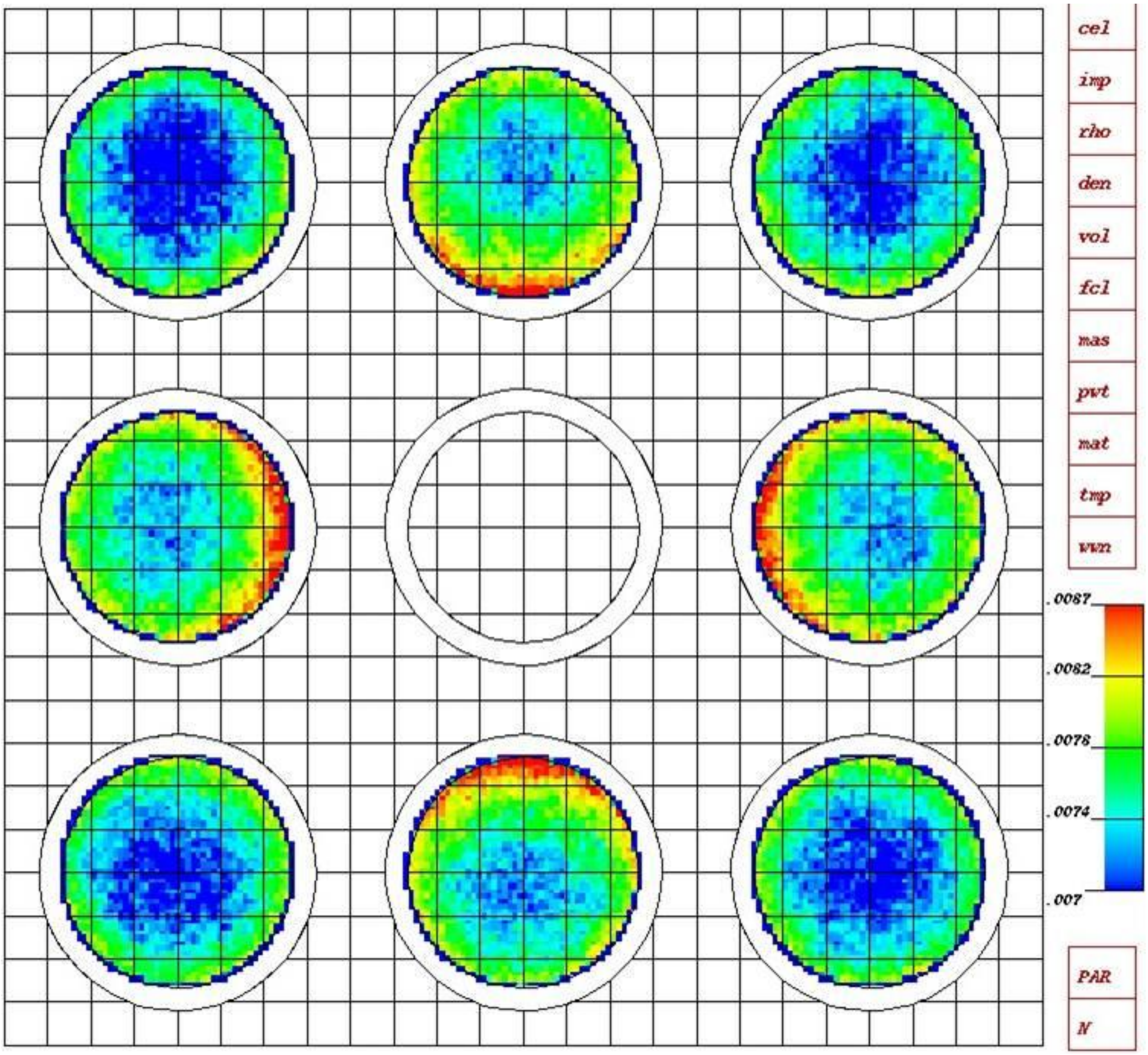

Figure 42. Radial Power Density Distribution at *z* = 117 cm (Iteration 3).

Figure 43 shows the axial distribution of fuel temperatures in element 2 for different radial distances from the fuel centerline. As seen in Figure 43, fuel cells near the center of the pin have higher temperatures. The maximum fuel temperature is about 922 K, occurring at *z* = 0.98 m.

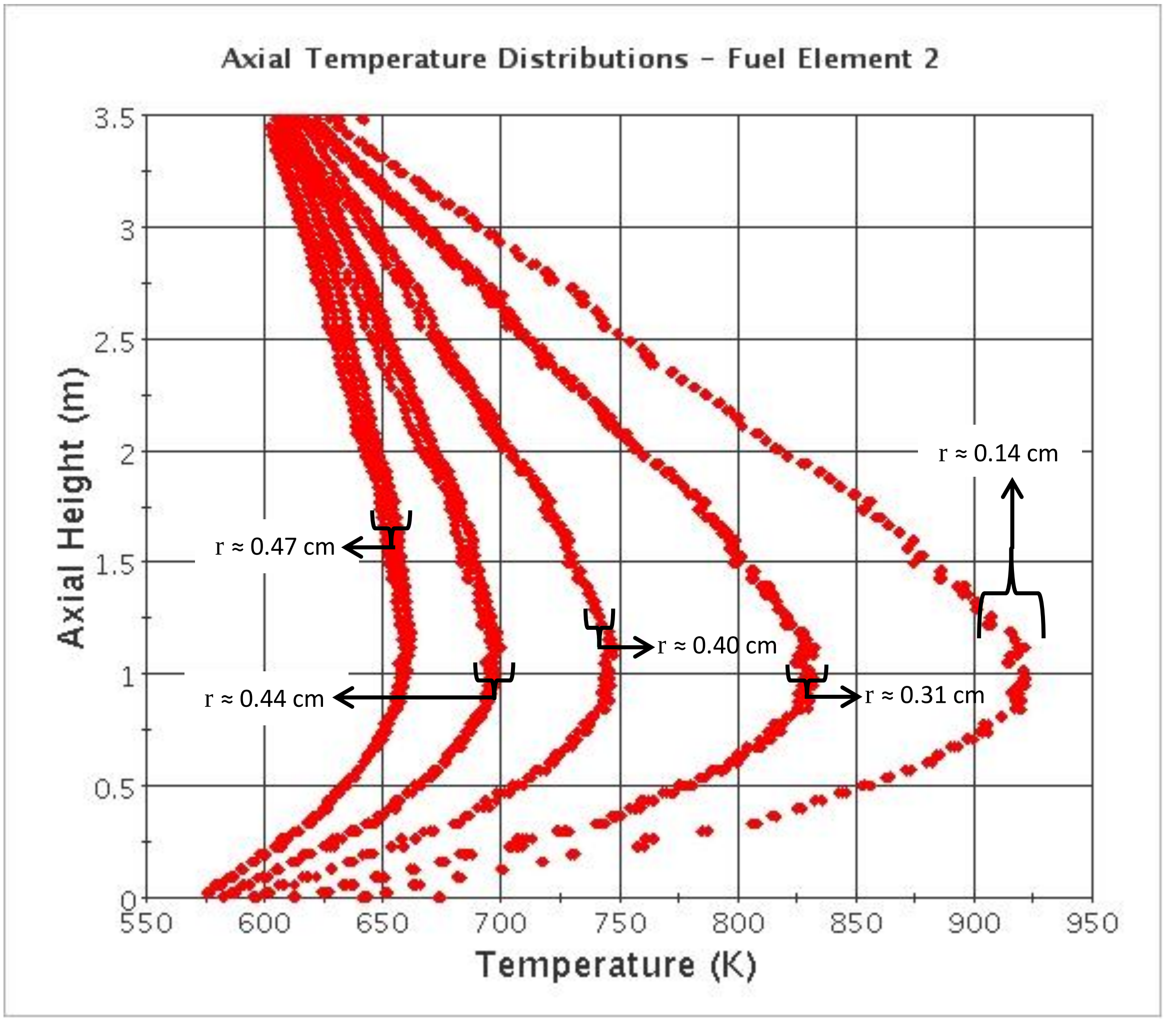

Figure 43. Axial Fuel Temperature Distributions for Different Radial Locations in Element 2 (Iteration 3).

Figure 44 shows the axial distribution of the maximum fuel temperatures at each axial level, comparing the first iteration to the third iteration. Figure 44 shows that the maximum fuel temperature for the third iteration is greater than that of the first iteration (and occurs lower in the model), which is due to the axial power distribution being compressed to the lower part of the model. The temperature distributions for the fuel, clad, and water regions for the second iteration nearly match those from the third iteration, and are therefore omitted from the following temperature plots.

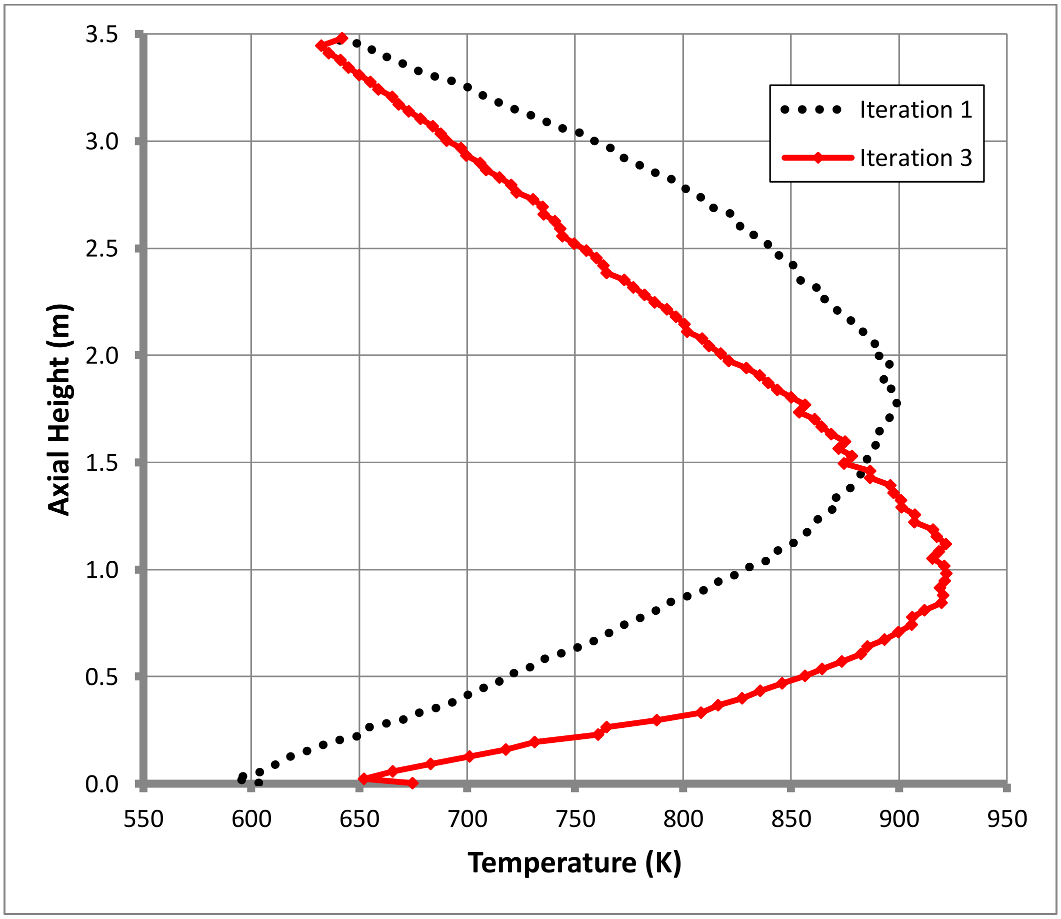

Figure 44. Maximum Axial Temperatures for Fuel Region in Element 2.

Figure 45 shows the axial distribution of the maximum cladding temperatures at each axial level, comparing the first iteration to the last iteration. Figure 45 shows that PCT for iteration 3 is approximately 629.4 K, occurring at *z* = 1.6 m. The PCT for iteration 3 occurs lower in the model than the PCT from iteration 1. PCT for iteration 3 is also slightly less (629.4 K compared to 632 K for iteration 1), most likely due to PCT being located in the lower region of the model where coolant temperatures are significantly less than they are in the upper region, thereby enhancing the cooling of the cladding region.

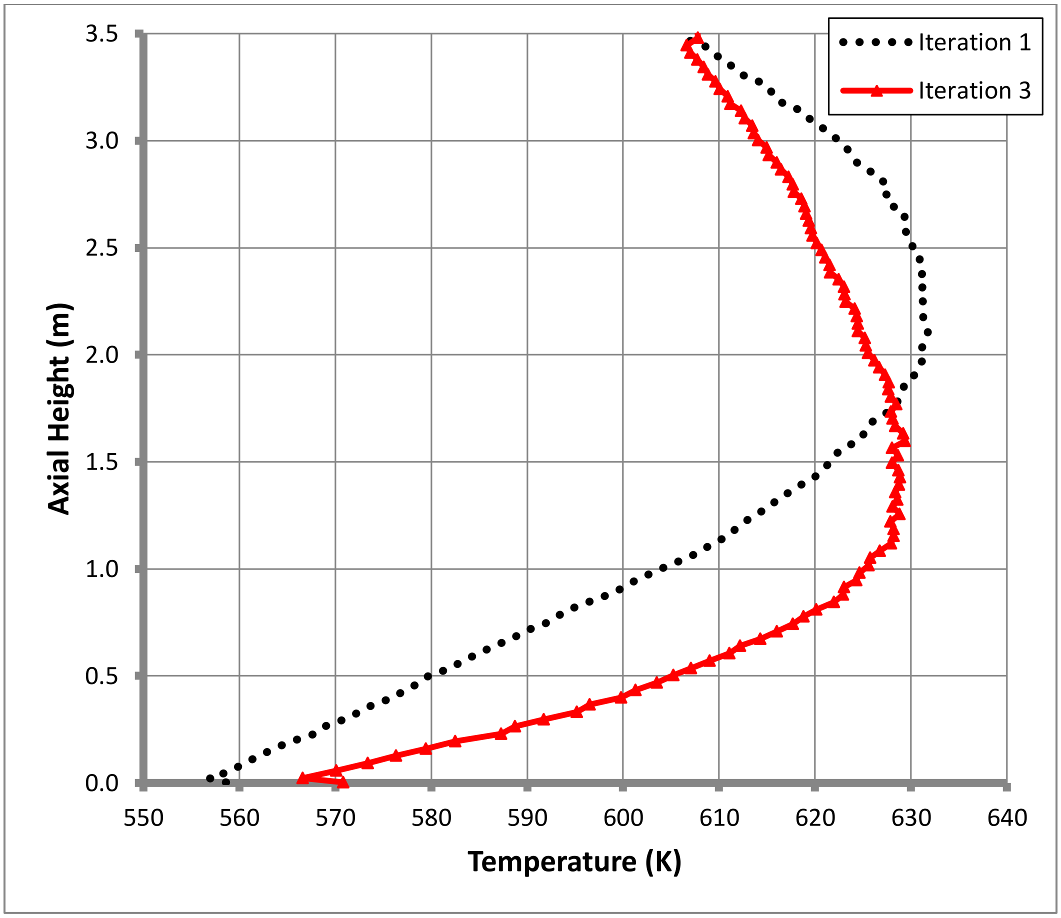

Figure 45. Maximum Axial Temperature Distribution for Clad Region in Element 2.

Figure 46 shows the axial distribution of average and maximum coolant temperatures at each axial node for the first and third iterations. For all of the MULTINUKE iterations, the coolant enters the model at 550 K and exits with an average temperature around 596 K (average ΔT ≈ 46 K). The temperature rise is so high due to the relatively slow inlet velocity (a constant 1 m/s) for the power level of the model (220 kW). The temperature-polynomial (eqn. (6.2)) for the water density may also need to be improved. The large temperature difference between the upper and lower regions of the model is the cause of the bottom-peaked power distribution shown in Figure 40. Figure 47 shows the axial distribution of average coolant density at each axial level. The coolant density in the lower region of the model is greater than the density in the upper region, which results in higher thermal neutron flux and power densities in the lower region.

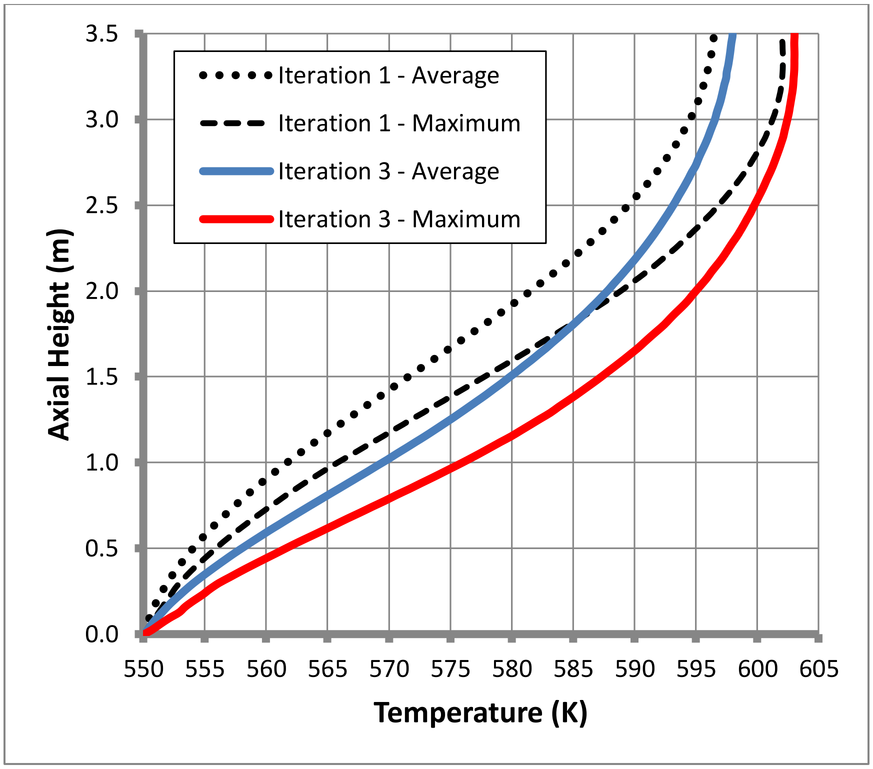

Figure 46. Axial Temperature Distributions for Coolant in Element 2.

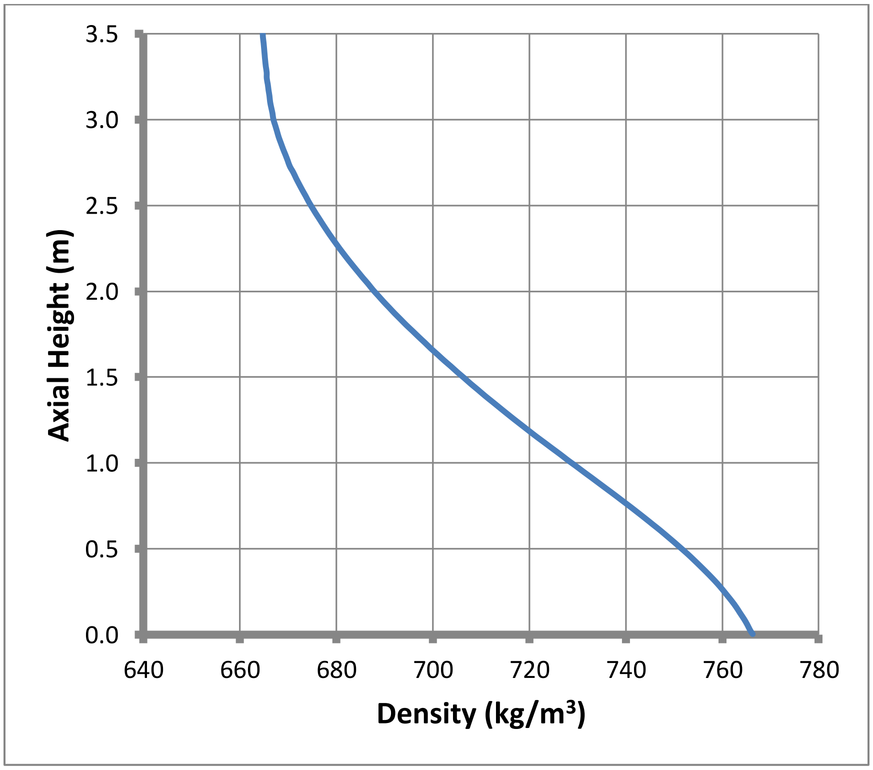

Figure 47. Axial Distribution of Average Coolant Density in Element 2 (Iteration 3).

Chapter 7. Summary

7.1. Conclusions

The MCNP5 Monte Carlo particle transport code has been coupled to the computational fluid dynamics code, STAR-CCM+, to provide a high fidelity multi-physics simulation tool for pressurized water nuclear reactors. The codes were executed separately and coupled externally through a Perl script that automated the exchange of temperature, density, and volumetric heating information between the codes using ASCII text data files.

The single PWR cell test case provided verification of the methodology used to couple the neutronic and CFD codes. The MCNP5 cell model provided evidence of converged eigenvalue and fission source distribution. Furthermore, the MCNP5 model had adequate tally statistics and intuitively expected reactivity coefficients. The STAR-CCM+ cell model had appropriate residuals convergence for the CFD simulations. A finer, unstructured, polyhedral mesh of the PWR cell model was compared to the base hexahedral mesh results – showing acceptable axial fuel temperature distribution agreement. Finally, the coupled MULTINUKE simulation demonstrated realistic and intuitive power distributions, temperature distributions, coolant densities, and fluid flow characteristics for a simple PWR model.

The shortened height of the first test model (20 cm PWR cell) did not allow for a very clear demonstration of thermal-hydraulic feedback influencing the axial power distribution. Considering the PWR cell model's inlet velocity and total power level, the resulting distribution of coolant density (lower near the exit and higher near the inlet) was not significant enough to push power peaking to the lower region in such a short model, as it would be for a BWR (or the 3 x 3 PWR lattice model). However, the cell model results from Chapter 6 were successful in demonstrating the effects that reduced coolant density and higher fuel temperatures have on overall reactivity. In addition, the power distributions calculated by MCNP5 had a clear impact on the temperature distributions in the fuel, clad, and coolant regions.

The simulation of the 3 x 3 PWR model expanded upon the results for the single 20 cm cell, demonstrating clearer feedback effects between the CFD and neutronic solvers, due to the more realistic size of the 3 x 3 model. Specifically, coolant temperatures increased more dramatically along the height of the model, thereby lowering coolant density in the upper region of the core, and resulting in a more bottom-peaked power distribution relative to the single PWR cell results. Fuel and clad temperatures peaked lower in the 3 x 3 model as a result. In the absence of control rods and axial variations of fuel and poison, the axial power peaking seen with this model is probably excessive for a PWR – meaning the inlet velocity, power level, and moderator density equation need some adjustments to obtain more realistic PWR behavior. The 3 x 3 PWR model has a water hole in the middle of the model due to the water-filled guide tube. Therefore, fission reaction rates (and power densities) were highest along the outer edge of the fuel pins nearest to the center guide tube, since thermal neutron flux was highest near the center of the 3 x 3 PWR model.

7.2. Further Work with MULTINUKE

The mesh for the 3 x 3 PWR model could be refined since it only has 89,856 CFD cells. In creating the 3 x 3 model, the same axial mesh (104 nodes) from the 20 cm PWR cell was used to avoid having the re-correlate the CFD mesh to the neutronic mesh. In addition, it preserved a one-to-one relation between the fuel and moderator cells for both meshes, bypassing the need add code to MULTINUKE to transfer data between two meshes of differing cell count and volume. Most importantly, building upon the old mesh allowed the 3 x 3 PWR simulation to run reasonably fast on a single quad-core machine. Eventually, the CFD mesh for the 3 x 3 model should be refined to approximately 400-600 axial nodes. The radial mesh should also be refined to better capture heat transfer and coolant flow behavior in the boundary layer. This is required for more accurate thermal-hydraulic simulation of a 3 x 3 model that is 400 cm tall. Higher fidelity turbulence models, such as the Reynolds Stress Transport model, would further increase the accuracy of the 3 x 3 PWR simulation. Some code would need to be added to MULTINUKE to transfer data between different MCNP5 and STAR-CCM+ meshes.

Beyond PWR assembly models, it is hoped that MULTINUKE may eventually be used for more advanced, time-dependent applications. Specifically, further development of MULTINUKE would include its implementation on massively parallel supercomputers. Calculation times for the simple PWR models analyzed in this work were between 8 and 130 hours on just four cores of a quad-processor machine. Massively parallel computing with MULTINUKE could analyze large nuclear reactor models with more complicated neutronic–thermal-hydraulic feedback effects, such as BWRs and fast reactors. For transient and accident analysis, STAR-CCM+ could be used in time-dependent mode, with MCNP5 providing updated power distributions at appropriate time intervals. (MCNP5 has the capability for time-dependent, *user-specified* sources and temperatures, but it has no direct transient or depletion capability.) Such advanced, high fidelity, multi-physics reactor simulations can assist in furthering the state-of-the-art through innovative validation of reactor safety and economic viability.

References

[1] F. B. Brown, J. T. Goorley, and J. E. Sweezy, "MCNP5 Parallel Processing Workshop," *Proceedings of ANS Mathematics & Computation Topical Meeting*, Gatlinburg, Tennessee, April 11 (2003).

[2] P. Finck, D. Keyes, and R. Stevens, “Workshop on Simulation and Modeling for Advanced Nuclear Energy Systems,” Washington, D.C., August 15-17 (2006). Available at http://www.er.doe.gov/ascr/Misc/gnep06-final.pdf.

[3] US Department of Energy Webpage, “Modeling & Simulation for Nuclear Reactors,” http://www.energy.gov/hubs/modeling_simulation_nuclear_reactors.htm, May 28 (2010). Accessed June 28, 2010.

[4] X-5 Monte Carlo Team, “MCNP – A General Monte Carlo N-Particle Transport Code, Version 5,” Los Alamos, New Mexico (2008).

[5] M. M. El-Wakil, *Nuclear Heat Transport*, The American Nuclear Society, La Grange Park, Illinois (1993).

[6] J. J. Duderstadt and L. J. Hamilton, *Nuclear Reactor Analysis*, John Wiley & Sons, New York, New York (1976).

[7] W. M. Stacey, *Nuclear Reactor Physics*, Wiley-VCH, Weinheim, Germany (2007).

[8] J. R. Lamarsh and A. J. Baratta, *Introduction to Nuclear Engineering*, Prentice Hall, Upper Saddle River, New Jersey (2001).

[9] T. M. Sutton, T. J. Donovan, T. H. Trumbull, P. S. Dobreff, E. Caro, D. P. Griesheimer, L. J. Tyburski, D. C. Carpenter, and H. Joo, “The MC21 Monte Carlo Transport Code,” *Proceedings of Joint International Topical Meeting on Mathematics & Computation and Supercomputing in Nuclear Applications*, Monterey, California, April 15-19 (2007).

[10] R. E. Macfarlane et al., “NJOY99.0: Code System for Producing Pointwise and Multigroup Neutron and Photon Cross Sections from ENDF/B Data,” Los Alamos, New Mexico (2000). Basic NJOY information available at http://t2.lanl.gov/njoy/.

[11] V. Seker, J. W. Thomas, and T. J. Downar, “Reactor Physics Simulations With Coupled Monte Carlo Calculation and Computational Fluid Dynamics,” *Proceedings of International Conference on Emerging Nuclear Energy Systems*, Istanbul, Turkey, June 3-8 (2007).

[12] S. Kimhy and A. Galperin, “Simple Model of Thermal-Hydraulic Feedback for Neutronic Analysis of PWR Cores,” *Annals of Nuclear Energy*, Vol. 15, No. 2, pp. 95-100 (1988).

[13] D. P. Weber et al., “High Fidelity LWR Analysis with the Numerical Nuclear Reactor,” *Nuclear Science and Engineering*, Vol. 155, pp. 1-14 (2007).

[14] J. Hu and Rizwan-uddin, “Coupled Neutronics and Thermal-Hydraulics Using MCNP and FLUENT,” *Transactions of the American Nuclear Society*, Vol. 98, pp. 606-608 (2008).

[15] CD-adapco Webpage. “Product Overview,” http://www.cd-adapco.com/products/, CD-adapco, (2010). Accessed October 15, 2010.

[16] X-5 Monte Carlo Team, “MCNP5 1.50 Release Notes,” Los Alamos, New Mexico (2008).

[17] T. J. Downar, A. Siegel, C. Unal, et al. “Science Based Nuclear Energy Systems Enabled by Advanced Modeling and Simulation at the Extreme Scale,” Crystal City, Virginia, May 11-12 (2009).

[18] The RELAP5-3D© Code Development Team, “RELAP5-3D© Code Manual Volume 1: Code Structure, System Models, and Solution Methods,” Idaho Falls, Idaho (2005).

[19] F. B. Brown, “The makxsf Code with Doppler Broadening,” Los Alamos, New Mexico (2008).

[20] G. K. Batchelor, *An Introduction to Fluid Dynamics*, Cambridge University Press, New York, New York (2000).

[21] N. E. Todreas and M. S. Kazimi, *Nuclear Systems I*, Taylor & Francis, New York, New York (1993).

[22] CD-adapco, “User Guide: STAR-CCM+ Version 2.10.017,” CD-adapco (2007).

[23] D. P. Weber, T. Sofu, T. H. Chun, H. G. Joo, J. W. Thomas, Z. Zhong, T. J. Downar, “Development of Comprehensive Modeling Capability Based on Rigorous Treatment of Multi-Physics Phenomena Influencing Reactor Core Design,” *Proceedings of International Congress on Advances in Nuclear Power Plants*, Pittsburgh, Pennsylvania, June 13-17 (2004).

[24] L. Snoj and M. Ravnik, "Calculation of Power Density with MCNP in TRIGA Reactor," *Proceedings of International Conference on Nuclear Energy for New Europe*, Portoroz, Slovenia, September 18-21 (2006).

[25] B. El Bakkari, T. El Bardouni, O. Merroun, C. El Younoussi, Y. Boulaich, and E. Chakir, “Development of an MCNP Tally Based Burnup Code and Validation Through PWR Benchmark Exercises,” *Annals of Nuclear Energy*, Vol. 36, pp. 626-633 (2009).

[26] Argonne National Laboratory Webpage for the International Nuclear Safety Center, “Thermal Conductivity and Thermal Diffusivity of Solid UO_2,” http://www.insc.anl.gov/matprop/uo2/cond/solid/thcsuo2.pdf, July (1999). Accessed August 8, 2010.

[27] Argonne National Laboratory Webpage for the International Nuclear Safety Center, “Zircaloy Thermal Conductivity,” http://www.insc.anl.gov/matprop/zircaloy/zirck.pdf, July (1999). Accessed May 4, 2010.

[28] Argonne National Laboratory Webpage for the International Nuclear Safety Center, “Zircaloy Heat Capacity,” http://www.insc.anl.gov/matprop/zircaloy/zirccp/fmt_orig.pdf, October (1997). Accessed May 4, 2010.

[29] F. B. Brown, W. Martine, J. Leppanen, W. Haeck, and B. Cochet, "Reactor Physics Analysis with Monte Carlo," *Proceedings of ANS PHYSOR-2010 Conference Workshop*, Pittsburgh, Pennsylvania, May 9 (2010).

APPENDIX A. Base Input Files for PWR Cell Model

Complete input files for the PWR cell model can be found in *multinuke.zip*.

A.1 MCNP5 Input File Excerpts

```
pin20cm : 5.0% enriched UO2 pin in H20 block - with grids
c
c             ****************************
c             *** cell definitions     ***
c             ****************************
c
c cell#  material#  density    surfaces   tmpTemperature  importance
c
c fuel cells 1-3328
   1 f_0001 6.874E-02 -1 12 -13 21 -22  99 -100 tmp=ft0001 imp:n=1 $ fuel pin grid block axial seg   1
   2 f_0002 6.874E-02 -1 13 -14 21 -22  99 -100 tmp=ft0002 imp:n=1 $ fuel pin grid block axial seg   1
   3 f_0003 6.874E-02 -1 14 -15 21 -22  99 -100 tmp=ft0003 imp:n=1 $ fuel pin grid block axial seg   1
   4 f_0004 6.874E-02 -1 15 -16 21 -22  99 -100 tmp=ft0004 imp:n=1 $ fuel pin grid block axial seg   1
   5 f_0005 6.874E-02 -1 11 -12 22 -23  99 -100 tmp=ft0005 imp:n=1 $ fuel pin grid block axial seg   1
   6 f_0006 6.874E-02 -1 12 -13 22 -23  99 -100 tmp=ft0006 imp:n=1 $ fuel pin grid block axial seg   1
   7 f_0007 6.874E-02 -1 13 -14 22 -23  99 -100 tmp=ft0007 imp:n=1 $ fuel pin grid block axial seg   1
   8 f_0008 6.874E-02 -1 14 -15 22 -23  99 -100 tmp=ft0008 imp:n=1 $ fuel pin grid block axial seg   1
   9 f_0009 6.874E-02 -1 15 -16 22 -23  99 -100 tmp=ft0009 imp:n=1 $ fuel pin grid block axial seg   1
  10 f_0010 6.874E-02 -1 16 -17 22 -23  99 -100 tmp=ft0010 imp:n=1 $ fuel pin grid block axial seg   1
  11 f_0011 6.874E-02 -1 11 -12 23 -24  99 -100 tmp=ft0011 imp:n=1 $ fuel pin grid block axial seg   1
  12 f_0012 6.874E-02 -1 12 -13 23 -24  99 -100 tmp=ft0012 imp:n=1 $ fuel pin grid block axial seg   1
  13 f_0013 6.874E-02 -1 13 -14 23 -24  99 -100 tmp=ft0013 imp:n=1 $ fuel pin grid block axial seg   1
  14 f_0014 6.874E-02 -1 14 -15 23 -24  99 -100 tmp=ft0014 imp:n=1 $ fuel pin grid block axial seg   1
  15 f_0015 6.874E-02 -1 15 -16 23 -24  99 -100 tmp=ft0015 imp:n=1 $ fuel pin grid block axial seg   1
  16 f_0016 6.874E-02 -1 16 -17 23 -24  99 -100 tmp=ft0016 imp:n=1 $ fuel pin grid block axial seg   1
  17 f_0017 6.874E-02 -1 11 -12 24 -25  99 -100 tmp=ft0017 imp:n=1 $ fuel pin grid block axial seg   1
  18 f_0018 6.874E-02 -1 12 -13 24 -25  99 -100 tmp=ft0018 imp:n=1 $ fuel pin grid block axial seg   1
  19 f_0019 6.874E-02 -1 13 -14 24 -25  99 -100 tmp=ft0019 imp:n=1 $ fuel pin grid block axial seg   1
  20 f_0020 6.874E-02 -1 14 -15 24 -25  99 -100 tmp=ft0020 imp:n=1 $ fuel pin grid block axial seg   1
  21 f_0021 6.874E-02 -1 15 -16 24 -25  99 -100 tmp=ft0021 imp:n=1 $ fuel pin grid block axial seg   1
  22 f_0022 6.874E-02 -1 16 -17 24 -25  99 -100 tmp=ft0022 imp:n=1 $ fuel pin grid block axial seg   1
  23 f_0023 6.874E-02 -1 11 -12 25 -26  99 -100 tmp=ft0023 imp:n=1 $ fuel pin grid block axial seg   1
  24 f_0024 6.874E-02 -1 12 -13 25 -26  99 -100 tmp=ft0024 imp:n=1 $ fuel pin grid block axial seg   1
  25 f_0025 6.874E-02 -1 13 -14 25 -26  99 -100 tmp=ft0025 imp:n=1 $ fuel pin grid block axial seg   1
  26 f_0026 6.874E-02 -1 14 -15 25 -26  99 -100 tmp=ft0026 imp:n=1 $ fuel pin grid block axial seg   1
  27 f_0027 6.874E-02 -1 15 -16 25 -26  99 -100 tmp=ft0027 imp:n=1 $ fuel pin grid block axial seg   1
  28 f_0028 6.874E-02 -1 16 -17 25 -26  99 -100 tmp=ft0028 imp:n=1 $ fuel pin grid block axial seg   1
  29 f_0029 6.874E-02 -1 12 -13 26 -27  99 -100 tmp=ft0029 imp:n=1 $ fuel pin grid block axial seg   1
  30 f_0030 6.874E-02 -1 13 -14 26 -27  99 -100 tmp=ft0030 imp:n=1 $ fuel pin grid block axial seg   1
  31 f_0031 6.874E-02 -1 14 -15 26 -27  99 -100 tmp=ft0031 imp:n=1 $ fuel pin grid block axial seg   1
  32 f_0032 6.874E-02 -1 15 -16 26 -27  99 -100 tmp=ft0032 imp:n=1 $ fuel pin grid block axial seg   1
  33 f_0033 6.874E-02 -1 12 -13 21 -22 100 -101 tmp=ft0033 imp:n=1 $ fuel pin grid block axial seg   2
  34 f_0034 6.874E-02 -1 13 -14 21 -22 100 -101 tmp=ft0034 imp:n=1 $ fuel pin grid block axial seg   2
  35 f_0035 6.874E-02 -1 14 -15 21 -22 100 -101 tmp=ft0035 imp:n=1 $ fuel pin grid block axial seg   2
  36 f_0036 6.874E-02 -1 15 -16 21 -22 100 -101 tmp=ft0036 imp:n=1 $ fuel pin grid block axial seg   2
  37 f_0037 6.874E-02 -1 11 -12 22 -23 100 -101 tmp=ft0037 imp:n=1 $ fuel pin grid block axial seg   2
  38 f_0038 6.874E-02 -1 12 -13 22 -23 100 -101 tmp=ft0038 imp:n=1 $ fuel pin grid block axial seg   2
  39 f_0039 6.874E-02 -1 13 -14 22 -23 100 -101 tmp=ft0039 imp:n=1 $ fuel pin grid block axial seg   2
  40 f_0040 6.874E-02 -1 14 -15 22 -23 100 -101 tmp=ft0040 imp:n=1 $ fuel pin grid block axial seg   2
  41 f_0041 6.874E-02 -1 15 -16 22 -23 100 -101 tmp=ft0041 imp:n=1 $ fuel pin grid block axial seg   2
  42 f_0042 6.874E-02 -1 16 -17 22 -23 100 -101 tmp=ft0042 imp:n=1 $ fuel pin grid block axial seg   2
  43 f_0043 6.874E-02 -1 11 -12 23 -24 100 -101 tmp=ft0043 imp:n=1 $ fuel pin grid block axial seg   2
  44 f_0044 6.874E-02 -1 12 -13 23 -24 100 -101 tmp=ft0044 imp:n=1 $ fuel pin grid block axial seg   2
  45 f_0045 6.874E-02 -1 13 -14 23 -24 100 -101 tmp=ft0045 imp:n=1 $ fuel pin grid block axial seg   2
  46 f_0046 6.874E-02 -1 14 -15 23 -24 100 -101 tmp=ft0046 imp:n=1 $ fuel pin grid block axial seg   2
  47 f_0047 6.874E-02 -1 15 -16 23 -24 100 -101 tmp=ft0047 imp:n=1 $ fuel pin grid block axial seg   2
  48 f_0048 6.874E-02 -1 16 -17 23 -24 100 -101 tmp=ft0048 imp:n=1 $ fuel pin grid block axial seg   2
  49 f_0049 6.874E-02 -1 11 -12 24 -25 100 -101 tmp=ft0049 imp:n=1 $ fuel pin grid block axial seg   2
  50 f_0050 6.874E-02 -1 12 -13 24 -25 100 -101 tmp=ft0050 imp:n=1 $ fuel pin grid block axial seg   2
  51 f_0051 6.874E-02 -1 13 -14 24 -25 100 -101 tmp=ft0051 imp:n=1 $ fuel pin grid block axial seg   2
  52 f_0052 6.874E-02 -1 14 -15 24 -25 100 -101 tmp=ft0052 imp:n=1 $ fuel pin grid block axial seg   2
  53 f_0053 6.874E-02 -1 15 -16 24 -25 100 -101 tmp=ft0053 imp:n=1 $ fuel pin grid block axial seg   2
  54 f_0054 6.874E-02 -1 16 -17 24 -25 100 -101 tmp=ft0054 imp:n=1 $ fuel pin grid block axial seg   2
  55 f_0055 6.874E-02 -1 11 -12 25 -26 100 -101 tmp=ft0055 imp:n=1 $ fuel pin grid block axial seg   2
  56 f_0056 6.874E-02 -1 12 -13 25 -26 100 -101 tmp=ft0056 imp:n=1 $ fuel pin grid block axial seg   2
  57 f_0057 6.874E-02 -1 13 -14 25 -26 100 -101 tmp=ft0057 imp:n=1 $ fuel pin grid block axial seg   2
  58 f_0058 6.874E-02 -1 14 -15 25 -26 100 -101 tmp=ft0058 imp:n=1 $ fuel pin grid block axial seg   2
  59 f_0059 6.874E-02 -1 15 -16 25 -26 100 -101 tmp=ft0059 imp:n=1 $ fuel pin grid block axial seg   2
  60 f_0060 6.874E-02 -1 16 -17 25 -26 100 -101 tmp=ft0060 imp:n=1 $ fuel pin grid block axial seg   2
  61 f_0061 6.874E-02 -1 12 -13 26 -27 100 -101 tmp=ft0061 imp:n=1 $ fuel pin grid block axial seg   2
  62 f_0062 6.874E-02 -1 13 -14 26 -27 100 -101 tmp=ft0062 imp:n=1 $ fuel pin grid block axial seg   2
  63 f_0063 6.874E-02 -1 14 -15 26 -27 100 -101 tmp=ft0063 imp:n=1 $ fuel pin grid block axial seg   2
  64 f_0064 6.874E-02 -1 15 -16 26 -27 100 -101 tmp=ft0064 imp:n=1 $ fuel pin grid block axial seg   2
  65 f_0065 6.874E-02 -1 12 -13 21 -22 101 -102 tmp=ft0065 imp:n=1 $ fuel pin grid block axial seg   3
  66 f_0066 6.874E-02 -1 13 -14 21 -22 101 -102 tmp=ft0066 imp:n=1 $ fuel pin grid block axial seg   3
  67 f_0067 6.874E-02 -1 14 -15 21 -22 101 -102 tmp=ft0067 imp:n=1 $ fuel pin grid block axial seg   3
  68 f_0068 6.874E-02 -1 15 -16 21 -22 101 -102 tmp=ft0068 imp:n=1 $ fuel pin grid block axial seg   3
  69 f_0069 6.874E-02 -1 11 -12 22 -23 101 -102 tmp=ft0069 imp:n=1 $ fuel pin grid block axial seg   3
  70 f_0070 6.874E-02 -1 12 -13 22 -23 101 -102 tmp=ft0070 imp:n=1 $ fuel pin grid block axial seg   3
  71 f_0071 6.874E-02 -1 13 -14 22 -23 101 -102 tmp=ft0071 imp:n=1 $ fuel pin grid block axial seg   3
  72 f_0072 6.874E-02 -1 14 -15 22 -23 101 -102 tmp=ft0072 imp:n=1 $ fuel pin grid block axial seg   3
  73 f_0073 6.874E-02 -1 15 -16 22 -23 101 -102 tmp=ft0073 imp:n=1 $ fuel pin grid block axial seg   3
  74 f_0074 6.874E-02 -1 16 -17 22 -23 101 -102 tmp=ft0074 imp:n=1 $ fuel pin grid block axial seg   3
  75 f_0075 6.874E-02 -1 11 -12 23 -24 101 -102 tmp=ft0075 imp:n=1 $ fuel pin grid block axial seg   3
  76 f_0076 6.874E-02 -1 12 -13 23 -24 101 -102 tmp=ft0076 imp:n=1 $ fuel pin grid block axial seg   3
  77 f_0077 6.874E-02 -1 13 -14 23 -24 101 -102 tmp=ft0077 imp:n=1 $ fuel pin grid block axial seg   3
  78 f_0078 6.874E-02 -1 14 -15 23 -24 101 -102 tmp=ft0078 imp:n=1 $ fuel pin grid block axial seg   3
  79 f_0079 6.874E-02 -1 15 -16 23 -24 101 -102 tmp=ft0079 imp:n=1 $ fuel pin grid block axial seg   3
  80 f_0080 6.874E-02 -1 16 -17 23 -24 101 -102 tmp=ft0080 imp:n=1 $ fuel pin grid block axial seg   3
  81 f_0081 6.874E-02 -1 11 -12 24 -25 101 -102 tmp=ft0081 imp:n=1 $ fuel pin grid block axial seg   3
  82 f_0082 6.874E-02 -1 12 -13 24 -25 101 -102 tmp=ft0082 imp:n=1 $ fuel pin grid block axial seg   3
  83 f_0083 6.874E-02 -1 13 -14 24 -25 101 -102 tmp=ft0083 imp:n=1 $ fuel pin grid block axial seg   3
  84 f_0084 6.874E-02 -1 14 -15 24 -25 101 -102 tmp=ft0084 imp:n=1 $ fuel pin grid block axial seg   3
  85 f_0085 6.874E-02 -1 15 -16 24 -25 101 -102 tmp=ft0085 imp:n=1 $ fuel pin grid block axial seg   3
  86 f_0086 6.874E-02 -1 16 -17 24 -25 101 -102 tmp=ft0086 imp:n=1 $ fuel pin grid block axial seg   3
  87 f_0087 6.874E-02 -1 11 -12 25 -26 101 -102 tmp=ft0087 imp:n=1 $ fuel pin grid block axial seg   3
  88 f_0088 6.874E-02 -1 12 -13 25 -26 101 -102 tmp=ft0088 imp:n=1 $ fuel pin grid block axial seg   3
  89 f_0089 6.874E-02 -1 13 -14 25 -26 101 -102 tmp=ft0089 imp:n=1 $ fuel pin grid block axial seg   3
  90 f_0090 6.874E-02 -1 14 -15 25 -26 101 -102 tmp=ft0090 imp:n=1 $ fuel pin grid block axial seg   3
  91 f_0091 6.874E-02 -1 15 -16 25 -26 101 -102 tmp=ft0091 imp:n=1 $ fuel pin grid block axial seg   3
  92 f_0092 6.874E-02 -1 16 -17 25 -26 101 -102 tmp=ft0092 imp:n=1 $ fuel pin grid block axial seg   3
  93 f_0093 6.874E-02 -1 12 -13 26 -27 101 -102 tmp=ft0093 imp:n=1 $ fuel pin grid block axial seg   3
  94 f_0094 6.874E-02 -1 13 -14 26 -27 101 -102 tmp=ft0094 imp:n=1 $ fuel pin grid block axial seg   3
  95 f_0095 6.874E-02 -1 14 -15 26 -27 101 -102 tmp=ft0095 imp:n=1 $ fuel pin grid block axial seg   3
  96 f_0096 6.874E-02 -1 15 -16 26 -27 101 -102 tmp=ft0096 imp:n=1 $ fuel pin grid block axial seg   3
  97 f_0097 6.874E-02 -1 12 -13 21 -22 102 -103 tmp=ft0097 imp:n=1 $ fuel pin grid block axial seg   4
  98 f_0098 6.874E-02 -1 13 -14 21 -22 102 -103 tmp=ft0098 imp:n=1 $ fuel pin grid block axial seg   4
  99 f_0099 6.874E-02 -1 14 -15 21 -22 102 -103 tmp=ft0099 imp:n=1 $ fuel pin grid block axial seg   4
 100 f_0100 6.874E-02 -1 15 -16 21 -22 102 -103 tmp=ft0100 imp:n=1 $ fuel pin grid block axial seg   4
 101 f_0101 6.874E-02 -1 11 -12 22 -23 102 -103 tmp=ft0101 imp:n=1 $ fuel pin grid block axial seg   4
 102 f_0102 6.874E-02 -1 12 -13 22 -23 102 -103 tmp=ft0102 imp:n=1 $ fuel pin grid block axial seg   4
 103 f_0103 6.874E-02 -1 13 -14 22 -23 102 -103 tmp=ft0103 imp:n=1 $ fuel pin grid block axial seg   4
 104 f_0104 6.874E-02 -1 14 -15 22 -23 102 -103 tmp=ft0104 imp:n=1 $ fuel pin grid block axial seg   4
 105 f_0105 6.874E-02 -1 15 -16 22 -23 102 -103 tmp=ft0105 imp:n=1 $ fuel pin grid block axial seg   4
 106 f_0106 6.874E-02 -1 16 -17 22 -23 102 -103 tmp=ft0106 imp:n=1 $ fuel pin grid block axial seg   4
 107 f_0107 6.874E-02 -1 11 -12 23 -24 102 -103 tmp=ft0107 imp:n=1 $ fuel pin grid block axial seg   4
 108 f_0108 6.874E-02 -1 12 -13 23 -24 102 -103 tmp=ft0108 imp:n=1 $ fuel pin grid block axial seg   4
 109 f_0109 6.874E-02 -1 13 -14 23 -24 102 -103 tmp=ft0109 imp:n=1 $ fuel pin grid block axial seg   4
 110 f_0110 6.874E-02 -1 14 -15 23 -24 102 -103 tmp=ft0110 imp:n=1 $ fuel pin grid block axial seg   4
 111 f_0111 6.874E-02 -1 15 -16 23 -24 102 -103 tmp=ft0111 imp:n=1 $ fuel pin grid block axial seg   4
```

.

.

(Fuel cell cards continue)

.

.

```
c (WATER CELLS)
4001 w_4001 wden_4001 2 10 -11 20 -21  99 -100 tmp=wt4001 imp:n=1 $ water grid block axial seg   1
4002 w_4002 wden_4002 2 11 -12 20 -21  99 -100 tmp=wt4002 imp:n=1 $ water grid block axial seg   1
4003 w_4003 wden_4003 2 12 -13 20 -21  99 -100 tmp=wt4003 imp:n=1 $ water grid block axial seg   1
4004 w_4004 wden_4004 2 13 -14 20 -21  99 -100 tmp=wt4004 imp:n=1 $ water grid block axial seg   1
4005 w_4005 wden_4005 2 14 -15 20 -21  99 -100 tmp=wt4005 imp:n=1 $ water grid block axial seg   1
4006 w_4006 wden_4006 2 15 -16 20 -21  99 -100 tmp=wt4006 imp:n=1 $ water grid block axial seg   1
4007 w_4007 wden_4007 2 16 -17 20 -21  99 -100 tmp=wt4007 imp:n=1 $ water grid block axial seg   1
4008 w_4008 wden_4008 2 17 -18 20 -21  99 -100 tmp=wt4008 imp:n=1 $ water grid block axial seg   1
4009 w_4009 wden_4009 2 10 -11 21 -22  99 -100 tmp=wt4009 imp:n=1 $ water grid block axial seg   1
4010 w_4010 wden_4010 2 11 -12 21 -22  99 -100 tmp=wt4010 imp:n=1 $ water grid block axial seg   1
4011 w_4011 wden_4011 2 12 -13 21 -22  99 -100 tmp=wt4011 imp:n=1 $ water grid block axial seg   1
4012 w_4012 wden_4012 2 15 -16 21 -22  99 -100 tmp=wt4012 imp:n=1 $ water grid block axial seg   1
4013 w_4013 wden_4013 2 16 -17 21 -22  99 -100 tmp=wt4013 imp:n=1 $ water grid block axial seg   1
4014 w_4014 wden_4014 2 17 -18 21 -22  99 -100 tmp=wt4014 imp:n=1 $ water grid block axial seg   1
4015 w_4015 wden_4015 2 10 -11 22 -23  99 -100 tmp=wt4015 imp:n=1 $ water grid block axial seg   1
```

```
4016 w_4016 wden_4016 2 11 -12 22 -23  99 -100 tmp=wt4016 imp:n=1 $ water grid block axial seg   1
4017 w_4017 wden_4017 2 16 -17 22 -23  99 -100 tmp=wt4017 imp:n=1 $ water grid block axial seg   1
4018 w_4018 wden_4018 2 17 -18 22 -23  99 -100 tmp=wt4018 imp:n=1 $ water grid block axial seg   1
4019 w_4019 wden_4019 2 10 -11 23 -24  99 -100 tmp=wt4019 imp:n=1 $ water grid block axial seg   1
4020 w_4020 wden_4020 2 17 -18 23 -24  99 -100 tmp=wt4020 imp:n=1 $ water grid block axial seg   1
4021 w_4021 wden_4021 2 10 -11 24 -25  99 -100 tmp=wt4021 imp:n=1 $ water grid block axial seg   1
4022 w_4022 wden_4022 2 17 -18 24 -25  99 -100 tmp=wt4022 imp:n=1 $ water grid block axial seg   1
4023 w_4023 wden_4023 2 10 -11 25 -26  99 -100 tmp=wt4023 imp:n=1 $ water grid block axial seg   1
4024 w_4024 wden_4024 2 11 -12 25 -26  99 -100 tmp=wt4024 imp:n=1 $ water grid block axial seg   1
4025 w_4025 wden_4025 2 16 -17 25 -26  99 -100 tmp=wt4025 imp:n=1 $ water grid block axial seg   1
4026 w_4026 wden_4026 2 17 -18 25 -26  99 -100 tmp=wt4026 imp:n=1 $ water grid block axial seg   1
4027 w_4027 wden_4027 2 10 -11 26 -27  99 -100 tmp=wt4027 imp:n=1 $ water grid block axial seg   1
4028 w_4028 wden_4028 2 11 -12 26 -27  99 -100 tmp=wt4028 imp:n=1 $ water grid block axial seg   1
4029 w_4029 wden_4029 2 12 -13 26 -27  99 -100 tmp=wt4029 imp:n=1 $ water grid block axial seg   1
4030 w_4030 wden_4030 2 15 -16 26 -27  99 -100 tmp=wt4030 imp:n=1 $ water grid block axial seg   1
4031 w_4031 wden_4031 2 16 -17 26 -27  99 -100 tmp=wt4031 imp:n=1 $ water grid block axial seg   1
4032 w_4032 wden_4032 2 17 -18 26 -27  99 -100 tmp=wt4032 imp:n=1 $ water grid block axial seg   1
4033 w_4033 wden_4033 2 10 -11 27 -28  99 -100 tmp=wt4033 imp:n=1 $ water grid block axial seg   1
4034 w_4034 wden_4034 2 11 -12 27 -28  99 -100 tmp=wt4034 imp:n=1 $ water grid block axial seg   1
4035 w_4035 wden_4035 2 12 -13 27 -28  99 -100 tmp=wt4035 imp:n=1 $ water grid block axial seg   1
4036 w_4036 wden_4036 2 13 -14 27 -28  99 -100 tmp=wt4036 imp:n=1 $ water grid block axial seg   1
4037 w_4037 wden_4037 2 14 -15 27 -28  99 -100 tmp=wt4037 imp:n=1 $ water grid block axial seg   1
4038 w_4038 wden_4038 2 15 -16 27 -28  99 -100 tmp=wt4038 imp:n=1 $ water grid block axial seg   1
4039 w_4039 wden_4039 2 16 -17 27 -28  99 -100 tmp=wt4039 imp:n=1 $ water grid block axial seg   1
4040 w_4040 wden_4040 2 17 -18 27 -28  99 -100 tmp=wt4040 imp:n=1 $ water grid block axial seg   1
4041 w_4041 wden_4041 2 10 -11 20 -21 100 -101 tmp=wt4041 imp:n=1 $ water grid block axial seg   2
4042 w_4042 wden_4042 2 11 -12 20 -21 100 -101 tmp=wt4042 imp:n=1 $ water grid block axial seg   2
4043 w_4043 wden_4043 2 12 -13 20 -21 100 -101 tmp=wt4043 imp:n=1 $ water grid block axial seg   2
4044 w_4044 wden_4044 2 13 -14 20 -21 100 -101 tmp=wt4044 imp:n=1 $ water grid block axial seg   2
4045 w_4045 wden_4045 2 14 -15 20 -21 100 -101 tmp=wt4045 imp:n=1 $ water grid block axial seg   2
4046 w_4046 wden_4046 2 15 -16 20 -21 100 -101 tmp=wt4046 imp:n=1 $ water grid block axial seg   2
4047 w_4047 wden_4047 2 16 -17 20 -21 100 -101 tmp=wt4047 imp:n=1 $ water grid block axial seg   2
4048 w_4048 wden_4048 2 17 -18 20 -21 100 -101 tmp=wt4048 imp:n=1 $ water grid block axial seg   2
4049 w_4049 wden_4049 2 10 -11 21 -22 100 -101 tmp=wt4049 imp:n=1 $ water grid block axial seg   2
4050 w_4050 wden_4050 2 11 -12 21 -22 100 -101 tmp=wt4050 imp:n=1 $ water grid block axial seg   2
4051 w_4051 wden_4051 2 12 -13 21 -22 100 -101 tmp=wt4051 imp:n=1 $ water grid block axial seg   2
4052 w_4052 wden_4052 2 15 -16 21 -22 100 -101 tmp=wt4052 imp:n=1 $ water grid block axial seg   2
4053 w_4053 wden_4053 2 16 -17 21 -22 100 -101 tmp=wt4053 imp:n=1 $ water grid block axial seg   2
4054 w_4054 wden_4054 2 17 -18 21 -22 100 -101 tmp=wt4054 imp:n=1 $ water grid block axial seg   2
4055 w_4055 wden_4055 2 10 -11 22 -23 100 -101 tmp=wt4055 imp:n=1 $ water grid block axial seg   2
4056 w_4056 wden_4056 2 11 -12 22 -23 100 -101 tmp=wt4056 imp:n=1 $ water grid block axial seg   2
4057 w_4057 wden_4057 2 16 -17 22 -23 100 -101 tmp=wt4057 imp:n=1 $ water grid block axial seg   2
4058 w_4058 wden_4058 2 17 -18 22 -23 100 -101 tmp=wt4058 imp:n=1 $ water grid block axial seg   2
4059 w_4059 wden_4059 2 10 -11 23 -24 100 -101 tmp=wt4059 imp:n=1 $ water grid block axial seg   2
4060 w_4060 wden_4060 2 17 -18 23 -24 100 -101 tmp=wt4060 imp:n=1 $ water grid block axial seg   2
4061 w_4061 wden_4061 2 10 -11 24 -25 100 -101 tmp=wt4061 imp:n=1 $ water grid block axial seg   2
4062 w_4062 wden_4062 2 17 -18 24 -25 100 -101 tmp=wt4062 imp:n=1 $ water grid block axial seg   2
4063 w_4063 wden_4063 2 10 -11 25 -26 100 -101 tmp=wt4063 imp:n=1 $ water grid block axial seg   2
4064 w_4064 wden_4064 2 11 -12 25 -26 100 -101 tmp=wt4064 imp:n=1 $ water grid block axial seg   2
4065 w_4065 wden_4065 2 16 -17 25 -26 100 -101 tmp=wt4065 imp:n=1 $ water grid block axial seg   2
4066 w_4066 wden_4066 2 17 -18 25 -26 100 -101 tmp=wt4066 imp:n=1 $ water grid block axial seg   2
4067 w_4067 wden_4067 2 10 -11 26 -27 100 -101 tmp=wt4067 imp:n=1 $ water grid block axial seg   2
4068 w_4068 wden_4068 2 11 -12 26 -27 100 -101 tmp=wt4068 imp:n=1 $ water grid block axial seg   2
4069 w_4069 wden_4069 2 12 -13 26 -27 100 -101 tmp=wt4069 imp:n=1 $ water grid block axial seg   2
4070 w_4070 wden_4070 2 15 -16 26 -27 100 -101 tmp=wt4070 imp:n=1 $ water grid block axial seg   2
4071 w_4071 wden_4071 2 16 -17 26 -27 100 -101 tmp=wt4071 imp:n=1 $ water grid block axial seg   2
4072 w_4072 wden_4072 2 17 -18 26 -27 100 -101 tmp=wt4072 imp:n=1 $ water grid block axial seg   2
4073 w_4073 wden_4073 2 10 -11 27 -28 100 -101 tmp=wt4073 imp:n=1 $ water grid block axial seg   2
4074 w_4074 wden_4074 2 11 -12 27 -28 100 -101 tmp=wt4074 imp:n=1 $ water grid block axial seg   2
4075 w_4075 wden_4075 2 12 -13 27 -28 100 -101 tmp=wt4075 imp:n=1 $ water grid block axial seg   2
4076 w_4076 wden_4076 2 13 -14 27 -28 100 -101 tmp=wt4076 imp:n=1 $ water grid block axial seg   2
4077 w_4077 wden_4077 2 14 -15 27 -28 100 -101 tmp=wt4077 imp:n=1 $ water grid block axial seg   2
4078 w_4078 wden_4078 2 15 -16 27 -28 100 -101 tmp=wt4078 imp:n=1 $ water grid block axial seg   2
4079 w_4079 wden_4079 2 16 -17 27 -28 100 -101 tmp=wt4079 imp:n=1 $ water grid block axial seg   2
4080 w_4080 wden_4080 2 17 -18 27 -28 100 -101 tmp=wt4080 imp:n=1 $ water grid block axial seg   2
4081 w_4081 wden_4081 2 10 -11 20 -21 101 -102 tmp=wt4081 imp:n=1 $ water grid block axial seg   3
4082 w_4082 wden_4082 2 11 -12 20 -21 101 -102 tmp=wt4082 imp:n=1 $ water grid block axial seg   3
4083 w_4083 wden_4083 2 12 -13 20 -21 101 -102 tmp=wt4083 imp:n=1 $ water grid block axial seg   3
4084 w_4084 wden_4084 2 13 -14 20 -21 101 -102 tmp=wt4084 imp:n=1 $ water grid block axial seg   3
4085 w_4085 wden_4085 2 14 -15 20 -21 101 -102 tmp=wt4085 imp:n=1 $ water grid block axial seg   3
4086 w_4086 wden_4086 2 15 -16 20 -21 101 -102 tmp=wt4086 imp:n=1 $ water grid block axial seg   3
4087 w_4087 wden_4087 2 16 -17 20 -21 101 -102 tmp=wt4087 imp:n=1 $ water grid block axial seg   3
4088 w_4088 wden_4088 2 17 -18 20 -21 101 -102 tmp=wt4088 imp:n=1 $ water grid block axial seg   3
4089 w_4089 wden_4089 2 10 -11 21 -22 101 -102 tmp=wt4089 imp:n=1 $ water grid block axial seg   3
4090 w_4090 wden_4090 2 11 -12 21 -22 101 -102 tmp=wt4090 imp:n=1 $ water grid block axial seg   3
4091 w_4091 wden_4091 2 12 -13 21 -22 101 -102 tmp=wt4091 imp:n=1 $ water grid block axial seg   3
```

```
4092 w_4092 wden_4092 2 15 -16 21 -22 101 -102 tmp=wt4092 imp:n=1 $ water grid block axial seg   3
4093 w_4093 wden_4093 2 16 -17 21 -22 101 -102 tmp=wt4093 imp:n=1 $ water grid block axial seg   3
4094 w_4094 wden_4094 2 17 -18 21 -22 101 -102 tmp=wt4094 imp:n=1 $ water grid block axial seg   3
4095 w_4095 wden_4095 2 10 -11 22 -23 101 -102 tmp=wt4095 imp:n=1 $ water grid block axial seg   3
4096 w_4096 wden_4096 2 11 -12 22 -23 101 -102 tmp=wt4096 imp:n=1 $ water grid block axial seg   3
4097 w_4097 wden_4097 2 16 -17 22 -23 101 -102 tmp=wt4097 imp:n=1 $ water grid block axial seg   3
4098 w_4098 wden_4098 2 17 -18 22 -23 101 -102 tmp=wt4098 imp:n=1 $ water grid block axial seg   3
4099 w_4099 wden_4099 2 10 -11 23 -24 101 -102 tmp=wt4099 imp:n=1 $ water grid block axial seg   3
4100 w_4100 wden_4100 2 17 -18 23 -24 101 -102 tmp=wt4100 imp:n=1 $ water grid block axial seg   3
4101 w_4101 wden_4101 2 10 -11 24 -25 101 -102 tmp=wt4101 imp:n=1 $ water grid block axial seg   3
4102 w_4102 wden_4102 2 17 -18 24 -25 101 -102 tmp=wt4102 imp:n=1 $ water grid block axial seg   3
4103 w_4103 wden_4103 2 10 -11 25 -26 101 -102 tmp=wt4103 imp:n=1 $ water grid block axial seg   3
4104 w_4104 wden_4104 2 11 -12 25 -26 101 -102 tmp=wt4104 imp:n=1 $ water grid block axial seg   3
4105 w_4105 wden_4105 2 16 -17 25 -26 101 -102 tmp=wt4105 imp:n=1 $ water grid block axial seg   3
4106 w_4106 wden_4106 2 17 -18 25 -26 101 -102 tmp=wt4106 imp:n=1 $ water grid block axial seg   3
4107 w_4107 wden_4107 2 10 -11 26 -27 101 -102 tmp=wt4107 imp:n=1 $ water grid block axial seg   3
4108 w_4108 wden_4108 2 11 -12 26 -27 101 -102 tmp=wt4108 imp:n=1 $ water grid block axial seg   3
4109 w_4109 wden_4109 2 12 -13 26 -27 101 -102 tmp=wt4109 imp:n=1 $ water grid block axial seg   3
4110 w_4110 wden_4110 2 15 -16 26 -27 101 -102 tmp=wt4110 imp:n=1 $ water grid block axial seg   3
4111 w_4111 wden_4111 2 16 -17 26 -27 101 -102 tmp=wt4111 imp:n=1 $ water grid block axial seg   3
4112 w_4112 wden_4112 2 17 -18 26 -27 101 -102 tmp=wt4112 imp:n=1 $ water grid block axial seg   3
4113 w_4113 wden_4113 2 10 -11 27 -28 101 -102 tmp=wt4113 imp:n=1 $ water grid block axial seg   3
4114 w_4114 wden_4114 2 11 -12 27 -28 101 -102 tmp=wt4114 imp:n=1 $ water grid block axial seg   3
4115 w_4115 wden_4115 2 12 -13 27 -28 101 -102 tmp=wt4115 imp:n=1 $ water grid block axial seg   3
4116 w_4116 wden_4116 2 13 -14 27 -28 101 -102 tmp=wt4116 imp:n=1 $ water grid block axial seg   3
4117 w_4117 wden_4117 2 14 -15 27 -28 101 -102 tmp=wt4117 imp:n=1 $ water grid block axial seg   3
4118 w_4118 wden_4118 2 15 -16 27 -28 101 -102 tmp=wt4118 imp:n=1 $ water grid block axial seg   3
4119 w_4119 wden_4119 2 16 -17 27 -28 101 -102 tmp=wt4119 imp:n=1 $ water grid block axial seg   3
4120 w_4120 wden_4120 2 17 -18 27 -28 101 -102 tmp=wt4120 imp:n=1 $ water grid block axial seg   3
4121 w_4121 wden_4121 2 10 -11 20 -21 102 -103 tmp=wt4121 imp:n=1 $ water grid block axial seg   4
4122 w_4122 wden_4122 2 11 -12 20 -21 102 -103 tmp=wt4122 imp:n=1 $ water grid block axial seg   4
4123 w_4123 wden_4123 2 12 -13 20 -21 102 -103 tmp=wt4123 imp:n=1 $ water grid block axial seg   4
4124 w_4124 wden_4124 2 13 -14 20 -21 102 -103 tmp=wt4124 imp:n=1 $ water grid block axial seg   4
4125 w_4125 wden_4125 2 14 -15 20 -21 102 -103 tmp=wt4125 imp:n=1 $ water grid block axial seg   4
4126 w_4126 wden_4126 2 15 -16 20 -21 102 -103 tmp=wt4126 imp:n=1 $ water grid block axial seg   4
4127 w_4127 wden_4127 2 16 -17 20 -21 102 -103 tmp=wt4127 imp:n=1 $ water grid block axial seg   4
4128 w_4128 wden_4128 2 17 -18 20 -21 102 -103 tmp=wt4128 imp:n=1 $ water grid block axial seg   4
4129 w_4129 wden_4129 2 10 -11 21 -22 102 -103 tmp=wt4129 imp:n=1 $ water grid block axial seg   4
4130 w_4130 wden_4130 2 11 -12 21 -22 102 -103 tmp=wt4130 imp:n=1 $ water grid block axial seg   4
4131 w_4131 wden_4131 2 12 -13 21 -22 102 -103 tmp=wt4131 imp:n=1 $ water grid block axial seg   4
4132 w_4132 wden_4132 2 15 -16 21 -22 102 -103 tmp=wt4132 imp:n=1 $ water grid block axial seg   4
4133 w_4133 wden_4133 2 16 -17 21 -22 102 -103 tmp=wt4133 imp:n=1 $ water grid block axial seg   4
4134 w_4134 wden_4134 2 17 -18 21 -22 102 -103 tmp=wt4134 imp:n=1 $ water grid block axial seg   4
4135 w_4135 wden_4135 2 10 -11 22 -23 102 -103 tmp=wt4135 imp:n=1 $ water grid block axial seg   4
4136 w_4136 wden_4136 2 11 -12 22 -23 102 -103 tmp=wt4136 imp:n=1 $ water grid block axial seg   4
4137 w_4137 wden_4137 2 16 -17 22 -23 102 -103 tmp=wt4137 imp:n=1 $ water grid block axial seg   4
4138 w_4138 wden_4138 2 17 -18 22 -23 102 -103 tmp=wt4138 imp:n=1 $ water grid block axial seg   4
4139 w_4139 wden_4139 2 10 -11 23 -24 102 -103 tmp=wt4139 imp:n=1 $ water grid block axial seg   4
4140 w_4140 wden_4140 2 17 -18 23 -24 102 -103 tmp=wt4140 imp:n=1 $ water grid block axial seg   4
4141 w_4141 wden_4141 2 10 -11 24 -25 102 -103 tmp=wt4141 imp:n=1 $ water grid block axial seg   4
4142 w_4142 wden_4142 2 17 -18 24 -25 102 -103 tmp=wt4142 imp:n=1 $ water grid block axial seg   4
4143 w_4143 wden_4143 2 10 -11 25 -26 102 -103 tmp=wt4143 imp:n=1 $ water grid block axial seg   4
4144 w_4144 wden_4144 2 11 -12 25 -26 102 -103 tmp=wt4144 imp:n=1 $ water grid block axial seg   4
4145 w_4145 wden_4145 2 16 -17 25 -26 102 -103 tmp=wt4145 imp:n=1 $ water grid block axial seg   4
4146 w_4146 wden_4146 2 17 -18 25 -26 102 -103 tmp=wt4146 imp:n=1 $ water grid block axial seg   4
4147 w_4147 wden_4147 2 10 -11 26 -27 102 -103 tmp=wt4147 imp:n=1 $ water grid block axial seg   4
4148 w_4148 wden_4148 2 11 -12 26 -27 102 -103 tmp=wt4148 imp:n=1 $ water grid block axial seg   4
4149 w_4149 wden_4149 2 12 -13 26 -27 102 -103 tmp=wt4149 imp:n=1 $ water grid block axial seg   4
4150 w_4150 wden_4150 2 15 -16 26 -27 102 -103 tmp=wt4150 imp:n=1 $ water grid block axial seg   4
4151 w_4151 wden_4151 2 16 -17 26 -27 102 -103 tmp=wt4151 imp:n=1 $ water grid block axial seg   4
4152 w_4152 wden_4152 2 17 -18 26 -27 102 -103 tmp=wt4152 imp:n=1 $ water grid block axial seg   4
4153 w_4153 wden_4153 2 10 -11 27 -28 102 -103 tmp=wt4153 imp:n=1 $ water grid block axial seg   4
4154 w_4154 wden_4154 2 11 -12 27 -28 102 -103 tmp=wt4154 imp:n=1 $ water grid block axial seg   4
4155 w_4155 wden_4155 2 12 -13 27 -28 102 -103 tmp=wt4155 imp:n=1 $ water grid block axial seg   4
4156 w_4156 wden_4156 2 13 -14 27 -28 102 -103 tmp=wt4156 imp:n=1 $ water grid block axial seg   4
4157 w_4157 wden_4157 2 14 -15 27 -28 102 -103 tmp=wt4157 imp:n=1 $ water grid block axial seg   4
4158 w_4158 wden_4158 2 15 -16 27 -28 102 -103 tmp=wt4158 imp:n=1 $ water grid block axial seg   4
4159 w_4159 wden_4159 2 16 -17 27 -28 102 -103 tmp=wt4159 imp:n=1 $ water grid block axial seg   4
```

.

.

(Coolant cell cards continue)

.

.

```
c
 9000 mclad -6.55                 1 -2 99 -203 tmp=cladt  imp:n=1 $ cladding (zirc-4)
c
 9999 0                  -10:18:-20:28:-99:203            imp:n=0 $ escape
c

c
c
c             ****************************
c             *** surface definitions  ***
c             ****************************
c
c cylindrical radial surfaces
   1       cz 0.5           $ fuel cylinder
   2       cz 0.6           $ outer clad surface
c
c radial grid surfaces
  *10      px -0.75         $ x-radial grid surfaces (*=reflective surface)
   11      px -0.5625
   12      px -0.375
   13      px -0.1875
   14      px  0.0
   15      px  0.1875
   16      px  0.375
   17      px  0.5625
  *18      px  0.75
c
  *20      py -0.75         $ y-radial grid surfaces (*=reflective surface)
   21      py -0.5625
   22      py -0.375
   23      py -0.1875
   24      py  0.0
   25      py  0.1875
   26      py  0.375
   27      py  0.5625
  *28      py  0.75
c
c axial grid surfaces
    99     pz       0.0000000   $ bottom of model
   100     pz       0.0195517
   101     pz       0.1367224
   102     pz       0.3320344
   103     pz       0.5273464
   104     pz       0.7226585
   105     pz       0.9179704
   106     pz       1.1132824
   107     pz       1.3085945
   108     pz       1.5039065
   109     pz       1.6992184
   110     pz       1.8945304
   111     pz       2.0898423
   112     pz       2.2851543
   113     pz       2.4804664
   114     pz       2.6757784
   115     pz       2.8710904
   116     pz       3.0664024
   117     pz       3.2617145
   118     pz       3.4570265
   119     pz       3.6523385
   120     pz       3.8476505
   121     pz       4.0429626
   122     pz       4.2382746
   123     pz       4.4335866
```

```
124      pz        4.6288986
125      pz        4.8242106
126      pz        5.0195227
127      pz        5.2148342
128      pz        5.4101462
129      pz        5.6054583
130      pz        5.8007703
131      pz        5.9960823
132      pz        6.1913943
133      pz        6.3867064
134      pz        6.5820184
135      pz        6.7773304
136      pz        6.9726424
137      pz        7.1679544
138      pz        7.3632665
139      pz        7.5585785
140      pz        7.7538905
141      pz        7.9492025
142      pz        8.1445141
143      pz        8.3398266
144      pz        8.5351381
145      pz        8.7304506
146      pz        8.9257622
147      pz        9.1210747
148      pz        9.3163862
149      pz        9.5116987
150      pz        9.7070103
151      pz        9.9023228
152      pz       10.0976343
153      pz       10.2929468
154      pz       10.4882584
155      pz       10.6835709
156      pz       10.8788824
157      pz       11.0741949
158      pz       11.2695065
159      pz       11.4648180
160      pz       11.6601305
161      pz       11.8554420
162      pz       12.0507545
163      pz       12.2460661
164      pz       12.4413786
165      pz       12.6366901
166      pz       12.8320026
167      pz       13.0273142
168      pz       13.2226267
169      pz       13.4179382
170      pz       13.6132507
171      pz       13.8085623
172      pz       14.0038748
173      pz       14.1991863
174      pz       14.3944988
175      pz       14.5898104
176      pz       14.7851229
177      pz       14.9804344
178      pz       15.1757460
179      pz       15.3710585
180      pz       15.5663700
181      pz       15.7616825
182      pz       15.9569941
183      pz       16.1523056
184      pz       16.3476181
185      pz       16.5429306
186      pz       16.7382431
```

```
   187     pz      16.9335537
   188     pz      17.1288662
   189     pz      17.3241787
   190     pz      17.5194912
   191     pz      17.7148018
   192     pz      17.9101143
   193     pz      18.1054268
   194     pz      18.3007393
   195     pz      18.4960499
   196     pz      18.6913624
   197     pz      18.8866749
   198     pz      19.0819874
   199     pz      19.2772980
   200     pz      19.4726105
   201     pz      19.6679230
   202     pz      19.8632336
   203     pz      19.9804039
c
c

c
c              ****************************
c              *** material definitions ***
c              ****************************
c
c m1: UO2 enriched to 5.0 w/o  (bin 1)
m1   8016.01c 1.98      &
    92234.01c 0.000055  &
    92235.01c 0.050000  &
    92238.01c 0.949945
c
c m2: UO2 enriched to 5.0 w/o  (bin 2)
m2   8016.02c 1.98      &
    92234.02c 0.000055  &
    92235.02c 0.050000  &
    92238.02c 0.949945
c
c m3: UO2 enriched to 5.0 w/o  (bin 3)
m3   8016.03c 1.98      &
    92234.03c 0.000055  &
    92235.03c 0.050000  &
    92238.03c 0.949945
c
c m4: UO2 enriched to 5.0 w/o  (bin 4)
m4   8016.04c 1.98      &
    92234.04c 0.000055  &
    92235.04c 0.050000  &
    92238.04c 0.949945
c
c m5: UO2 enriched to 5.0 w/o  (bin 5)
m5   8016.05c 1.98      &
    92234.05c 0.000055  &
    92235.05c 0.050000  &
    92238.05c 0.949945
c
c m6: UO2 enriched to 5.0 w/o  (bin 6)
m6   8016.06c 1.98      &
    92234.06c 0.000055  &
    92235.06c 0.050000  &
    92238.06c 0.949945
c
c m7: UO2 enriched to 5.0 w/o  (bin 7)
m7   8016.07c 1.98      &
```

```
    92234.07c 0.000055  &
    92235.07c 0.050000  &
    92238.07c 0.949945
c
c m8: UO2 enriched to 5.0 w/o  (bin 8)
m8   8016.08c 1.98      &
    92234.08c 0.000055  &
    92235.08c 0.050000  &
    92238.08c 0.949945
c
c m9: UO2 enriched to 5.0 w/o  (bin 9)
m9   8016.09c 1.98      &
    92234.09c 0.000055  &
    92235.09c 0.050000  &
    92238.09c 0.949945
c
c m10: UO2 enriched to 5.0 w/o  (bin 10)
m10  8016.10c 1.98      &
    92234.10c 0.000055  &
    92235.10c 0.050000  &
    92238.10c 0.949945
c
c m11: UO2 enriched to 5.0 w/o  (bin 11)
m11  8016.11c 1.98      &
    92234.11c 0.000055  &
    92235.11c 0.050000  &
    92238.11c 0.949945
c
c m12: UO2 enriched to 5.0 w/o  (bin 12)
m12  8016.12c 1.98      &
    92234.12c 0.000055  &
    92235.12c 0.050000  &
    92238.12c 0.949945
c
c m13: UO2 enriched to 5.0 w/o  (bin 13)
m13  8016.13c 1.98      &
    92234.13c 0.000055  &
    92235.13c 0.050000  &
    92238.13c 0.949945
c
c m14: UO2 enriched to 5.0 w/o  (bin 14)
m14  8016.14c 1.98      &
    92234.14c 0.000055  &
    92235.14c 0.050000  &
    92238.14c 0.949945
c
c m15: UO2 enriched to 5.0 w/o  (bin 15)
m15  8016.15c 1.98      &
    92234.15c 0.000055  &
    92235.15c 0.050000  &
    92238.15c 0.949945
c
c m21: zircaloy-4 cladding: 6.55g/cc (4.28234e-2 atom/b-cm), 98.2%Zr, 1.5%Sn, 0.20%Fe,
c 0.1%Cr
m21 24050.21c   4.3450e-05   &
    24052.21c   8.3789e-04   &
    24053.21c   9.5010e-05   &
    24054.21c   2.3650e-05   &
    26054.21c   1.1600e-04   &
    26056.21c   1.8344e-03   &
    26057.21c   4.4000e-05   &
    26058.21c   5.6000e-06   &
c
```

```
    50112.21c   1.4550e-04   &
    50114.21c   9.9000e-05   &
    50115.21c   5.1000e-05   &
    50116.21c   2.1810e-03   &
    50117.21c   1.1520e-03   &
    50118.21c   3.6330e-03   &
    50119.21c   1.2885e-03   &
    50120.21c   4.8870e-03   &
    50122.21c   6.9450e-04   &
    50124.21c   8.6850e-04   &
c
    40090.21c   0.5052390    &
    40091.21c   0.1101804    &
    40092.21c   0.1684130    &
    40094.21c   0.1706716    &
    40096.21c   0.0274960
c
c m22: zircaloy-4 cladding: 6.55g/cc (4.28234e-2 atom/b-cm), 98.2%Zr, 1.5%Sn, 0.20%Fe,
c 0.1%Cr
m22 24050.22c   4.3450e-05   &
    24052.22c   8.3789e-04   &
    24053.22c   9.5010e-05   &
    24054.22c   2.3650e-05   &
    26054.22c   1.1600e-04   &
    26056.22c   1.8344e-03   &
    26057.22c   4.4000e-05   &
    26058.22c   5.6000e-06   &
c
    50112.22c   1.4550e-04   &
    50114.22c   9.9000e-05   &
    50115.22c   5.1000e-05   &
    50116.22c   2.1810e-03   &
    50117.22c   1.1520e-03   &
    50118.22c   3.6330e-03   &
    50119.22c   1.2885e-03   &
    50120.22c   4.8870e-03   &
    50122.22c   6.9450e-04   &
    50124.22c   8.6850e-04   &
c
    40090.22c   0.5052390    &
    40091.22c   0.1101804    &
    40092.22c   0.1684130    &
    40094.22c   0.1706716    &
    40096.22c   0.0274960
c
c m23: zircaloy-4 cladding: 6.55g/cc (4.28234e-2 atom/b-cm), 98.2%Zr, 1.5%Sn, 0.20%Fe,
c 0.1%Cr
m23 24050.23c   4.3450e-05   &
    24052.23c   8.3789e-04   &
    24053.23c   9.5010e-05   &
    24054.23c   2.3650e-05   &
    26054.23c   1.1600e-04   &
    26056.23c   1.8344e-03   &
    26057.23c   4.4000e-05   &
    26058.23c   5.6000e-06   &
c
    50112.23c   1.4550e-04   &
    50114.23c   9.9000e-05   &
    50115.23c   5.1000e-05   &
    50116.23c   2.1810e-03   &
    50117.23c   1.1520e-03   &
    50118.23c   3.6330e-03   &
    50119.23c   1.2885e-03   &
    50120.23c   4.8870e-03   &
    50122.23c   6.9450e-04   &
    50124.23c   8.6850e-04   &
c
    40090.23c   0.5052390    &
    40091.23c   0.1101804    &
    40092.23c   0.1684130    &
    40094.23c   0.1706716    &
    40096.23c   0.0274960
c
c
c m31: water moderator           (water bin 1)
m31   1001.31c  2.0          &
      8016.31c  1.0
mt31  lwtr.31t
c
c m32: water moderator           (water bin 2)
m32   1001.32c  2.0          &
      8016.32c  1.0
mt32  lwtr.32t
c
c m33: water moderator           (water bin 3)
m33   1001.33c  2.0          &
      8016.33c  1.0
mt33  lwtr.33t
c
c m34: water moderator           (water bin 4)
m34   1001.34c  2.0          &
      8016.34c  1.0
mt34  lwtr.34t
c
c m35: water moderator           (water bin 5)
m35   1001.35c  2.0          &
      8016.35c  1.0
mt35  lwtr.35t
c
c m36: water moderator           (water bin 6)
m36   1001.36c  2.0          &
      8016.36c  1.0
mt36  lwtr.36t
c
c m37: water moderator           (water bin 7)
m37   1001.37c  2.0          &
      8016.37c  1.0
mt37  lwtr.37t
c
c m38: water moderator           (water bin 8)
m38   1001.38c  2.0          &
      8016.38c  1.0
mt38  lwtr.38t
c
c m39: water moderator           (water bin 9)
m39   1001.39c  2.0          &
      8016.39c  1.0
mt39  lwtr.39t
c
c
c ------------------------------
c isothermal 293 K materials
c ------------------------------
c
c m41: UO2 enriched to 5.0 w/o
m41  8016.70c 1.98      &
```

```
    92234.70c 0.000055  &
    92235.70c 0.050000  &
    92238.70c 0.949945
c
c m42: zircaloy-4 cladding: 6.55g/cc (4.28234e-2 atom/b-cm), 98.2%Zr, 1.5%Sn, 0.20%Fe,
0.1%Cr
m42 24050.70c   4.3450e-05   &
    24052.70c   8.3789e-04   &
    24053.70c   9.5010e-05   &
    24054.70c   2.3650e-05   &
    26054.70c   1.1600e-04   &
    26056.70c   1.8344e-03   &
    26057.70c   4.4000e-05   &
    26058.70c   5.6000e-06   &
c
    50112.70c   1.4550e-04   &
    50114.70c   9.9000e-05   &
    50115.70c   5.1000e-05   &
    50116.70c   2.1810e-03   &
    50117.70c   1.1520e-03   &
    50118.70c   3.6330e-03   &
    50119.70c   1.2885e-03   &
    50120.70c   4.8870e-03   &
    50122.70c   6.9450e-04   &
    50124.70c   8.6850e-04   &
c
    40090.70c   0.5052390    &
    40091.70c   0.1101804    &
    40092.70c   0.1684130    &
    40094.70c   0.1706716    &
    40096.70c   0.0274960
c
c
c m43: water moderator
m43  1001.70c  2.0           &
     8016.70c  1.0
mt43 lwtr.10t
c
c
c             ****************************
c             *** physics/fission src  ***
c             ****************************
c
c neutron/photon physics options:
mode n
totnu
kcode 15000 1.0 10 160
c
c source definition:
sdef erg=d1 rad=d2 axs=0 0 1 ext=d3 pos=0.0 0.0 0.0
sp1     -3
si2    0.0 0.5
sp2    -21 1
si3      0 19.98
sp3    -21 0
c
c
c             ******************************
c             *** fisson rxn rate tally  ***
c             ******************************
c
c use f14 with fm14 below to get fission tally
c f14:n  fm14 (1 1 -6)
```

```
f14:n &
    1    2    3    4    5    6    7    8 &
    9   10   11   12   13   14   15   16 &
   17   18   19   20   21   22   23   24 &
   25   26   27   28   29   30   31   32 &
   33   34   35   36   37   38   39   40 &
   41   42   43   44   45   46   47   48 &
   49   50   51   52   53   54   55   56 &
   57   58   59   60   61   62   63   64 &
   65   66   67   68   69   70   71   72 &
   73   74   75   76   77   78   79   80 &
   81   82   83   84   85   86   87   88 &
   89   90   91   92   93   94   95   96 &
   97   98   99  100  101  102  103  104 &
  105  106  107  108  109  110  111  112 &
  113  114  115  116  117  118  119  120 &
```

…

(Cropped: list of all fuel cell numbers for fission reaction rate tally)

…

```
 3249 3250 3251 3252 3253 3254 3255 3256 &
 3257 3258 3259 3260 3261 3262 3263 3264 &
 3265 3266 3267 3268 3269 3270 3271 3272 &
 3273 3274 3275 3276 3277 3278 3279 3280 &
 3281 3282 3283 3284 3285 3286 3287 3288 &
 3289 3290 3291 3292 3293 3294 3295 3296 &
 3297 3298 3299 3300 3301 3302 3303 3304 &
 3305 3306 3307 3308 3309 3310 3311 3312 &
 3313 3314 3315 3316 3317 3318 3319 3320 &
 3321 3322 3323 3324 3325 3326 3327 3328
fm14 (1 1 -6)
sd14 &
0.0001346 0.0006456 0.0006634 0.0001514 &   $ bottom node volumes
0.0001471 0.0013561 0.0014901 0.0014901 &
0.0013559 0.0001401 0.0006706 0.0014901 &
0.0014901 0.0014901 0.0014901 0.0006656 &
0.0006683 0.0014901 0.0014901 0.0014901 &
0.0014901 0.0006654 0.0001464 0.0013578 &
0.0014901 0.0014901 0.0013560 0.0001402 &
0.0001353 0.0006468 0.0006631 0.0001513 &
0.0007170 0.0033041 0.0033204 0.0007195 &   $ middle node volumes
0.0007171 0.0066793 0.0074506 0.0074506 &
0.0067400 0.0006910 0.0032764 0.0074506 &
0.0074506 0.0074506 0.0074506 0.0032991 &
0.0032866 0.0074506 0.0074506 0.0074506 &
0.0074506 0.0033185 0.0007105 0.0067400 &
0.0074506 0.0074506 0.0067770 0.0006949 &
0.0007097 0.0032655 0.0033259 0.0007546 &
0.0007170 0.0033041 0.0033204 0.0007195 &
0.0007171 0.0066793 0.0074506 0.0074506 &
0.0067400 0.0006910 0.0032764 0.0074506 &
0.0074506 0.0074506 0.0074506 0.0032991 &
0.0032866 0.0074506 0.0074506 0.0074506 &
0.0074506 0.0033185 0.0007105 0.0067400 &
0.0074506 0.0074506 0.0067770 0.0006949 &
0.0007097 0.0032655 0.0033259 0.0007546 &
0.0007170 0.0033041 0.0033204 0.0007195 &
```

…

(Cropped: list of all fuel cell volumes for fission reaction rate tally)

…

```
0.0074506 0.0033185 0.0007105 0.0067400 &
0.0074506 0.0074506 0.0067770 0.0006949 &
```

```
0.0007097 0.0032655 0.0033259 0.0007546 &
0.0001346 0.0006456 0.0006634 0.0001514 &   $ top node volumes
0.0001471 0.0013561 0.0014901 0.0014901 &
0.0013559 0.0001401 0.0006706 0.0014901 &
0.0014901 0.0014901 0.0014901 0.0006656 &
0.0006683 0.0014901 0.0014901 0.0014901 &
0.0014901 0.0006654 0.0001464 0.0013578 &
0.0014901 0.0014901 0.0013560 0.0001402 &
0.0001353 0.0006468 0.0006631 0.0001513
c
c             ****************************************
c             *** fission energy deposition tally  ***
c             ****************************************
c
f17:n &
    1    2    3    4    5    6    7    8 &
    9   10   11   12   13   14   15   16 &
   17   18   19   20   21   22   23   24 &
   25   26   27   28   29   30   31   32 &
   33   34   35   36   37   38   39   40 &
   41   42   43   44   45   46   47   48 &
   49   50   51   52   53   54   55   56 &
   57   58   59   60   61   62   63   64 &
   65   66   67   68   69   70   71   72 &
   73   74   75   76   77   78   79   80 &
   81   82   83   84   85   86   87   88 &
   89   90   91   92   93   94   95   96 &
   97   98   99  100  101  102  103  104 &
  105  106  107  108  109  110  111  112 &
  113  114  115  116  117  118  119  120 &
  121  122  123  124  125  126  127  128 &
  129  130  131  132  133  134  135  136 &
  137  138  139  140  141  142  143  144 &
  145  146  147  148  149  150  151  152 &
  153  154  155  156  157  158  159  160 &
  161  162  163  164  165  166  167  168 &
  169  170  171  172  173  174  175  176 &
  177  178  179  180  181  182  183  184 &
  185  186  187  188  189  190  191  192 &
  193  194  195  196  197  198  199  200 &
  201  202  203  204  205  206  207  208 &
  209  210  211  212  213  214  215  216 &
  217  218  219  220  221  222  223  224 &
```

…

(Cropped: list of all fuel cell numbers for fission energy deposition tally)

…

```
3193 3194 3195 3196 3197 3198 3199 3200 &
 3201 3202 3203 3204 3205 3206 3207 3208 &
 3209 3210 3211 3212 3213 3214 3215 3216 &
 3217 3218 3219 3220 3221 3222 3223 3224 &
 3225 3226 3227 3228 3229 3230 3231 3232 &
 3233 3234 3235 3236 3237 3238 3239 3240 &
 3241 3242 3243 3244 3245 3246 3247 3248 &
 3249 3250 3251 3252 3253 3254 3255 3256 &
 3257 3258 3259 3260 3261 3262 3263 3264 &
 3265 3266 3267 3268 3269 3270 3271 3272 &
 3273 3274 3275 3276 3277 3278 3279 3280 &
 3281 3282 3283 3284 3285 3286 3287 3288 &
 3289 3290 3291 3292 3293 3294 3295 3296 &
 3297 3298 3299 3300 3301 3302 3303 3304 &
 3305 3306 3307 3308 3309 3310 3311 3312 &
 3313 3314 3315 3316 3317 3318 3319 3320 &
 3321 3322 3323 3324 3325 3326 3327 3328
sd17 &
0.0013867 0.0066496 0.0068325 0.0015597 &   $ bottom node masses
0.0015149 0.0139679 0.0153482 0.0153482 &
0.0139656 0.0014431 0.0069069 0.0153482 &
0.0153482 0.0153482 0.0153482 0.0068554 &
0.0068840 0.0153482 0.0153482 0.0153482 &
0.0153482 0.0068533 0.0015078 0.0139849 &
0.0153482 0.0153482 0.0139673 0.0014442 &
0.0013932 0.0066619 0.0068301 0.0015584 &
0.0073855 0.0340327 0.0341999 0.0074105 &   $ middle node masses
0.0073865 0.0687971 0.0767410 0.0767410 &
0.0694219 0.0071172 0.0337467 0.0767410 &
0.0767410 0.0767410 0.0767410 0.0339808 &
0.0338524 0.0767410 0.0767410 0.0767410 &
0.0767410 0.0341808 0.0073177 0.0694216 &
0.0767410 0.0767410 0.0698032 0.0071578 &
0.0073095 0.0336348 0.0342565 0.0077726 &
0.0073855 0.0340327 0.0341999 0.0074105 &
0.0073865 0.0687971 0.0767410 0.0767410 &
0.0694219 0.0071172 0.0337467 0.0767410 &
0.0767410 0.0767410 0.0767410 0.0339808 &
0.0338524 0.0767410 0.0767410 0.0767410 &
0.0767410 0.0341808 0.0073177 0.0694216 &
0.0767410 0.0767410 0.0698032 0.0071578 &
0.0073095 0.0336348 0.0342565 0.0077726 &
0.0073855 0.0340327 0.0341999 0.0074105 &
```

…

(Cropped: list of all fuel cell masses for fission energy deposition tally)

…

```
0.0073865 0.0687971 0.0767410 0.0767410 &
0.0694219 0.0071172 0.0337467 0.0767410 &
0.0767410 0.0767410 0.0767410 0.0339808 &
0.0338524 0.0767410 0.0767410 0.0767410 &
0.0767410 0.0341808 0.0073177 0.0694216 &
0.0767410 0.0767410 0.0698032 0.0071578 &
0.0073095 0.0336348 0.0342565 0.0077726 &
0.0087638 0.0420258 0.0431815 0.0098571 &  $ top node masses
0.0095739 0.0882773 0.0970006 0.0970006 &
0.0882626 0.0091203 0.0436516 0.0970006 &
0.0970006 0.0970006 0.0970006 0.0433263 &
0.0435068 0.0970006 0.0970006 0.0970006 &
0.0970006 0.0433126 0.0095291 0.0883844 &
0.0970006 0.0970006 0.0882732 0.0091276 &
0.0088048 0.0421032 0.0431662 0.0098490
c
```

A.2 STAR-CCM+ Simulation File

The STAR-CCM+ simulation file is not available as a text file. An electronic copy of the 20 cm PWR cell model (called *pin20cm.sim*) can be found in the *multinuke.zip* file.

A.3 MAKXSF Input File (*specs*)

```
# datapath to old xsdir not necessary - in DATAPATH enviroment variable
#
# Old xsdir name (just orig xsdir)  |  New xsdir name
      xsdir                              xsdir_broad1
#
#
#  new library name/type
   library_broad1   1
#

#  1st fuel temperature bin 600 K - 650 K: broaden to 625 K
    8016.01c  625.00    8016.71c    8016.73c
   92234.01c  625.00   92234.71c   92234.73c
   92235.01c  625.00   92235.71c   92235.73c
   92238.01c  625.00   92238.71c   92238.73c
#
#  2nd fuel temperature bin 650 K - 700 K: broaden to 675 K
    8016.02c  675.00    8016.71c    8016.73c
   92234.02c  675.00   92234.71c   92234.73c
   92235.02c  675.00   92235.71c   92235.73c
   92238.02c  675.00   92238.71c   92238.73c
#
#  3rd fuel temperature bin 700 K - 750 K: broaden to 725 K
    8016.03c  725.00    8016.71c    8016.73c
   92234.03c  725.00   92234.71c   92234.73c
   92235.03c  725.00   92235.71c   92235.73c
   92238.03c  725.00   92238.71c   92238.73c
#
#  4th fuel temperature bin 750 K - 800 K: broaden to 775 K
    8016.04c  775.00    8016.71c    8016.73c
   92234.04c  775.00   92234.71c   92234.73c
   92235.04c  775.00   92235.71c   92235.73c
   92238.04c  775.00   92238.71c   92238.73c
#
#  5th fuel temperature bin 800 K - 850 K: broaden to 825 K
    8016.05c  825.00    8016.71c    8016.73c
   92234.05c  825.00   92234.71c   92234.73c
   92235.05c  825.00   92235.71c   92235.73c
   92238.05c  825.00   92238.71c   92238.73c
#
#  6th fuel temperature bin 850 K - 900 K: broaden to 875 K
    8016.06c  875.00    8016.71c    8016.73c
   92234.06c  875.00   92234.71c   92234.73c
   92235.06c  875.00   92235.71c   92235.73c
   92238.06c  875.00   92238.71c   92238.73c
#
#  7th fuel temperature bin 900 K - 950 K: broaden to 925 K
    8016.07c  925.00    8016.71c    8016.73c
   92234.07c  925.00   92234.71c   92234.73c
   92235.07c  925.00   92235.71c   92235.73c
   92238.07c  925.00   92238.71c   92238.73c
#
#  8th fuel temperature bin 950 K - 1000 K: broaden to 975 K
    8016.08c  975.00    8016.71c    8016.73c
   92234.08c  975.00   92234.71c   92234.73c
   92235.08c  975.00   92235.71c   92235.73c
   92238.08c  975.00   92238.71c   92238.73c
#
#  9th fuel temperature bin 1000 K - 1050 K: broaden to 1025 K
    8016.09c  1025.00    8016.71c    8016.73c
   92234.09c  1025.00   92234.71c   92234.73c
   92235.09c  1025.00   92235.71c   92235.73c
   92238.09c  1025.00   92238.71c   92238.73c
#
#  10th fuel temperature bin 1050 K - 1100 K: broaden to 1075 K
    8016.10c  1075.00    8016.71c    8016.73c
   92234.10c  1075.00   92234.71c   92234.73c
   92235.10c  1075.00   92235.71c   92235.73c
   92238.10c  1075.00   92238.71c   92238.73c
#
#  11th fuel temperature bin 1100 K - 1150 K: broaden to 1125 K
    8016.11c  1125.00    8016.71c    8016.73c
   92234.11c  1125.00   92234.71c   92234.73c
   92235.11c  1125.00   92235.71c   92235.73c
   92238.11c  1125.00   92238.71c   92238.73c
#
#  12th fuel temperature bin 1150 K - 1200 K: broaden to 1175 K
    8016.12c  1175.00    8016.71c    8016.73c
   92234.12c  1175.00   92234.71c   92234.73c
   92235.12c  1175.00   92235.71c   92235.73c
   92238.12c  1175.00   92238.71c   92238.73c
#
#  13th fuel temperature bin 1200 K - 1250 K: broaden to 1225 K
    8016.13c  1225.00    8016.73c    8016.74c
   92234.13c  1225.00   92234.73c   92234.74c
   92235.13c  1225.00   92235.73c   92235.74c
   92238.13c  1225.00   92238.73c   92238.74c
#
#  14th fuel temperature bin 1250 K - 1300 K: broaden to 1275 K
    8016.14c  1275.00    8016.73c    8016.74c
   92234.14c  1275.00   92234.73c   92234.74c
   92235.14c  1275.00   92235.73c   92235.74c
   92238.14c  1275.00   92238.73c   92238.74c
#
#  15th fuel temperature bin 1300 K - 1350 K: broaden to 1325 K
    8016.15c  1325.00    8016.73c    8016.74c
   92234.15c  1325.00   92234.73c   92234.74c
   92235.15c  1325.00   92235.73c   92235.74c
   92238.15c  1325.00   92238.73c   92238.74c
#
#  1st clad temperature bin 500 K - 600 K: broaden to 550 K
   24050.21c  550.00   24050.70c   24050.72c
   24052.21c  550.00   24052.70c   24052.72c
   24053.21c  550.00   24053.70c   24053.72c
   24054.21c  550.00   24054.70c   24054.72c
   26054.21c  550.00   26054.70c   26054.72c
   26056.21c  550.00   26056.70c   26056.72c
   26057.21c  550.00   26057.70c   26057.72c
   26058.21c  550.00   26058.70c   26058.72c
   50112.21c  550.00   50112.70c   50112.72c
   50114.21c  550.00   50114.70c   50114.72c
   50115.21c  550.00   50115.70c   50115.72c
   50116.21c  550.00   50116.70c   50116.72c
   50117.21c  550.00   50117.70c   50117.72c
   50118.21c  550.00   50118.70c   50118.72c
   50119.21c  550.00   50119.70c   50119.72c
   50120.21c  550.00   50120.70c   50120.72c
   50122.21c  550.00   50122.70c   50122.72c
   50124.21c  550.00   50124.70c   50124.72c
   40090.21c  550.00   40090.70c   40090.72c
   40091.21c  550.00   40091.70c   40091.72c
   40092.21c  550.00   40092.70c   40092.72c
   40094.21c  550.00   40094.70c   40094.72c
   40096.21c  550.00   40096.70c   40096.72c
#
#  2nd clad temperature bin 600 K - 700 K: broaden to 650 K
   24050.22c  650.00   24050.70c   24050.72c
   24052.22c  650.00   24052.70c   24052.72c
   24053.22c  650.00   24053.70c   24053.72c
   24054.22c  650.00   24054.70c   24054.72c
   26054.22c  650.00   26054.70c   26054.72c
   26056.22c  650.00   26056.70c   26056.72c
   26057.22c  650.00   26057.70c   26057.72c
   26058.22c  650.00   26058.70c   26058.72c
   50112.22c  650.00   50112.70c   50112.72c
   50114.22c  650.00   50114.70c   50114.72c
   50115.22c  650.00   50115.70c   50115.72c
   50116.22c  650.00   50116.70c   50116.72c
   50117.22c  650.00   50117.70c   50117.72c
   50118.22c  650.00   50118.70c   50118.72c
   50119.22c  650.00   50119.70c   50119.72c
   50120.22c  650.00   50120.70c   50120.72c
   50122.22c  650.00   50122.70c   50122.72c
   50124.22c  650.00   50124.70c   50124.72c
   40090.22c  650.00   40090.70c   40090.72c
   40091.22c  650.00   40091.70c   40091.72c
   40092.22c  650.00   40092.70c   40092.72c
   40094.22c  650.00   40094.70c   40094.72c
   40096.22c  650.00   40096.70c   40096.72c
#
#  3rd clad temperature bin 700 K - 800 K: broaden to 750 K
   24050.23c  750.00   24050.70c   24050.72c
   24052.23c  750.00   24052.70c   24052.72c
   24053.23c  750.00   24053.70c   24053.72c
   24054.23c  750.00   24054.70c   24054.72c
   26054.23c  750.00   26054.70c   26054.72c
   26056.23c  750.00   26056.70c   26056.72c
   26057.23c  750.00   26057.70c   26057.72c
   26058.23c  750.00   26058.70c   26058.72c
   50112.23c  750.00   50112.70c   50112.72c
   50114.23c  750.00   50114.70c   50114.72c
   50115.23c  750.00   50115.70c   50115.72c
   50116.23c  750.00   50116.70c   50116.72c
   50117.23c  750.00   50117.70c   50117.72c
   50118.23c  750.00   50118.70c   50118.72c
   50119.23c  750.00   50119.70c   50119.72c
   50120.23c  750.00   50120.70c   50120.72c
   50122.23c  750.00   50122.70c   50122.72c
   50124.23c  750.00   50124.70c   50124.72c
   40090.23c  750.00   40090.70c   40090.72c
   40091.23c  750.00   40091.70c   40091.72c
   40092.23c  750.00   40092.70c   40092.72c
   40094.23c  750.00   40094.70c   40094.72c
   40096.23c  750.00   40096.70c   40096.72c
#
```

```
#  1st water temperature bin 550 K - 560 K: broaden to 555 K
    1001.31c  555.00    1001.70c    1001.72c
    8016.31c  555.00    8016.70c    8016.72c
    lwtr.31t  555.00    lwtr.61t    lwtr.63t
#
#  2nd water temperature bin 560 K - 570 K: broaden to 570 K
    1001.32c  570.00    1001.70c    1001.72c
    8016.32c  570.00    8016.70c    8016.72c
    lwtr.32t  570.00    lwtr.61t    lwtr.63t
#
#  3rd water temperature bin 570 K - 575 K: broaden to 572.5 K
    1001.33c  572.50    1001.70c    1001.72c
    8016.33c  572.50    8016.70c    8016.72c
    lwtr.33t  572.50    lwtr.61t    lwtr.63t
#
#  4th water temperature bin 575 K - 580 K: broaden to 577.5 K
    1001.34c  577.50    1001.70c    1001.72c
    8016.34c  577.50    8016.70c    8016.72c
    lwtr.34t  577.50    lwtr.61t    lwtr.63t
#
#  5th water temperature bin 580 K - 585 K: broaden to 582.5 K
    1001.35c  582.50    1001.70c    1001.72c
    8016.35c  582.50    8016.70c    8016.72c
    lwtr.35t  582.50    lwtr.61t    lwtr.63t
#
#  6th water temperature bin 585 K - 590 K: broaden to 587.5 K
    1001.36c  587.50    1001.70c    1001.72c
    8016.36c  587.50    8016.70c    8016.72c
    lwtr.36t  587.50    lwtr.61t    lwtr.63t
#
#  7th water temperature bin 590 K - 595 K: broaden to 592.5 K
    1001.37c  592.50    1001.70c    1001.72c
    8016.37c  592.50    8016.70c    8016.72c
    lwtr.37t  592.50    lwtr.61t    lwtr.63t
#
#  8th water temperature bin 595 K - 600 K: broaden to 597.5 K
    1001.38c  597.50    1001.70c    1001.72c
    8016.38c  597.50    8016.70c    8016.72c
    lwtr.38t  597.50    lwtr.61t    lwtr.63t
#
#  9th water temperature bin 600 K - 610 K: broaden to 605.0 K
    1001.39c  605.00    1001.70c    1001.72c
    8016.39c  605.00    8016.70c    8016.72c
    lwtr.39t  605.00    lwtr.61t    lwtr.63t
#
#  isothermal data copied over -
    lwtr.10t
    lwtr.11t
    lwtr.12t
    lwtr.13t
    lwtr.14t
    lwtr.15t
    lwtr.16t
    lwtr.17t
    lwtr.18t
    1001.70c
    8016.70c
    24050.70c
    24052.70c
    24053.70c
    24054.70c
    26054.70c
    26056.70c
    26057.70c
    26058.70c
    40090.70c
    40091.70c
    40092.70c
    40094.70c
    40096.70c
    50112.70c
    50114.70c
    50115.70c
    50116.70c
    50117.70c
    50118.70c
    50119.70c
    50120.70c
    50122.70c
    50124.70c
    92234.70c
    92235.70c
    92238.70c
#

# done
```

A.4 MULTINUKE Input File for PWR Cell Model – *multiSpecs_base.txt*

```
mcnpInputFile       = pin20cm
mcnpOutputFile      = pin20cmo
rhoFuel_g_cc        = 10.3
powerW              = 4700.0
Q_MeVperFission     = 200.0
iteration_start     = 1
iteration_max       = 5
converge_eigenvalue = 0.0005
converge_heat       = 0.02
MCNPisothermJob     = 293
MCNPwaterIndexStart = 4000
```

APPENDIX B. MULTINUKE Programs

B.1 MULTINUKE Perl Script

```
#!/usr/bin/perl

# read multiSpecs_base input file
open(multispecsINPUT, "multiSpecs_base.txt") || die "multiSpecs_base.txt file not found\n";
while(<multispecsINPUT>) {
 if (/mcnpInputFile/) {
   $mcnpInputFile_line = $_;
   @mcnpInputFile0 = split("=", $mcnpInputFile_line);
   @mcnpInputFile1 = split(" ", $mcnpInputFile0[1]);
 }
 if (/mcnpOutputFile/) {
   $mcnpOutputFile_line = $_;
   @mcnpOutputFile0 = split("=", $mcnpOutputFile_line);
   @mcnpOutputFile1 = split(" ", $mcnpOutputFile0[1]);
 }
 if (/iteration_start/) {
   $iteration_start_line = $_;
   @iteration_start0 = split("=", $iteration_start_line);
   @iteration_start1 = split(" ", $iteration_start0[1]);
 }
 if (/iteration_max/) {
   $iteration_max_line = $_;
   @iteration_max0 = split("=", $iteration_max_line);
   @iteration_max1 = split(" ", $iteration_max0[1]);
 }
 if (/converge_eigenvalue/) {
   $converge_eigenvalue_line = $_;
   @converge_eigenvalue0 = split("=", $converge_eigenvalue_line);
   @converge_eigenvalue1 = split(" ", $converge_eigenvalue0[1]);
 }
 if (/converge_heat/) {
   $converge_heat_line = $_;
   @converge_heat0 = split("=", $converge_heat_line);
   @converge_heat1 = split(" ", $converge_heat0[1]);
 }
 if (/MCNPisothermJob/) {
   $MCNPisothermJob_line = $_;
   @MCNPisothermJob0 = split("=", $MCNPisothermJob_line);
   @MCNPisothermJob1 = split(" ", $MCNPisothermJob0[1]);
 }
 if (/MCNPwaterIndexStart/) {
   $MCNPwaterIndexStart_line = $_;
   @MCNPwaterIndexStart0 = split("=", $MCNPwaterIndexStart_line);
   @MCNPwaterIndexStart1 = split(" ", $MCNPwaterIndexStart0[1]);
 }
}
close multispecsINPUT;

# =========================================================
# multiphysics script run parameters
# $iterationStart --> starting iteration #, for restarts
# $iterationMax   --> max. # of iterations
# =========================================================
$iterationStart =  $iteration_start1[0];

$iterationMax   = $iteration_max1[0];

$iterationEnd   = $iterationStart + $iterationMax;
```

```
# ============================================================
# multiphysics script convergence criteria
# $convergeMCNP5     --> converges by k-eff (units = delta k)
# $convergeSTARCCM   --> converges by an avg error value of fuel and water temperature
# ============================================================

$convergeMCNP5   = $converge_eigenvalue1[0]; # units of delta k (k_new - k_old)

$convergeSTARCCM = $converge_heat1[0];       # avg relative error in fuel/clad/water temperatures

# ==========================================
# input MCNP water cell index start
# input jobs name - determines mcnp file names
# ==========================================
$MCNPwaterIndexStart = $MCNPwaterIndexStart1[0];

$JOB_NAME = $mcnpInputFile1[0];

$append_firstMCNPrun = $MCNPisothermJob1[0];

$append_baseMCNPfile = "_base";

#--------------------------------------------------
$isothermMCNPfile = $JOB_NAME.$append_firstMCNPrun;

$isothermMCNPoutfile = $JOB_NAME.$append_firstMCNPrun.o;

$MCNPbaseFile = $JOB_NAME.$append_baseMCNPfile;

$k = 8.617E-11;

$isoTemp = $k * $append_firstMCNPrun;

$numFuelCells = 3328;

$numWaterCells = 4160;

# open summary text file for keff and temperature convergence data
open(summaryFile, ">convergenceSummary.txt");

# set stack size unlimited ------------------------
system("ulimit -s unlimited");

# set links to enormous doppler broadened library and xsdir file
system("ln -s -f /home/jcardoni2/thesis/XSdir_broad2/xsdir_broad1 xsdir_broad1");
system("ln -s -f /home/jcardoni2/thesis/XSdir_broad2/library_broad1 library_broad1");

# $Niter is the iteration number - increases after a MCNP5 run and STARCCM+ run (1 iteration)
$Niter = 0;
$oForOutput="o";
$rForRestart="r";
$sForSource="s";

# ------------------------------------------------------------------------------------------------------------------------------------------------------------------------
##################################################################################################
#>>>>>>>>>>>>>>>>>>>>>>>>>>>> correlate STARCCM+ and MCNP5 mesh indexes <<<<<<<<<<<<<<<<<<<<<<<<<<<<<<<<<<<<<<<<
#                                                                ( only need to run this once )
##################################################################################################
#-------------------------------------------------------------------------------------------------------------------------------------------------------------------------

##################################################
##### read MCNP5-to-STARCCM+ fuel index    #####
##################################################

open(fuelMesh, "fuel-STARcell_equals_MCNPcell.txt") || die "fuel mesh correlation file not found\n";
readline(fuelMesh);  # skip first line

$i = 0;
while(<fuelMesh>) {
  $i = $i + 1;
  $linevalues = $_;

  @values = split(" ",$linevalues);
  $fuelIndexSTAR[$i] = $values[0];
  $fuelIndexMCNP[$i] = $values[2];
}
close fuelMesh;

################################################
##### read MCNP5-to-STARCCM+ water index   #####
################################################

open(waterMesh, "water-STARcell_equals_MCNPcell.txt") || die "water mesh correlation file not found\n";
readline(waterMesh);  # skip first line

$i = 0;
while(<waterMesh>) {
  $i = $i + 1;
  $linevalues = $_;

  @values = split(" ",$linevalues);
  $waterIndexSTAR[$i] = $values[0];
  $waterIndexMCNP[$i] = $values[2];
}
close waterMesh;

# ------------------------------------------------------------------------------------------------------------------------------------------------------------------
################################################################################################
################################################################################################
# ------------------------------------------------------------------------------------------------------------------------------------------------------------------
# prep mcnp post-processing specs file (for f90 post-processing code)
$i = 0;
open(specsBASE, "multiSpecs_base.txt") || die "multiSpecs_base.txt file not found\n";
@multispecsLines = <specsBASE>;
close specsBASE;

# open actual working java file with working directory in it
open(MCNPspecs, ">multiSpecs.txt");

foreach $specsline (@multispecsLines) {
  $specsline =~ s/$JOB_NAME/$isothermMCNPfile/g;
  $specsline =~ s/$JOB_NAME$oForOutput/$isothermMCNPoutfile/g;
  print MCNPspecs $specsline;
}
close MCNPspecs;

###################################################################
##### load fuel isothermal material numbers and temperatures #####
###################################################################

$i=0;
open (MCNPfile_base0, "$MCNPbaseFile") || die "base MCNP file not found\n";
while(<MCNPfile_base0>){
  $i=$i+1;
  if (/f_$numFuelCells/) {
    $FUELlineNumberMax = $i;
    print "Loading isothermal fuel materials and $append_firstMCNPrun kT temps.\n";
  }
}
seek(MCNPfile_base0,0,0);
@mcnpBase0 = <MCNPfile_base0>;
close MCNPfile_base0;

$i = 0;
foreach $line (@mcnpBase0) {
  $i=$i+1;
  $linearray[$i] = $line;
}
```

```
$numberLines=$i;

$j = 0;
for ($i = 1; $i <= $FUELlineNumberMax; $i++) {
  if ($linearray[$i] =~ /f_/) {
    $j=$j+1;
    if ($j < 10 ) {
      $linearray[$i] =~ s/f_000$j/41/g;
      $linearray[$i] =~ s/ft000$j/$isoTemp/g;
    }
    elsif ($j < 100) {
      $linearray[$i] =~ s/f_00$j/41/g;
      $linearray[$i] =~ s/ft00$j/$isoTemp/g;
    }
    elsif ($j < 1000) {
      $linearray[$i] =~ s/f_0$j/41/g;
      $linearray[$i] =~ s/ft0$j/$isoTemp/g;
    }
    else {
      $linearray[$i] =~ s/f_$j/41/g;
      $linearray[$i] =~ s/ft$j/$isoTemp/g;
    }
  }
}

open (MCNPruntmp0, ">grid20cm_main293.tmp0");
for ($i = 1; $i <= $numberLines; $i++) {
  print MCNPruntmp0 $linearray[$i] ;
}

close MCNPruntmp0;

######################################################################
##### load water isothermal material numbers, temps, and densities #####
######################################################################

open (MCNPfile_base1, "grid20cm_main293.tmp0");
$i=0;
$waterLookForNumber=$numWaterCells+$MCNPwaterIndexStart;
while(<MCNPfile_base1>){
  $i=$i+1;
  if (/w_$waterLookForNumber/) {
    $H20lineNumberMax = $i;
    print "Loading isothermal water materials and temperatures. \n";
  }
}
seek(MCNPfile_base1,0,0);
@mcnpBase1 = <MCNPfile_base1>;
close MCNPfile_base1;

$i = 0;
foreach $line (@mcnpBase1) {
  $i=$i+1;
  $linearray[$i] = $line;
}

$j=$MCNPwaterIndexStart;
for ($i = $FUELlineNumberMax; $i <= $H20lineNumberMax; $i++) {
  if ($linearray[$i] =~ /w_/) {
    $j=$j+1;
    $linearray[$i] =~ s/w_$j/43/g;
    $linearray[$i] =~ s/wden_$j/-1.0/g;
    $linearray[$i] =~ s/wt$j/$isoTemp/g;
  }
}

open (MCNPruntmp1, ">grid20cm_main293.tmp1");
for ($j = 1; $j <= $numberLines; $j++) {
  print MCNPruntmp1 $linearray[$j];
}
close MCNPruntmp1;

##################################################################
##### load clad isothermal material numbers and temperatures #####
##################################################################

open (MCNPfile_base2, "grid20cm_main293.tmp1");
@mcnpBase2 = <MCNPfile_base2>;
close MCNPfile_base2;

open (MCNPruntmp2, ">$isothermMCNPfile");

foreach $line (@mcnpBase2) {
  $line =~ s/mclad/42/g;
  $line =~ s/cladt/$isoTemp/g;
  print MCNPruntmp2 $line ;
}

close MCNPruntmp2;

system("chmod 775 *");

# remove temporary files
system("rm grid20cm_main293.tmp*");

#^^^^^^^^^^^^^^^^^^^^^^^^^^^^^^^^^^^^^^^^^^^^^^^^^^^^^^^^^^^^^^^^^^^^^^^^^^^^^
#^^^^^^^^^^^^^^^^^^^^^^^^^^^^^^^^^^^^^^^^^^^^^^^^^^^^^^^^^^^^^^^^^^^^^^^^^^^^^
#   run first MCNP5 job at isothermal conditions, uniform water density
#--------------------------------------------------------------------------------
#^^^^^^^^^^^^^^^^^^^^^^^^^^^^^^^^^^^^^^^^^^^^^^^^^^^^^^^^^^^^^^^^^^^^^^^^^^^^^
#^^^^^^^^^^^^^^^^^^^^^^^^^^^^^^^^^^^^^^^^^^^^^^^^^^^^^^^^^^^^^^^^^^^^^^^^^^^^^

system("mpirun -n 4 mcnp5.mpi n=$isothermMCNPfile xsdir=xsdir_broad1");

# run f90 post processor to extract W/m^3 heat source
# GETHEAT will create "heat.xy" file for STARCCM+'s java file to read in

system("./GETHEAT");

# make sure all files are executable and readable
system("chmod 775 *");

system("mv Heat.xy Heat_$Niter.xy");
system("mv RPDoutPut.txt RPDoutPut_$Niter.txt");
system("mv absoluteHeating.txt absoluteHeating_$Niter.txt");
system("mv fissionHeatingData.txt fissionHeatingData_$Niter.txt");

# extract k-eff from MCNP output file, calculate difference from previous iteration
open(MCNPoutIsotherm, "$isothermMCNPoutfile") || die "MCNP5 isothermal output file missing for keff extraction.\n";

while(<MCNPoutIsotherm>) {
  if (/the final estimated combined collision/) {
    $keffLineString = $_;
  }
}
close MCNPoutIsotherm;

@keffValues0 = split("=", $keffLineString);
@keffValues1 = split(" ", $keffValues0[1]);
$keff[$Niter] = $keffValues1[0];
$reactDk[$Niter] = $keff[$Niter] - $keff[$Niter-1];
$keff_diff[$Niter] = abs $reactDk[$Niter];

print "iso keff = $keff[$Niter] \n";
print summaryFile "iso keff = $keff[$Niter] \n";
```

```
#^^^^^^^^^^^^^^^^^^^^^^^^^^^^^^^^^^^^^^^^^^^^^^^^^^^^^^^^^^^^^^^^^^^^^^
#^^^^^^^^^^^^^^^^^^^^^^^^^^^^^^^^^^^^^^^^^^^^^^^^^^^^^^^^^^^^^^^^^^^^^^
#   start main MULTINUKE “while” iteration loop ---> loops until convergence criteria satisfied
#---------------------------------------------------------------------------------------------------------------------
#^^^^^^^^^^^^^^^^^^^^^^^^^^^^^^^^^^^^^^^^^^^^^^^^^^^^^^^^^^^^^^^^^^^^^^
#^^^^^^^^^^^^^^^^^^^^^^^^^^^^^^^^^^^^^^^^^^^^^^^^^^^^^^^^^^^^^^^^^^^^^^
use Cwd;
$workdir = cwd;

$keff_diff[$Niter] = 1000.0;
$percentTemperatureDiff[$Niter] = 1000.0;

while (($keff_diff[$Niter] > $convergeMCNP5) && ($percentTemperatureDiff[$Niter] > $convergeSTARCCM)) {

open(STARJAVAFILE, "loadHeat_runStarJob_base.java") || die "STARCCM java base file not found, iteration = $Niter\n";
@starlines_array = <STARJAVAFILE>;
close STARJAVAFILE;

open(STARJAVANEW, ">loadHeat_runStarJob.java");

$NiterPlus1 = $Niter+1;
foreach $starline (@starlines_array) {
  $starline =~ s/_WORKDIR_/$workdir/g;
  $starline =~ s/_ITERATION_/$Niter/g;
  $starline =~ s/_ITERATION1_/$NiterPlus1/g;
  print STARJAVANEW $starline;
}
close STARJAVANEW;

system("chmod 775 *");

#^^^^^^^^^^^^^^^^^^^^^^^^^^^^^^^^^^^^^^^^^^^^^^^^^^^^^^^^^^^^^^^^^^^^^^
#^^^^^^^^^^^^^^^^^^^^^^^^^^^^^^^^^^^^^^^^^^^^^^^^^^^^^^^^^^^^^^^^^^^^^^
#   run STARCCM+ with MCNP5 generated heat.xy file
#---------------------------------------------------------------------------------------------------------------------
#^^^^^^^^^^^^^^^^^^^^^^^^^^^^^^^^^^^^^^^^^^^^^^^^^^^^^^^^^^^^^^^^^^^^^^
#^^^^^^^^^^^^^^^^^^^^^^^^^^^^^^^^^^^^^^^^^^^^^^^^^^^^^^^^^^^^^^^^^^^^^^

system("starccm+ -np 4 -batch loadHeat_runStarJob.java $JOB_NAME.sim");

system("mv $JOB_NAME\@04000.sim $JOB_NAME\@04000\_$NiterPlus1.sim");

$Niter = $Niter + 1;
# kill script if max # of iterations exceeded
if ($Niter > $iterationEnd) {
  die "maximum iterations exceeded.  Sorry, I'm dead.\n";
}

system("chmod 775 *");

#^^^^^^^^^^^^^^^^^^^^^^^^^^^^^^^^^^^^^^^^^^^^^^^^^^^^^^^^^^^^^^^^^^^^^^
#^^^^^^^^^^^^^^^^^^^^^^^^^^^^^^^^^^^^^^^^^^^^^^^^^^^^^^^^^^^^^^^^^^^^^^
#   read in STARCCM+ output csv files, assign materials
#-------------------------------------------------------------------------
#^^^^^^^^^^^^^^^^^^^^^^^^^^^^^^^^^^^^^^^^^^^^^^^^^^^^^^^^^^^^^^^^^^^^^^
#^^^^^^^^^^^^^^^^^^^^^^^^^^^^^^^^^^^^^^^^^^^^^^^^^^^^^^^^^^^^^^^^^^^^^^

##########################################################
#####    read STARCCM+ fuel  temperature output       #####
##########################################################

open (STARtempDens_fuel, "STARCCMfuel_out\_$Niter.csv") || die "STARCCM fuel output file not found, iteration = $Niter\n";

readline(STARtempDens_fuel);

$i = 0;
while (<STARtempDens_fuel>) {
  $i = $i + 1;
  $linevalues = $_;
  @values = split(" ",$linevalues);
  $FuelcellNum[$i]          = $values[0];
  $FuelcellTemp[$i][$Niter] = $values[2];
}
$numFuelCells=$i;

### assign MCNP fuel material numbers

for ($i = 1; $i <= $numFuelCells; $i++) {
  if ($FuelcellTemp[$i][$Niter] < 650) {                                                    # fuel bin 1: broadened to 625 K (600 K - 650 K)
    $FuelMat_Num[$i] = 1;
  }
  elsif (($FuelcellTemp[$i][$Niter] >= 650) && ($FuelcellTemp[$i][$Niter] < 700)) {   # fuel bin 2: broadened to 675 K (650 K - 700 K)
    $FuelMat_Num[$i] = 2;
  }
  elsif (($FuelcellTemp[$i][$Niter] >= 700) && ($FuelcellTemp[$i][$Niter] < 750)) {   # fuel bin 3: broadened to 725 K (700 K - 750 K)
    $FuelMat_Num[$i] = 3;
  }
  elsif (($FuelcellTemp[$i][$Niter] >= 750) && ($FuelcellTemp[$i][$Niter] < 800)) {   # fuel bin 4: broadened to 775 K (750 K - 800 K)
    $FuelMat_Num[$i] = 4;
  }
  elsif (($FuelcellTemp[$i][$Niter] >= 800) && ($FuelcellTemp[$i][$Niter] < 850)) {   # fuel bin 5: broadened to 825 K (800 K - 850 K)
    $FuelMat_Num[$i] = 5;
  }
  elsif (($FuelcellTemp[$i][$Niter] >= 850) && ($FuelcellTemp[$i][$Niter] < 900)) {   # fuel bin 6: broadened to 875 K (850 K - 900 K)
    $FuelMat_Num[$i] = 6;
  }
  elsif (($FuelcellTemp[$i][$Niter] >= 900) && ($FuelcellTemp[$i][$Niter] < 950)) {   # fuel bin 7: broadened to 925 K (900 K - 950 K)
    $FuelMat_Num[$i] = 7;
  }
  elsif (($FuelcellTemp[$i][$Niter] >= 950) && ($FuelcellTemp[$i][$Niter] < 1000)) {  # fuel bin 8: broadened to 975 K (950 K - 1000 K)
    $FuelMat_Num[$i] = 8;
  }
  elsif (($FuelcellTemp[$i][$Niter] >= 1000) && ($FuelcellTemp[$i][$Niter] < 1050)){# fuel bin 9: broadened to 1025 K (1000 K - 1050 K)
    $FuelMat_Num[$i] = 9;
  }
  elsif (($FuelcellTemp[$i][$Niter] >= 1050) && ($FuelcellTemp[$i][$Niter] < 1100)){# fuel bin 10: broadened to 1075 K (1050K-1100 K)
    $FuelMat_Num[$i] = 10;
  }
  elsif (($FuelcellTemp[$i][$Niter] >= 1100) && ($FuelcellTemp[$i][$Niter] < 1150)){#fuel bin 11: broadened to 1125 K (110 K - 1150 K)
    $FuelMat_Num[$i] = 11;
  }
  elsif (($FuelcellTemp[$i][$Niter] >= 1150) && ($FuelcellTemp[$i][$Niter] < 1200)){#fuel bin 12: broadened to 1175 K (1150K -1200 K)
    $FuelMat_Num[$i] = 12;
  }
  elsif (($FuelcellTemp[$i][$Niter] >= 1200) && ($FuelcellTemp[$i][$Niter] < 1250)) {#fuel bin 13: broadened to 1225 K (1200K-1250 K)
    $FuelMat_Num[$i] = 13;
  }
  elsif (($FuelcellTemp[$i][$Niter] >= 1250) && ($FuelcellTemp[$i][$Niter] < 1300)){# fuel bin 14: broadened to 1275 K (1250K-1300 K)
    $FuelMat_Num[$i] = 14;
  }
  else {
    $FuelMat_Num[$i] = 15;                                                                   # fuel bin 15: broadened to 1325 K (1300 K - 1350 K)
  }
}

###########################################################
#####    read STARCCM+ clad  temperature output       #####
###########################################################

open (STARtempDens_clad, "STARCCMclad_out\_$Niter.csv") || die "STARCCM clad output file not found, iteration = $Niter\n";

readline(STARtempDens_clad);

$i = 0;
while (<STARtempDens_clad>) {
  $i = $i + 1;
  $linevalues = $_;
```

```
 @values = split(" ",$linevalues);
 $CladcellNum[$i]          = $values[0];
 $CladcellTemp[$i][$Niter]   = $values[2];
 $CladcellVolume[$i]        = $values[3] * (10.0**6.0); # 1 m^3 = 1,000,000 cm^3
}
$numCladCells=$i;

### calculate volume-weighted average clad temperature

$totalCladVolume=0.0;
for ($i = 1; $i <= $numCladCells; $i++) {
 $totalCladVolume = $totalCladVolume + $CladcellVolume[$i];
}

$numerator_avgCladTemp=0.0;
for ($i = 1; $i <= $numCladCells; $i++) {
 $numerator_avgCladTemp = $numerator_avgCladTemp + $CladcellTemp[$i][$Niter] * $CladcellVolume[$i];
}

$avgCladTemp = $numerator_avgCladTemp / $totalCladVolume;

### assign MCNP clad material number

if ($avgCladTemp < 600) {
 $CladMat_Num = 21;      # clad bin 1: broadened to 550 K
}
elsif (($avgCladTemp >= 600) && ($avgCladTemp < 700)) {
 $CladMat_Num = 22;      # clad bin 2: broadened to 650 K
}
else{
 $CladMat_Num = 23;      # clad bin 3: broadened to 750 K
}


##########################################################
##### read STARCCM+ water density/temperature output  #####
##########################################################

open (STARtempDens_water, "STARCCMwater_out\_$Niter.csv") || die "STARCCM water output file not found, iteration = $Niter\n";

readline(STARtempDens_water);

$i = 0;
while (<STARtempDens_water>) {
 $i = $i + 1;
 $linevalues = $_;

 @values = split(" ",$linevalues);
 $H2OcellNum[$i]         = $values[0];
 $H2OcellDens[$i]        = $values[1] * 0.001*(-1.0);  # convert kg/m^3 to g/cc, make negative for MCNP5 cell cards
 $H2OcellTemp[$i][$Niter] = $values[2];
}
$numWaterCells=$i;

$i = 0;

close STARtempDens_water;

### assign MCNP water material numbers

for ($i = 1; $i <= $numWaterCells; $i++) {
 if ($H2OcellTemp[$i][$Niter] < 560) {                                                # water bin 1: broadened to 555.0 K (550 K - 560 K)
  $WaterMat_Num[$i] = 31;
 }
 elsif (($H2OcellTemp[$i][$Niter] >= 560) && ($H2OcellTemp[$i][$Niter] < 570)) {   # water bin 2: broadened to 570.0 K (560 K -570 K)
  $WaterMat_Num[$i] = 32;
 }
 elsif (($H2OcellTemp[$i][$Niter] >= 570) && ($H2OcellTemp[$i][$Niter] < 575)) {   # water bin 3: broadened to 572.5 K (570 K - 575 K)
```

```
   $WaterMat_Num[$i] = 33;
  }
  elsif (($H2OcellTemp[$i][$Niter] >= 575) && ($H2OcellTemp[$i][$Niter] < 580)) {   # water bin 4: broadened to 577.5 K (575 K - 580 K)
   $WaterMat_Num[$i] = 34;
  }
  elsif (($H2OcellTemp[$i][$Niter] >= 580) && ($H2OcellTemp[$i][$Niter] < 585)) {   # water bin 5: broadened to 582.5 K (580 K - 585 K)
   $WaterMat_Num[$i] = 35;
  }
  elsif (($H2OcellTemp[$i][$Niter] >= 585) && ($H2OcellTemp[$i][$Niter] < 590)) {   # water bin 6: broadened to 587.5 K (585 K - 590 K)
   $WaterMat_Num[$i] = 36;
  }
  elsif (($H2OcellTemp[$i][$Niter] >= 590) && ($H2OcellTemp[$i][$Niter] < 595)) {   # water bin 7: broadened to 592.5 K (590 K - 595 K)
   $WaterMat_Num[$i] = 37;
  }
  elsif (($H2OcellTemp[$i][$Niter] >= 595) && ($H2OcellTemp[$i][$Niter] < 600)) {   # water bin 8: broadened to 597.5 K (595 K - 600 K)
   $WaterMat_Num[$i] = 38;
  }
  else{                                                                              # water bin 9: broadened to 605.0 K (600 K - 610 K)
   $WaterMat_Num[$i] = 39;
  }
}


#########################################################################################
##### calculate avg % difference in STAR cell temperatures from previous iteration #####
#########################################################################################
# avg relative error in fuel/water temperature distribution avg{ (T_new[i]-T_old[i]) / [(T_new[i]+T_old[i])/2] }

$SUMfuel=0.0;
for ($i = 1; $i <= $numFuelCells; $i++) {
  $FuelcellTemp[$i][0] = $append_firstMCNPrun;
  $FuelPercentDiff[$i] = abs( ($FuelcellTemp[$i][$Niter]-$FuelcellTemp[$i][$Niter-1]) /
(($FuelcellTemp[$i][$Niter]+$FuelcellTemp[$i][$Niter-1])/2.0) );
}
for ($i = 1; $i <= $numFuelCells; $i++) {
  $SUMfuel = $SUMfuel + $FuelPercentDiff[$i];
}

$SUMclad=0.0;
for ($i = 1; $i <= $numCladCells; $i++) {
  $CladcellTemp[$i][0] = $append_firstMCNPrun;
  $CladPercentDiff[$i] = abs( ($CladcellTemp[$i][$Niter]-$CladcellTemp[$i][$Niter-1]) /
(($CladcellTemp[$i][$Niter]+$CladcellTemp[$i][$Niter-1])/2.0) );
}
for ($i = 1; $i <= $numCladCells; $i++) {
  $SUMclad = $SUMclad + $CladPercentDiff[$i];
}

$SUMwater=0.0;
for ($i = 1; $i <= $numWaterCells; $i++) {
  $H2OcellTemp[$i][0] = $append_firstMCNPrun;
  $WaterPercentDiff[$i] = abs( ($H2OcellTemp[$i][$Niter]-$H2OcellTemp[$i][$Niter-1]) /
(($H2OcellTemp[$i][$Niter]+$H2OcellTemp[$i][$Niter-1])/2.0) );
}
for ($i = 1; $i <= $numWaterCells; $i++) {
  $SUMwater = $SUMwater + $WaterPercentDiff[$i];
}

$AVGFuelPercentDiff  = $SUMfuel/$numFuelCells;
$AVGCladPercentDiff  = $SUMclad/$numCladCells;
$AVGWaterPercentDiff = $SUMwater/$numWaterCells;

print "Iter = $Niter, Fuel%Diff = $AVGFuelPercentDiff, Clad%Diff = $AVGCladPercentDiff, Water%Diff = $AVGWaterPercentDiff\n";
print summaryFile "Iter = $Niter, Fuel%Diff = $AVGFuelPercentDiff, Clad%Diff = $AVGCladPercentDiff, Water%Diff =
$AVGWaterPercentDiff\n";

$percentTemperatureDiff[$Niter] = ($AVGFuelPercentDiff+$AVGCladPercentDiff+$AVGWaterPercentDiff)/3.0;

print "Iter = $Niter, percentTemperatureDiff = $percentTemperatureDiff[$Niter]\n";
print summaryFile "Iter = $Niter, percentTemperatureDiff = $percentTemperatureDiff[$Niter]\n";

################################################
##### load fuel material numbers and temps #####
################################################

$i=0;
open (MCNPfile_base0, "$MCNPbaseFile") || die "base MCNP file not found, iteration = $Niter\n";
while(<MCNPfile_base0>){
 $i=$i+1;
 if (/f_$numFuelCells/) {
  $FUELlineNumberMax = $i;
  print "Loading fuel materials and temperatures.  This will take a few seconds...\n";
 }
}
seek(MCNPfile_base0,0,0);
@mcnpBase0 = <MCNPfile_base0>;
close MCNPfile_base0;

$i = 0;
foreach $line (@mcnpBase0) {
 $i=$i+1;
 $linearray[$i] = $line;
}
$numberLines=$i;

for ($i = 1; $i <= $numFuelCells; $i++) {
 $FuelcellTempKT[$i] = $FuelcellTemp[$i][$Niter]*$k;
}

for ($i = 1; $i <= $numFuelCells; $i++) {
 for ($j = 1; $j <= $FUELlineNumberMax; $j++) {
  if ($fuelIndexMCNP[$i] < 10 ) {
   if ($linearray[$j] =~ s/f_000$fuelIndexMCNP[$i]/$FuelMat_Num[$i]/g) {
    $linearray[$j] =~ s/ft000$fuelIndexMCNP[$i]/$FuelcellTempKT[$i]/g;
   }
  }
  elsif ($fuelIndexMCNP[$i] < 100) {
   if ($linearray[$j] =~ s/f_00$fuelIndexMCNP[$i]/$FuelMat_Num[$i]/g) {
    $linearray[$j] =~ s/ft00$fuelIndexMCNP[$i]/$FuelcellTempKT[$i]/g;
   }
  }
  elsif ($fuelIndexMCNP[$i] < 1000) {
   if ($linearray[$j] =~ s/f_0$fuelIndexMCNP[$i]/$FuelMat_Num[$i]/g) {
    $linearray[$j] =~ s/ft0$fuelIndexMCNP[$i]/$FuelcellTempKT[$i]/g;
   }
  }
  else {
   if ($linearray[$j] =~ s/f_$fuelIndexMCNP[$i]/$FuelMat_Num[$i]/g) {
    $linearray[$j] =~ s/ft$fuelIndexMCNP[$i]/$FuelcellTempKT[$i]/g;
   }
  }
 }
}

open (MCNPruntmp0, ">$JOB_NAME.tmp0");
for ($j = 1; $j <= $numberLines; $j++) {
 print MCNPruntmp0 $linearray[$j] ;
}

close MCNPruntmp0;

##############################################################
##### load water material numbers, densities, and temps #####
##############################################################
open (MCNPfile_base1, "$JOB_NAME.tmp0");
$i=0;
$waterLookForNumber=$numWaterCells+$MCNPwaterIndexStart;
while(<MCNPfile_base1>){
  $i=$i+1;
  if (/w_$waterLookForNumber/) {
    $H20lineNumberMax = $i;
    print "Loading water materials, densities, and temperatures.  This will take a few seconds...\n";
  }
}
seek(MCNPfile_base1,0,0);
@mcnpBase1 = <MCNPfile_base1>;
close MCNPfile_base1;

$i = 0;
foreach $line (@mcnpBase1) {
  $i=$i+1;
  $linearray[$i] = $line;
}

for ($i = 1; $i <= $numWaterCells; $i++) {
  $H2OcellTempKT[$i] = $H2OcellTemp[$i][$Niter]*$k;
}

for ($i = 1; $i <= $numWaterCells; $i++) {
  $waterIndexReplace[$i]=$waterIndexMCNP[$i]+$MCNPwaterIndexStart;
  for ($j = $FUELlineNumberMax; $j <= $H20lineNumberMax; $j++) {
    if ($linearray[$j] =~ s/w_$waterIndexReplace[$i]/$WaterMat_Num[$i]/g) {
      $linearray[$j] =~ s/wden_$waterIndexReplace[$i]/$H2OcellDens[$i]/g;
      $linearray[$j] =~ s/wt$waterIndexReplace[$i]/$H2OcellTempKT[$i]/g;
    }
  }
}

open (MCNPruntmp1, ">$JOB_NAME.tmp1");

for ($j = 1; $j <= $numberLines; $j++) {
  print MCNPruntmp1 $linearray[$j];
}

close MCNPruntmp1;

#################################################
#####    load clad material number         #####
#################################################

open (MCNPfile_base2, "$JOB_NAME.tmp1");
@mcnpBase2 = <MCNPfile_base2>;
close MCNPfile_base2;

open (MCNPruntmp2, ">$JOB_NAME\_$Niter");

$avgCladTempKT = $avgCladTemp*$k;
print "Loading clad materials and temperatures.\n";
foreach $line (@mcnpBase2) {
  $line =~ s/mclad/$CladMat_Num/g;
  $line =~ s/cladt/$avgCladTempKT/g;
  print MCNPruntmp2 $line ;
}

close MCNPruntmp2;

system("chmod 775 *");

# remove temporary files
system("rm $JOB_NAME.tmp*");

#^^^^^^^^^^^^^^^^^^^^^^^^^^^^^^^^^^^^^^^^^^^^^^^^^^^^^^^^^^^^^^^^^^^^^^^^^^^^^^^
#^^^^^^^^^^^^^^^^^^^^^^^^^^^^^^^^^^^^^^^^^^^^^^^^^^^^^^^^^^^^^^^^^^^^^^^^^^^^^^^
#   rerun MCNP5 once with STARCCM+ output
#------------------------------------------------------------------------------------------
#^^^^^^^^^^^^^^^^^^^^^^^^^^^^^^^^^^^^^^^^^^^^^^^^^^^^^^^^^^^^^^^^^^^^^^^^^^^^^^^
#^^^^^^^^^^^^^^^^^^^^^^^^^^^^^^^^^^^^^^^^^^^^^^^^^^^^^^^^^^^^^^^^^^^^^^^^^^^^^^^
```

```
open(specsBASE, "multiSpecs_base.txt") || die "STARCCM java base file not found, iteration = $Niter\n";
@multispecsLines = <specsBASE>;
close specsBASE;

open(MCNPspecs, ">multiSpecs.txt");

foreach $specsline (@multispecsLines) {
  $specsline =~ s/$JOB_NAME/$JOB_NAME\_$Niter/g;
  $specsline =~ s/$JOB_NAME$oForOutput/$JOB_NAME\_$Niter$oForOutput/g;
  print MCNPspecs $specsline;
}
close MCNPspecs;

system("mpirun -n 4 mcnp5.mpi n=$JOB_NAME\_$Niter xsdir=xsdir_broad1");
system("./GETHEAT");
system("chmod 775 *");
system("mv Heat.xy Heat_$Niter.xy");
system("mv RPDoutPut.txt RPDoutPut\_$Niter.txt");
system("mv absoluteHeating.txt absoluteHeating\_$Niter.txt");
system("mv fissionHeatingData.txt fissionHeatingData\_$Niter.txt");
system("rm $JOB_NAME\_$Niter$rForRestart");
system("rm $JOB_NAME\_$Niter$sForSource");

# extract k-eff from MCNP output file, calculate difference from previous iteration
open(MCNPoutKeff, "$JOB_NAME\_$Niter$oForOutput") || die "MCNP5 output file missing for keff extraction. Iteration = $Niter\n";

while(<MCNPoutKeff>) {
  if (/the final estimated combined collision/) {
    $keffLineString = $_;
  }
}
close MCNPoutKeff;

@keffValues0 = split("=", $keffLineString);
@keffValues1 = split(" ", $keffValues0[1]);
$keff[$Niter] = $keffValues1[0];
$reactDk[$Niter] = $keff[$Niter] - $keff[$Niter-1];
$keff_diff[$Niter] = abs $reactDk[$Niter];

print "iteration = $Niter, keff difference = $keff_diff[$Niter]\n";
print summaryFile "iteration = $Niter, keff difference = $keff_diff[$Niter]\n";

if (($keff_diff[$Niter] <= $convergeMCNP5) && ($percentTemperatureDiff[$Niter] <= $convergeSTARCCM)) {
  print summaryFile "Solutions appear converged.  Ending MULTINUKE...\n";
  print "Solutions appear converged.  Ending MULTINUKE...\n";
  close summaryFile;
}

} #closing bracket for iterating while loop in MULTINUKE
```

B.2 GETHEAT.f90 MCNP5 Post Processor

```
module data_constants
! ==================================================
! contains global variables, parameters
!
! ==================================================
  integer                        :: io_number=0
  integer, parameter             :: fuelCellsPerNode=32
  integer, parameter             :: axialNodes=104
  character (len=10), parameter  :: specsFile='multiSpecs'

  type paramStrings
  ! strings to look for that mark appropriate data in specs file
    character (len=13)  :: param1 = 'mcnpInputFile'
    character (len=14)  :: param2 = 'mcnpOutputFile'
    character (len=12)  :: param3 = 'rhoFuel_g_cc'
    character (len=6)   :: param4 = 'powerW'
    character (len=15)  :: param5 = 'Q_MeVperFission'
  end type paramStrings

end module data_constants


module physicsData
! ==================================================
! model data: cell volumes, centroids
! ==================================================
 real, dimension(32)  :: vols_topNode = &
 (/0.000134629, &
   0.000645597, &
   0.000663351, &
   0.000151424, &
   0.000147074, &
   0.001356109, &
   0.001490116, &
   0.001490116, &
   0.001355884, &
   0.000140106, &
   0.000670572, &
   0.001490116, &
   0.001490116, &
   0.001490116, &
   0.001490116, &
   0.000665575, &
   0.000668348, &
   0.001490116, &
   0.001490116, &
   0.001490116, &
   0.001490116, &
   0.000665365, &
   0.000146386, &
   0.001357754, &
   0.001490116, &
   0.001490116, &
   0.001356047, &
   0.000140217, &
   0.000135259, &
   0.000646786, &
   0.000663116, &
   0.000151299/)

 real, dimension(32)  :: vols_bottomNode = &
 (/0.000134629, &
   0.000645597, &
   0.000663351, &
   0.000151424, &
   0.000147074, &
   0.001356109, &
   0.001490116, &
   0.001490116, &
   0.001355884, &
   0.000140106, &
   0.000670572, &
   0.001490116, &
   0.001490116, &
   0.001490116, &
   0.001490116, &
   0.000665575, &
   0.000668348, &
   0.001490116, &
   0.001490116, &
   0.001490116, &
   0.001490116, &
   0.000665365, &
   0.000146386, &
   0.001357754, &
   0.001490116, &
   0.001490116, &
   0.001356047, &
   0.000140217, &
   0.000135259, &
   0.000646786, &
   0.000663116, &
   0.000151299/)

 real, dimension(32)  :: vols_middleNodes  = &
 (/0.000717041, &
   0.003304147, &
   0.003320380, &
   0.000719466, &
   0.000717134, &
   0.006679333, &
   0.007450581, &
   0.007450581, &
   0.006739989, &
   0.000690994, &
   0.003276380, &
   0.007450581, &
   0.007450581, &
   0.007450581, &
   0.007450581, &
   0.003299103, &
   0.003286638, &
   0.007450581, &
   0.007450581, &
   0.007450581, &
   0.007450581, &
   0.003318527, &
   0.000710452, &
   0.006739960, &
   0.007450581, &
   0.007450581, &
   0.006777007, &
   0.000694928, &
   0.000709665, &
   0.003265519, &
   0.003325870, &
   0.000754623/)

 real, dimension(32)  :: xc = &
 (/ -0.231434, &
    -0.089682, &
     0.090564, &
     0.233300, &
    -0.412725, &
    -0.286159, &
    -0.097656, &
     0.097656, &
     0.285981, &
     0.412210, &
    -0.435431, &
    -0.292969, &
    -0.097656, &
     0.097656, &
     0.292969, &
     0.435160, &
    -0.435272, &
    -0.292969, &
    -0.097656, &
     0.097656, &
     0.292969, &
     0.435118, &
    -0.412474, &
    -0.286230, &
    -0.097656, &
     0.097656, &
     0.285989, &
     0.412213, &
    -0.231538, &
    -0.089758, &
     0.090536, &
     0.233303/)

 real, dimension(32)  :: yc = &
 (/ -0.411868, &
    -0.433834, &
    -0.434847, &
    -0.413297, &
    -0.233430, &
    -0.285896, &
    -0.292969, &
    -0.292969, &
    -0.286094, &
    -0.232169, &
    -0.089565, &
    -0.097656, &
    -0.097656, &
    -0.097656, &
    -0.097656, &
    -0.089350, &
     0.089444, &
     0.097656, &
     0.097656, &
     0.097656, &
     0.097656, &
     0.089475, &
     0.233648, &
     0.285977, &
     0.292969, &
     0.292969, &
     0.286101, &
     0.232199, &
     0.411906, &
     0.433899, &
     0.434837, &
     0.413273/)

 real, dimension(104)  :: zc = &
 (/ 0.00977585, &
    0.07813705, &
    0.2343784, &
    0.4296904, &
    0.62500245, &
    0.82031445, &
    1.0156264, &
    1.21093845, &
    1.4062505, &
    1.60156245, &
    1.7968744, &
    1.99218635, &
    2.1874983, &
    2.38281035, &
    2.5781224, &
    2.7734344, &
    2.9687464, &
    3.16405845, &
    3.3593705, &
    3.5546825, &
    3.7499945, &
    3.94530655, &
    4.1406186, &
    4.3359306, &
    4.5312426, &
    4.7265546, &
```

```
4.92186665, &
5.11717845, &
5.3124902, &
5.50780225, &
5.7031143, &
5.8984263, &
6.0937383, &
6.28905035, &
6.4843624, &
6.6796744, &
6.8749864, &
7.0702984, &
7.26561045, &
7.4609225, &
7.6562345, &
7.8515465, &
8.0468583, &
8.24217035, &
8.43748235, &
8.63279435, &
8.8281064, &
9.02341845, &
9.21873045, &
9.41404245, &
9.6093545, &
9.80466655, &
9.99997855, &
10.19529055, &
10.3906026, &
10.58591465, &
10.78122665, &
10.97653865, &
11.1718507, &
11.36716225, &
11.56247425, &
11.75778625, &
11.95309825, &
12.1484103, &
12.34372235, &
12.53903435, &
12.73434635, &
12.9296584, &
13.12497045, &
13.32028245, &
13.51559445, &
13.7109065, &
13.90621855, &
14.10153055, &
14.29684255, &
14.4921546, &
14.68746665, &
14.88277865, &
15.0780902, &
15.27340225, &
15.46871425, &
15.66402625, &
15.8593383, &
16.05464985, &
16.24996185, &
16.44527435, &
16.64058685, &
16.8358984, &
17.03120995, &
17.22652245, &
17.42183495, &
17.6171465, &
17.81245805, &
18.00777055, &
18.20308305, &
18.3983946, &
18.59370615, &
18.78901865, &
18.98433115, &
19.1796427, &
19.37495425, &
19.57026675, &
```

```
    19.7655783, &
    19.92181875/)

end module physicsData


!\\\\\\\\\\\\\\\\\\\\\\\\\\\\\\\\\\\\\\\\\\\\\\\\\\\\\\\\\\\\\\\\\\\\\\\\\\\\\\\\\\\\\\\\\\\\\\\\\\\\\\
! ****************************************************************************************
!/////////////////////////////////////////////////////////////////////////////////////////


Program getHeat
! ===================================================
! main program
!
! ===================================================

  use data_constants

  implicit none

  logical               :: exist_specsFile
  character (len=60)    :: mcnpInfile
  character (len=60)    :: mcnpOutfile
  character             :: tmp
  character             :: findequal = 'o'
  real, dimension(4000) :: volume
  real                  :: rhoFuel
  real                  :: power
  real                  :: Q_MeVperFiss
  real                  :: eigenvalue
  real                  :: Nu

  inquire( file=specsFile//'.txt', exist=exist_specsFile )
  if ( .not.exist_specsFile ) then
    write(*,'(a,a,a)') 'Cannot find specs file: ',specsFile//'.txt',', exiting program.'
    write(*,'(a)') 'Hit any key and enter to close.'
    read(*,*)
    call exit()
  endif

  call loadVolumes(volume)                                                 ! load mcnp cell volumes

  call readSpecsInput(mcnpInfile,mcnpOutfile,rhoFuel,power,Q_MeVperFiss) ! read input

  call axialPowerDist(mcnpInfile,mcnpOutfile,volume)                     ! extract axial power

  call readEigenvalueNu(mcnpOutfile,eigenvalue,Nu)                       ! extract k-eff and Nu

  call FissionHeating(mcnpInfile,mcnpOutfile,volume,rhoFuel,power,Q_MeVperFiss,eigenvalue,Nu)

write(*,*)
write(*,*) '*****************************************'
write(*,*) '*****************************************'
write(*,*)
write(*,*) 'Done reading heat.'
write(*,*)
end program getHeat


!\\\\\\\\\\\\\\\\\\\\\\\\\\\\\\\\\\\\\\\\\\\\\\\\\\\\\\\\\\\\\\\\\\\\\\\\\\\\\\\\\\\\\\\\\\\\\\\\\\\\\\
! ****************************************************************************************
!/////////////////////////////////////////////////////////////////////////////////////////


subroutine readSpecsInput(mcnpInfile,mcnpOutfile,rhoFuel,power,Q_MeVperFiss)
! ===================================================
! extracts input data from multispecs.txt input file
! --> order of input data doesn't matter
! ===================================================

  use data_constants
  implicit none
  type(paramStrings)               :: specString
  character (len=60), intent(out) :: mcnpInfile
  character (len=60), intent(out) :: mcnpOutfile
  character (len=60)              :: tmp
  character                       :: findequal='o'
  real, intent(out)               :: rhoFuel
  real, intent(out)               :: power
  real, intent(out)               :: Q_MeVperFiss

  io_number=io_number+1
  open( unit=io_number, file=specsFile//'.txt', status='old')
loop1: do while( .not.eof(io_number) )
         do while( tmp /= specString%param1 )
           if( eof(io_number) ) then
             write(*,'(a,a,a)') 'Could not find ', specString%param1, ' in specs file, exiting', &
                                                                        ' program.'
             write(*,'(a)') 'Hit any key and enter to close.'
             read(*,*)
             call exit()
           endif
           100 continue
           read(io_number,'(a13)', advance='no', EOR=100) tmp
           if( tmp == specString%param1) then
             do while( findequal /= '=')
               read(io_number,'(a)',advance='no') findequal
               if( findequal == '=') then
                 read(io_number,'(1x,a60)') mcnpInfile
                 write(*,'(a,a)') 'Found mcnp input file in specs file ', mcnpInfile
               endif
             enddo
             exit loop1
           endif
         enddo
       enddo loop1
  rewind(io_number)
  findequal='o'

loop2: do while( .not.eof(io_number) )
         do while( tmp /= specString%param2 )
           if( eof(io_number) ) then
             write(*,'(a,a,a)') 'Could not find ', specString%param2, ' in specs file, exiting', &
                                                                        ' program.'
             write(*,'(a)') 'Hit any key and enter to close.'
             read(*,*)
             call exit()
           endif
           105 continue
           read(io_number,'(a14)', advance='no', EOR=105) tmp
           if( tmp == specString%param2) then
             do while( findequal /= '=')
               read(io_number,'(a)',advance='no') findequal
               if( findequal == '=') then
                 read(io_number,'(1x,a60)') mcnpOutfile
                 write(*,'(a,a)') 'Found mcnp output file in specs file ', mcnpOutfile
               endif
             enddo
             exit loop2
           endif
         enddo
       enddo loop2
  rewind(io_number)
  findequal='o'

loop3: do while( .not.eof(io_number) )
         do while( tmp /= specString%param3 )
           if( eof(io_number) ) then
             write(*,'(a,a,a)') 'Could not find ', specString%param3, ' in specs file, exiting', &
                                                                        ' program.'
             write(*,'(a)') 'Hit any key and enter to close.'
             read(*,*)
             call exit()
           endif
           110 continue
           read(io_number,'(a12)', advance='no', EOR=110) tmp
           if( tmp == specString%param3) then
             do while( findequal /= '=')
               read(io_number,'(a)',advance='no') findequal
               if( findequal == '=') then
                 read(io_number,*) rhoFuel
                 write(*,'(a,f)') 'Found fuel density = ', rhoFuel
               endif
             enddo
             exit loop3
           endif
         enddo
       enddo loop3
  rewind(io_number)
  findequal='o'

loop4: do while( .not.eof(io_number) )
         do while( tmp /= specString%param4 )
           if( eof(io_number) ) then
             write(*,'(a,a,a)') 'Could not find ', specString%param4, ' in specs file, exiting', &
                                                                      ' program.'
             write(*,'(a)') 'Hit any key and enter to close.'
             read(*,*)
             call exit()
           endif
           115 continue
           read(io_number,'(a7)', advance='no', EOR=115) tmp
           if( tmp == specString%param4) then
             do while( findequal /= '=')
               read(io_number,'(a)',advance='no') findequal
               if( findequal == '=') then
                 read(io_number,*) power
                 write(*,'(a,f)') 'Found power = ', power
               endif
             enddo
             exit loop4
           endif
         enddo
       enddo loop4
  rewind(io_number)
  findequal='o'

loop5: do while( .not.eof(io_number) )
         do while( tmp /= specString%param5 )
           if( eof(io_number) ) then
             write(*,'(a,a,a)') 'Could not find ', specString%param5, ' in specs file, exiting', &
                                                                      ' program.'
             write(*,'(a)') 'Hit any key and enter to close.'
             read(*,*)
             call exit()
           endif
           120 continue
           read(io_number,'(a15)', advance='no', EOR=120) tmp
           if( tmp == specString%param5) then
             do while( findequal /= '=')
               read(io_number,'(a)',advance='no') findequal
               if( findequal == '=') then
                 read(io_number,*) Q_MeVperFiss
                 write(*,'(a,f5.1)') 'Found MeV/fission = ', Q_MeVperFiss
               endif
             enddo
             exit loop5
           endif
         enddo
       enddo loop5
  rewind(io_number)
  findequal='o'

  close(io_number)
end subroutine readSpecsInput


!\\\\\\\\\\\\\\\\\\\\\\\\\\\\\\\\\\\\\\\\\\\\\\\\\\\\\\\\\\\\\\\\\\\\\\\\\\\\\\\\\\\\\\\\\\\\\\\\\\
! ****************************************************************************************
!/////////////////////////////////////////////////////////////////////////////////////////


subroutine loadVolumes(volume)
! ==================================================
! assigns volumes to mcnp cells
! ==================================================
  use physicsData
  use data_constants
  implicit none
  real, dimension(4000), intent(out) :: volume
  integer                            :: i=0
  integer                            :: n=0
  integer                            :: z

  !load in bottom volumes
  do i = 1, fuelCellsPerNode
    n=n+1
    volume(n) = vols_bottomNode(i)
  enddo

  !load in middle volumes
  do z = 2, axialNodes-1
    do i = 1,fuelCellsPerNode
      n=n+1
      volume(n) = vols_middleNodes(i)
    enddo
  enddo

  !load in top volumes
  do i = 1, fuelCellsPerNode
    n=n+1
    volume(n) = vols_topNode(i)
  enddo
end subroutine loadVolumes



!\\\\\\\\\\\\\\\\\\\\\\\\\\\\\\\\\\\\\\\\\\\\\\\\\\\\\\\\\\\\\\\\\\\\\\\\\\\\\\\\\\\\\\\\\\\\\\\\\\\\
! ***************************************************************************************
!////////////////////////////////////////////////////////////////////////////////////////


subroutine axialPowerDist(mcnpInfile,mcnpOutfile,volume)
! ==================================================
! extracts and prints axial power distribution
! ( point/avg fission reaction rates )
! ==================================================

  use data_constants
  implicit none
  character (len=60), intent(in)  :: mcnpInfile
  character (len=60), intent(in)  :: mcnpOutfile
  real,dimension(4000),intent(in) :: volume

  character (len=46)              :: findFissionRxnRates
  logical                         :: exist_mcnpOutfile
  integer                         :: numFuelBins
  integer                         :: i=0
  integer                         :: z=0
  integer                         :: n=0
  integer                         :: radialStart=1
  real, dimension(axialNodes)     :: axialsum=0.0
  real, dimension(4000)           :: fission
  real, dimension(4000)           :: error
  real                            :: avgFiss
  real                            :: avgAxialFiss
  real, dimension(4000)           :: normPowerDist
  real, dimension(axialNodes)     :: axialFiss
  real                            :: sum_Weighted_Fission=0.0

  inquire( file=trim(mcnpOutfile), exist=exist_mcnpOutfile )
  if ( .not.exist_mcnpOutfile ) then
    write(*,'(a,a,a)') 'Cannot find mcnp output file for fission rxn rate: ',trim(mcnpOutfile), &
                                                                                 ' exiting program.'
    write(*,'(a)') 'Hit any key and enter to close.'
    read(*,*)
    call exit()
  endif

  io_number=io_number+1
  open( unit=io_number, file=trim(mcnpOutfile), status='old' )
  do while( .not.eof(io_number) )
    read(io_number,'(a46)') findFissionRxnRates
    if ( findFissionRxnRates == ' multiplier bin:   1.00000E+00    1         -6' ) then
      i=i+1
      read(io_number,'(17x,E11.5E3,1x,f6.4)') fission(i), error(i)
    endif
  enddo
  numFuelBins = i

  close(io_number)

  do i = 1, numFuelBins
    sum_Weighted_Fission = sum_Weighted_Fission + fission(i) * volume(i)
  enddo

  avgFiss = sum_Weighted_Fission /numFuelBins

  !calculate 3d relative power distribution
  do i = 1, numFuelBins
    normPowerDist(i) = fission(i) * volume(i)/ avgFiss
  enddo

  radialStart=1
  !integrate radially at each axial node
  do z = 1, axialNodes
    do i = radialStart, fuelCellsPerNode+radialStart-1
      axialsum(z) = axialsum(z) + fission(i) * volume(i)
    enddo
    radialStart = radialStart + fuelCellsPerNode
  enddo

  avgAxialFiss = sum(axialsum) / axialNodes

  !calculate normalized axial fission reaction rates
  do z = 1, axialNodes
    axialFiss(z) = axialsum(z) / avgAxialFiss
  enddo

  io_number=io_number+1
  open( unit=io_number, file='RPDoutPut.txt')
  do i = 1, numFuelBins
    write(io_number,'(i4,a,f9.7)') i,' ', normPowerDist(i)
  enddo

  write(io_number,*)
  write(io_number,*)
  write(io_number,*)

  do z = 1, axialNodes
    write(io_number,'(a13,i3,a,f9.7)') 'axial node = ',z,' ',axialFiss(z)
  enddo

  close(io_number)

end subroutine axialPowerDist


!\\\\\\\\\\\\\\\\\\\\\\\\\\\\\\\\\\\\\\\\\\\\\\\\\\\\\\\\\\\\\\\\\\\\\\\\\\\\\\\\\\\\\\\\\\\\\\\\\\\\\
! ***************************************************************************************
!////////////////////////////////////////////////////////////////////////////////////////


subroutine readEigenvalueNu(mcnpOutfile,eigenvalue,Nu)
! ==================================================
! read eigenvalue and Nu value from MCNP output file
! ==================================================

  use data_constants
  implicit none
  character (len=60), intent(in)  :: mcnpOutfile

  real, intent(out)               :: eigenvalue
  real, intent(out)               :: Nu
  logical                         :: exist_mcnpOutfile
  character (len=73)              :: tmp
  character (len=57)              :: tmp2

  inquire( file=trim(mcnpOutfile), exist=exist_mcnpOutfile )
  if ( .not.exist_mcnpOutfile ) then
    write(*,'(a,a,a)') 'Cannot find mcnp output file: ',trim(mcnpOutfile),', exiting program.'
    write(*,'(a)') 'Hit any key and enter to close.'
    read(*,*)
    call exit()
  endif

  io_number=io_number+1
  open( unit=io_number, file=trim(mcnpOutfile), status='old' )
  loop10:do while( .not.eof(io_number) )
          do while( tmp /= " | the final estimated combined collision/absorption/track-length keff = ")
           if( eof(io_number) ) then
               write(*,'(a)') 'getHeat.f90 :: Could not find keff in MCNP5 outpuf file.'
               write(*,'(a)') 'Hit any key and enter to close.'
               read(*,*)
               call exit()
           endif
           200 continue
           read(io_number,'(a73)', advance='no', EOR=200) tmp
           if( tmp == " | the final estimated combined collision/absorption/track-length keff = ") then
                read(io_number,'(f7.5)') eigenvalue
                write(*,'(a,f7.5)') 'Found keff = ', eigenvalue
                exit loop10
           endif
          enddo
        enddo loop10
  rewind(io_number)

  loop11:do while( .not.eof(io_number) )
           do while( tmp2 /= " | the average number of neutrons produced per fission = ")
             if( eof(io_number) ) then
               write(*,'(a)') 'getHeat.f90 :: Could not find Nu in MCNP5 outpuf file.'
               write(*,'(a)') 'Hit any key and enter to close.'
               read(*,*)
               call exit()
             endif
             205 continue
             read(io_number,'(a57)', advance='no', EOR=205) tmp2
             if( tmp2 == " | the average number of neutrons produced per fission = ") then
                read(io_number,'(f5.3)') Nu
                write(*,'(a,f5.3)') 'Found Nu = ', Nu
                exit loop11
             endif
           enddo
         enddo loop11
  close(io_number)

end subroutine readEigenvalueNu


!\\\\\\\\\\\\\\\\\\\\\\\\\\\\\\\\\\\\\\\\\\\\\\\\\\\\\\\\\\\\\\\\\\\\\\\\\\\\\\\\\\\\\\\\\\\\
! **************************************************************************************
!///////////////////////////////////////////////////////////////////////////////////////


subroutine FissionHeating(mcnpInfile,mcnpOutfile,volume,rhoFuel,power,Q_MeVperFiss,eigenvalue,Nu)
! ==================================================
! extracts and prints fission energy deposition
! ==================================================
  use physicsData
  use data_constants

  implicit none
  character (len=60), intent(in)  :: mcnpInfile
  character (len=60), intent(in)  :: mcnpOutfile
  real,dimension(4000),intent(in) :: volume
  real, intent(in)                :: rhoFuel
  real, intent(in)                :: power
  real, intent(in)                :: Q_MeVperFiss
  real, intent(in)                :: eigenvalue
  real, intent(in)                :: Nu

  character (len=17)     :: findFissionHeating
  character (len=6)      :: findHeatCell
  logical                :: exist_mcnpOutfile
  integer                :: numFuelBins
  integer               :: i=0
  integer               :: z=0
  integer               :: n=1
  integer               :: radialStart=1
  real, dimension(4000)  :: heating
  real, dimension(4000)  :: heating_W_m3
  real, dimension(4000)  :: Heat_error
  real, dimension(4000)  :: absolute_Heat
  real                   :: PwrFactor
  real, parameter        :: volConvert_cc_m3=10.0**-6

  inquire( file=trim(mcnpOutfile), exist=exist_mcnpOutfile )
  if ( .not.exist_mcnpOutfile ) then
    write(*,'(a,a,a)') 'Cannot find mcnp output file: ',trim(mcnpOutfile),', exiting program.'
    write(*,'(a)') 'Hit any key and enter to close.'
    read(*,*)
    call exit()
  endif

  ! this loop will find the track length fission heating tally.
  ! It does not have a "multiplier bin" before each tally bin like the fission rxn rate tally (14)
  io_number=io_number+1
  open( unit=io_number, file=trim(mcnpOutfile), status='old' )
loop20: do while( .not.eof(io_number) )
          read(io_number,'(a17)') findFissionHeating
          if ( findFissionHeating == '           masses' ) then
            do while(findHeatCell /= ' cell ')
              read(io_number,'(a6)') findHeatCell
              if (findHeatCell == ' cell ') then
                exit loop20
              endif
            enddo
          endif
        enddo loop20

  ! read in the heat tally data
loop21: do while( findHeatCell == ' cell ')
          i=i+1
          read(io_number,'(17x,E11.5E3,1x,f6.4)') heating(i), Heat_error(i)
          read(io_number,*)  ! skip the empty blank line following the heat tally bin
          read(io_number,'(a6)') findHeatCell
          if (findHeatCell /=' cell ') then
            exit loop21
          endif
        enddo loop21
  numFuelBins = i
  close(io_number)

  ! ***************************************************
  ! ***************************************************
  ! convert normalized MeV/g tally to real W/m^3 units
  ! ***************************************************
  ! ***************************************************
  do i=1, numFuelBins
    heating_W_m3(i) = ( heating(i)*power*Nu / (1.602e-13*Q_MeVperFiss*eigenvalue) ) &
                    * ( rhoFuel*(1/volConvert_cc_m3)*1.602e-13 )
  enddo

  ! write 3d heat distribution data (not normalized to anything)
  io_number=io_number+1
  open(io_number, file='fissionHeatingData.txt')
  do i=1, numFuelBins
    write(io_number, '(i4,a,E13.7E2)') i,' ',heating(i)
  enddo
  close(io_number)

  ! calculate/write absolute heat source (Watts in each cell, not W/m^3)
  do i = 1, numFuelBins
    absolute_Heat(i) = heating_W_m3(i) * volume(i) * volConvert_cc_m3
  enddo

  PwrFactor = power / sum(absolute_Heat) ! keeps total power level constant for sake of correct
                                         ! temperature values for non-realistic reactivities
  io_number=io_number+1
  open(io_number, file='Heat.xy')
  write(io_number,'(a)') "X Y Z Heat"
  n = 1 ! count for heating array
  do z = 1, axialNodes
    do i= 1, fuelCellsPerNode
      write(io_number,'(f10.6,f10.6,f10.6,a,E13.7E2)') xc(i)/100.0, yc(i)/100.0, zc(z)/100.0,' ',&
                                                       heating_W_m3(n)*PwrFactor
      n=n+1
    enddo
  enddo
  close(io_number)

  io_number=io_number+1
  open(io_number, file='absoluteHeating.txt')
  do i = 1, numFuelBins
    write(io_number, *) i,absolute_Heat(i)*PwrFactor
  enddo
  write(io_number,*)
  write(io_number,*)
  write(io_number,*) 'total absolute heat = ', sum(absolute_Heat)*PwrFactor, ' Watts'
  close(io_number)

  write(*,*) 'total absolute heat = ', sum(absolute_Heat)*PwrFactor, ' Watts'

end subroutine FissionHeating
```

B.3 STAR-CCM+ Java Script

```
// STAR-CCM+ macro: loadHeat_runStarJob.java
package macro;

import java.util.*;

import star.common.*;
import star.base.neo.*;
import star.energy.*;


public class loadHeat_runStarJob extends StarMacro {

  public void execute() {

    Simulation simulation_0 =
      getActiveSimulation();

// load in MCNP generated volumetric energy (heat) source
    FileTable fileTable_0 =
      (FileTable) simulation_0.getTableManager().createFromFile(resolvePath("_WORKDIR_/Heat__ITERATION_.xy"));

// apply "Heat" data column to "fuel" region as energy source
    Region region_0 =
      simulation_0.getRegionManager().getRegion("fuel");

    EnergyUserSource energyUserSource_0 =
      region_0.getValues().get(EnergyUserSource.class);

    energyUserSource_0.setMethod(XyzTabularScalarProfileMethod.class);

    ((XyzTabularScalarProfileMethod) energyUserSource_0.getMethod()).setTable(fileTable_0);

    ((XyzTabularScalarProfileMethod) energyUserSource_0.getMethod()).setData("Heat");


// run STARCCM+ job with MCNP generated fission heat source
    Solution solution_0 =
      simulation_0.getSolution();

    solution_0.initializeSolution();

    simulation_0.getSimulationIterator().run(true);


// STARCCM+ job done - now create, fill, and export STARCCM+ generated density/temperature output

// ************************************************************************************************
// xyzInternalTable_0 is the fuel region csv output table
// ************************************************************************************************

    XyzInternalTable xyzInternalTable_0 =
      simulation_0.getTableManager().createInternal(XyzInternalTable.class);

    xyzInternalTable_0.setPresentationName("Fuel_OutPut");

    xyzInternalTable_0.getParts().setObjects(region_0);
  xyzInternalTable_0.getParts().setObjects(region_0);

// set primitive field functions to be used in each region for table output: fuel, clad, and water
  PrimitiveFieldFunction primitiveFieldFunction_0 =
   ((PrimitiveFieldFunction) simulation_0.getFieldFunctionManager().getFunction("LocalCellIndex"));

  PrimitiveFieldFunction primitiveFieldFunction_1 =
   ((PrimitiveFieldFunction) simulation_0.getFieldFunctionManager().getFunction("Density"));

  PrimitiveFieldFunction primitiveFieldFunction_2 =
   ((PrimitiveFieldFunction) simulation_0.getFieldFunctionManager().getFunction("Temperature"));

  PrimitiveFieldFunction primitiveFieldFunction_3 =
   ((PrimitiveFieldFunction) simulation_0.getFieldFunctionManager().getFunction("Volume"));

  CompiledFieldFunction compiledFieldFunction_0 =
   ((CompiledFieldFunction) simulation_0.getFieldFunctionManager().getFunction("Centroid_0"));

  CompiledFieldFunction compiledFieldFunction_1 =
   ((CompiledFieldFunction) simulation_0.getFieldFunctionManager().getFunction("Centroid_1"));

  CompiledFieldFunction compiledFieldFunction_2 =
   ((CompiledFieldFunction) simulation_0.getFieldFunctionManager().getFunction("Centroid_2"));

  xyzInternalTable_0.setFieldFunctions(new NeoObjectVector(new Object[] {primitiveFieldFunction_0,
primitiveFieldFunction_1, primitiveFieldFunction_2, primitiveFieldFunction_3, compiledFieldFunction_0,
compiledFieldFunction_1, compiledFieldFunction_2}));

  FieldFunctionColumnDescriptor fieldFunctionColumnDescriptor_0 =
   ((FieldFunctionColumnDescriptor) xyzInternalTable_0.getColumnDescriptor("Cell Index"));

  fieldFunctionColumnDescriptor_0.setPosition(0);

  FieldFunctionColumnDescriptor fieldFunctionColumnDescriptor_1 =
   ((FieldFunctionColumnDescriptor) xyzInternalTable_0.getColumnDescriptor("Density"));

  fieldFunctionColumnDescriptor_1.setPosition(1);

  FieldFunctionColumnDescriptor fieldFunctionColumnDescriptor_2 =
   ((FieldFunctionColumnDescriptor) xyzInternalTable_0.getColumnDescriptor("Temperature"));

  fieldFunctionColumnDescriptor_2.setPosition(2);

  FieldFunctionColumnDescriptor fieldFunctionColumnDescriptor_3 =
   ((FieldFunctionColumnDescriptor) xyzInternalTable_0.getColumnDescriptor("Volume"));

  fieldFunctionColumnDescriptor_3.setPosition(3);

  FieldFunctionColumnDescriptor fieldFunctionColumnDescriptor_4 =
   ((FieldFunctionColumnDescriptor) xyzInternalTable_0.getColumnDescriptor("Centroid: X-Component"));

  fieldFunctionColumnDescriptor_4.setPosition(4);

  FieldFunctionColumnDescriptor fieldFunctionColumnDescriptor_5 =
   ((FieldFunctionColumnDescriptor) xyzInternalTable_0.getColumnDescriptor("Centroid: Y-Component"));

  fieldFunctionColumnDescriptor_5.setPosition(5);

  FieldFunctionColumnDescriptor fieldFunctionColumnDescriptor_6 =
   ((FieldFunctionColumnDescriptor) xyzInternalTable_0.getColumnDescriptor("Centroid: Z-Component"));
  fieldFunctionColumnDescriptor_6.setPosition(6);

  xyzInternalTable_0.setFieldFunctions(new NeoObjectVector(new Object[] {primitiveFieldFunction_0,
primitiveFieldFunction_1, primitiveFieldFunction_2, primitiveFieldFunction_3, compiledFieldFunction_0,
compiledFieldFunction_1, compiledFieldFunction_2}));

  fieldFunctionColumnDescriptor_0.setPosition(0);

  fieldFunctionColumnDescriptor_1.setPosition(1);

  fieldFunctionColumnDescriptor_2.setPosition(2);

  fieldFunctionColumnDescriptor_3.setPosition(3);

  fieldFunctionColumnDescriptor_4.setPosition(4);

  fieldFunctionColumnDescriptor_5.setPosition(5);

  fieldFunctionColumnDescriptor_6.setPosition(6);


// **************************************************************************************************
// xyzInternalTable_1 is the cladding csv output table file
// **************************************************************************************************

  XyzInternalTable xyzInternalTable_1 =
   simulation_0.getTableManager().createInternal(XyzInternalTable.class);

  xyzInternalTable_1.setPresentationName("Clad_OutPut");

  Region region_1 =
   simulation_0.getRegionManager().getRegion("clad");

  xyzInternalTable_1.getParts().setObjects(region_1);

  xyzInternalTable_1.getParts().setObjects(region_1);

  xyzInternalTable_1.setFieldFunctions(new NeoObjectVector(new Object[] {primitiveFieldFunction_0,
primitiveFieldFunction_1, primitiveFieldFunction_2, primitiveFieldFunction_3, compiledFieldFunction_0,
compiledFieldFunction_1, compiledFieldFunction_2}));

  FieldFunctionColumnDescriptor fieldFunctionColumnDescriptor_7 =
   ((FieldFunctionColumnDescriptor) xyzInternalTable_1.getColumnDescriptor("Cell Index"));

  fieldFunctionColumnDescriptor_7.setPosition(0);

  FieldFunctionColumnDescriptor fieldFunctionColumnDescriptor_8 =
   ((FieldFunctionColumnDescriptor) xyzInternalTable_1.getColumnDescriptor("Density"));

  fieldFunctionColumnDescriptor_8.setPosition(1);

  FieldFunctionColumnDescriptor fieldFunctionColumnDescriptor_9 =
   ((FieldFunctionColumnDescriptor) xyzInternalTable_1.getColumnDescriptor("Temperature"));

  fieldFunctionColumnDescriptor_9.setPosition(2);

  FieldFunctionColumnDescriptor fieldFunctionColumnDescriptor_10 =
   ((FieldFunctionColumnDescriptor) xyzInternalTable_1.getColumnDescriptor("Volume"));

  fieldFunctionColumnDescriptor_10.setPosition(3);
```

```
  FieldFunctionColumnDescriptor fieldFunctionColumnDescriptor_11 = 
    ((FieldFunctionColumnDescriptor) xyzInternalTable_1.getColumnDescriptor("Centroid: X-Component"));

  fieldFunctionColumnDescriptor_11.setPosition(4);

  FieldFunctionColumnDescriptor fieldFunctionColumnDescriptor_12 = 
    ((FieldFunctionColumnDescriptor) xyzInternalTable_1.getColumnDescriptor("Centroid: Y-Component"));

  fieldFunctionColumnDescriptor_12.setPosition(5);

  FieldFunctionColumnDescriptor fieldFunctionColumnDescriptor_13 = 
    ((FieldFunctionColumnDescriptor) xyzInternalTable_1.getColumnDescriptor("Centroid: Z-Component"));

  fieldFunctionColumnDescriptor_13.setPosition(6);

  xyzInternalTable_1.setFieldFunctions(new NeoObjectVector(new Object[] {primitiveFieldFunction_0, 
primitiveFieldFunction_1, primitiveFieldFunction_2, primitiveFieldFunction_3, compiledFieldFunction_0, 
compiledFieldFunction_1, compiledFieldFunction_2}));

  fieldFunctionColumnDescriptor_7.setPosition(0);

  fieldFunctionColumnDescriptor_8.setPosition(1);

  fieldFunctionColumnDescriptor_9.setPosition(2);

  fieldFunctionColumnDescriptor_10.setPosition(3);

  fieldFunctionColumnDescriptor_11.setPosition(4);

  fieldFunctionColumnDescriptor_12.setPosition(5);

  fieldFunctionColumnDescriptor_13.setPosition(6);


// *************************************************************************************************
// xyzInternalTable_2 is the water csv output table file
// *************************************************************************************************

  XyzInternalTable xyzInternalTable_2 = 
    simulation_0.getTableManager().createInternal(XyzInternalTable.class);

  xyzInternalTable_2.setPresentationName("Water_OutPut");

  Region region_2 = 
    simulation_0.getRegionManager().getRegion("water");

  xyzInternalTable_2.getParts().setObjects(region_2);

  xyzInternalTable_2.getParts().setObjects(region_2);

  xyzInternalTable_2.setFieldFunctions(new NeoObjectVector(new Object[] {primitiveFieldFunction_0, 
primitiveFieldFunction_1, primitiveFieldFunction_2, primitiveFieldFunction_3, compiledFieldFunction_0, 
compiledFieldFunction_1, compiledFieldFunction_2}));

  FieldFunctionColumnDescriptor fieldFunctionColumnDescriptor_14 = 
    ((FieldFunctionColumnDescriptor) xyzInternalTable_2.getColumnDescriptor("Cell Index"));

  fieldFunctionColumnDescriptor_14.setPosition(0);

  FieldFunctionColumnDescriptor fieldFunctionColumnDescriptor_15 = 
    ((FieldFunctionColumnDescriptor) xyzInternalTable_2.getColumnDescriptor("Density"));
```

```
   fieldFunctionColumnDescriptor_15.setPosition(1);

   FieldFunctionColumnDescriptor fieldFunctionColumnDescriptor_16 =
    ((FieldFunctionColumnDescriptor) xyzInternalTable_2.getColumnDescriptor("Temperature"));

   fieldFunctionColumnDescriptor_16.setPosition(2);

   FieldFunctionColumnDescriptor fieldFunctionColumnDescriptor_17 =
    ((FieldFunctionColumnDescriptor) xyzInternalTable_2.getColumnDescriptor("Volume"));

   fieldFunctionColumnDescriptor_17.setPosition(3);

   FieldFunctionColumnDescriptor fieldFunctionColumnDescriptor_18 =
    ((FieldFunctionColumnDescriptor) xyzInternalTable_2.getColumnDescriptor("Centroid: X-Component"));

   fieldFunctionColumnDescriptor_18.setPosition(4);

   FieldFunctionColumnDescriptor fieldFunctionColumnDescriptor_19 =
    ((FieldFunctionColumnDescriptor) xyzInternalTable_2.getColumnDescriptor("Centroid: Y-Component"));

   fieldFunctionColumnDescriptor_19.setPosition(5);

   FieldFunctionColumnDescriptor fieldFunctionColumnDescriptor_20 =
    ((FieldFunctionColumnDescriptor) xyzInternalTable_2.getColumnDescriptor("Centroid: Z-Component"));

   fieldFunctionColumnDescriptor_20.setPosition(6);

   xyzInternalTable_2.setFieldFunctions(new NeoObjectVector(new Object[] {primitiveFieldFunction_0,
primitiveFieldFunction_1, primitiveFieldFunction_2, primitiveFieldFunction_3, compiledFieldFunction_0,
compiledFieldFunction_1, compiledFieldFunction_2}));

   fieldFunctionColumnDescriptor_14.setPosition(0);

   fieldFunctionColumnDescriptor_15.setPosition(1);

   fieldFunctionColumnDescriptor_16.setPosition(2);

   fieldFunctionColumnDescriptor_17.setPosition(3);

   fieldFunctionColumnDescriptor_18.setPosition(4);

   fieldFunctionColumnDescriptor_19.setPosition(5);

   fieldFunctionColumnDescriptor_20.setPosition(6);


// ***********************************************************************************************
//  export STARCCM+ generated temperature/density output for subsequent MCNP5 execution
// ***********************************************************************************************

   xyzInternalTable_0.export(resolvePath("_WORKDIR_/STARCCMfuel_out__ITERATION1_.csv"), 0);

   xyzInternalTable_1.export(resolvePath("_WORKDIR_/STARCCMclad_out__ITERATION1_.csv"), 0);

   xyzInternalTable_2.export(resolvePath("_WORKDIR_/STARCCMwater_out__ITERATION1_.csv"), 0);

 }
}
```

APPENDIX C. Data File Formats

C.1 MCNP5 to STAR-CCM+: Heat.xy Volumetric Heat Source File Excerpt

Below, (X,Y,Z) is the centroid of the MCNP5 cell in meters. Heat is the power density in each cell in W/m^3.

```
X Y Z Heat
 -0.002314 -0.004119  0.000098 0.5730506E+08
 -0.000897 -0.004338  0.000098 0.4047297E+08
  0.000906 -0.004348  0.000098 0.3333602E+08
  0.002333 -0.004133  0.000098 0.5421250E+08
 -0.004127 -0.002334  0.000098 0.4626177E+08
 -0.002862 -0.002859  0.000098 0.2874447E+08
 -0.000977 -0.002930  0.000098 0.2483536E+08
  0.000977 -0.002930  0.000098 0.2358711E+08
  0.002860 -0.002861  0.000098 0.2792769E+08
  0.004122 -0.002322  0.000098 0.5138924E+08
 -0.004354 -0.000896  0.000098 0.3456092E+08
 -0.002930 -0.000977  0.000098 0.2431238E+08
 -0.000977 -0.000977  0.000098 0.2438148E+08
  0.000977 -0.000977  0.000098 0.2386235E+08
  0.002930 -0.000977  0.000098 0.2694028E+08
  0.004352 -0.000893  0.000098 0.3700510E+08
 -0.004353  0.000894  0.000098 0.3218361E+08
 -0.002930  0.000977  0.000098 0.2638603E+08
 -0.000977  0.000977  0.000098 0.2515003E+08
  0.000977  0.000977  0.000098 0.2425299E+08
  0.002930  0.000977  0.000098 0.2453624E+08
  0.004351  0.000895  0.000098 0.3629155E+08
 -0.004125  0.002336  0.000098 0.5619471E+08
 -0.002862  0.002860  0.000098 0.2699767E+08
 -0.000977  0.002930  0.000098 0.2517076E+08
  0.000977  0.002930  0.000098 0.2657661E+08
  0.002860  0.002861  0.000098 0.2698103E+08
  0.004122  0.002322  0.000098 0.6107013E+08
 -0.002315  0.004119  0.000098 0.6315418E+08
 -0.000898  0.004339  0.000098 0.3628746E+08
  0.000905  0.004348  0.000098 0.3516224E+08
  0.002333  0.004133  0.000098 0.5715716E+08
 -0.002314 -0.004119  0.000781 0.7674357E+08
 -0.000897 -0.004338  0.000781 0.4743583E+08
  0.000906 -0.004348  0.000781 0.4584070E+08
  0.002333 -0.004133  0.000781 0.7622444E+08
 -0.004127 -0.002334  0.000781 0.7234044E+08
 -0.002862 -0.002859  0.000781 0.3797202E+08
 -0.000977 -0.002930  0.000781 0.3304345E+08
  0.000977 -0.002930  0.000781 0.3324944E+08
  0.002860 -0.002861  0.000781 0.3678525E+08
  0.004122 -0.002322  0.000781 0.7878394E+08
 -0.004354 -0.000896  0.000781 0.4902124E+08
 -0.002930 -0.000977  0.000781 0.3411621E+08
 -0.000977 -0.000977  0.000781 0.3059442E+08
  0.000977 -0.000977  0.000781 0.3184674E+08
  0.002930 -0.000977  0.000781 0.3545682E+08
  0.004352 -0.000893  0.000781 0.4881287E+08
 -0.004353  0.000894  0.000781 0.4939116E+08
 -0.002930  0.000977  0.000781 0.3251755E+08
```

C.2 STAR-CCM+ to MCNP5: CSV Temperature and Density Data File Excerpt

The CSV files are automatically generated by STAR-CCM+ with assistance from the Java script (Appendix B.3). The headers at the top of the CSV files describe the quantity and units given in each column.

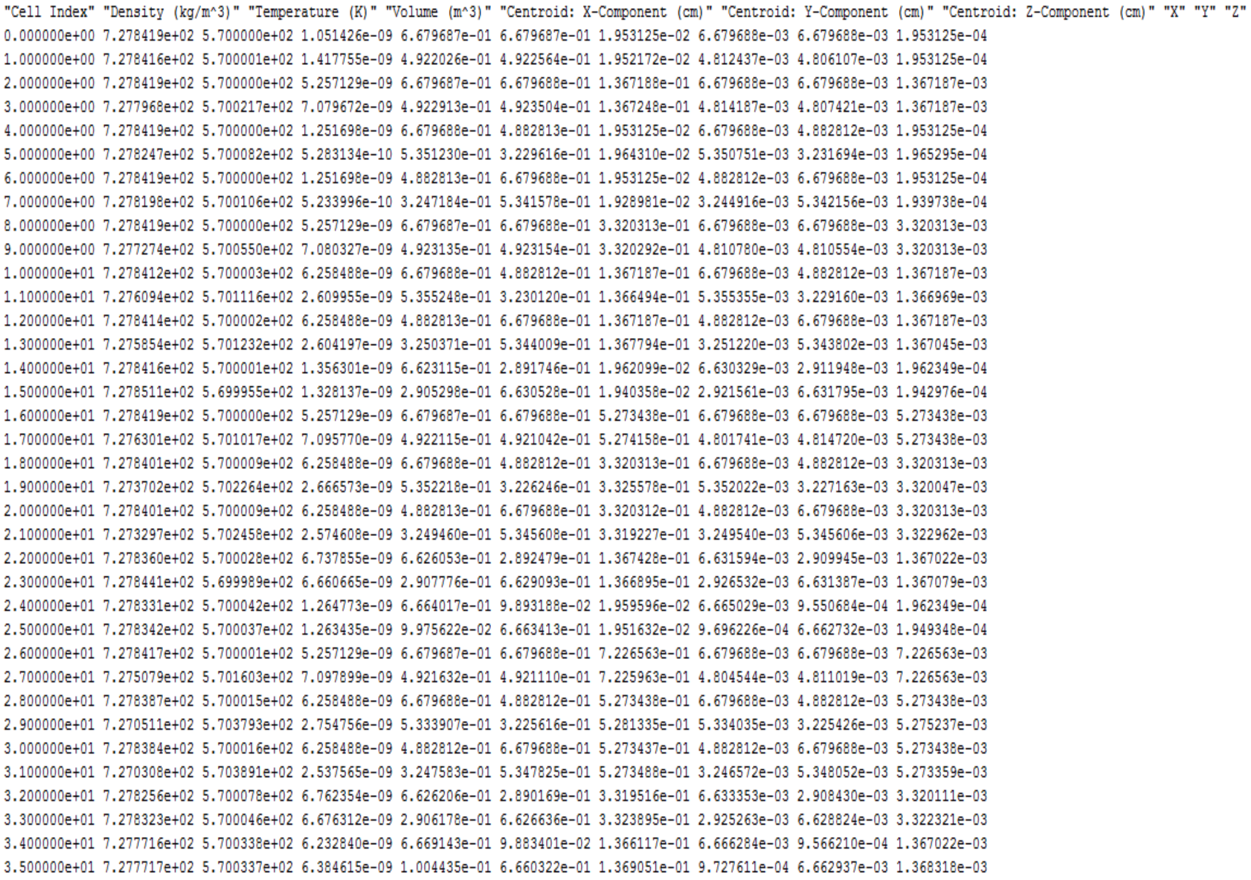

```
"Cell Index" "Density (kg/m^3)" "Temperature (K)" "Volume (m^3)" "Centroid: X-Component (cm)" "Centroid: Y-Component (cm)" "Centroid: Z-Component (cm)" "X" "Y" "Z"
0.000000e+00 7.278419e+02 5.700000e+02 1.051426e-09 6.679687e-01 6.679687e-01 1.953125e-02 6.679688e-03 6.679688e-03 1.953125e-04
1.000000e+00 7.278416e+02 5.700001e+02 1.417755e-09 4.922026e-01 4.922564e-01 1.952172e-02 4.812437e-03 4.806107e-03 1.953125e-04
2.000000e+00 7.278419e+02 5.700000e+02 5.257129e-09 6.679687e-01 6.679688e-01 1.367188e-01 6.679688e-03 6.679688e-03 1.367187e-03
3.000000e+00 7.277968e+02 5.700217e+02 7.079672e-09 4.922913e-01 4.923504e-01 1.367248e-01 4.814187e-03 4.807421e-03 1.367187e-03
4.000000e+00 7.278419e+02 5.700000e+02 1.251698e-09 6.679688e-01 4.882813e-01 1.953125e-02 6.679688e-03 4.882812e-03 1.953125e-04
5.000000e+00 7.278247e+02 5.700082e+02 5.283134e-10 5.351230e-01 3.229616e-01 1.964310e-02 5.350751e-03 3.231694e-03 1.965295e-04
6.000000e+00 7.278419e+02 5.700000e+02 1.251698e-09 4.882813e-01 6.679688e-01 1.953125e-02 4.882812e-03 6.679688e-03 1.953125e-04
7.000000e+00 7.278198e+02 5.700106e+02 5.233996e-10 3.247184e-01 5.341578e-01 1.928981e-02 3.244916e-03 5.342156e-03 1.939738e-04
8.000000e+00 7.278419e+02 5.700000e+02 5.257129e-09 6.679687e-01 6.679688e-01 3.320313e-01 6.679688e-03 6.679688e-03 3.320313e-03
9.000000e+00 7.277274e+02 5.700550e+02 7.080327e-09 4.923135e-01 4.923154e-01 3.320292e-01 4.810780e-03 4.810554e-03 3.320313e-03
1.000000e+01 7.278412e+02 5.700003e+02 6.258488e-09 6.679688e-01 4.882812e-01 1.367187e-01 6.679688e-03 4.882812e-03 1.367187e-03
1.100000e+01 7.276094e+02 5.701116e+02 2.609955e-09 5.355248e-01 3.230120e-01 1.366494e-01 5.355355e-03 3.229160e-03 1.366969e-03
1.200000e+01 7.278414e+02 5.700002e+02 6.258488e-09 4.882813e-01 6.679688e-01 1.367187e-01 4.882812e-03 6.679688e-03 1.367187e-03
1.300000e+01 7.275854e+02 5.701232e+02 2.604197e-09 3.250371e-01 5.344009e-01 1.367794e-01 3.251220e-03 5.343802e-03 1.367045e-03
1.400000e+01 7.278416e+02 5.700001e+02 1.356301e-09 6.623115e-01 2.891746e-01 1.962099e-02 6.630329e-03 2.911948e-03 1.962349e-04
1.500000e+01 7.278511e+02 5.699955e+02 1.328137e-09 2.905298e-01 6.630528e-01 1.940358e-02 2.921561e-03 6.631795e-03 1.942976e-04
1.600000e+01 7.278419e+02 5.700000e+02 5.257129e-09 6.679687e-01 6.679688e-01 5.273438e-01 6.679688e-03 6.679688e-03 5.273438e-03
1.700000e+01 7.276301e+02 5.701017e+02 7.095770e-09 4.922115e-01 4.921042e-01 5.274158e-01 4.801741e-03 4.814720e-03 5.273438e-03
1.800000e+01 7.278401e+02 5.700009e+02 6.258488e-09 6.679688e-01 4.882812e-01 3.320313e-01 6.679688e-03 4.882812e-03 3.320313e-03
1.900000e+01 7.273702e+02 5.702264e+02 2.666573e-09 5.352218e-01 3.226246e-01 3.325578e-01 5.352022e-03 3.227163e-03 3.320047e-03
2.000000e+01 7.278401e+02 5.700009e+02 6.258488e-09 4.882813e-01 6.679688e-01 3.320312e-01 4.882812e-03 6.679688e-03 3.320313e-03
2.100000e+01 7.273297e+02 5.702458e+02 2.574608e-09 3.249460e-01 5.345608e-01 3.319227e-01 3.249540e-03 5.345606e-03 3.322962e-03
2.200000e+01 7.278360e+02 5.700028e+02 6.737855e-09 6.626053e-01 2.892479e-01 1.367428e-01 6.631594e-03 2.909945e-03 1.367022e-03
2.300000e+01 7.278441e+02 5.699989e+02 6.660665e-09 2.907776e-01 6.629093e-01 1.366895e-01 2.926532e-03 6.631387e-03 1.367079e-03
2.400000e+01 7.278331e+02 5.700042e+02 1.264773e-09 6.664017e-01 9.893188e-02 1.959596e-02 6.665029e-03 9.550684e-04 1.962349e-04
2.500000e+01 7.278342e+02 5.700037e+02 1.263435e-09 9.975622e-02 6.663413e-01 1.951632e-02 9.696226e-04 6.662732e-03 1.949348e-04
2.600000e+01 7.278417e+02 5.700001e+02 5.257129e-09 6.679687e-01 6.679688e-01 7.226563e-01 6.679688e-03 6.679688e-03 7.226563e-03
2.700000e+01 7.275079e+02 5.701603e+02 7.097899e-09 4.921632e-01 4.921110e-01 7.225963e-01 4.804544e-03 4.811019e-03 7.226563e-03
2.800000e+01 7.278387e+02 5.700015e+02 6.258488e-09 6.679688e-01 4.882812e-01 5.273438e-01 6.679688e-03 4.882812e-03 5.273438e-03
2.900000e+01 7.270511e+02 5.703793e+02 2.754756e-09 5.333907e-01 3.225616e-01 5.281335e-01 5.334035e-03 3.225426e-03 5.275237e-03
3.000000e+01 7.278384e+02 5.700016e+02 6.258488e-09 4.882812e-01 6.679688e-01 5.273437e-01 4.882812e-03 6.679688e-03 5.273438e-03
3.100000e+01 7.270308e+02 5.703891e+02 2.537565e-09 3.247583e-01 5.347825e-01 5.273488e-01 3.246572e-03 5.348052e-03 5.273359e-03
3.200000e+01 7.278256e+02 5.700078e+02 6.762354e-09 6.626206e-01 2.890169e-01 3.319516e-01 6.633353e-03 2.908430e-03 3.320111e-03
3.300000e+01 7.278323e+02 5.700046e+02 6.676312e-09 2.906178e-01 6.626636e-01 3.323895e-01 2.925263e-03 6.628824e-03 3.322321e-03
3.400000e+01 7.277716e+02 5.700338e+02 6.232840e-09 6.669143e-01 9.883401e-02 1.366117e-01 6.666284e-03 9.566210e-04 1.367022e-03
3.500000e+01 7.277717e+02 5.700337e+02 6.384615e-09 1.004435e-01 6.660322e-01 1.369051e-01 9.727611e-04 6.662937e-03 1.368318e-03
```

APPENDIX D. Running MULTINUKE: An Overview of the Required Files

Figure 33 is a screen shot of a directory containing all the files required to run a MULTINUKE simulation. Table 17 describes each file required to be located in the working directory to run MULTINUKE. A comparable setup should allow the user to execute the MULTINUKE code, assuming the user has made the necessary preparations to the MCNP5 input file, STAR-CCM+ simulation file and Java script, mesh correlation files, and the *multiSpecs_base.txt* file (as described in Chapter 5, Section 5.2: Solver Preparation). Furthermore, the example directory assumes the user has created a temperature dependent cross section library, and has proper access to MCNP5 and STAR-CCM+ parallel executables. Depending on the operating system settings, the user may be required to manually set the stacksize to unlimited to allow sufficient memory allocation for MCNP5 and STAR-CCM+.

The MULTINUKE coupled solver is executed by running the Perl script:

```
./runMultiNuke.pl
```

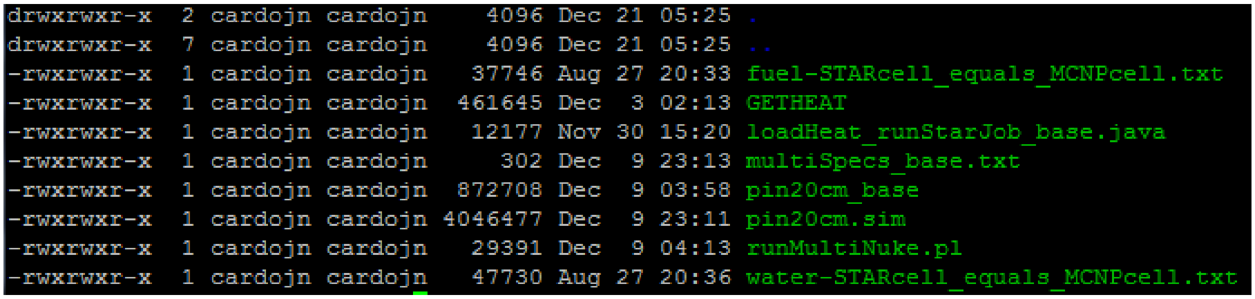

```
drwxrwxr-x  2 cardojn cardojn    4096 Dec 21 05:25 .
drwxrwxr-x  7 cardojn cardojn    4096 Dec 21 05:25 ..
-rwxrwxr-x  1 cardojn cardojn   37746 Aug 27 20:33 fuel-STARcell_equals_MCNPcell.txt
-rwxrwxr-x  1 cardojn cardojn  461645 Dec  3 02:13 GETHEAT
-rwxrwxr-x  1 cardojn cardojn   12177 Nov 30 15:20 loadHeat_runStarJob_base.java
-rwxrwxr-x  1 cardojn cardojn     302 Dec  9 23:13 multiSpecs_base.txt
-rwxrwxr-x  1 cardojn cardojn  872708 Dec  9 03:58 pin20cm_base
-rwxrwxr-x  1 cardojn cardojn 4046477 Dec  9 23:11 pin20cm.sim
-rwxrwxr-x  1 cardojn cardojn   29391 Dec  9 04:13 runMultiNuke.pl
-rwxrwxr-x  1 cardojn cardojn   47730 Aug 27 20:36 water-STARcell_equals_MCNPcell.txt
```

Figure D1. Example of Working Directory for Running MULTINUKE.

Table D1. Required Files in MULTINUKE Working Directory.

File Name	Description
fuel-STARcell_equals_MCNPcell.txt	Fuel mesh correlation file.
GETHEAT	Fortran90 post-processor for MCNP5.
loadHeat_runStarJob_base.java	Base Java script for STAR-CCM+.
multiSpecs_base.txt	Input file for MULTINUKE.
pin20cm_base	MCNP5 base input file.
pin20cm.sim	STAR-CCM+ simulation file.
runMultiNuke.pl	Main MULTINUKE Perl Script.
water-STARcell_equals_MCNPcell.txt	Coolant mesh correlation file.

Author’s Biography

Jeffrey Neil Cardoni was born on October 15, 1984. He graduated from Normal Community West High School in 2003. In 2007, he earned a Bachelor of Science in Nuclear Engineering from the University of Illinois at Urbana-Champaign, graduating with highest honors. After working in various DOE laboratories, he returned to graduate school in 2009 to obtain an MS in Nuclear Engineering from the University of Illinois.